



Title	Photocatalytic Redox Reactions by Aqueous Suspension of Titanium Dioxide
Author(s)	Ohtani, Bunsho
Citation	Kyoto University. 博士(Engineering)
Issue Date	1985-03-23
Doc URL	<a href="http://hdl.handle.net/2115/32340">http://hdl.handle.net/2115/32340</a>
Type	theses (doctoral)
File Information	thesis.pdf



[Instructions for use](#)

PHOTOCATALYTIC REDOX REACTIONS BY AQUEOUS  
SUSPENSION OF TITANIUM DIOXIDE

1 9 8 4

BUNSHO OHTANI

DEPARTMENT OF HYDROCARBON CHEMISTRY  
FACULTY OF ENGINEERING  
KYOTO UNIVERSITY  
KYOTO

## PREFACE

The studies presented in this thesis have been carried out under the direction of Professor Dr. Tsutomu Kagiya, Department of Hydrocarbon Chemistry, Faculty of Engineering, Kyoto University during 1981-1984.

The author wishes to express his sincerest gratitude to Professor Dr. Tsutomu Kagiya for his constant guidance, helpful discussions, and hearty encouragement throughout this work. He is also deeply grateful to Associate Professor Dr. Takeo Shimidzu and Dr. Sei-ichi Nishimoto for their pertinent guidance, stimulating discussion and constant encouragement during the course of the study. Acknowledgement is also made to Professor Dr. Satohiro Yoshida and Dr. Eiichiro Nakayama for generous support of facilities and kind advice in the measurements. Furthermore, he wishes to express his appreciation to his colleague, Messrs. Tadao Yoshikawa and Hiroshi Shirai for their collaborations and insightful discussions. He is equally grateful to Messrs. Akira Sakamoto, Hiroshi Kajiwara, Haruyoshi Osaki, and Yoshitaka Okugawa for their collaborations and helpful discussions. He is indebted to all the members of the research group of Professor Dr. Tsutomu Kagiya. He would also like to express his gratitude to Kyoei Fund for the financial support during 1981-1984.

Finally, the author sincerely thanks his parents and his wife Kaoru for their understanding and encouragement.

Bunsho Ohtani

November 1984

## CONTENTS

General Introduction .....	1
----------------------------	---

### PART I

#### Photocatalytic Reaction of Organic Compounds by Aqueous Suspension of Platinized TiO<sub>2</sub>

Chapter 1 Photocatalytic Dehydrogenation of Aliphatic Alcohols by Aqueous Suspension of Platinized TiO <sub>2</sub> .....	15
Chapter 2 Photocatalytic Degradation and Dimerization of 2-Methyl-2-propanol by Aqueous Suspension of Platinized TiO <sub>2</sub> .....	34
Chapter 3 Photocatalytic Reaction of Poly(vinyl alcohol) by Aqueous Suspension of Platinized TiO <sub>2</sub> .....	60
Chapter 4 Photocatalytic Degradation and Prolongation of Poly(ethylene oxide) by Aqueous Suspension of Platinized TiO <sub>2</sub> .....	73
Chapter 5 Photocatalytic Deaminoalkylation and Cyclization of Aliphatic Amines by Aqueous Suspension of Platinized TiO <sub>2</sub> .....	97

### PART II

#### Photocatalytic Oxidations of 2-Propanol and Water Along with Silver Metal Deposition by TiO<sub>2</sub> Suspension

Chapter 6	Photocatalytic Oxygen Formation and Silver Metal Deposition by $\text{TiO}_2$ Suspension in Aqueous Solution of Various Silver Salts .....	146
Chapter 7	Photocatalytic Oxidations of 2-Propanol and Water by $\text{TiO}_2$ Suspension in Aqueous Solution of Various Silver Salts .....	169
Chapter 8	Effect of the Concentrations of 2-Propanol and Silver Sulfate on Photocatalytic Oxidations of 2-Propanol and Water Along with Silver Metal Deposition by $\text{TiO}_2$ Suspension .....	189

### PART III

Correlation of Photocatalytic Activity of  $\text{TiO}_2$  for Redox Reaction in Aqueous 2-Propanol and Silver Salt Solution with Crystal Form and Surface Structure of  $\text{TiO}_2$

Chapter 9	Photocatalytic Activity of $\text{TiO}_2$ Prepared from Titanium Sulfate for Dehydrogenation of 2-Propanol in Aqueous Solution .....	219
Chapter 10	Correlation between Crystal Form of $\text{TiO}_2$ Prepared from Titanium Tetra-2-propoxide and Photocatalytic Activity for Redox Reaction in Aqueous 2-Propanol and Silver Salt Solutions .....	245
Chapter 11	Influence of pH on the Photocatalytic Activity of $\text{TiO}_2$ Powders Suspended in Aqueous Silver Nitrate Solution and on Chemical Structure of $\text{TiO}_2$ Surface .....	273

Summary ..... 303  
List of Publications ..... 308

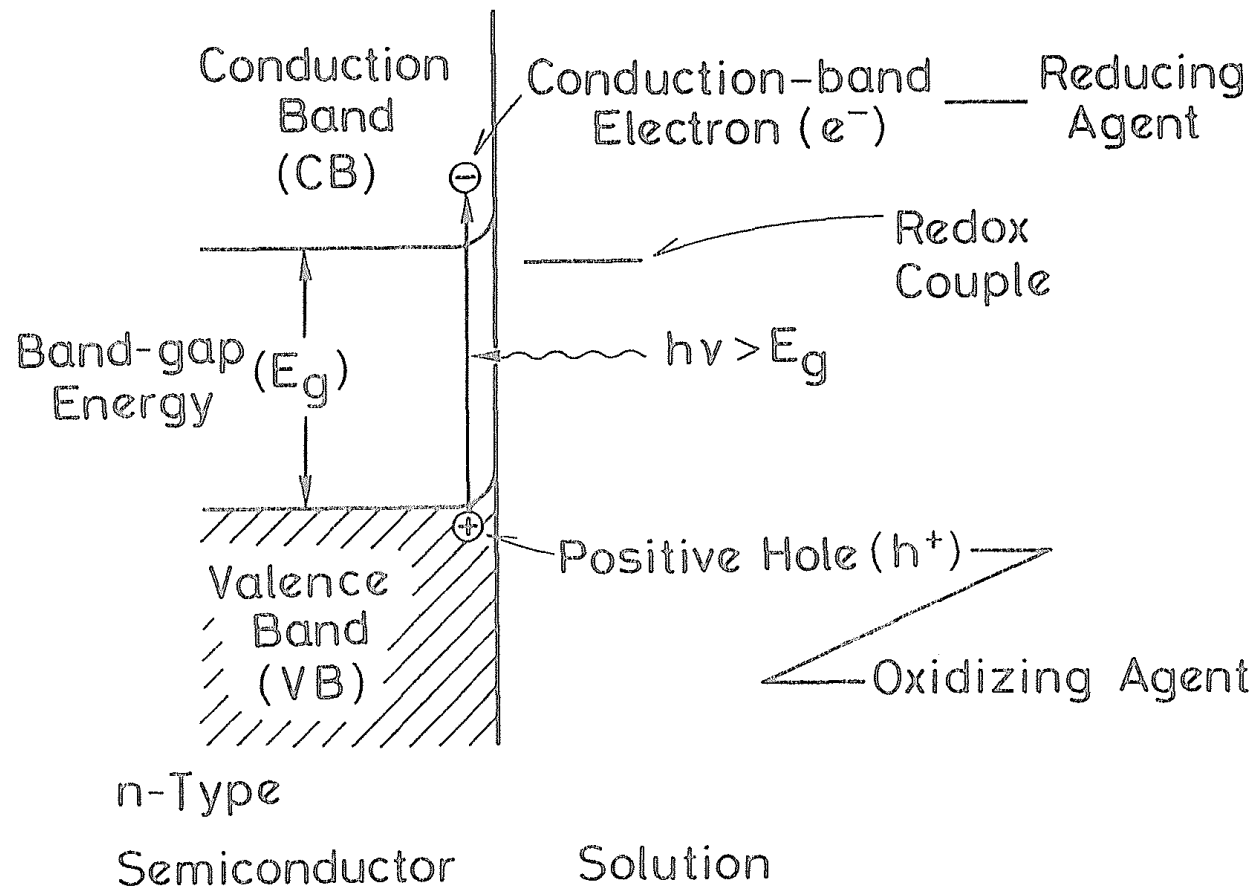
## GENERAL INTRODUCTION

### 1. Background

One of the current interests in the photochemical research is semiconductor photocatalysis, i.e., redox-including chemical reaction induced by the photoirradiated semiconductor surface.<sup>1</sup> In such photocatalysis primary step involves the absorption of light energy by semiconductor which is characterized by band structure, i.e., a filled valence band separated by an energy gap from a vacant conduction band (Scheme 1). The light of energy greater than the band gap promotes excitation of an electron from the valence band to the conduction band, leaving an electron deficiency, i.e., positive hole in the valence band. These active species can respectively reduce or oxidize substrates in the solution. Ability of the photoirradiated semiconductor for chemical reaction is attributable to the photoexcitation and subsequent charge transfer through semiconductor solution interface.<sup>2</sup>

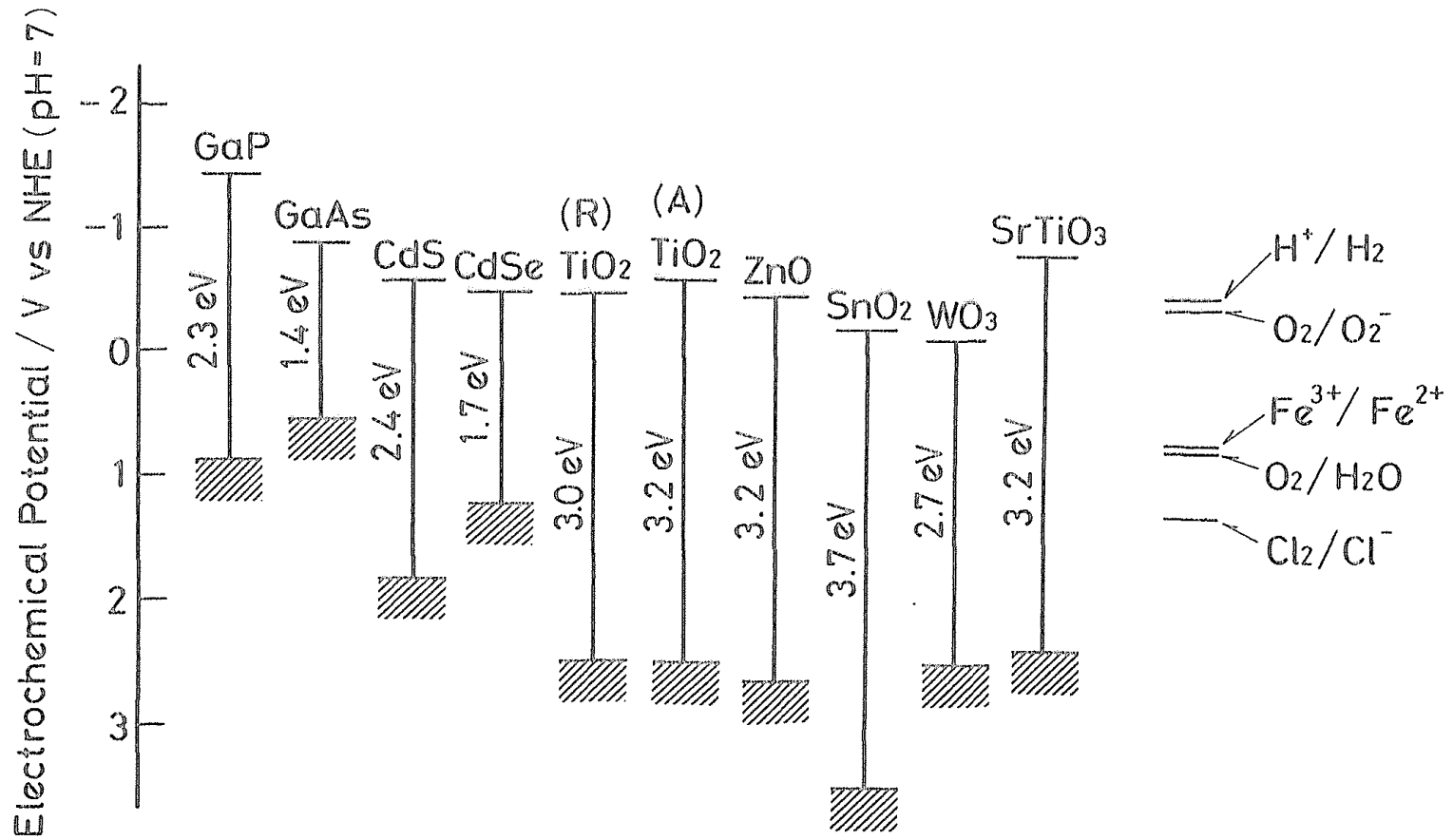
Among semiconductor materials n-type titanium dioxide ( $\text{TiO}_2$ ) has been extensively used as a stable photocatalyst suspended in an aqueous solution. From the electrochemical studies on  $\text{TiO}_2$  photoanode,<sup>3</sup> the energies of the electron and the positive hole are evaluated to be sufficient even for the reduction and oxidation of water into hydrogen and oxygen, respectively (Scheme 2).<sup>4</sup>

Noticeable attempts have been made to utilize the photogenerated active species separately without their mutual recombination. One of the effort toward this efficient charge separation is modification of the  $\text{TiO}_2$  surface by partial coverage with metal and/or metal



Scheme 1 Photoexcitation of n-type semiconductor by photoabsorption ( $h\nu > E_g$ ) to produce a pair of conduction band electron and positive hole.

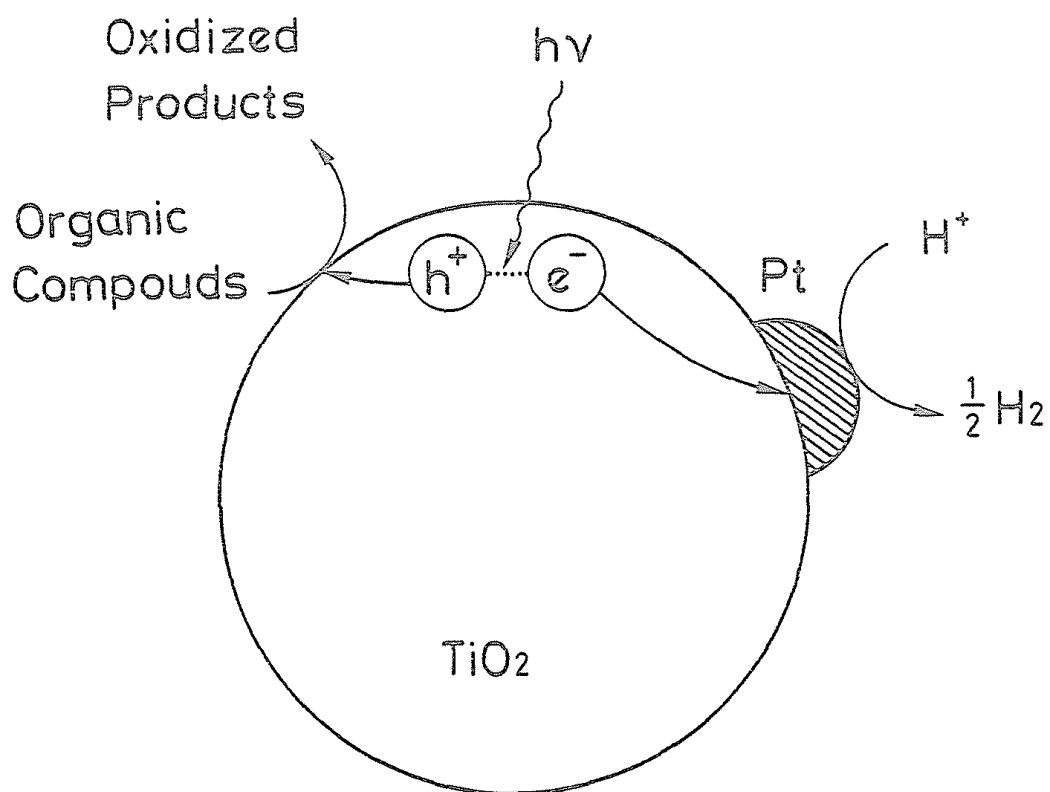




Scheme 2 Potential of conduction and valence bands of various semiconductors; (A) and (R) show anatase and rutile  $TiO_2$ , respectively.

oxide, such as platinum<sup>5</sup> and/or ruthenium dioxide,<sup>6</sup> according to the idea of coupling semiconductor anode and metal cathode which has been used separately in the photoelectrochemical cell.<sup>7</sup> In the modified, typically platinized, TiO<sub>2</sub> particles the photoexcited electrons could effectively reduce proton into hydrogen on the metal surface<sup>8</sup> to result in the enhancement of total photocatalytic activity (Scheme 3). Such platinized TiO<sub>2</sub> (TiO<sub>2</sub>/Pt) powder has been successfully prepared by in situ photoreduction of hexachloroplatinum ion<sup>9</sup> or simply by mixing with platinum black.<sup>10</sup> The thus prepared photocatalyst has sufficient ability to decompose gaseous water into oxygen and hydrogen<sup>11</sup> or to oxidize organic compounds, such as methanol,<sup>12</sup> ethanol,<sup>13</sup> or sugar,<sup>14</sup> with the simultaneous formation of hydrogen. Similarly, carboxylic acids undergo decarboxylation to produce alkane and CO<sub>2</sub> in the TiO<sub>2</sub>/Pt photocatalyzed system, through a proposed reaction pathway involving an oxidative decomposition of carboxylate by the positive hole and reduction of resulting alkyl radical by the electron on the Pt site.<sup>15</sup>

Thus, the metallized TiO<sub>2</sub> catalyst has been favorably applied to photoinduced reaction of several organic compounds. In these systems, however, the fate of organic substrates other than simple alcohols or acids has been so far poorly characterized, particularly in the primary stage of the reaction,<sup>16</sup> because significant attention has been paid to the production of hydrogen from water<sup>17</sup> not to the oxidation products. Consequently, detailed characterization of the semiconductor photocatalysis is desired. In this respect, Part I of this thesis is concerned with reaction characteristics of a series of organic compounds including polymeric materials.



Scheme 3 Oxidation of organic compounds along with  $\text{H}_2$  formation by platinized  $\text{TiO}_2$  particle.

Another effort for the effective utilization of photogenerated active species has been made using electron acceptors<sup>18</sup> and donors<sup>19</sup> for the trapping of electron and positive hole, respectively, to avoid their mutual recombination. One of the most reasonable example is the conventional photocatalysis on  $\text{TiO}_2$ <sup>20</sup> or  $\text{ZnO}$ <sup>21</sup> under aerated conditions owing to the characteristic electron acceptability of oxygen. The aerated systems have been successfully used in the oxidation of organic compounds, such as alkenes<sup>22</sup> or alkylbenzenes<sup>23</sup> into ketones or phenols, respectively, in respect of synthetic application. Similarly, metal ions can also enhance the  $\text{TiO}_2$  photocatalytic ability by trapping the photogenerated electrons. Accordingly, Part II of this thesis deals with enhancement of  $\text{TiO}_2$ -photocatalytic activity by the surface adsorption of electron acceptor and donors.

Throughout the above mentioned photocatalysis, one of the factor governing the photocatalytic activity is the crystal and surface structure of semiconductor powders. In most of the reported photocatalytic reaction systems commercially available  $\text{TiO}_2$  powders have been used and there are few descriptions on the dependence on their structure.<sup>24</sup> In order to obtain highly active photocatalyst, detailed investigations concerning the correlations between the photocatalytic activity and these physical properties are desirable. In Part III, relevant studies are described on the correlations obtained using prepared  $\text{TiO}_2$  powders in the various types of photocatalytic reactions.

## 2. Survey of This Thesis

The outline of this thesis is given as follows.

Part I, which is composed of five chapters (Chapters 1-5), deals with photocatalytic reactions of various organic materials by aqueous  $\text{TiO}_2$  or platinized  $\text{TiO}_2$  suspensions under deaerated conditions at room temperature. Particular emphasis is placed on the characteristic of reaction mechanism of each substrate.

In Chapter 1, the photoinduced reaction of a series of aliphatic alcohols in aqueous  $\text{TiO}_2$  and platinized  $\text{TiO}_2$  suspension is described. Platinization of  $\text{TiO}_2$  leads to the enhancement of the  $\text{TiO}_2$  photocatalytic activity and stoichiometric formation of oxidation and reduction products. The reactivities of primary, secondary, and tertiary alcohols are characterized on the basis of the product distributions. A linear relationship between the initial photoreaction rate and the reactivity of the alcohols toward OH radical suggests the photo-oxidation process via OH radical intermediate generated from  $\text{OH}^-$  with photogenerated positive hole.

Chapter 2 is concerned with detailed characterization of the  $\text{TiO}_2$ -photocatalytic reaction of 2-methyl-2-propanol (t-BuOH) in aqueous solution under deaerated or aerated conditions. Comparison with the product distribution in the t-BuOH oxidation by Fenton's reagent and by ionizing radiation reveals that the photoreaction pathway involves 2-hydroxyl-2-methylpropyl radical intermediate to undergo recombination into dimeric product or to degrade into methyl radical and acetone, in accord with the prediction in Chapter 1.

Chapter 3 states the photocatalytic decomposition of poly(vinyl alcohol) in aqueous suspension of  $\text{TiO}_2/\text{Pt}$  catalyst. Ultraviolet

spectroscopic and viscometric measurements reveals the photoreaction pathway involving  $\alpha$ -hydroxy polymer radical induced by photo-generated positive hole. The intermediate radical undergoes both further oxidation into polymer ketone and  $\beta$ -scission to yield terminal acetyl group.

Chapter 4 deals with the photoinduced degradation of poly(ethylene oxide) in aqueous solution by platinized  $\text{TiO}_2$  under deaerated conditions. Prolongation and degradation of the polymer chain are observed in the basic and acidic solutions, respectively. This behavior is interpreted by the pH dependent modification of the  $\text{TiO}_2$  surface.

Chapter 5 describes the results of photoinduced reaction of aliphatic amines in aqueous solution by platinized  $\text{TiO}_2$  catalyst. Aliphatic linear primary amines give corresponding secondary amines by the dual function of platinized  $\text{TiO}_2$  catalyst; photogenerated positive hole oxidizes the amines into imines and photogenerated electron reduces the intermediate Schiff base derived from the starting amine with the imine or its hydrated derivative, aldehyde. GC-MS analysis of the product secondary amine from  $\text{D}_2\text{O}$  solution confirms the proposed mechanism. Attempts are made to apply the photocatalytic reaction to synthesize cyclic secondary amines from diamines.

Part II, which consists of three chapters (Chapter 6-8), is concerned with the  $\text{TiO}_2$ -photocatalyzed reaction in the aqueous suspension containing silver salt. The significance of this study is based on the fact that photogenerated reductive species, electron, is effectively trapped by the silver ion adsorbed on the  $\text{TiO}_2$

surface.

Chapter 6 describes the photoinduced oxygen formation and silver metal deposition by  $\text{TiO}_2$  suspension in the presence of a series of silver salts. Mass spectroscopic analysis of isotope distribution of product oxygen from  $\text{H}_2^{16}\text{O}/\text{H}_2^{18}\text{O}$  clarifies that water molecules are oxidized into oxygen in the present photoreaction system. The effect of counter anion on the photoreaction yield is rationalized by the fact that  $\text{TiO}_2$  activity is significantly dependent on the pH of the reaction mixture.

Chapter 7 states the effect of 2-propanol addition to the photoreaction system of  $\text{TiO}_2$  suspension in aqueous silver salt solution. 2-Propanol and water are competitively oxidized with the photogenerated positive hole into acetone and oxygen, respectively, while the concomitantly formed electron reduces silver ion to silver metal deposit.

Chapter 8 provides a physicochemical behavior of surface adsorbates in the  $\text{TiO}_2$  photocatalytic system in aqueous silver sulfate and 2-propanol solution. A proposed mechanism including Langmuir adsorption of both silver ion and 2-propanol and trapping of the photogenerated active species by surface adsorbates interprets the observed dependence of photocatalytic reaction rate on the concentrations of the silver salt and 2-propanol.

Part III, which consists of three chapters (Chapters 9-11), is concerned with the correlation of photocatalytic activity with the crystal and surface structure of  $\text{TiO}_2$ .

Chapter 9 describes the photocatalytic activity of  $\text{TiO}_2$  prepared by hydrolysis of titanium sulfate followed by calcination at various

temperatures up to 1000 °C. Crystal structure of TiO<sub>2</sub> predominantly influences on the activity of platinized TiO<sub>2</sub> for the dehydrogenation of 2-propanol in aqueous solution. The activity of anatase polycrystalline is sufficient and increased with the crystal growth, while that of rutile polycrystalline is negligible.

Chapter 10 describes the photocatalytic activity of anion-free TiO<sub>2</sub> prepared by hydrolysis of titanium tetra-2-propoxide and subsequent calcination at various temperatures up to 1000 °C. The photocatalytic activity dependences on the calcination temperature observed in three different reactions, dehydrogenation of 2-propanol with platinized catalyst, oxygen formation and Ag metal deposition from aqueous silver salt solution, and 2-propanol oxidation and Ag metal deposition from aqueous silver salt and 2-propanol solution, provide a correlation with TiO<sub>2</sub> crystal structure, in accord with the prediction demonstrated in Chapter 9.

Chapter 11 deals with the pH dependent nature of surface hydroxyl group on the two types of TiO<sub>2</sub> powder, anatase and rutile, suspended in an aqueous solution, and their effects on the photocatalytic activity in the aqueous silver salt solution. The pH dependent behavior that the TiO<sub>2</sub> activity decreased with the decreasing pH is suggested to relate with protonation - deprotonation equilibria of the surface hydroxyl groups.



## References

- 1 (a) A. J. Bard, *J. Photochem.*, 10, 59 (1979) (b) A. J. Bard, *Science*, 207, 139 (1980).
- 2 (a) A. J. Nozik, *Ann. Rev. Phys. Chem.*, 29, 189 (1978) (b) M. S. Wrighton, *Acc. Chem. Res.*, 12, 303 (1979).
- 3 E. C. Dutoit, F. Cardon, and W. P. Gomes, *Ber. Bunsenges. Phys. Chem.*, 80, 475 (1976).
- 4 A. J. Bard, *J. Phys. Chem.*, 86, 172 (1982).
- 5 J.-M. Lehn, J.-P. Sauvage, and R. Ziessel, *Nouv. J. Chim.*, 4, 623 (1980).
- 6 K. Kalyanasundaram, E. Borgarello, and M. Grätzel, *Helv. Chim. Acta*, 64, 362 (1981).
- 7 (a) A. Fujishima and K. Honda, *Bull. Chem. Soc. Jpn*, 44, 1148 (1971) (b) A. Fujishima and K. Honda, *Nature (London)*, 238, 37 (1972).
- 8 R. Baba, S. Nakabayashi, A. Fujishima, and K. Honda, 48th Annual Meeting of Chemical Society of Japan, 4011 (1983).
- 9 (a) B. Kraeutler and A. J. Bard, *J. Am. Chem. Soc.*, 100, 4318 (1978) (b) W. W. Dunn and A. J. Bard, *Nouv. J. Chim.*, 5, 651 (1981).
- 10 T. Kawai, T. Sakata, *J. Chem. Soc., Chem. Commun.*, 1047 (1979).
- 11 S. Sato and J. M. White, *J. Catal.*, 69, 128 (1980).
- 12 T. Kawai and T. Sakata, *J. Chem. Soc., Chem. Commun.*, 694 (1980).
- 13 P. Pichat, J.-M. Herrmann, J. Disdier, H. Courbon, and M.-N. Mozzanega, *Nouv. J. Chim.*, 5, 627, (1981).

- 14 (a) T. Kawai and T. Sakata, *Chem. Lett.*, 81 (1981) (b) M. R. St. John, A. J. Furgala, and A. F. Sammells, *J. Phys. Chem.*, 87, 801 (1983).
- 15 (a) B. Kraeutler and A. J. Bard, *J. Am. Chem. Soc.*, 100, 5985 (1978) (b) H. Yoneyama, Y. Takao, H. Tamura, *J. Phys. Chem.*, 87, 1417 (1983).
- 16 T. Kawai and T. Sakata, *Nature*, 286, 474 (1980).
- 17 T. Sakata and T. Kawai, *Nouv. J. Chim.*, 5, 279 (1981).
- 18 (a) A. A. Krasnovskii, G. P. Brin, and Z. Aliev, *Dokl. Akad. Nauk SSSR*, 199, 952 (1971) (b) E. Borgarello, J. Kiwi, M. Grätzel, E. Pellizzetti, and M. Visca, *J. Am. Chem. Soc.*, 104, 2996 (1982) (c) A. Mills and G. Porter, *J. Chem. Soc., Faraday Trans. 1*, 78, 3659 (1982) (d) P. D. Fleischauer, H. K. Alen Kan, and J. R. Schepherd, *J. Am. Chem. Soc.*, 94, 283 (1972) (e) A. W. Adamson and P. D. Fleischauer, *Concepts of Inorganic Photochemistry* (Wiley, New York, 1975), p. 400.
- 19 (a) S. Sato and J. M. White, *J. Phys. Chem.*, 85, 336 (1981) (b) S. Sato and J. M. White, *J. Am. Chem. Soc.*, 102, 7206 (1980) (c) Y. Oosawa, *J. Chem. Soc., Chem. Commun.*, 221 (1982) (d) S. Teratani, J. Nakamichi, K. Taya, and K. Tanaka, *Bull. Chem. Soc. Jpn*, 55, 1688 (1982) (e) K. Domen, S. Naito, T. Ohnishi, and K. Tamaru, *Chem. Lett.*, 555 (1982).
- 20 P. R. Harvey, R. Rudham, and S. Ward, *J. Chem. Soc., Faraday Trans. 1*, 79, 1381 (1983) and references therein.
- 21 I. Komuro, Y. Fujita, and T. Kwan, *Bull. Chem. Soc. Jpn*, 32, 882 (1959).
- 22 M. A. Fox and C. C. Chen, *Tetrahedron Lett.*, 24, 547 (1983).

- 23 M. Fujihira, Y. Satoh, and T. Osa, Bull. Chem. Soc. Jpn, 55, 666  
(1982).
- 24 M. V. Rao, K. Rajeshwar, V. R. Pal Verneker, and J. DuBow, J.  
Phys. Chem., 84, 1987 (1980).

Part I

Photocatalytic Reaction of Organic Compounds by Aqueous  
Suspension of Platinized  $\text{TiO}_2$

## Chapter 1

### Photocatalytic Dehydrogenation of Aliphatic Alcohols by Aqueous Suspension of Platinized TiO<sub>2</sub>

#### ABSTRACT

Photoirradiation ( $\lambda_{ex} > 300$  nm) of aqueous 2-propanol solution gave hydrogen and acetone in the presence of platinum and/or ruthenium oxide loaded TiO<sub>2</sub>. The photocatalytic activity of anatase TiO<sub>2</sub> significantly depended on these metal or metal oxide deposits; the activity increased in the order, platinum black  $\gg$  platinum powder  $>$  ruthenium oxide. The photocatalytic activity of rutile TiO<sub>2</sub> was negligible even when loaded with platinum black. The effective wavelength for this photocatalytic dehydrogenation of 2-propanol was below ca. 390 nm, which practically agreed with the photoabsorption edge of TiO<sub>2</sub>. In the similar way, aliphatic primary, secondary, and tertiary alcohols underwent photocatalytic oxidation by the platinized TiO<sub>2</sub>, accompanied by the hydrogen liberation. The primary and secondary alcohols gave corresponding carbonyl derivatives with stoichiometric hydrogen evolution, while the tertiary alcohol, 2-methyl-2-propanol, gave a dimeric product.

## INTRODUCTION

Recently, photocatalytic activities of titanium dioxide ( $\text{TiO}_2$ ) and its modifications have been discussed considerably in the oxidation of organic compounds such as methanol and carbohydrates in aqueous solution.<sup>1</sup> The reactivities of the substrates have, however, not yet been characterized comprehensively in these photocatalytic oxidation systems. In the present work, photocatalyzed reactions of a series of aliphatic alcohols by platinized  $\text{TiO}_2$  powder are reported. Correlation of the initial oxidation rate in aqueous suspension with the corresponding rate constant of hydrogen abstraction by hydroxyl radical in a homogeneous system is discussed.

## EXPERIMENTAL

Materials. Titanium dioxide powder (anatase > 99 %;  $\text{SO}_4^{2-}$ , 0,05 %;  $\text{Cl}^-$ , 0.01 %) was supplied from Merck and used without further activation. Rutile  $\text{TiO}_2$  powder was prepared by calcination of above mentioned  $\text{TiO}_2$  at 1200 °C for 10 h in an electric furnace. This treatment led to the crystal transition to rutile which was confirmed by X-ray diffraction analysis (see Chapter 6). Platinum (Pt black or Pt powder, 5 wt%) or ruthenium oxide ( $\text{RuO}_2$ , 10 wt%) was mixed with  $\text{TiO}_2$  powder in an agate mortar<sup>1</sup> to prepare catalyst. Water was passed through an ion-exchange resin and distilled immediately before use. Acetone and aliphatic alcohols (2-methyl-2-propanol, methanol, ethylene glycol, ethanol, and 2-propanol) were obtained commercially and used without further purification.

Photoirradiation. The powdered catalyst (50 mg) was suspended in aqueous solution ( $5.0 \text{ cm}^3$ ) of substrate (0.5 mmol) under neutral or

alkaline ( $6 \text{ mol dm}^{-3}$  NaOH) conditions in a glass tube ( $15 \text{ mm}\phi \times 180 \text{ mm}$ , transparent for the light of wavelengths  $> 300 \text{ nm}$ ). The magnetically stirred solution under Ar was irradiated at  $> 300 \text{ nm}$  using a merry-go-round apparatus equipped with a 400-W high-pressure mercury arc (Eiko-sha 400).

Monochromatic Photoirradiation. In an experiment of quantum yield measurement, the platinized  $\text{TiO}_2$  powder 30 mg and  $6 \text{ mol dm}^{-3}$  NaOH aqueous solution  $4.0 \text{ cm}^3$  were placed in a rectangular quartz cell ( $1.0 \text{ cm}$  path) with an upper part of pyrex tube ( $10 \text{ mm}\phi$ , ca.  $15 \text{ cm}$ ) and purged of air by Ar stream. The above prepared suspension was photoirradiated by Philips SP 500 ultra high-pressure mercury arc (operated at 750 W) through a grating monochromator (Japan Spectroscopic Co., Ltd, CT 25N). Number of the photons incident upon the suspension through the monochromator and the quartz window were evaluated by ferric oxalate actinometry.<sup>2</sup>

Ultraviolet absorption spectrum of  $\text{TiO}_2$  suspension was recorded on Hitachi EPS-3T spectrophotometer equipped with a R-10A integrating sphere.

Product Analysis. After the irradiation, the gas phase of the sealed sample was analyzed by gas chromatography using Shimadzu GC 4A equipped with a TCD and a 60-80 mesh Molecular Sieve 5A column ( $3 \text{ mm}\phi \times 3 \text{ m}$ , at  $130 \text{ }^\circ\text{C}$  with Ar carrier). The suspension was centrifuged to filter off the catalyst and the solution was subjected to product analysis by gas chromatography (Shimadzu GC 6A with an FID and  $\text{N}_2$  carrier). The typical conditions were as follows; 20 % Polyethylene Glycol 20M on 60-80 mesh Celite 545 ( $3 \text{ mm}\phi \times 3 \text{ m}$ ) at  $70 \text{ }^\circ\text{C}$  for 2-propanol, acetone, 2-methyl-2-propanol, methanol, ethanol

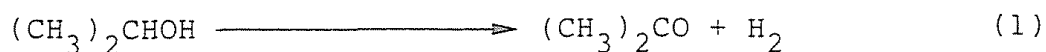
and acetaldehyde; Tenax GC (3 mmφ × 1 m) at 200 °C for the other products. Formaldehyde was determined quantitatively in the form of 1,4-dihydro-3,5-diacetyl-2,6-lutidine derived with 2,4-pentanedione and ammonium acetate<sup>3</sup> ( $\lambda_{\text{max}}$  in CHCl<sub>3</sub>, 396 nm).

## RESULTS AND DISCUSSION

### Photocatalytic Activity of Platinum and/or Ruthenium Oxide Loaded TiO<sub>2</sub> Powder for 2-Propanol Dehydrogenation.

Table 1 shows the hydrogen yield in the photocatalytic system including 2-propanol under deaerated conditions in the presence of platinum and/or ruthenium oxide loaded TiO<sub>2</sub> suspension. Though the activities of both anatase and rutile TiO<sub>2</sub> without loaded metal were negligible in neutral and basic solutions, small amount of metal deposit enhanced the activity of anatase TiO<sub>2</sub> to larger extent. Note that only 5 wt% of platinum black loading enhanced the activity approximately 100 fold both in the neutral and basic conditions. The other additives, Pt powder and RuO<sub>2</sub>, were also effective for the photocatalytic hydrogen formation, but the enhancement ratios were relatively small when compared with platinum black.

In these modified anatase TiO<sub>2</sub> systems acetone was also liberated in the aqueous solution. The acetone yield was almost identical to that of hydrogen and to the consumption of 2-propanol, showing that dehydrogenation of 2-propanol proceeds photocatalytically.<sup>4</sup>



The enhanced activity of the platinum-black-loaded TiO<sub>2</sub> is possibly



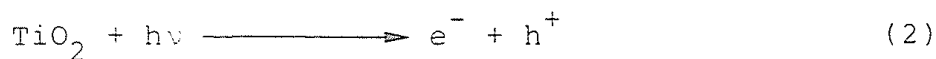
Table 1 Photoreaction of aqueous 2-propanol solutions catalyzed by  $\text{TiO}_2$  and Pt and/or  $\text{RuO}_2$  loaded  $\text{TiO}_2$ .<sup>a</sup>

Run	Catalyst	$\text{H}_2\text{O}$		6 M NaOH
		$\text{H}_2$	acetone	$\text{H}_2/\mu\text{mol}$
1	$\text{TiO}_2$	0.7	1.6	2.6
2	$\text{TiO}_2$ + Pt powder (5 %)	13	11	38
3	$\text{TiO}_2$ + Pt black (5 %)	93	79	200
4	$\text{TiO}_2$ + $\text{RuO}_2$ (10 %)	8.9	9.0	30
5	$\text{TiO}_2$ + Pt black (5 %) + $\text{RuO}_2$ (10 %)	130	132	210
6	$\text{TiO}_2^{\text{b}}$	0.1	0.6	1.3
7	$\text{TiO}_2^{\text{b}}$ + Pt black (5 %)	0.4	4.3	2.4

<sup>a</sup>Catalyst 50 mg, 6 mol  $\text{dm}^{-3}$  NaOH aqueous solution 5.0  $\text{cm}^3$ , and 2-propanol 38  $\text{mm}^3$  (500  $\mu\text{mol}$ ) were placed in a test tube and irradiated with 500-W high-pressure mercury arc under Ar at room temperature.

<sup>b</sup>Rutile crystal.

accounted for by the facilitated reduction of  $H^+$  on the metal surface to result in efficient charge separation of photogenerated electron ( $e^-$ ) - positive hole ( $h^+$ ) pairs,<sup>5</sup> as in the case of  $RuO_2$ .<sup>6</sup>

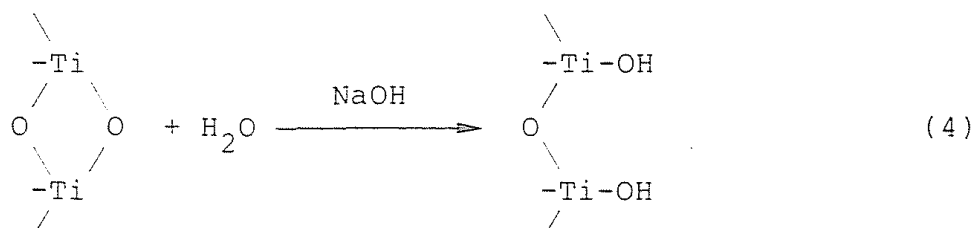


Smaller enhancement by platinum powder may be due to its small surface area and thereby poor contact with  $TiO_2$ , since the crystallite size of the platinum powder is in same order (> 200 nm) of the anatase  $TiO_2$  while that of platinum black is ca. 6 nm evaluated from X-ray diffraction patterns using Scherrer equation.<sup>7</sup>

On the other hand, the activity of rutile  $TiO_2$  was negligible even when loaded with platinum black. From the electrochemical studies of  $TiO_2$  electrodes little difference in the flat band potential between anatase and rutile  $TiO_2$  has been pointed out; the potential of anatase was evaluated to be approximately 0.2 V negative compared with that of rutile<sup>8</sup> (see also Scheme 2 in the general introduction). Since the potential lies close to the redox potential of  $H^+/H_2$  pair, the small activity of the rutile powder for the reaction including hydrogen formation is attributable to the disadvantage in the reduction step using photogenerated electron.

The effect of alkaline addition was evident in the present systems; 1.5-3 fold larger amount of hydrogen was obtained than that in the neutral solution (see Table 1). Kawai and Sakata pointed out the similar enhancement of  $TiO_2$  activity for the dehydrogenation of

alcohols under strongly alkaline ( $5 \text{ mol dm}^{-3} \text{ NaOH}$ ) conditions.<sup>1</sup> Although there has been no structural evidence at present, surface modification induced by the alkaline treatment possibly accounts for the enhancement, as schematically shown below.<sup>10</sup>



The surface hydroxyl is expected to be a hole trapping site, as discussed in the last section.

Wavelength Dependence of 2-Propanol Dehydrogenation by Suspended Platinized  $\text{TiO}_2$  Catalyst.

Figure 1 shows the dependence of quantum efficiency of the photocatalytic dehydrogenation of 2-propanol on the irradiation wavelength. The anatase  $\text{TiO}_2$  powder loaded with platinum black ( $\text{TiO}_2/\text{Pt}$ ) was used as photocatalyst and  $6 \text{ mol dm}^{-3}$  aqueous  $\text{NaOH}$  solution as solvent. The quantum efficiency was defined as the ratio of twice of hydrogen to the number of incident photons, according to reactions (2) and (3) in which two photons are required for the formation of one hydrogen molecule.<sup>11</sup> The efficiency over the wavelength range 260-380 nm was apparently constant (0.6-0.8 %) and decreased drastically at the wavelength ca. 380-400 nm. Photoirradiation of the light of wavelength above 400 nm could produce negligible amount of hydrogen. The thus obtained action spectrum of anatase  $\text{TiO}_2$  reasonably corresponds to the absorption spectrum as also shown in Figure 1. These facts indicate clearly that the 2-propanol dehydrogenation is initiated by photoexcitation

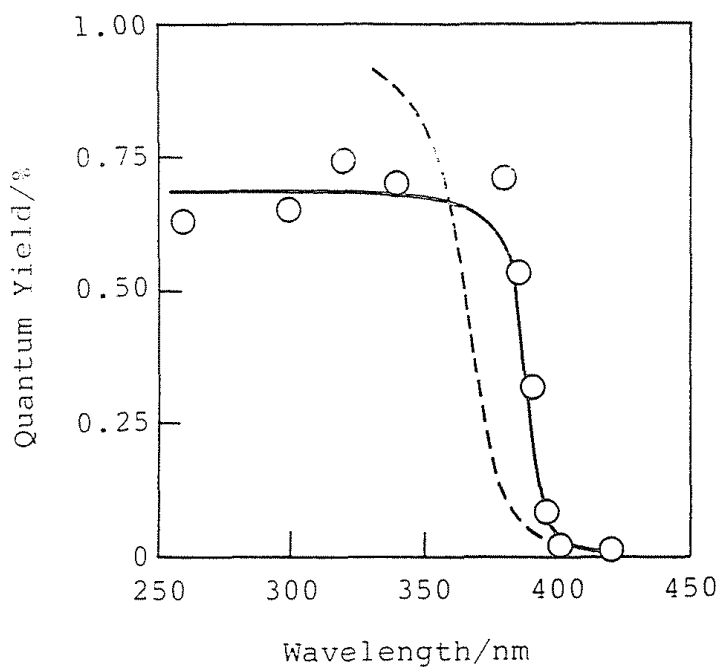


Figure 1 Variation in the quantum yield of photocatalytic dehydrogenation of 2-propanol in  $\text{TiO}_2/\text{Pt}$  suspension under Ar as a function of wavelength of monochromatic light. Broken line shows the absorption spectrum of aqueous anatase  $\text{TiO}_2$  suspension.

of electron of the filled valence band into vacant conduction band with the light of energy greater than the band gap (ca. 3.2 eV (corresponds to ca. 390 nm) for anatase  $\text{TiO}_2$ <sup>8</sup>) as described above (reaction 2).

Influence of the 2-Propanol Concentration. Figure 2(a) shows the initial rate of  $\text{H}_2$  formation ( $r(\text{H}_2)$ ) by the  $\text{TiO}_2/\text{Pt}$  photocatalyst as a function of the initial concentration of 2-propanol (C). A sharp increase of ( $r(\text{H}_2)$ ) with the increasing concentration C was observed in a lower region of C ( $< 100 \text{ mmol dm}^{-3}$ ). In the higher C region,  $r(\text{H}_2)$  was practically constant ( $\approx 3.5 \text{ } \mu\text{mol h}^{-1}$ ). Replots of the data in Figure 2(A) according to a Langmuir adsorption isotherm,  $1/r(\text{H}_2) = f(1/C^n)$  ( $n = 1$  or  $1/2$ ), are shown in Figure 2(b). Linear relation for  $n=1$  (molecular adsorption) was obtained, which is clearly better than that for  $n = 1/2$  (dissociative adsorption). Pichat and co-workers suggested the dissociative adsorption of methanol in the photocatalytic reaction by platinized  $\text{TiO}_2$ .<sup>1b</sup> In the present system, however, the molecular adsorption of 2-propanol is more probable. The amount of the adsorbed 2-propanol possibly dominated the over all reaction (equation 1), as discussed in the following section.

Photocatalytic Reaction of a Series of Aliphatic Alcohols by Platinized  $\text{TiO}_2$ . Table 2 shows the representative results of the photoreactions of a series of aliphatic alcohols and acetone in distilled water in the presence of  $\text{TiO}_2/\text{Pt}$ . These reactions could not be observed neither in the dark nor in the absence of  $\text{TiO}_2/\text{Pt}$ . Accordingly, all the products listed in Table 2 are attributable to the photocatalytic action of  $\text{TiO}_2/\text{Pt}$ .

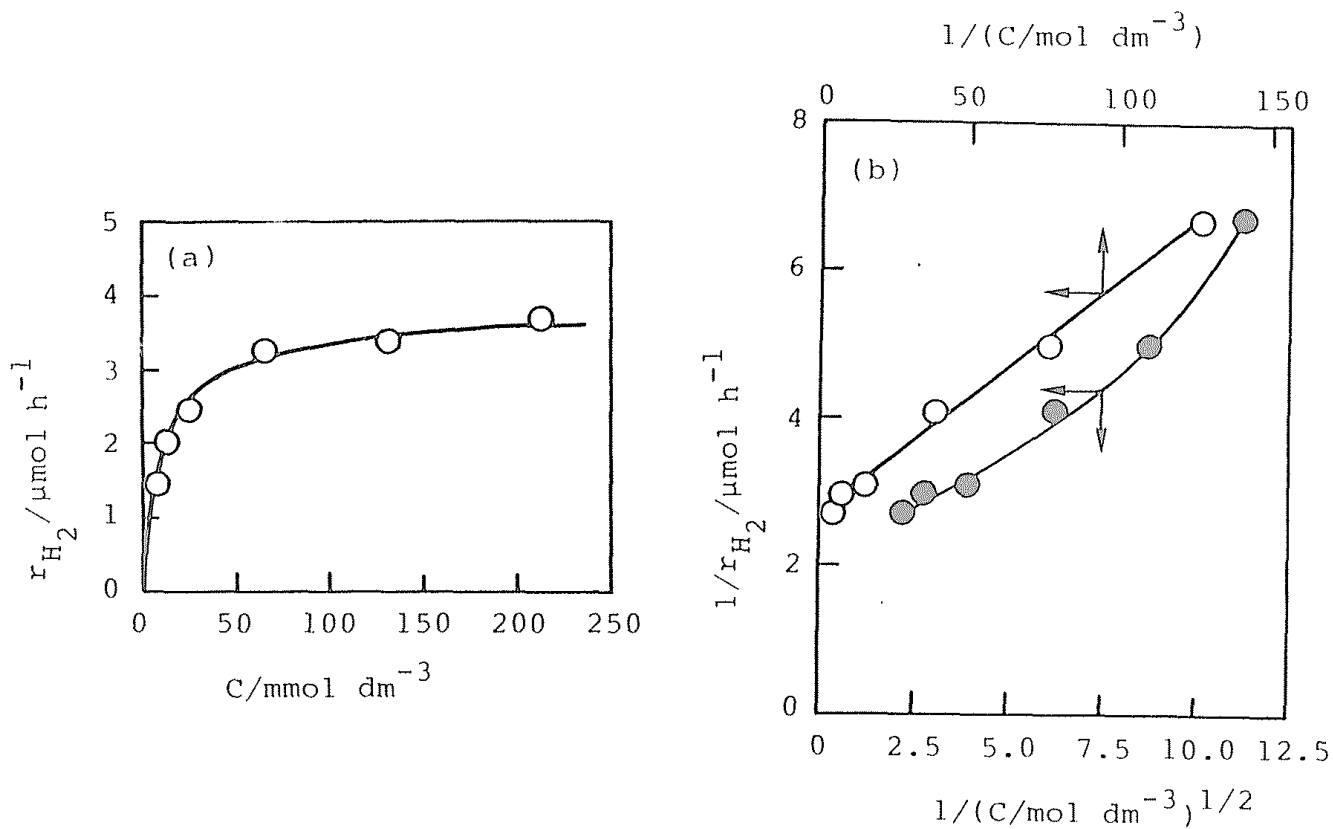


Figure 2 (a) Dependence of rate of H<sub>2</sub> formation ( $r_{H_2}$ ) on the concentration of 2-propanol ( $C$ ), and (b) linear transform  $(1/r_{H_2}) = f(1/C^n)$  for  $n = 1$  (O) and  $n = 1/2$  (●).

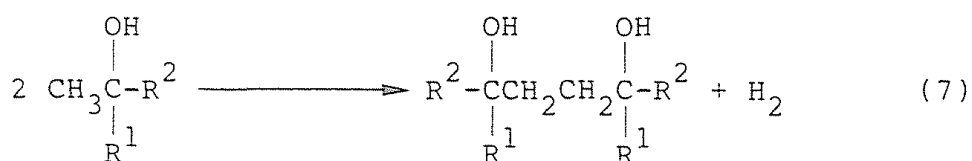
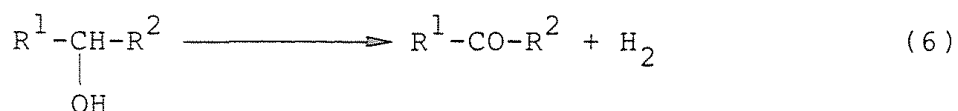
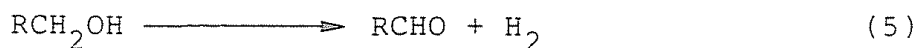
Table 2 Photocatalytic oxidation of alcohols and acetone by aqueous suspension of platinized TiO<sub>2</sub>.

Substrate	H <sub>2</sub> /μmol	Organic Product/μmol	
CH <sub>3</sub> COCH <sub>3</sub>	3.3	(CH <sub>3</sub> COCH <sub>2</sub> -) <sub>2</sub>	5.9
(CH <sub>3</sub> ) <sub>3</sub> COH	18	[(CH <sub>3</sub> ) <sub>2</sub> CH(OH)CH <sub>2</sub> -] <sub>2</sub>	18
		CH <sub>3</sub> COCH <sub>3</sub>	1.6
CH <sub>3</sub> OH	20	HCHO	14
CH <sub>2</sub> (OH)CH <sub>2</sub> OH	16	HOCH <sub>2</sub> CHO	14
		CH <sub>3</sub> CHO	5.3
CH <sub>3</sub> CH <sub>2</sub> OH	20	CH <sub>3</sub> CHO	17
(CH <sub>3</sub> ) <sub>2</sub> CHOH	54	CH <sub>3</sub> COCH <sub>3</sub>	46

Substrate (0.50 mmol) in water (5.0 cm<sup>3</sup>) was irradiated in the presence of platinized TiO<sub>2</sub> (50 mg) for 10 h under Ar at room temperature.

As Table 2 shows, mono-alcohols except for 2-methyl-2-propanol gave carbonyl derivatives identical to those obtained by Kawai and Sakata,<sup>12</sup> and by Pichat and co-workers.<sup>1b</sup> Similarly, ethylene glycol gave 2-hydroxyethanal. In the case of 2-methyl-2-propanol, a dimeric product 2,5-dimethyl-2,5-hexanediol as reported by Arimitsu and co-workers,<sup>13</sup> with small amounts of acetone and 2-methyl-1-butanol were obtained. Acetone, which is the product from 2-propanol and 2-methyl-2-propanol, was less reactive and gave only a small amount of dimeric product 2,5-hexanedione.

Hydrogen evolution was observed simultaneously in each photoreaction system. It is seen from Table 2 that the yield of hydrogen is virtually equal to that of the carbonyl and dimeric<sup>14</sup> products derived from alcohols. Thus, the formal scheme for the photocatalytic reaction of alcohols at the initial stage can be given by



Apparently, the reactivity in the above reaction varies in the order secondary > primary > tertiary alcohols (Table 2). This order agrees with that observed in the conventional oxidation of alcohols.



Figure 3 shows a plot of the initial rate of hydrogen evolution in each aqueous alcohol solution ( $0.1 \text{ mol dm}^{-3}$ ) against the rate constant of hydrogen abstraction by hydroxyl radical in aqueous solution.<sup>15</sup> Thus, the activities are correlated reasonably with the hydrogen abstraction rate constants, in both neutral and alkaline conditions. In the similar experiments using platinized  $\text{TiO}_2$  Kawai and co-workers pointed out that the ionization potential of organic substrates could partly interpret their reactivity in the photocatalytic reaction.<sup>16</sup>

A possible mechanism, rationalizing the above mentioned results, for the dehydrogenation of the alcohols are as follows. The enhanced ability, for  $\text{H}^+$  reduction to produce  $\text{H}_2$  (reaction 3), of platinized  $\text{TiO}_2$  possibly enable the sufficient consumption of excess excited electron, left in the  $\text{TiO}_2$  particle by the hole trapping by the alcohol or by hydroxyl group on the  $\text{TiO}_2$  surface, as reported by Dunn and co-workers using  $\text{TiO}_2$ -slurry electrode.<sup>17</sup> In such situation, the quantum efficiency could be expressed with the efficiency of the hole trapping ( $k_{\text{ox}}[\text{ROH}]$ ) and geminate electron-hole recombination ( $k_{\text{d}}$ ), since the oxidation step dominates the overall efficiency.

$$\phi = k_{\text{ox}}[\text{ROH}] / (k_{\text{d}} + k_{\text{ox}}[\text{ROH}]) \quad (8)$$

Under the conditions where  $\phi \ll 1$ , i.e.,  $k_{\text{d}} \gg k_{\text{ox}}[\text{ROH}]$  (see Figure 1),  $\phi$  is approximately in proportion to  $k_{\text{ox}}[\text{ROH}]$ .

$$\phi (\propto \text{rate of } \text{H}_2 \text{ formation}) \propto k_{\text{ox}}[\text{ROH}] \quad (9)$$

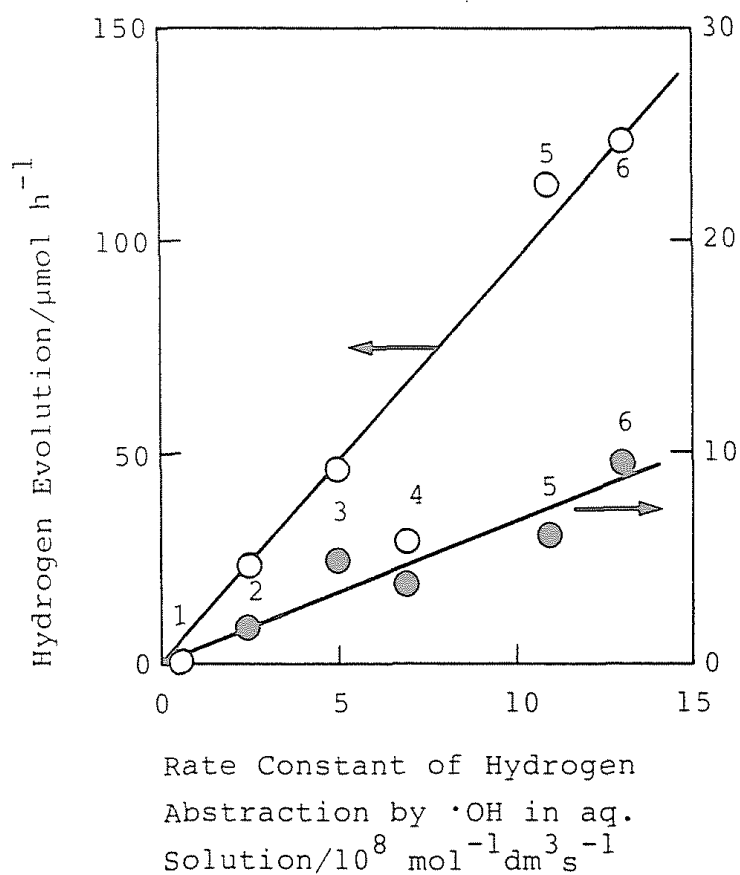
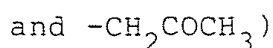
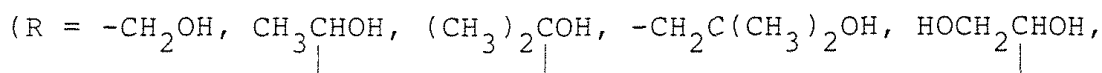
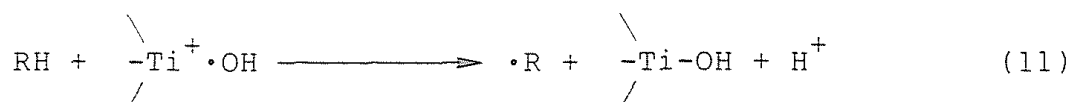
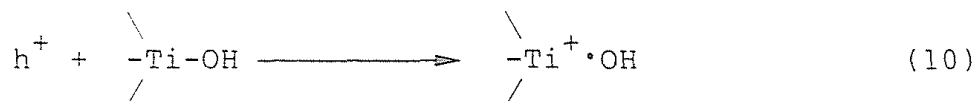
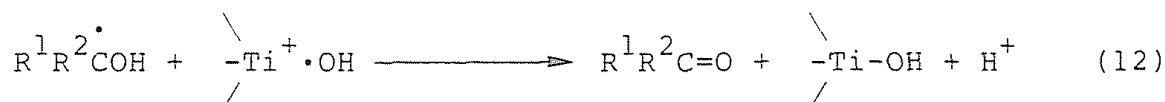


Figure 3 Hydrogen evolution rate<sup>a</sup> vs rate constant of hydrogen abstraction by hydroxyl radical in aqueous solution (reference 14).  
<sup>a</sup>500 mol of substrate and 50 mg of  $\text{TiO}_2/\text{Pt}$  (platinum black, 5 wt%) in  $5.0 \text{ cm}^3$  of water ( $\bullet$ ) and  $6 \text{ mol dm}^{-3}$  NaOH aqueous solution ( $\circ$ ) were irradiated for 2.5 h or 0.5 h, respectively.  
 1 : acetone, 2 : 2-methyl-2-propanol, 3 : methanol, 4 : ethylene glycol, 5 : ethanol, and 6 : 2-propanol

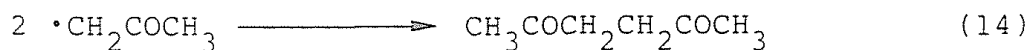
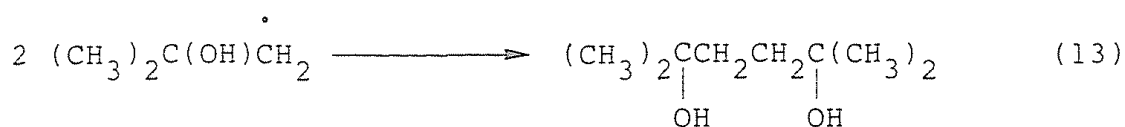
On the assumption that the effective concentration of each alcohol ([ROH]) is identical (i.e., the amount of alcohol adsorbed on the TiO<sub>2</sub> surface is almost saturated, see Figure 2),  $\phi$  is estimated with  $k_{ox}$ , coefficient of the hole trapping by alcohol. From the linear relations shown in Figure 3, it is suggested that the hole trapping proceeds via hydrogen abstraction from the alcohol molecule. On the basis of these results, mechanism of the photocatalytic oxidation, involving surface hydroxyl radical<sup>18</sup> intermediate, is schematically shown as follows (where  $\begin{array}{c} \diagdown \\ -Ti-OH \\ \diagup \end{array}$  represents the surface hydroxyl group).



In the case of the primary and secondary alcohols, the hydroxyalkyl radicals<sup>19</sup> undergo further oxidation to carbonyl derivatives.



On the other hand, the radical produced from 2-methyl-2-propanol and acetone mainly undergo recombination into dimeric derivatives.



In conclusion, these results demonstrate that platinized  $\text{TiO}_2$  enables that dehydrogenation of alcohols, the quantum efficiency of which depends on the efficiency of the oxidation by photogenerated  $h^+$ . The detailed investigation of the photocatalytic reaction of 2-methyl-2-propanol and poly(vinyl alcohol) are described in Chapters 2 and 3, respectively. Moreover, the photocatalytic oxidation of 2-propanol in the presence of silver salt, as an electron acceptor, is shown in Chapters 7 and 8.

## REFERENCES AND NOTES

- 1 (a) T. Kawai and T. Sakata, Chem. Lett., 81 (1981) (b) P. Pichat, J.-M. Herrmann, J. Disdier, H. Courbon, and M.-N. Mozzanega, Nouv. J. Chim., 5, 627 (1981) (c) M. R. St. John, A. J. Furgala, and A. F. Sommells, J. Phys. Chem., 87, 801 (1983).
- 2 C. A. Parker, Proc. Royal Soc. London, A220, 104 (1953).
- 3 Japan Industrial Standard K 0102 (1974).
- 4 (a) S. Teratani, J. Nakamichi, K. Taya, and K. Tanaka, Bull. Chem. Soc. Jpn, 55, 1688 (1982) (b) K. Domen, S. Naito, T. Ohnishi, and K. Tamaru, Chem. Lett., 555 (1982).
- 5 A. J. Bard, J. Phys. Chem., 86, 172 (1982).
- 6 Sakata and Kawai<sup>1,2</sup> previously suggested that RuO<sub>2</sub> catalyzed the oxidation with the photogenerated h<sup>+</sup>. However, recently they reported the results of electrochemical studies suggesting the catalytic function of RuO<sub>2</sub> for the H<sub>2</sub> formation; T. Sakata, K. Hashimoto, and T. Kawai, Annual Meeting of Electrochemical Society, Japan, E 209 (1983).
- 7 H. Klug, L. E. Alexander, "X-ray Diffraction Procedures", 2nd Ed. John Wiley and Sons, Inc., New York, N. Y. (1974) p. 618.
- 8 V. N. Pak and N. G. Ventov, Russ. J. Phys. Chem. (English Transl.), 49, 1489 (1975).
- 9 B. Kraeutler and A. J. Bard, J. Am. Chem. Soc., 100, 5985 (1978).
- 10 Increase in the specific surface area and the amount surface hydroxyl groups by the alkaline treatment has been reported; S. Okazaki and T. Kanto, Nippon Kagaku Kaishi, 404 (1976).

- 11 The efficiency is essentially defined with the number of photons absorbed by the catalyst. In the present system, the efficiency was evaluated by the use of the number of incident photons, instead of that of the absorbed photons, because of the difficulty in the measurement of exact number of the absorbed photons. The true efficiency should be somewhat larger than the apparent efficiency shown in Figure 1, since dispersion and/or reflection diminish the number of the absorbed photons.
- 12 T. Kawai and T. Sakata, J. Chem. Soc., Chem. Commun., 694 (1980).
- 13 S. Arimitsu, T. Imafuku, and I. Shiojima, Symposium on Photochemistry, Japan, IIIA-301 (1980).
- 14 Minor products, methane, ethane and 2-methyl-2-propanol were also observed in this system (detailed stoichiometry and mechanism are described in the following chapter (Chapter 2); S. Nishimoto, B. Ohtani, H. Shirai, and T. Kagiya, to be submitted in J. Am. Chem. Soc.). The amount of  $e^-$  and  $h^+$  consumed in this reaction is possibly estimated as sum of  $CH_4$  and twice of  $H_2$ . In this chapter, however, the  $H_2$  yield was used for convenience since the  $CH_4$  yield was negligible under these conditions.
- 15 M. Anbar and P. Neta, Int. J. Appl. Radiat. Isot., 18, 493 (1967).
- 16 T. Kawai, T. Sakata, K. Hashimoto, and M. Kawai, Nippon Kagaku Kaishi, 277 (1984).
- 17 (a) W. W. Dunn, Y. Aikawa, and A. J. Bard, J. Am. Chem. Soc., 103, 3456 (1981) (b) W. W. Dunn, Y. Aikawa, and A. J. Bard, J.

Electrochem. Soc., 128, 222 (1981) (c) C. Bahnemann, A. Henglein, J. Lilie, and L. Spanhal, J. Phys. Chem., 88, 709 (1984).

18 Hydroxyl radical formation in the water photolysis by platinized  $\text{TiO}_2$  has been suggested; C. D. Jaeger and A. J. Bard, J. Phys. Chem., 83, 3146 (1979).

19 Nakabayashi and Fujishima have reported that the formation of the hydroxyl and hydroxyalkyl radicals could be observed by ESR; Post Conference (Osaka University) of the 5th International Symposium on Photochemical Conversion and Storage of Solar Energy (Osaka, Japan (1984)).

## Chapter 2

### Photocatalytic Degradation and Dimerization of 2-Methyl-2-propanol by Aqueous Suspension of Platinized TiO<sub>2</sub>

#### ABSTRACT

Photoirradiation ( $\lambda_{\text{ex}} > 300$  nm) on Ar-purged aqueous suspension of platinized TiO<sub>2</sub> containing 2-methyl-2-propanol at room temperature led to the formations of hydrogen, methane, and ethane in the gas phase of the reaction mixture. Simultaneous formations of acetone, 2-methyl-2-butanol (t-AmOH), and 2,5-dimethyl-2,5-hexanediol (2,5-DH) were observed in the liquid phase of the reaction mixture. The product distributions were reasonably interpreted by the mechanism involving intermediate, 2-hydroxy-2-methylpropyl radical, to undergo recombination into 2,5-DH and/or  $\beta$ -cleavage into acetone and methyl radical, which is the precursor of methane and ethane. Acetone formation predominated in the product distributions under aerated conditions or in the presence of silver salt, suggesting another reaction pathway of oxidative trapping of the intermediate radicals.



## INTRODUCTION

Among semiconductor materials n-type titanium dioxide ( $\text{TiO}_2$ ) has been used as a stable photocatalyst suspended in an aqueous solution. The sufficient ability of the photoirradiated  $\text{TiO}_2$  to oxidize and to reduce organic or inorganic substrates is responsible to the formation of the electron and positive hole upon irradiation of near ultraviolet light.<sup>1,2</sup> One of the efforts toward the efficient charge separation is modification of the  $\text{TiO}_2$  surface by partial coverage with metal and/or metal oxide, such as platinum or ruthenium dioxide, according to the idea of coupling semiconductor anode and metal cathode used separately in the photoelectrochemical cell.<sup>3</sup> In the modified, in most of studies platinized,  $\text{TiO}_2$  particles the photoexcited electrons effectively reduce proton into hydrogen on the metal surface<sup>4</sup> to result in the enhancement of total photocatalytic activity. Organic compounds, such as methanol,<sup>5a</sup> ethanol,<sup>5b</sup> or sugar,<sup>6</sup> undergo photocatalytic oxidation by the platinized  $\text{TiO}_2$  suspension, along with the simultaneous hydrogen liberation.<sup>7</sup>

In Chapter 1 of this thesis, photocatalytic reaction of aliphatic alcohols in aqueous suspension of platinized  $\text{TiO}_2$  under deaerated conditions has been demonstrated. 2-Methyl-2-propanol gave dimeric product along with the formation of acetone (see Table 2 in Chapter 1) while the other primary or secondary alcohols gave corresponding carbonyl derivatives. In the present study, detailed investigation on the photocatalytic reaction of 2-methyl-2-propanol under deaerated or aerated conditions is reported. The product distributions are discussed in comparison with the other oxidation

process using ionizing radiation or Fenton's reagent. Particular emphasis is placed on the characteristic reactivity of intermediate radical formed by the oxidation of the alcohol with photogenerated positive hole.

## EXPERIMENTAL

Materials. Titanium dioxide powder (anatase > 99 %,  $\text{TiO}_2(\text{A})$ ) was obtained from Merck and used without further activation. Rutile  $\text{TiO}_2$  powder ( $\text{TiO}_2(\text{R})$ ) was prepared by calcination of above mentioned  $\text{TiO}_2$  at 1150 °C for 10 h in an electric furnace. This treatment made almost all crystals into rutile, which was determined by X-ray diffraction analysis. The detailed results were reported elsewhere.<sup>8</sup> Platinized  $\text{TiO}_2$  catalyst was prepared by powdering a mixture of the anatase or rutile  $\text{TiO}_2$  with 5 wt% platinum black (Nakai Chemicals). Palladium (Pd) and ruthenium dioxide ( $\text{RuO}_2$ ) loading were performed in the similar way. Water was passed through an ion exchange resin and distilled immediately before use. The other chemicals including 2-methyl-2-propanol (t-BuOH) were obtained commercially and used as received.

Apparatus. A 400-W high-pressure mercury arc (Eiko-sha 400) equipped with a merry-go-round apparatus was used as the light source.

Gaseous products under irradiation ( $\lambda_{\text{ex}} > 300 \text{ nm}$ ) were measured by gas chromatography, using Shimadzu GC 4A (for  $\text{H}_2$  and  $\text{O}_2$ , equipped with a TCD, column 60-80 mesh Molecular Sieve 5A (3 mm $\phi$  × 3 m), Ar carrier at 130 °C) and GC 6A (for  $\text{CH}_4$  and  $\text{C}_2\text{H}_6$ , equipped with an FID, column 50-80 mesh Porapak R (3 mm $\phi$  × 2 m),  $\text{N}_2$  carrier at 90 °C). Quantitative analyses of the organic products in the reaction

mixture were carried out using Shimadzu GC 6A (for acetone, t-BuOH, and 2-methyl-2-butanol, equipped with an FID, column 20 % Poly(ethylene glycol) 20 M on 60-80 mesh Celite 545 (3 mm $\phi$   $\times$  2 m), N<sub>2</sub> carrier at 90 °C) and GC 7A (for 2,5-dimethyl-2,5-hexanediol, equipped with an FID, column 60-80 mesh Tenax GC (3 mm $\phi$   $\times$  1 m), N<sub>2</sub> carrier at 200 °C). Atomic absorption spectroscopic measurement of Ag<sup>+</sup> ion was carried out on Jarrel-Ash AA 8200 spectrometer.

Procedure. The powdered catalyst (TiO<sub>2</sub>/Pt, typically 50 mg) and solvent (distilled water, aqueous NaOH (1 mol dm<sup>-3</sup>) solution, or aqueous Ag<sub>2</sub>SO<sub>4</sub> (0.025 mol dm<sup>-3</sup>) solution; 5.0 cm<sup>3</sup>) was placed in a glass tube (18 mm $\phi$   $\times$  180 mm, transparent for the light of wavelength  $>$  300 nm), purged for 30 min with Ar, and then sealed off with a rubber stopper. An aerated suspension was prepared in the similar way using O<sub>2</sub> stream. The substrate t-BuOH was injected just before irradiation through the stopper by micro syringe. The thus prepared suspension was stirred magnetically throughout the irradiation.

After the irradiation at room temperature, the gaseous products under irradiation were first determined. The suspension was centrifuged to separate the catalyst and the aqueous solution was subjected to the gas chromatographic measurements.

In the experiment using silver salt, the separated TiO<sub>2</sub> powder was washed repeatedly with distilled water, dried overnight at 70 °C and treated with HNO<sub>3</sub> (ca. 13 mol dm<sup>-3</sup>) to dissolve photodeposited silver metal. The resulting suspension of bleached TiO<sub>2</sub> was diluted with distilled water and centrifuged to measure Ag<sup>+</sup> concentration by atomic absorption spectroscopy.

Ionizing radiation on the aqueous t-BuOH solution was carried

out in the sealed glass tubes at room temperature with a  $^{60}\text{Co}$   $\gamma$ -ray source at a dose rate of  $380 \text{ Gy h}^{-1}$ . Oxidation of t-BuOH with Fenton's reagent was performed using aqueous  $\text{FeSO}_4$  and  $\text{H}_2\text{O}_2$  solutions.

## RESULTS AND DISCUSSION

### Photoreaction of t-BuOH in Aqueous Solution by Platinized $\text{TiO}_2$ Catalyst.

Irradiation on  $\text{TiO}_2/\text{Pt}$  powders suspended in an Ar-purged aqueous t-BuOH solution led to  $\text{H}_2$ ,  $\text{CH}_4$ , and  $\text{C}_2\text{H}_6$  formations in the gas phase of the reaction mixture. Simultaneous formations of 2,5-dimethyl-2,5-hexanediol (2,5-DH), acetone, and 2-methyl-2-propanol (t-AmOH) were observed in the liquid phase, as Table 1 shows.<sup>9</sup> In this case apparent optimum yield was obtained under the alkaline conditions; the  $\text{TiO}_2/\text{Pt}$  activity was 2-60 fold enhanced in the NaOH solution compared with that in the neutral or acidic solutions. Similar products were obtained upon irradiation of  $\text{TiO}_2$ , without Pt, suspension, but the product yields were negligible.

Figure 1 shows the time-course of the so obtained reaction products in the alkaline solution under deaerated conditions. Each product and the starting material, t-BuOH, increased and decreased, respectively, linearly with the irradiation time up to 6 h. Further irradiation was not so effective for the photocatalytic reaction. One of the most probable reason for such deactivation of the  $\text{TiO}_2/\text{Pt}$  catalyst is detachment of Pt particle from the  $\text{TiO}_2$  surface by the magnetic stirring. Actually, Pt aggregation was observed after lengthened irradiation. These facts suggested the importance of contact between the Pt particle and the  $\text{TiO}_2$  surface.

Figure 2 is replot of data shown in Figure 1, indicating the

Table 1 Product distribution in the decomposition of aqueous 2-methyl-2-propanol solutions.

Run	Cat. <sup>c</sup>	Condition	Product/ $\mu\text{mol}$						
			H <sub>2</sub>	CH <sub>4</sub>	C <sub>2</sub> H <sub>6</sub>	Me <sub>2</sub> CO	t-AmOH	2,5-DH	
1	T(A)	NaOH	Ar <sup>a</sup>	0.1	0.4	$\approx 0$	0.6	$\approx 0$	0.2
2	T/Pt	H <sub>2</sub> O	Ar <sup>b</sup>	2.5	0.2	$\approx 0$	1.0	0.2	6.1
3	T/Pt	NaOH	Ar <sup>b</sup>	35.3	12.1	1.3	15.1	7.4	15.9
4	T/Pt	H <sub>2</sub> SO <sub>4</sub>	Ar <sup>b</sup>	0.2	0.2	$\approx 0$	1.3	$\approx 0$	0.8
5	T/Pt	H <sub>2</sub> O	O <sub>2</sub> <sup>b</sup>	$\approx 0$	0.3	$\approx 0$	28.2	0.2	5.8
6	T/Pt	NaOH	O <sub>2</sub> <sup>b</sup>	17.6	6.8	0.7	28.8	5.3	9.9
7	T/Pt	H <sub>2</sub> SO <sub>4</sub>	O <sub>2</sub> <sup>b</sup>	$\approx 0$	0.9	$\approx 0$	39.6	$\approx 0$	1.4
8	T/Pd	H <sub>2</sub> O	Ar <sup>a</sup>	3.6	0.4	$\approx 0$	1.3	0.3	7.5
9	T/Pd	NaOH	Ar <sup>a</sup>	16.4	10.1	0.6	14.3	5.4	14.5
10	T/RO	H <sub>2</sub> O	Ar <sup>a</sup>	0.2	$\approx 0$	$\approx 0$	0.2	$\approx 0$	1.3
11	T/RO	NaOH	Ar <sup>a</sup>	1.2	0.6	$\approx 0$	1.1	0.2	0.9
12 <sup>f</sup>	T/Pt	Ag <sub>2</sub> SO <sub>4</sub>	Ar <sup>a</sup>	$\approx 0$	1.5	2.1	41.3	0.1	$\approx 0$
13 <sup>f</sup>	T(A)	Ag <sub>2</sub> SO <sub>4</sub>	Ar <sup>a</sup>	$\approx 0$	1.5	3.0	35.5	0.1	$\approx 0$
14 <sup>f</sup>	T(R)	Ag <sub>2</sub> SO <sub>4</sub>	Ar <sup>a</sup>	$\approx 0$	$\approx 0$	$\approx 0$	9.1	$\approx 0$	$\approx 0$
15 <sup>g</sup>	—	H <sub>2</sub> O	N <sub>2</sub> O <sup>d</sup>	1.7	0.2	$\approx 0$	2.2	0.4	4.9
16 <sup>g</sup>	—	NaOH	N <sub>2</sub> O <sup>d</sup>	1.9	0.7	0.2	4.4	2.0	3.8
17	—	FeSO <sub>4</sub>	Ar <sup>e</sup>	$\approx 0$	—	—	4.1	$\approx 0$	19.8

<sup>a</sup>5-h irradiation ( $\lambda_{\text{ex}} > 300$  nm). <sup>b</sup>10-h irradiation. <sup>c</sup>T(A) : anatase TiO<sub>2</sub>(Merck), T/Pt : anatase TiO<sub>2</sub> + 5 wt% platinum black, T/Pd : anatase TiO<sub>2</sub> + 5 wt% palladium black, T/RO : anatase TiO<sub>2</sub> + 10 wt% ruthenium dioxide, and T(R) : rutile TiO<sub>2</sub>. <sup>d</sup>Co<sup>60</sup>  $\gamma$ -ray radiation (728 Krad). <sup>e</sup>Fenton's reagent containing H<sub>2</sub>O<sub>2</sub> 180  $\mu\text{mol}$ . <sup>f</sup>Ag-metal deposition was also observed; 12 : 212.5, 13 : 169.8, and 14 : 121.2  $\mu\text{mol}$ . <sup>g</sup>N<sub>2</sub> was also determined; 15 : 13.7, and 16 : 15.8  $\mu\text{mol}$ .

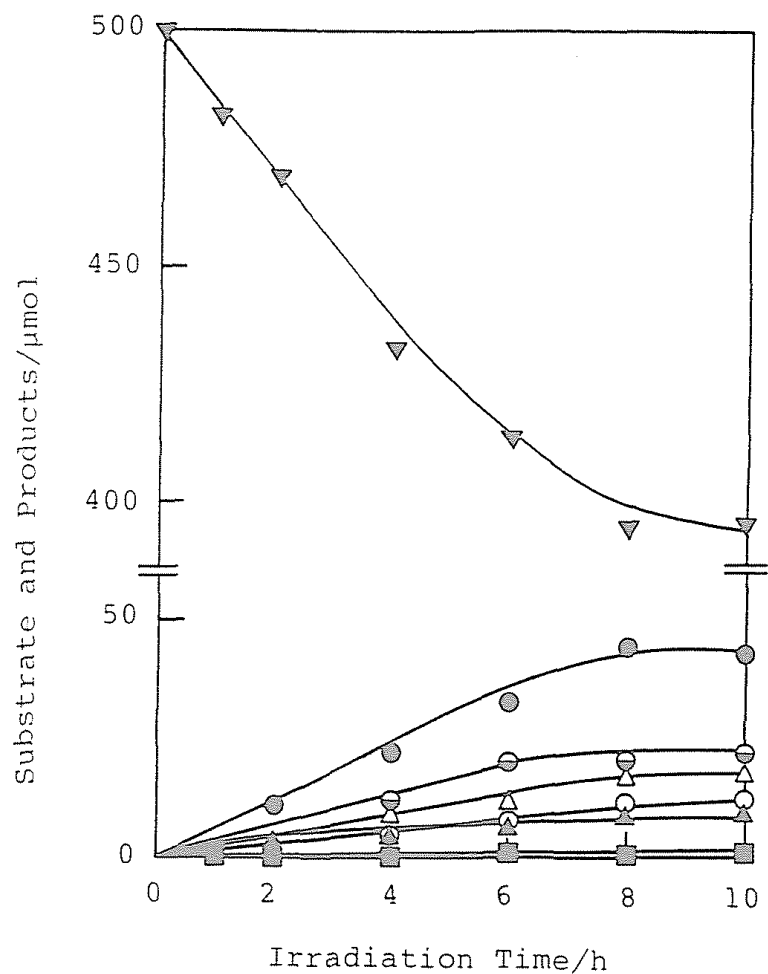
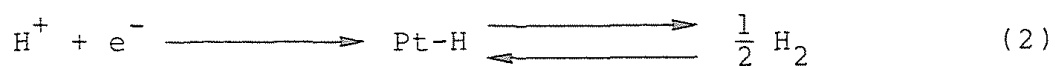
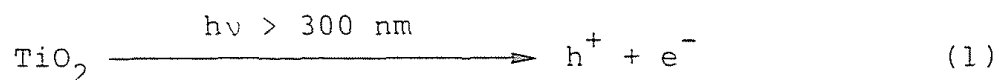


Figure 1 Time-course of the photocatalytic reaction of t-BuOH in 1 mol dm<sup>-3</sup> NaOH. ( ▽ : t-BuOH, ● : H<sub>2</sub>, ⊖ : 2,5-DH, △ : acetone, ○ : CH<sub>4</sub>, ▲ : t-AmOH, and ■ : C<sub>2</sub>H<sub>6</sub> )

t-BuOH (0.500 mmol), 1 mol dm<sup>-3</sup> NaOH (5.0 cm<sup>3</sup>), and TiO<sub>2</sub>/Pt (50 mg) were placed in a test tube and irradiated under Ar.

reasonably satisfied material balance concerning carbon atom; more than 70 % of consumed t-BuOH was recovered in the form of acetone, 2,5-DH, and t-AmOH. Among these products, the 2,5-DH and t-AmOH liberations require the formation of C-C bond while that of acetone is accounted for by the scission of C-C bond of t-BuOH.

On the basis of these results, a possible mechanism of the above mentioned photoinduced reaction is outlined as follows (see also Chapter 1). The photoreaction is initiated by the TiO<sub>2</sub>-photoabsorption to generate the electron (e<sup>-</sup>) and the positive hole (h<sup>+</sup>), which is confirmed by the results that the t-BuOH decomposition could be observed neither in the dark nor in the absence of TiO<sub>2</sub>. Loaded Pt particle could catalyze reduction of H<sup>+</sup> into H by the photogenerated electron to result in the efficient promotion of the charge separation.<sup>10</sup>



Concomitantly generated positive hole is used in the oxidation of t-BuOH to produce intermediate species, 2-hydroxy-2-methylpropyl radical. Although an alkoxy radical, 2-methyl-2-propoxy radical, is also expected to liberate by one-electron oxidation process, the reaction products (2,5-DH and t-AmOH) suggests the predominant formation of the hydroxyalkyl radical, presumably via hydrogen abstraction by surface hydroxyl radical.

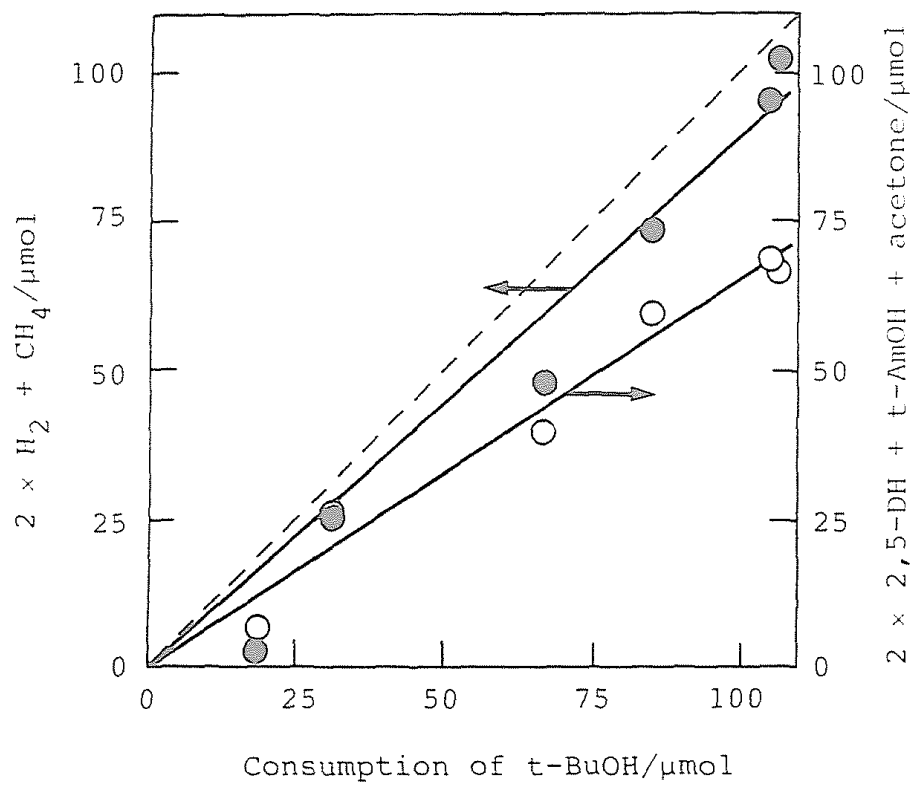
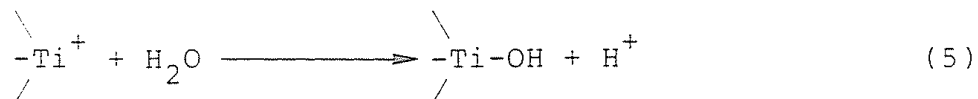
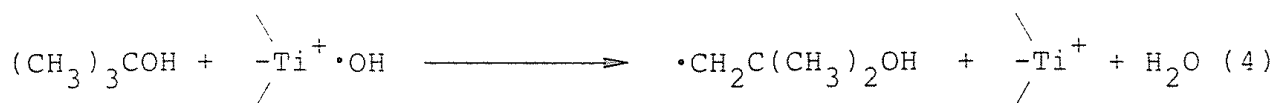
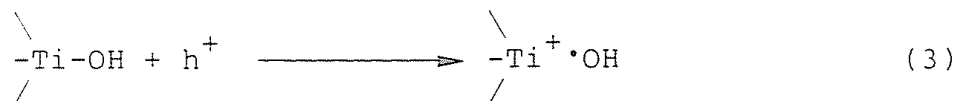
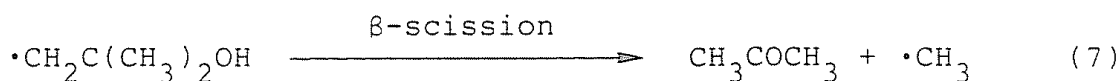
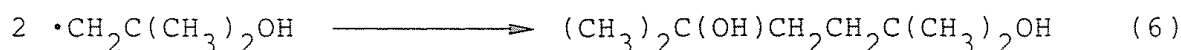


Figure 2 Material balance in the photocatalytic reaction of t-BuOH by TiO<sub>2</sub>/Pt.

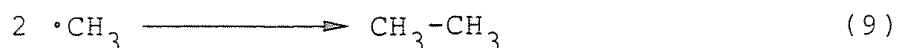




In this system, the intermediate radical gives 2,5-DH by the recombination and acetone by the  $\beta$ -cleavage with simultaneous formation of methyl radical.



The formation of t-AmOH, possessing the extended backbone, is attributable to the recombination of the hydroxyalkyl radical and the thus formed methyl radical. The other fate of methyl radical involves both self-recombination into ethane and recombination with H on the Pt surface into methane.



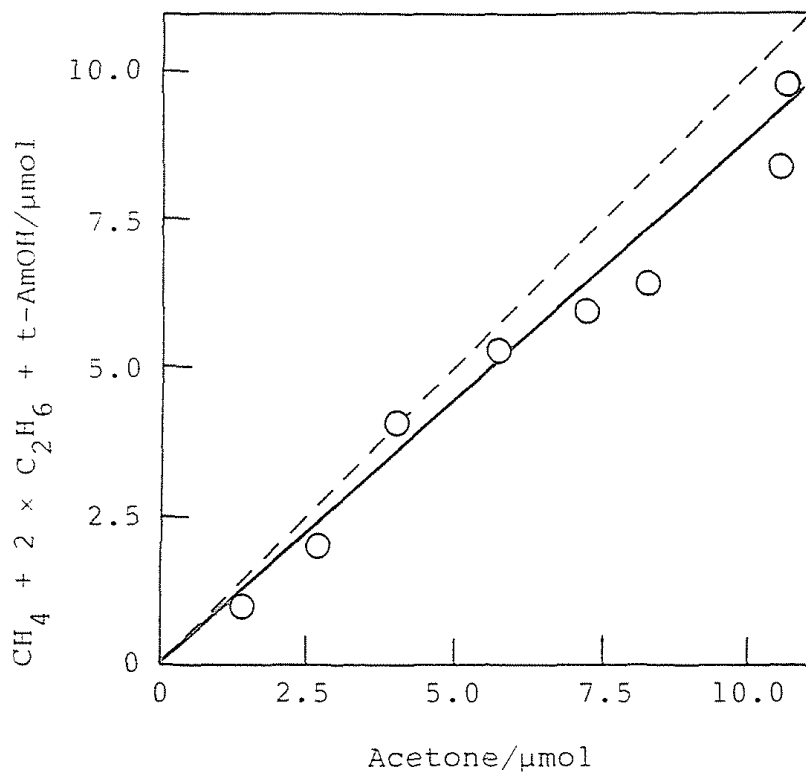


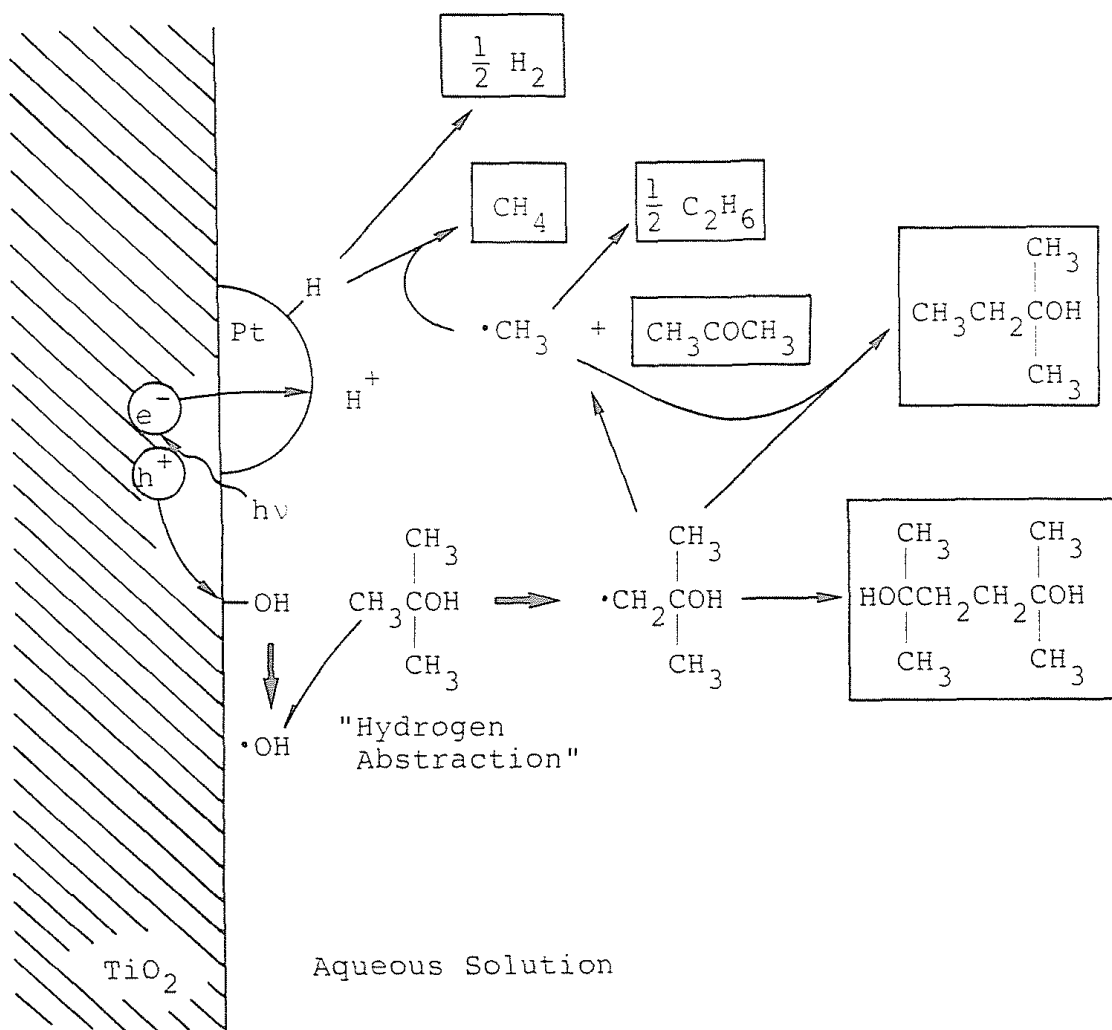
Figure 3 Material balance in the  $\beta$ -cleavage of  $\cdot\text{CH}_2\text{C}(\text{CH}_3)_2\text{OH}$  formed in the photocatalytic decomposition of t-BuOH by  $\text{TiO}_2/\text{Pt}$ .

t-BuOH (106  $\mu\text{mol}$ ), 1 mol  $\text{dm}^{-3}$  NaOH (5.0  $\text{cm}^3$ ), and  $\text{TiO}_2/\text{Pt}$  (50 mg) were placed in a test tube and irradiated with a 400-W high pressure mercury arc under Ar.

The above proposed mechanism requires the coincidence in the amounts of the consumed electron and positive hole as is shown in Figure 2. Because the amount of the consumed positive hole must be same as that of consumed t-BuOH (equation 3), a good linear relation, in Figure 2, between the amounts of oxidation (consumed t-BuOH) and reduction (sum of methane and twice of hydrogen) confirms the mechanism. Another requirement in the mechanism is the material balance in the  $\beta$ -cleavage of the hydroxyalkyl radical; equimolar amount of acetone and methyl radical should be observed in the photoreaction products. Figure 3 shows the reasonable agreement between the amount of acetone and that of methyl radical originated products, methane, ethane, and t-AmOH.

On the basis of these results, schematic diagram of the photocatalytic reaction is shown in Scheme 1. The platinum deposit catalyzes not only  $H_2$  formation but also reduction of methyl radical to methane. Bard and co-workers have reported "photo Kolbe" reaction of organic acids and suggested the similar mechanism of the methane formation on the Pt site.<sup>11,12</sup> Thus, one of the most characteristic function of the platinized  $TiO_2$  photocatalyst is due to the close existence of the oxidation and reduction sites, in contrast to conventional electrolysis systems. The function is also demonstrated in the photocatalytic reaction of aliphatic amines (see Chapter 5).

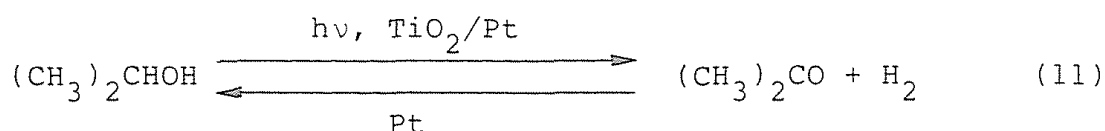
Effect of Pt Loading on the Product Distribution. Figures 4 and 5 show the product yields in gas and solution phases, respectively, as a function of the amount of Pt loading. The gaseous products  $H_2$  and methane increased with the increasing Pt amount up to 15-20 wt%,



Scheme 1 Photocatalytic reaction of t-BuOH by platinized TiO<sub>2</sub> particle; platinum catalyzes reduction, by photoexcited electron, of not only H<sup>+</sup> but also methyl radical.

while the ethane yield was relatively small and not so influenced by the Pt amount. According to the proposed mechanism, the increased yields of reduction products  $H_2$  and  $CH_4$  are accounted for by the enhancement of reducing activity of  $TiO_2/Pt$  catalyst along with the Pt increase. Similar behavior of the increasing yield was observed for the products in the aqueous solution; both 2,5-DH and acetone yields increased similarly up to 10-15 wt%. On the other hand in the case of t-AmOH almost constant yield was observed in the Pt amount range above 5 wt%. Although the dependence of the secondary products (such as  $CH_4$  or t-AmOH, see Scheme 1) was rather complicated, the amount of decomposed t-BuOH is not so affected by the Pt loading over 15 wt%.

The Pt deposit also catalyzes the thermal hydrogenation in the presence of  $H_2$ ; acetone which is liberated by the photocatalyzed reaction of 2-propanol is easily reduced back to 2-propanol.



Increase in the Pt amount facilitates not only the photocatalytic dehydrogenation but also the thermal hydrogenation. Therefore, the overall reaction yield was increased with the Pt increase but not so affected in the Pt amount region over ca. 5 wt%, as shown in Figure 8 of Chapter 9. On the contrary, the present system of t-BuOH is irreversible; the products can not give starting material t-BuOH by thermal hydrogenation. Accordingly, it is reasonable that the overall conversion increased with the increase of Pt up to ca. 15 wt%, which is larger than that observed in the reversible 2-propanol

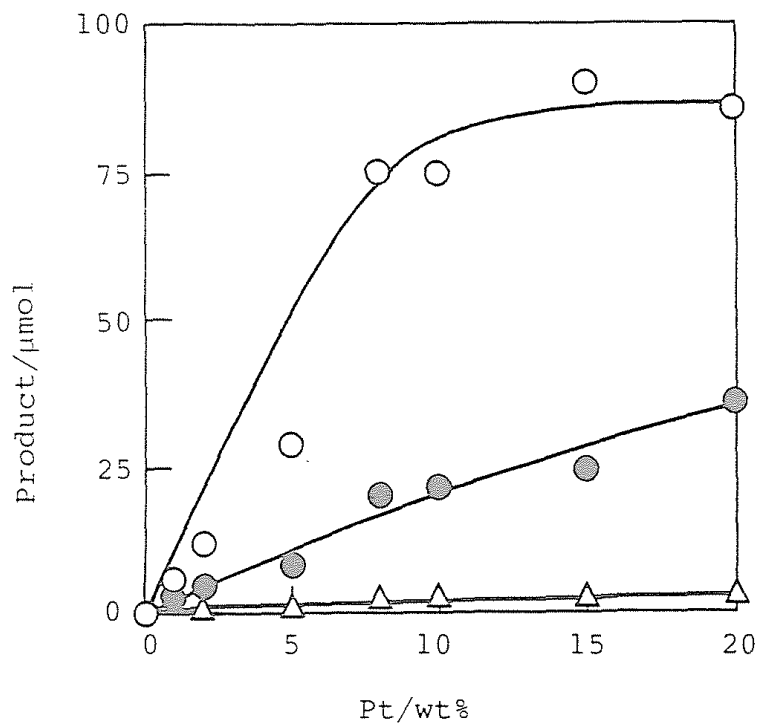


Figure 4 Influence of the amount of Pt loading on the yields of gaseous products obtained by TiO<sub>2</sub>/Pt catalyst; t-BuOH (500 μmol), 1 mol dm<sup>-3</sup> NaOH (5.0 cm<sup>3</sup>), and TiO<sub>2</sub>/Pt (TiO<sub>2</sub> 50 mg) were placed in a test tube and irradiated under Ar for 10 h.

○ : H<sub>2</sub>, ● : CH<sub>4</sub>, △ : C<sub>2</sub>H<sub>6</sub>.

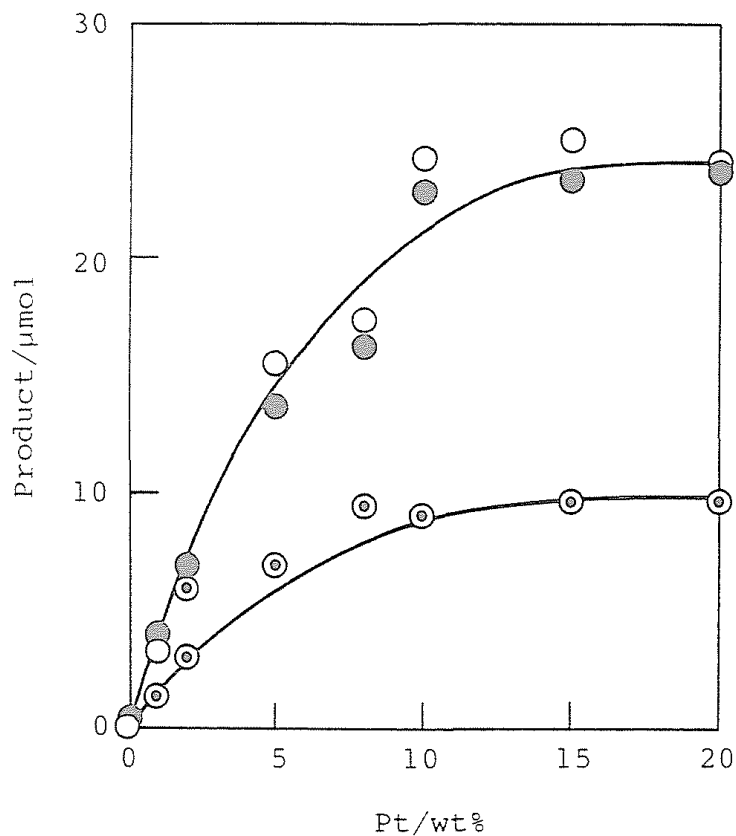


Figure 5 Influence of the amount of Pt loading on the yields of products in the aqueous solution obtained by  $\text{TiO}_2/\text{Pt}$  catalyst; *t*-BuOH (500  $\mu\text{mol}$ ),  $1 \text{ mol dm}^{-3}$  NaOH (5.0  $\text{cm}^3$ ), and  $\text{TiO}_2/\text{Pt}$  ( $\text{TiO}_2$  50 mg) were placed in a test tube and irradiated under Ar for 10 h.

○ : 2,5-DH, ● : acetone, and ⊙ : *t*-AmOH.

system.

Effect of t-BuOH Concentration. Figure 6 illustrates the influence of concentration of t-BuOH on the yield of products in the photocatalytic reaction. The amount of each product increased gradually along with the concentration, and was saturated over the concentration region of 200-600 mmol dm<sup>-3</sup>.

As demonstrated in Chapter 1, the overall efficiency of the photocatalytic reaction predominantly depends on the oxidation step under these condition. Assuming a Langmuir adsorption of t-BuOH on the TiO<sub>2</sub> surface, the photocatalytic reaction yield (Y) is represented using efficiency coefficient k as follows (see also Chapter 1, equation (9)).

$$Y = k a b [t\text{-BuOH}] / (1 + a[t\text{-BuOH}]) \quad (12)$$

where, [t-BuOH] is concentration of t-BuOH in the solution and a, b are constants. Figure 7 shows the linear relation between [t-BuOH]/Y and [t-BuOH], showing the reasonable fit of experimental data with equation (12). These results confirm the mechanism involving the adsorption of t-BuOH on the TiO<sub>2</sub> surface and the hole trapping, mentioned above.

The product distribution was also influenced by the t-BuOH concentration; acetone was predominantly liberated at the concentration region less than 20 mmol dm<sup>-3</sup>. These results suggest that the increase of t-BuOH concentration increases the steady state concentration of the hydroxyalkyl radical on the TiO<sub>2</sub> surface to result in the increase in possibility of bi-molecular recombination into



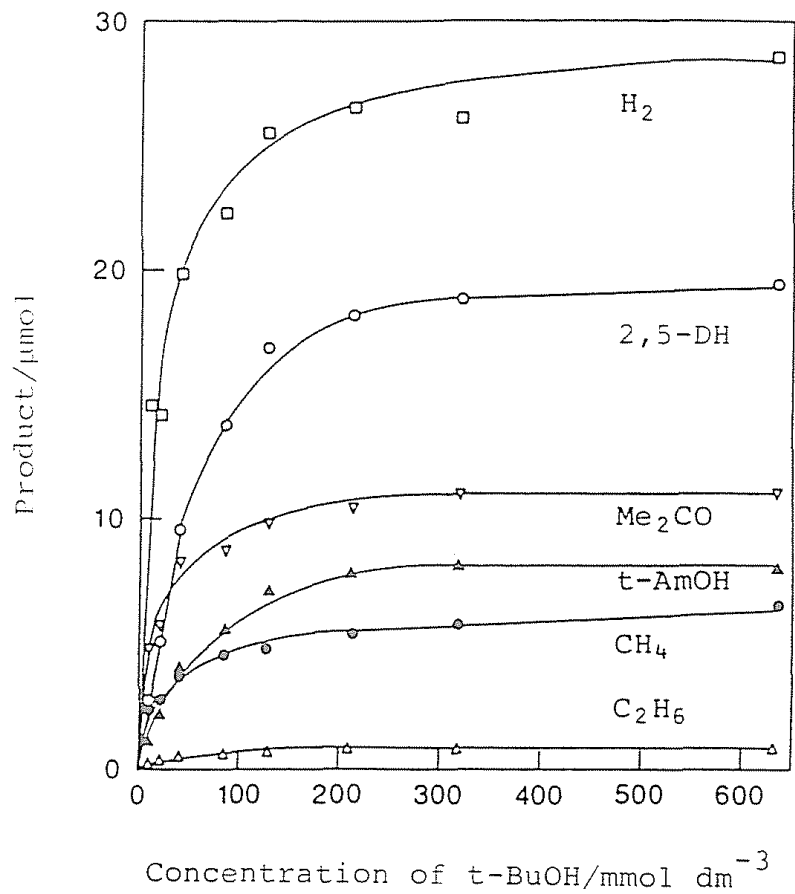


Figure 6 Influence of the concentration of t-BuOH on the yield of products in the photocatalytic reaction with TiO<sub>2</sub>/Pt.

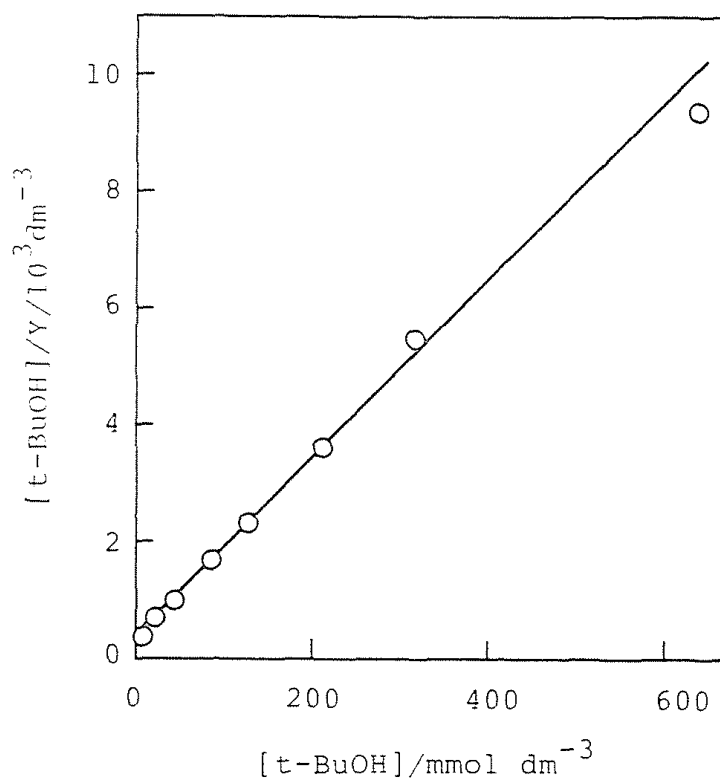
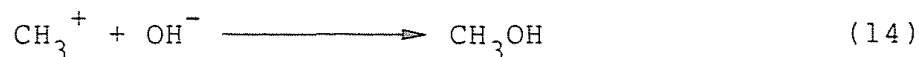


Figure 7 Linear relation between  $[t\text{-BuOH}]/Y$  and  $[t\text{-BuOH}]$

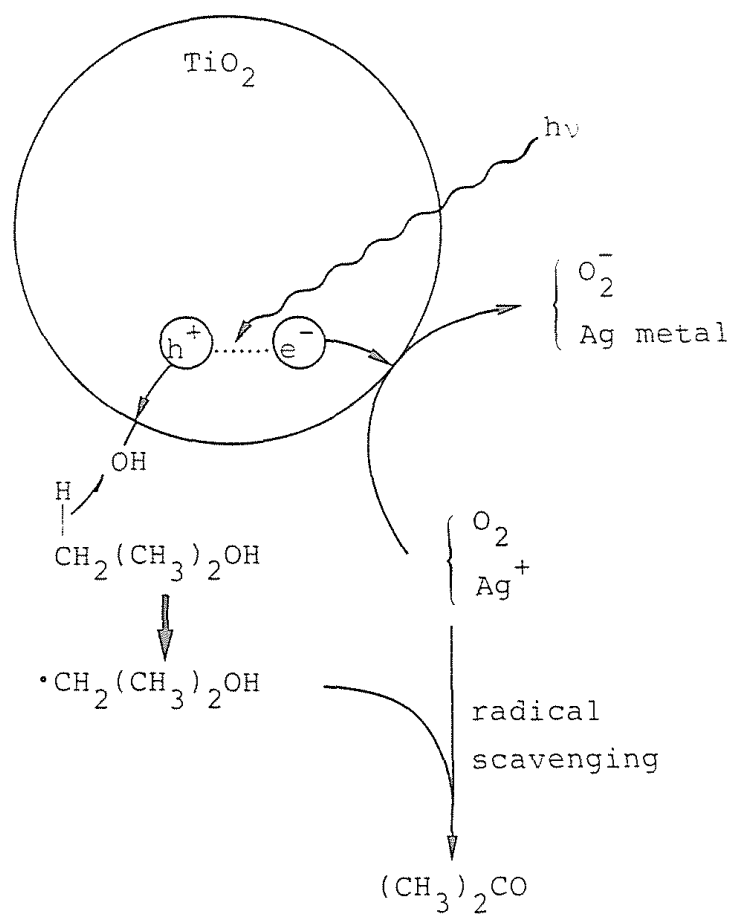
2,5-DH.

Photocatalytic Reaction of t-BuOH by Suspended TiO<sub>2</sub>/Pt Catalyst in the Presence of Oxygen or Silver Salt. Addition of O<sub>2</sub> to the above described photoreaction system enhanced the acetone yield approximately twice but decreased the yields of the other products drastically (Table 1). Because O<sub>2</sub> could be reduced by the photogenerated electron of TiO<sub>2</sub> to yield O<sub>2</sub><sup>-</sup>,<sup>13</sup> the relative decrease of reduction products (H<sub>2</sub> and CH<sub>4</sub>) is reasonable. More probable participation of O<sub>2</sub> in this system is the scavenging of the intermediate, 2-hydroxy-2-methylpropyl radical. Djeghri and co-workers<sup>14</sup> pointed out the acetone formation from t-BuOH during the course of TiO<sub>2</sub> photocatalyzed reaction of 2-methylpropane in vapor phase.

The effect of silver ion is also evident; acetone was predominantly liberated. Silver ion can accept the photogenerated electron to deposit onto the TiO<sub>2</sub> surface (Table 1).<sup>8,15,16</sup> Therefore the negligible H<sub>2</sub> yield is attributable to the effective trapping of electron by silver ion. The radical scavenging by silver ion is also probable because negligible amount of 2,5-DH could be obtained in the presence of silver ion. Following reaction is presumable.



Scheme 2 summarizes the photocatalytic reaction in the presence of the electron acceptors, which trap the photogenerated electron effectively even in the absence of the Pt deposit (see Runs 12 and 13

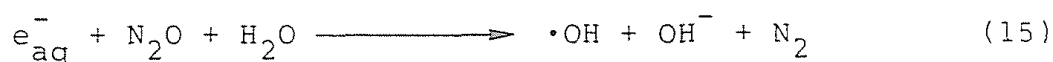


Scheme 2 Photocatalytic reaction of t-BuOH by suspended TiO<sub>2</sub> in the presence of electron acceptor.

in Table 1).

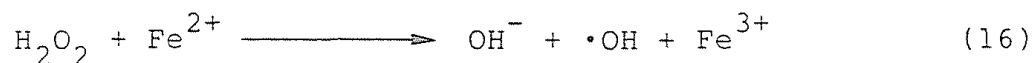
Oxidation of t-BuOH by Ionizing Radiation and by Fenton's Reagent.

Table 1 also shows the results of t-BuOH decomposition by ionizing radiation under N<sub>2</sub>O atmosphere. The observed product distributions are practically identical to that obtained in the photocatalytic system under both neutral and alkaline conditions, except for H<sub>2</sub>.<sup>17</sup> Because of the low concentration of t-BuOH (100 mmol), the radiation induced reaction is due to the indirect action via reactive species originating from the decomposition of water,<sup>18</sup> especially by •OH and e<sup>-</sup><sub>aq</sub>. In the presence of N<sub>2</sub>O saturated in aqueous solution, e<sup>-</sup><sub>aq</sub> is successfully converted into •OH radical,<sup>21</sup> as follows.



In the present system, therefore, mainly generated active species is •OH, which selectively abstracts hydrogen from t-BuOH to produce 2-hydroxy-2-methylpropyl radical,<sup>19,20</sup> which is the same proposed in the photocatalytic mechanism.

Similarly, Fenton's reagent includes the •OH formation through reductive decomposition of H<sub>2</sub>O<sub>2</sub>.<sup>21</sup>



As shown in Table 1, treatment of t-BuOH with Fenton's reagent gave 2,5-DH and acetone. The negligible yield of t-AmOH is probably due to the low pH (< 2) of the Fenton's reagent. Such decrease of t-AmOH yield was also observed in the photocatalytic system using

aqueous  $\text{H}_2\text{SO}_4$  solution.

The similarity between the product distribution of the  $\text{TiO}_2/\text{Pt}$  photocatalyzed reaction and those in the oxidation by  $\cdot\text{OH}$  mentioned above further confirmed the mechanism of the photocatalytic reaction shown in Scheme 1.

In conclusion, the above mentioned behavior of  $t\text{-BuOH}$  resembles that of organic acid in "photo Kolbe" reaction, due to the dual function of the platinized  $\text{TiO}_2$  photocatalyst.

## REFERENCES AND NOTES

- 1 (a) A. J. Bard, *J. Photochem.*, 10, 59 (1979) (b) A. J. Bard, *Science*, 207, 139 (1980).
- 2 (a) A. J. Nozik, *Ann. Rev. Phys. Chem.*, 29, 189 (1978) (b) M. S. Wrighton, *Acc. Chem. Res.*, 12, 303 (1979).
- 3 (a) A. Fujishima and K. Honda, *Bull. Chem. Soc. Jpn*, 44, 1148 (1971) (b) A. Fujishima and K. Honda, *Nature (London)*, 238, 37 (1972).
- 4 R. Baba, S. Nakabayashi, A. Fujishima, and K. Honda, 48th Annual Meeting of Chemical Society of Japan, 4011 (1983).
- 5 (a) T. Kawai and T. Sakata, *J. Chem. Soc., Chem. Commun.*, 694 (1980) (b) P. Pichat, J.-M. Herrmann, J. Disdier, H. Courbon, and M.-N. Mozzanega, *Nouv. J. Chim.*, 5, 627 (1981).
- 6 (a) T. Kawai and T. Sakata, *Chem. Lett.*, 81 (1981) (b) M. R. St. John, A. J. Furgala, and A. F. Sammells, *J. Phys. Chem.*, 87, 801 (1983).
- 7 (a) S. Sato and J. M. White, *J. Phys. Chem.*, 85, 336 (1981) (b) S. Sato and J. M. White, *J. Am. Chem. Soc.*, 102, 7206 (1980) (c) Y. Oosawa, *J. Chem. Soc., Chem. Commun.*, 221 (1982) (d) S. Teratani, J. Nakamichi, K. Taya; and K. Tanaka, *Bull. Chem. Soc. Jpn*, 55, 1688 (1982) (e) K. Domen, S. Naito, T. Ohnishi, and K. Tamaru, *Chem. Lett.*, 555 (1982).
- 8 S. Nishimoto, B. Ohtani, H. Kajiwara, and T. Kagiya, *J. Chem. Soc., Faraday Trans. 1*, 79, 2685 (1983).
- 9 The formation of dimeric product was firstly reported by Arimitsu and co-workers; Arimitsu, T. Imafuku, and I. Shiojima,

Symposium on Photochemistry, Japan, IIIA-301 (1980).

- 10 J.-M. Lehn, J.-P. Sauvage, and R. Ziessel, *Nouv. J. Chem.*, 4, 623 (1980).
- 11 (a) B. Kraeutler and A. J. Bard, *J. Am. Chem. Soc.*, 100, 2239  
(b) B. Kraeutler and A. J. Bard, *J. Am. Chem. Soc.*, 100, 5985.
- 12 I. Izumi, W. W. Dunn, K. O. Wilbourn, F. F. Fan, and A. J. Bard, *J. Phys. Chem.*, 84, 3207 (1980).
- 13 M. A. Fox and C. C. Chen, *Tetrahedron Lett.*, 24, 547 (1983).
- 14 N. Djeghri, M. Formenti, F. Jullet, and S. J. Teichner, *Disc. Faraday Soc.*, 58, 185 (1974).
- 15 S. Nishimoto, B. Ohtani, and T. Kagiya, *J. Photochem.*, in contribution.
- 16 (a) E. Borgarello, J. Kiwi, M. Gratzel, E. Pellizzetti, and M. Visca, *J. Am. Chem. Soc.*, 104, 2996 (1982) (b) P. D. Fleischauer, H. K. Alen Kan, and J. R. Shepherd, *J. Am. Chem. Soc.*, 94, 283 (1972) (c) A. W. Adamson and P. D. Fleischauer, *Concepts of Inorganic Photochemistry* (Wiley, New York, 1975), p. 400.
- 17 In this radiolysis, H<sub>2</sub> formation is attributable to hydrogen abstraction by H produced by radiolysis of water.<sup>18</sup>
- 18 Primary active species of hydrated electron ( $e_{aq}^-$ , G = 2.7), hydroxyl radical ( $\cdot OH$ , 2.7), and hydrogen atom ( $\cdot H$ , 0.55) are produced. G value shows the number of molecule produced or changed per 100 eV of energy absorbed in the solution. For recent review see H. A. Schwarz, *J. Chem. Ed.*, 58, 101 (1981).
- 19 A. J. Swallow, *Prog. Reaction Kinetics*, 9, 195 (1978).
- 20 D. Bahenemann, A. Henglein, J. Lilie, and L. Spanhel, *J. Phys. Chem.*, 88, 709 (1984).



21 W. C. Schumb, C. N. Satterfield, and R. L. Wentworth, "Hydrogen Peroxides", Reinhold, New York (1955).

## Chapter 3

### Photocatalytic Reaction of Poly(vinyl alcohol) by Aqueous Suspension of Platinized $\text{TiO}_2$

#### ABSTRACT

Poly(vinyl alcohol) (PVA) and its low-molecular-weight model compounds, 2-propanol and 2,4-pentanediol in aqueous solution were decomposed along with  $\text{H}_2$  liberation by photoirradiation ( $\lambda_{\text{ex}} > 300$  nm) of suspended  $\text{TiO}_2/\text{Pt}$  powder under Ar at room temperature. Viscometric and ultraviolet spectroscopic studies revealed that the PVA decomposition mainly includes dehydrogenation of the secondary alcohol to form ketone on the main chain ( $\beta$ -ketol) and small extent of oxidative cleavage of the PVA chain occurs simultaneously.

## INTRODUCTION

Many studies concerning heterogeneous photocatalytic reactions by metallized semiconductor materials such as platinized  $\text{TiO}_2$  powder have been carried out with the aim of solar energy conversion.<sup>1-3</sup> Considerable efforts have also been made to extend the photocatalytic action of semiconductor powders to synthetic chemistry.<sup>4-11</sup> On the other hand, in relation to utilization of waste materials for catalytic splitting of water to produce hydrogen gas, decomposition of organic materials by the  $\text{TiO}_2/\text{Pt}$  photocatalyst suspended in the aqueous solution has been reported.<sup>12,13</sup> In these studies, however, particular emphasis was placed on the efficiency of hydrogen formation not on the fate of the organic substrates. In order to clarify the mechanism of the  $\text{TiO}_2/\text{Pt}$  photocatalysis and to utilize for modification of polymeric materials, photolysis of poly(vinyl alcohol) (PVA) by  $\text{TiO}_2/\text{Pt}$  catalyst has been studied in detail under de-aerated conditions at room temperature. In the present work, characteristics in the PVA decomposition are discussed on the basis of viscometric and ultraviolet spectroscopic measurement and results of low-molecular-weight model compounds.

## EXPERIMENTAL

Materials. In the typical experiment, anatase  $\text{TiO}_2$  powder (Merck) was mixed with 5 wt% of platinum black (Pt),<sup>14</sup> and used without further activation. Characterization of the  $\text{TiO}_2$  powder were given elsewhere.<sup>15</sup> PVA (degree of polymerization  $\approx$  500, degree of saponification 86-89 % (Nakarai Chemicals)) was further saponified by refluxing with methanol and sulfuric acid, separated by filtration,

and freeze-dried. Water was passed through ion-exchange resin and distilled immediately before use. IR spectroscopic (Japan Spectroscopic A 302) analysis demonstrated that the content of residual acetate in the resulting PVA is less than 1 %. 2-Hydroxy-4-pentanone was prepared from 2,4-pentanedione from 2,4-pentanedione by reduction with  $\text{NaBH}_4$  in the aqueous solution. The other materials were obtained commercially and used without further purification.

Procedure. An Ar-purged suspension of the  $\text{TiO}_2/\text{Pt}$  powder (30 mg) in  $3.0 \text{ cm}^3$  of aqueous PVA (48-410  $\mu\text{mol}$  monomer unit) solution in a glass tube (18 mm $\phi$   $\times$  180 mm, transparent for the light of wavelength  $> 300 \text{ nm}$ ) was irradiated at room temperature under magnetic stirring with a 400-W or 500-W high-pressure mercury arc (Eiko-sha 400 and 500) equipped with a merry-go-round apparatus. Preparative photolysis of 1.80 g of PVA in water ( $180 \text{ cm}^3$ ) with 600 mg of  $\text{TiO}_2/\text{Pt}$  were carried out with a three-necked flask in which a glass-filtered high-pressure mercury arc (100 W,  $\lambda_{\text{ex}} > 300 \text{ nm}$ ) was incorporated.

Product Analysis. Gaseous products in the gas phase of the reaction mixture was analyzed by gas chromatography using a Shimadzu GC 4A equipped with a Molecular Sieves 5A column (3 mm $\phi$   $\times$  2 m) and a TCD. The suspension was centrifuged to filter off the catalyst and was subjected to viscometric (40  $^\circ\text{C}$ ) and ultraviolet (UV) spectroscopic (Shimadzu UV-200S) measurements. Amount of  $\text{CO}_2$  generated in the preparative photolysis of PVA was measured in the form of  $\text{BaCO}_3$  derived by purging the reaction mixture with  $\text{N}_2$  stream and trapping in aqueous  $\text{NaOH}$  and  $\text{Ba}(\text{OH})_2$  solution. Average number of main chain scission (N) was determined from the viscometric results by the use of viscosity-molecular weight relationship,<sup>20,21</sup> as follows.

$$[\eta] = 2.0 \times 10^{-4} (1.89 \times \bar{M}_n)$$

$$N = 1.8 [ 1 / (\bar{M}_n)_t - 1 / (\bar{M}_n)_0 ]$$

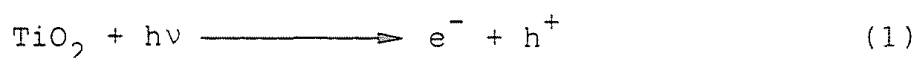
where  $[\eta]$  is intrinsic viscosity,  $(\bar{M}_n)_t$  and  $(\bar{M}_n)_0$  are number average molecular weight after and before photocatalytic reaction, respectively.

Procedure of the photocatalytic reaction of 2-propanol and 2,4-pentanediol was essentially identical to that of PVA, and reported elsewhere.<sup>16</sup>

## RESULTS AND DISCUSSION

### Photolysis of PVA Along with H<sub>2</sub> Formation by TiO<sub>2</sub>/Pt Catalyst

Photoirradiation ( $\lambda_{ex} > 300$  nm) of TiO<sub>2</sub>/Pt-suspended aqueous PVA solution led to the formation of H<sub>2</sub> in the gas phase of the reaction system. Figure 1 shows the dependence of the H<sub>2</sub> formation on the amount of Pt loading. Negligible amount of H<sub>2</sub> could be obtained by unplatized TiO<sub>2</sub> powder. The H<sub>2</sub> yield over the irradiation period of 20 h increased drastically upon increasing Pt up to 1.0 wt%, and was practically constant over the Pt content of 5-20 wt%. Thus, the small amount of Pt loading is very effective for the H<sub>2</sub> formation in the present system. Furthermore, the reaction could be observed neither in the dark nor with Pt alone, indicating that the reaction is initiated by photoabsorption ( $h\nu < ca. 390$  nm)<sup>17</sup> of anatase TiO<sub>2</sub> to form an electron-hole pair as primary active species.



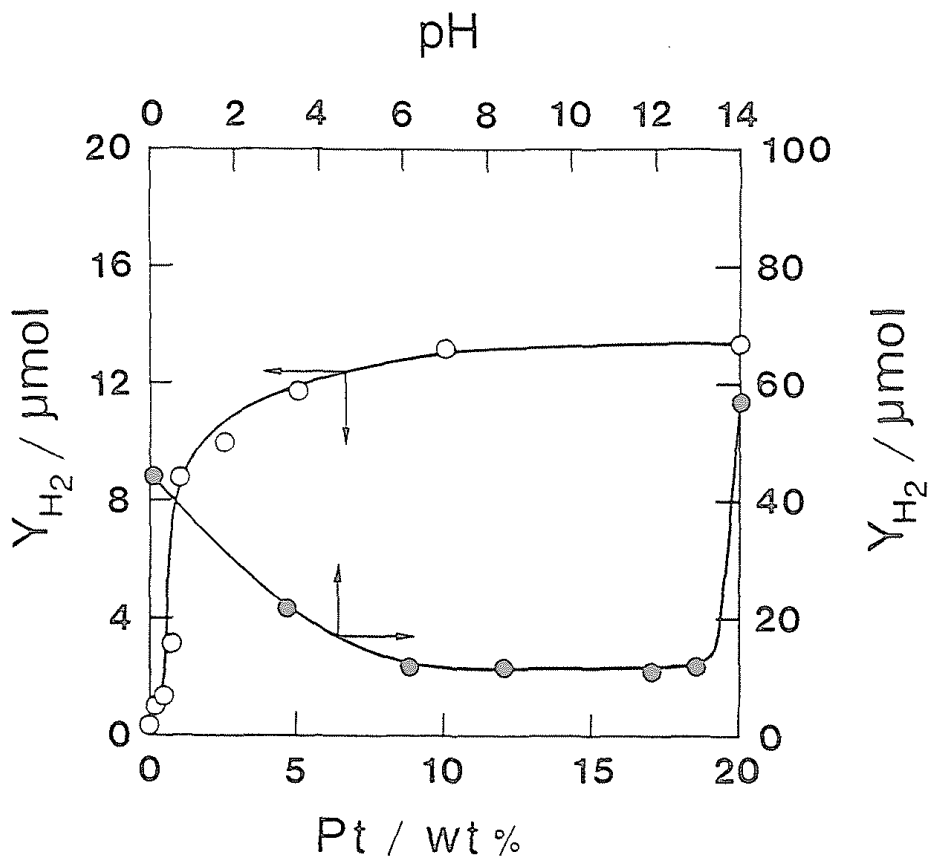


Figure 1 Influences of Pt loading ( O ) and pH of the reaction mixture ( ● ) on the photocatalytic H<sub>2</sub> formation from aqueous TiO<sub>2</sub>/Pt (30 mg) suspension (3.0 cm<sup>3</sup>) containing poly(vinyl alcohol) (410 μmol monomer unit). The suspensions were irradiated by 500-W high pressure mercury arc for 20 h.

The electron thus formed would reduce proton at the Pt side of the photocatalyst<sup>18</sup> to produce H<sub>2</sub>.

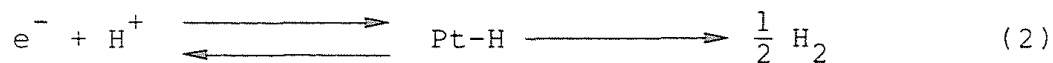


Figure 1 also shows the pH dependence of the H<sub>2</sub> formation by TiO<sub>2</sub>/Pt (5 wt%). The H<sub>2</sub> yield (Y<sub>H<sub>2</sub></sub>) by the irradiation for 20 h was almost constant (12-20 μmol) in the pH range of 3 to 13, while drastically increased in either lower (3 M H<sub>2</sub>SO<sub>4</sub>) or higher (6M NaOH) pH regions, although PVA was much less soluble in alkaline solution (pH > 11). Similar enhancement of the TiO<sub>2</sub>/Pt activity in the higher pH region (5 M NaOH) has been reported by Kawai and Sakata.<sup>12</sup> Such a pH-dependence is possibly attributable to surface modification of the TiO<sub>2</sub> powder by strong acid or base treatment.<sup>19</sup> Along with the H<sub>2</sub> formation, the intrinsic viscosity (η) of the PVA solution decreased as a result of the main-chain scission of PVA. By the use of viscosity-molecular weight relationship,<sup>20,21</sup> the average number of the scission was evaluated as 32 μmol at 190 μmol of H<sub>2</sub> liberation in the preparative photolysis for 150 h. In this photolysis, 18 μmol of CO<sub>2</sub> was also detected in the form of BaCO<sub>3</sub>.

#### Photocatalytic Formation of Carbonyl Group on the Polymer Chain.

In the same manner as the PVA system, photocatalytic reactivities of model compounds 2-propanol and 2,4-pentanediol (PDO) were studied in aqueous TiO<sub>2</sub>/Pt suspension (Table 1). In both cases H<sub>2</sub> was liberated in the gas phase together with almost equimolar amount of corresponding carbonyl compound, acetone or 2-hydroxy-4-pentanone (HPO).<sup>16,22</sup>

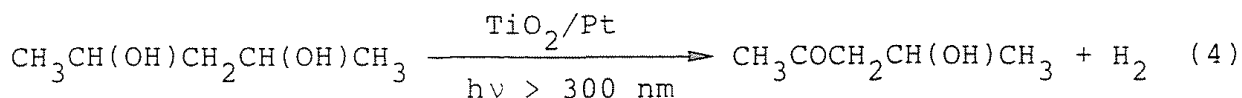
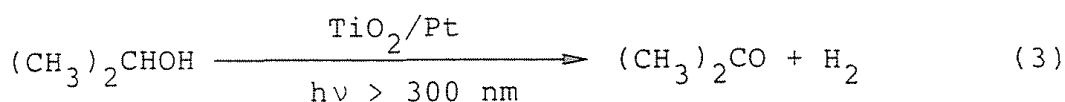
Table 1 Photocatalytic Reaction of PVA and Model Compounds by TiO<sub>2</sub>/Pt Catalyst.<sup>a</sup>

Substrate	-OH <sup>b</sup> / μmol	H <sub>2</sub> / μmol
poly(vinyl alcohol) <sup>c</sup>	410	8.7
2,4-pentanediol	820	16
2-propanol	500	81

<sup>a</sup>Substrate, TiO<sub>2</sub>/Pt (5 wt%, 30 mg), and distilled water (3.0 cm<sup>3</sup>) were placed in a test tube (18 mmφ × 180 mm) and irradiated by 400-W high-pressure mercury arc under Ar at room temperature for 20 h.

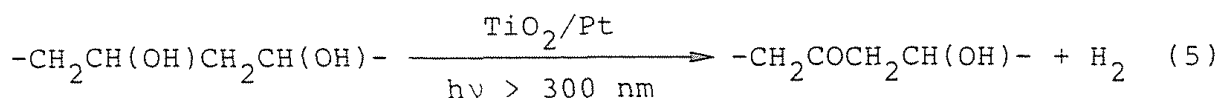
<sup>b</sup>Number of OH group in the starting materials.  $\overline{C_{M_n}} \approx 10500$ , degree of saponification > 99 %.



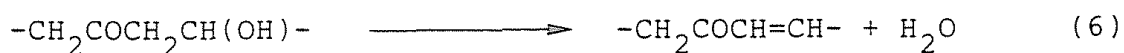


The amount of  $\text{H}_2$  liberated over the 20-h irradiation decreased with the increasing molecular weight (Table 1); approximately 10-fold larger amount of  $\text{H}_2$  was obtained using 2-propanol compared with that from PVA solution. These facts are possibly accounted for by the adsorption ability of the alcohols on the hydrophilic  $\text{TiO}_2$  surface.<sup>23</sup>

The formation of carbonyl group on the PVA chain was also suggested by comparison of the UV spectra of photoirradiated aqueous solutions of PVA and these model compounds (Fig. 2). Characteristic absorption band of PVA solution at  $\lambda_{\text{max}} \approx 270 \text{ nm}$ , which increased upon increasing the irradiation period, is assigned to  $\beta$ -ketol structure by reference to the spectrum of HPO ( $\lambda_{\text{max}} \approx 280 \text{ nm}$ ).



Another absorption appeared at  $\lambda_{\text{max}} \approx 230 \text{ nm}$  by the further irradiation ( $> 50 \text{ h}$ ). Since the dehydrated derivative of HPO, 3-penten-2-one, shows similar absorption spectrum,<sup>24</sup> the shorter wavelength absorption band is possibly due to the formation of  $\alpha,\beta$ -unsaturated ketone by dehydration of the  $\beta$ -ketol.



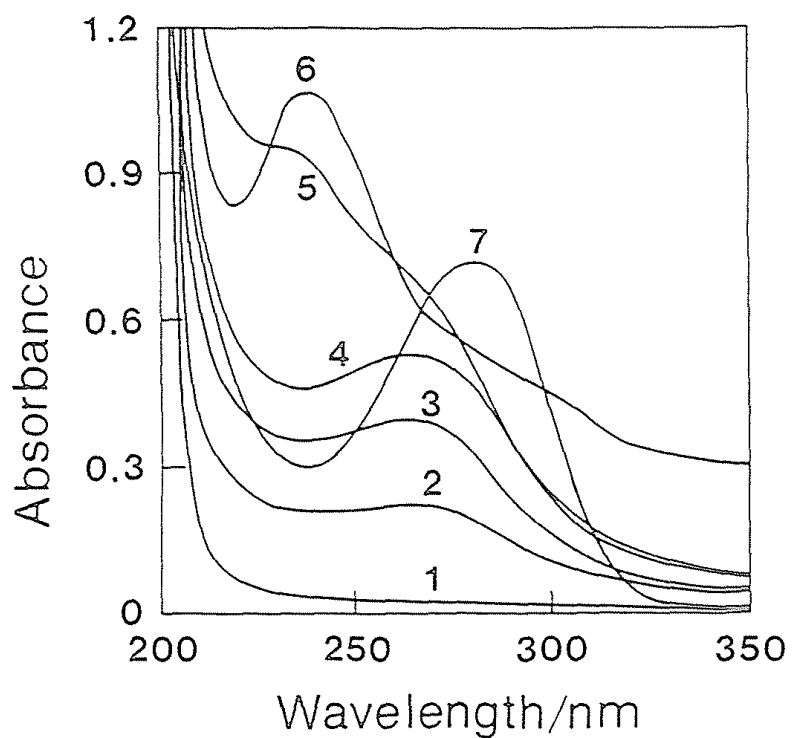
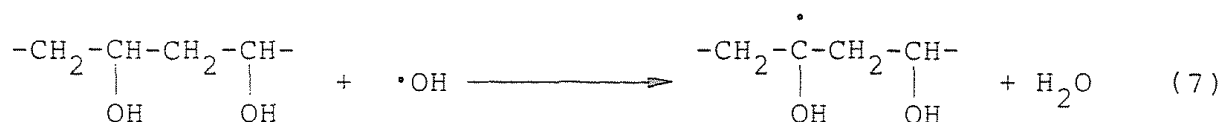


Figure 2 Ultraviolet absorption spectra of aqueous poly(vinyl alcohol) solution (48  $\mu\text{mol}$  monomer unit in 3.0  $\text{cm}^3$  of water) photo-irradiated ( $\lambda_{\text{ex}} > 300$  nm) with  $\text{TiO}_2/\text{Pt}$  catalyst (30 mg) by a 400-W high-pressure mercury arc: 1, 0 h; 2, 5 h; 3, 24 h; 4, 37 h; 5, 75 h; 6, freeze-dried sample of poly(vinyl alcohol) irradiated for 150 h; 7, authentic sample of 4-hydroxy-2-pentanone.

However, the proportion of the  $\alpha,\beta$ -unsaturated ketone must be small compared with the  $\beta$ -ketol, because the molar extinction coefficients ( $\epsilon$ ) of such  $\alpha,\beta$ -unsaturated ketones are usually larger ( $\log \epsilon \approx 4$ ) than those of the  $\beta$ -ketols ( $\log \epsilon = 1-2$ ).<sup>24</sup>

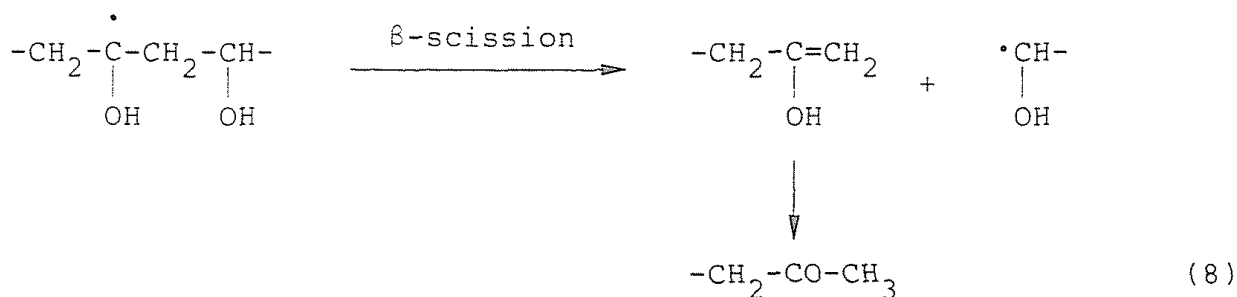
Since these two absorption bands were also observed even after freeze-drying of the photoirradiated PVA (see also Figure 2), the PVA chain is suggested to bear the ketones. The number of the ketones on the PVA chain was evaluated, for convenience by the use of the reported molar extinction coefficient of HPO ( $63 \text{ M}^{-1} \text{ cm}^{-1}$ ),<sup>24</sup> to be of the same order as the liberated  $\text{H}_2$  (10 and 5.0  $\mu\text{mol}$ , respectively, by 24-h irradiation).

Mechanism of the Photocatalytic Decomposition of PVA. A possible mechanism of the photocatalytic reaction including the formation of polymer radical is outlined as follows. The positive holes, which are produced together with electrons on the irradiated  $\text{TiO}_2$  (eqn 1), are strong oxidizing agents enough to oxidize surface hydroxyl group into hydroxyl radical adsorbed on the  $\text{TiO}_2$  surface.



Jaeger and Bard has been demonstrated the formation of hydroxyl radical in the ESR study on the  $\text{TiO}_2/\text{Pt}$  suspension.<sup>25</sup> The hydroxyl radical presumably abstracts hydrogen from the polymer chain to form  $\alpha$ -hydroxy radical.<sup>26</sup> The ketone formation on the polymer chain could occur by the subsequent oxidation of the polymer radical or by less possible disproportionation of the polymer radicals. It is

likely that the  $\alpha,\beta$ -unsaturated ketone is derived by dehydration of the ketol (eqn 6). On the other hand, the main chain cleavage is accounted for by the  $\beta$ -scission of the polymer radical with simultaneous formation of a ketone (terminal acetyl group).



Kawai and Sakata reported the photocatalytic  $\text{CO}_2$  formation by  $\text{TiO}_2/\text{Pt}$  suspension from various organic compounds as a result of complete oxidation of the backbone.<sup>12</sup> However, in the present system it seems more likely that the  $\text{CO}_2$  formation in the preparative photolysis is due to the decomposition<sup>4,5</sup> of a small amount of acetate ion eliminated catalytically or photocatalytically from the residual acetyl groups on the PVA, because maximally 200  $\mu\text{mol}$  of acetyl groups are estimated to remain in 1.8 g of PVA.

## REFERENCES AND NOTES

- 1 A. J. Bard, *J. Photochem.*, 10, 5 (1979).
- 2 A. J. Nozik, *Annu. Rev. Phys. Chem.*, 29, 189 (1978).
- 3 M. S. Wrighton, P. T. Wolczanski, and A. B. Ellis, *J. Solid. State Chem.*, 22, 17 (1977).
- 4 B. Kraeutler and A. J. Bard, *J. Am. Chem. Soc.*, 100, 2239 (1978).
- 5 I. Izumi, W. W. Dunn, K. O. Wilbourn, F. F. Fan, and A. J. Bard, *J. Phys. Chem.*, 84, 3207 (1980).
- 6 T. Kanno, T. Oguchi, H. Sakuragi, and K. Tokumaru, *Tetrahedron Lett.*, 21, 467 (1980).
- 7 M. A. Fox and C. C. Chen, *J. Am. Chem. Soc.*, 103, 6757 (1981).
- 8 M. A. Fox and M-J. Chen, *J. Am. Chem. Soc.*, 105, 4497 (1983).
- 9 J. W. Pavlik and S. Tantayanon, *J. Am. Chem. Soc.*, 103, 6755 (1981).
- 10 M. Fujihira, Y. Sato, and T. Osa, *Bull. Chem. Soc. Jpn*, 55, 666 (1982).
- 11 S. Nishimoto, B. Ohtani, T. Yoshikawa, and T. Kagiya, *J. Am. Chem. Soc.*, 105, 7180 (1983).
- 12 T. Kawai and T. Sakata, *Chem. Lett.*, 81 (1981).
- 13 T. Sakata and T. Kawai, *Nouv. J. Chim.*, 5, 279 (1981).
- 14 T. Kawai, T. Sakata, K. Hashimoto, and M. Kawai, *Nippon Kagaku Kaishi*, 277 (1984).
- 15 S. Nishimoto, B. Ohtani, H. Kajiwara, and T. Kagiya, *J. Chem. Soc., Faraday Soc.*, 79, 2685 (1983).
- 16 S. Nishimoto, B. Ohtani, A. Sakamoto, and T. Kagiya, *Nippon*

- Kagaku Kaishi, 246 (1984).
- 17 V. N. Pak and N. G. Ventov, Russ. J. Phys. Chem. (English Transl.), 49, 1489 (1975).
  - 18 B. Kraeutler and A. J. Bard, J. Am. Chem. Soc., 100, 5985 (1978).
  - 19 Increase in the specific surface area and the amount of surface hydroxyl groups induced by the alkaline or acid treatment has been reported; S. Okazaki and T. Kanto, Nippon Kagaku Kaishi, 404 (1976).
  - 20 K. Hayashi and T. Otsu, Makromol. Chem., 127, 54 (1969).
  - 21 P. J. Flory and F. S. Leutner, J. Polymer Sci., 3, 880 (1948).
  - 22 (a) S. Teratani, J. Nakamichi, K. Taya, and K. Tanaka, Bull. Chem. Soc. Jpn, 55, 1688 (1982) (b) P. Pichat, J.-M. Herrmann, J. Disdier, H. Courbon, and M.-N. Mozzanega, Nouv. J. Chim., 5, 627 (1981).
  - 23 H. P. Boehm, Disc. Faraday Soc., 52, 264 (1971).
  - 24 J. T. Clarke and E. R. Blout, J. Polym. Sci., 1, 419 (1946).
  - 25 C. D. Jaeger and A. J. Bard, J. Phys. Chem., 83, 3146 (1979).
  - 26 D. Bahneman and co-workers reported the formation of  $\alpha$ -hydroxy polymer radical via hydrogen abstraction by hydroxyl radical ( $\cdot\text{OH}$ ) generated by  $\gamma$ -ray radiolysis in homogeneous system; D. Bahnemann, A. Henglein, J. Lilie, and L. Spanhal, J. Phys. Chem., 88, 709 (1984).

## Chapter 4

### Photocatalytic Degradation and Prolongation of Poly(ethylene oxide) by Aqueous Suspension of Platinized $\text{TiO}_2$

#### ABSTRACT

Photoinduced reaction ( $\lambda_{\text{ex}} > 300 \text{ nm}$ ) of poly(ethylene oxide) (PEO) by platinized  $\text{TiO}_2$  ( $\text{TiO}_2/\text{Pt}$ ) in deaerated aqueous solution was studied at room temperature. Gel permeation chromatography of the photoirradiated PEO showed that the polymer chain of PEO was cleaved to give small molecules under the acidic conditions while the molecular weight of the chain increased under the neutral and the basic conditions.  $\text{H}_2$  formed simultaneously and the amount from the NaOH solution was 3-5 times larger than that from neutral and acidic solution. Remarkable formations of  $\text{CH}_4$ ,  $\text{C}_2\text{H}_6$ ,  $\text{CO}$ ,  $\text{CH}_3\text{CHO}$ ,  $\text{HCHO}$ , and  $\text{HOCH}_2\text{CH}_2\text{OH}$  were observed only under the acidic conditions. No influence on the yields of  $\text{H}_2$  and  $\text{CH}_3\text{CHO}$  was observed by shielding the gas phase of the reaction mixture against the photoirradiation, while those of  $\text{CH}_4$ ,  $\text{C}_2\text{H}_6$ ,  $\text{CO}$ , and  $\text{HCHO}$  decreased significantly. Photoirradiation on the  $\text{CH}_3\text{CHO}$  solution with or without  $\text{TiO}_2/\text{Pt}$  led to the formation of  $\text{CH}_4$ ,  $\text{C}_2\text{H}_6$ , and  $\text{CO}$  in the ratio (ca. 4 : 2 : 7) similar to that observed in the  $\text{TiO}_2/\text{Pt}$  photocatalyzed reaction of PEO under the acidic conditions. On the basis of these results, molecular mechanism of the photocatalytic reaction of PEO by  $\text{TiO}_2/\text{Pt}$  is discussed.

## INTRODUCTION

Recent investigations concerning heterogeneous photocatalysis by metallized semiconductor materials, such as platinized  $\text{TiO}_2$ , have attempted the utilization of solar energy to decompose water into  $\text{H}_2$  and  $\text{O}_2$ ,<sup>1-3</sup> or to produce  $\text{H}_2$  from water with the aid of sacrificial electron donors. Typically, alcohols or waste materials<sup>4-9</sup> have been used for the photocatalytic  $\text{H}_2$  evolution as has been demonstrated in Chapters 1 and 2 of this thesis. In the preceding chapter of this thesis, photoinduced reaction of polymeric material possessing secondary alcohol moiety, poly(vinyl alcohol) (PVA), by aqueous suspension of platinized  $\text{TiO}_2$  under deaerated conditions was described in detail. The formation of carbonyl group on the PVA chain, with the simultaneous  $\text{H}_2$  liberation, was observed by viscometric and ultraviolet spectroscopic measurements. The behavior of PVA in the photocatalytic system is essentially identical to those of the low-molecular-weight model compounds, 2-propanol and 2,4-pentanediol, to give dehydrogenated derivative by the treatment with the platinized  $\text{TiO}_2$ .

Few reports concerning the photocatalytic decomposition of ethers have been so far published.<sup>10</sup> In this chapter, the photocatalytic reaction of water-soluble polymer containing ether linkage, poly(ethylene oxide) (PEO), by aqueous suspension of platinized  $\text{TiO}_2$  under Ar at room temperature is described. In this photoreaction system, the formation of not only  $\text{H}_2$  but also  $\text{CH}_4$ ,  $\text{C}_2\text{H}_6$ , and CO were observed in the gas phase of the reaction mixture when photoirradiated ( $\lambda_{\text{ex}} > 300 \text{ nm}$ ) under acidic conditions, while  $\text{H}_2$  was obtained as a sole gaseous product under alkaline conditions. These gas



evolutions were characteristic of the photoinduced reaction of PEO in the presence of platinized  $\text{TiO}_2$ ; no gas evolution other than  $\text{H}_2$  could be observed in the case of PVA. Particular emphasis is placed on the pH-dependent behavior of the photocatalytic reaction of PEO in aqueous solution.

## EXPERIMENTAL

Materials. Polycrystalline  $\text{TiO}_2$  powder was supplied by Merck and the anatase structure (> 99 %) was confirmed by X-ray diffraction analysis (for detailed characterization see Chapter 6). Platinized  $\text{TiO}_2$  catalyst ( $\text{TiO}_2/\text{Pt}$ ) was prepared by mixing and braying the  $\text{TiO}_2$  powder with platinum black (Pt, Nakarai Chemicals, typically 5 wt%) in an agate mortar.<sup>4</sup> Poly(ethylene oxide) (PEO,  $\bar{M}$  570-630, mp 19-23 °C) was obtained from Nakarai Chemicals and used without further purification. Authentic samples of PEO were supplied by Nakarai Chemicals. Acetaldehyde was obtained commercially and used as received.

Photoirradiation. PEG 22 mg was dissolved in 5.0 cm<sup>3</sup> of solvent (NaOH aq., distilled water, or  $\text{H}_2\text{SO}_4$  aq.) containing 50 mg of the platinized  $\text{TiO}_2$  ( $\text{TiO}_2/\text{Pt}$ ) catalyst. The resulting suspension in a glass tube (18 mm $\phi$   $\times$  180 mm, transparent for the light of wavelength > 300 nm) was purged of air by Ar for at least 30 min and sealed off with a rubber stopper. Photoirradiation was performed at room temperature under magnetic stirring by 400-W high-pressure mercury arc (Eiko-sha 400) equipped with a merry-go-round apparatus. The gas phase of the reaction mixture was shielded with aluminum foil against the photoirradiation for the observation of the reaction in

the liquid phase.

Product Analysis. After the photoirradiation a portion of gaseous products liberated in the gas phase of the reaction mixture was collected through the rubber cap with a syringe and was analyzed by gas chromatography (GC) using a Shimadzu GC 4A equipped with a TCD and a Molecular Sieve 5A column (3 mm $\phi$   $\times$  2 m). The photoirradiated suspension was centrifuged to separate the TiO<sub>2</sub>/Pt catalyst and the aqueous solution was subjected to the GC and gel permeation chromatography (GPC). Typical conditions for the GC analysis are as follows; acetaldehyde and the other low boiling point compounds were analyzed with a Shimadzu GC 6A gas chromatograph equipped with an FID and a column (3 mm $\phi$   $\times$  2 m) packed with 20 % Polyethylene Glycol 20M on 60-80 mesh Celite 545. Higher boiling point compounds such as ethylene glycol were analyzed using a Tenax GC (3 mm $\phi$   $\times$  1 m) column.

Formaldehyde (HCHO) was analyzed by the acetylacetone method<sup>11</sup> (see Chapter 1).

The photoirradiated solution was neutralized by adding aqueous NaOH or H<sub>2</sub>SO<sub>4</sub> solution. After evaporation to dryness at below 35 °C, the residue (except inorganic salt) was dissolved in tetrahydrofuran (THF) and subjected to GPC analysis. In the case of NaIO<sub>4</sub> treatment, the residue was dissolved in an aqueous NaIO<sub>4</sub> solution, allowed to stand for 2 h, and evaporated to dryness. The residual PEO derivative was analyzed in the same manner as above. Typical conditions were as follows: Toyo Soda HLC-802 UR high speed liquid chromatograph equipped with G2000H8 columns (2  $\times$  7.5 mm $\phi$   $\times$  600 mm), eluted with THF at a flow rate of 1.0 cm<sup>3</sup> min<sup>-1</sup> at 40 °C (70 kg

cm<sup>-2</sup>).

## RESULTS AND DISCUSSION

TiO<sub>2</sub>/Pt Photocatalytic Reaction of PEO in Aqueous Solution. Figure 1 shows the GPC elution patterns of PEO before and after the photoirradiation (through a glass tube,  $\lambda_{\text{ex}} > 300$  nm) in the presence of TiO<sub>2</sub>/Pt catalyst. The samples from the 0.5 mol dm<sup>-3</sup> H<sub>2</sub>SO<sub>4</sub> solution (B-E) included the fraction which was eluted slower than the original PEO sample (A). This indicates that degradation of the PEO molecule took place. The most intensive peak (elution volume 26-27 cm<sup>3</sup>) among the degraded products corresponds to trimer or tetramer of ethylene oxide. The prolonged irradiation brought about the decrease in the molecular weight of PEO and the original PEO fraction disappeared almost by 72-h irradiation.

On the contrary, the samples from the photoirradiated aqueous NaOH solution and neutral solution were eluted in the region identical or of molecular weight larger than that of the original sample. The larger molecular weight peak (elution volume 18-19 cm<sup>3</sup>) corresponds to PEO of molecular weight of ca. 1300-2000. The degraded products as in the case of the H<sub>2</sub>SO<sub>4</sub> solution could be detected negligibly (see also Table 1).

Control experiment showed that no dark reaction occurs in the presence of TiO<sub>2</sub>/Pt suspended in the acidic, neutral, and basic solutions. Moreover, photoreaction of PEO in the absence of TiO<sub>2</sub>/Pt could not be observed. Therefore, the degradation and the increase of the molecular weight shown above are attributable to the photocatalytic action of TiO<sub>2</sub>/Pt, as follows.

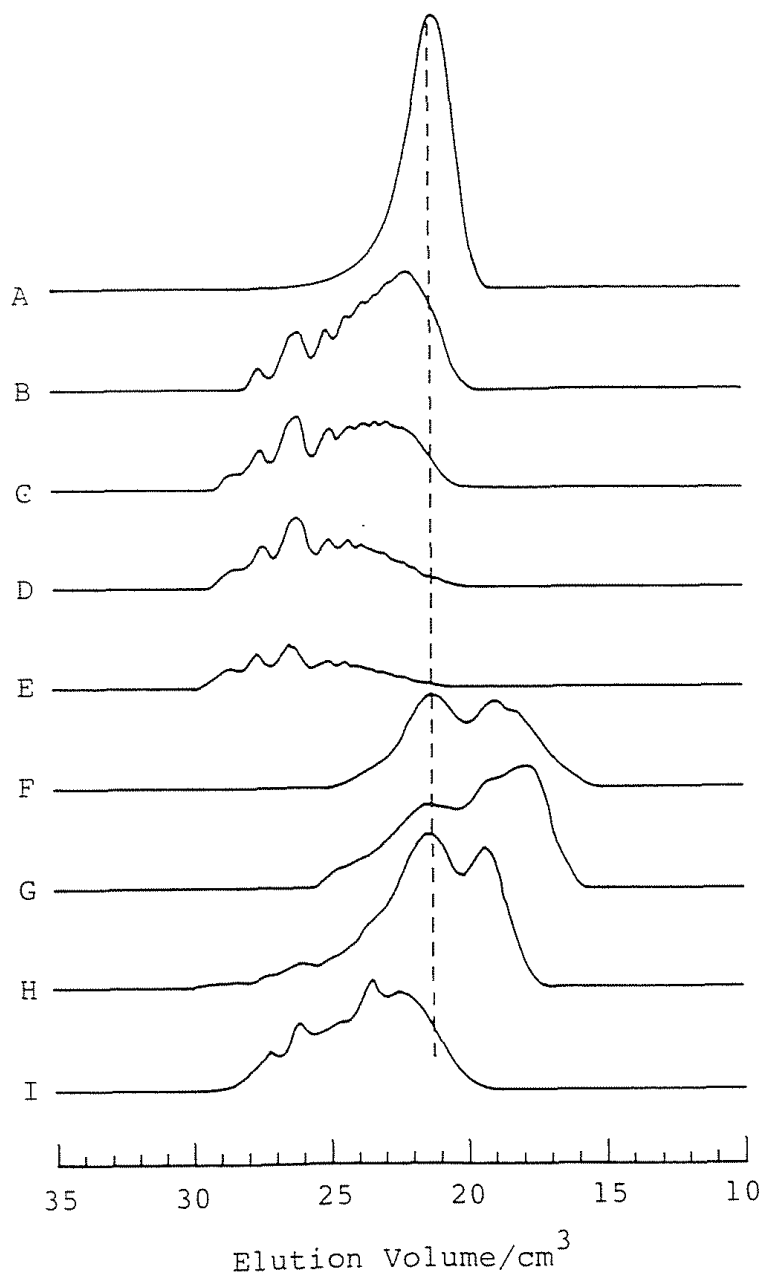
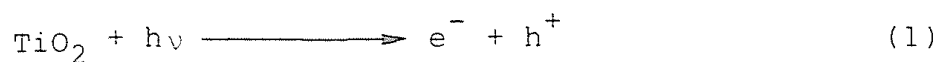
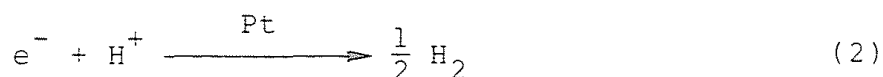


Figure 1 GPC elution patterns of PEO before (A) and after photoirradiation in 0.5 M  $\text{H}_2\text{SO}_4$  solution (B : 12 h, C : 24 h, D : 48 h, and E : 72 h), and in 1 M NaOH solution (G : 72 h, H : 24 h). Sample H was treated with  $\text{NaIO}_4$  to decompose into Sample I.

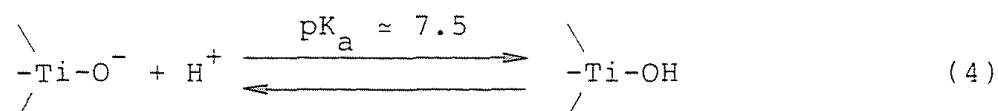
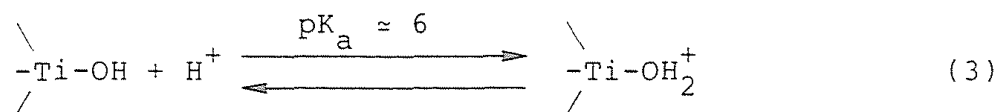


The photoexcited electron ( $e^-$ ) reduces  $\text{H}^+$  into  $\text{H}_2$  at the Pt site as discussed in later section (Table 1).



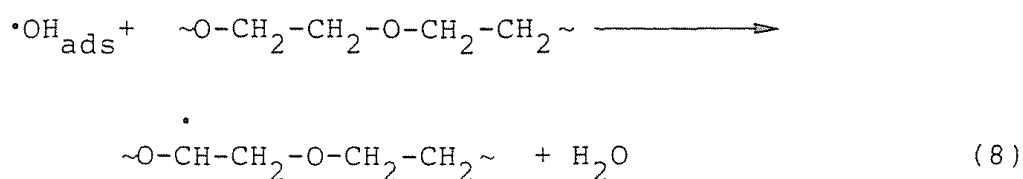
The positive hole ( $h^+$ ) generated simultaneously could remain to oxidize substrate without recombination with the photoexcited electron.

The  $\text{TiO}_2$  surface is positively and negatively charged under the acidic and basic conditions, respectively, due to the acid-base equilibria of surface hydroxyl group, as is described in Chapter 11.

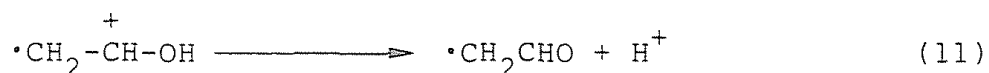
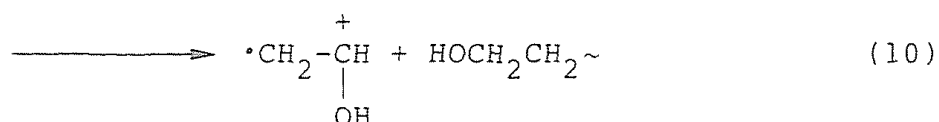
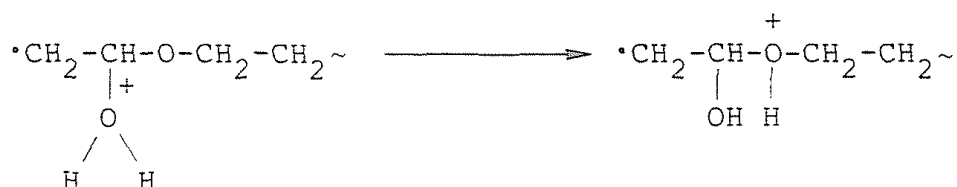
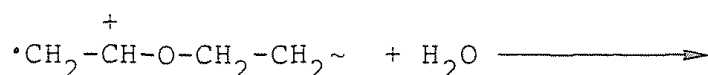
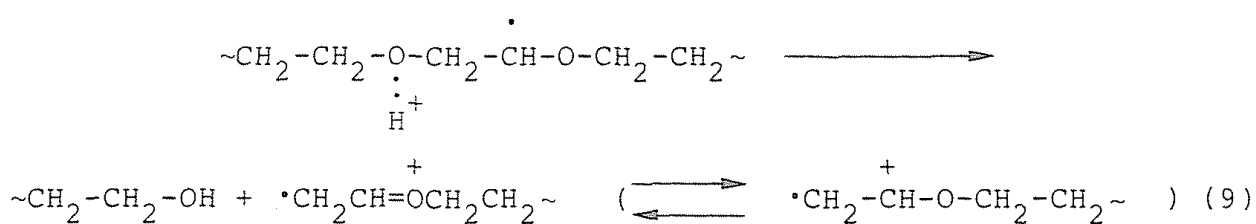


Most part of the hydroxyl group is expected to be positively charged ( $\equiv\text{Ti-OH}_2^+$ ) in the  $0.5 \text{ mol dm}^{-3} \text{ H}_2\text{SO}_4$  solution and negatively charged ( $\equiv\text{Ti-O}^-$ ) in the  $1 \text{ mol dm}^{-3} \text{ NaOH}$  solution. The most possible site, on the  $\text{TiO}_2$  surface, which traps the hole is the surface hydroxyl group to give surface hydroxyl radical ( $\cdot\text{OH}_{\text{ads}}$ ) or oxygen anion radical ( $\text{O}_{\text{ads}}^-$ ).



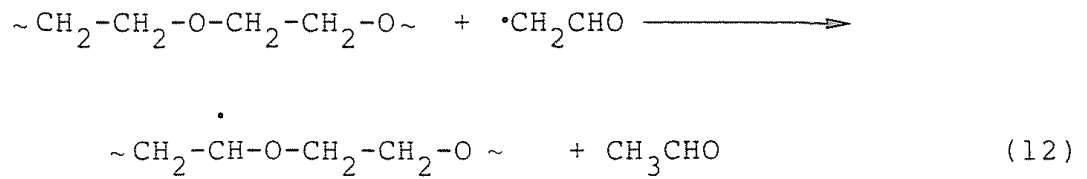


The polymer radical would undergo acid-catalyzed degradation, as observed in the decomposition of 1,2-dimethoxy radical,<sup>12</sup> through oxonium cation radical intermediate.

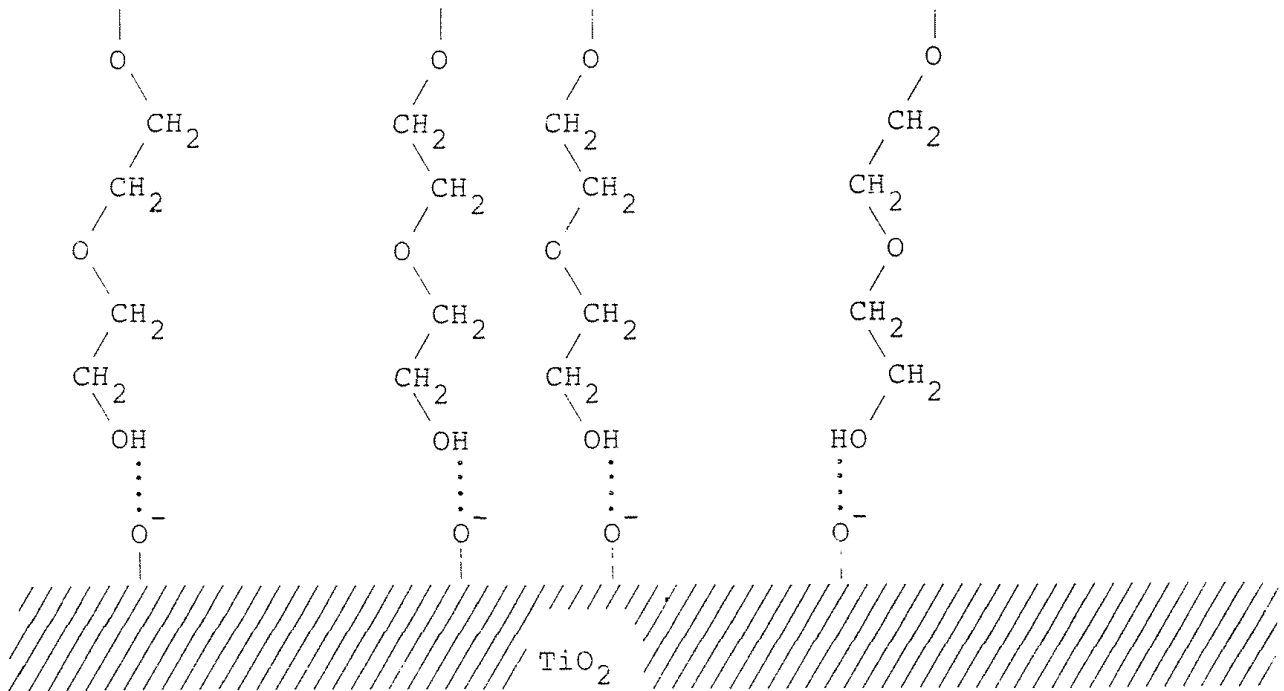


The resulting formylmethyl radical could abstract hydrogen from the polymer chain to produce  $\text{CH}_3\text{CHO}$  (as described in the following section (Table 1)) and the polymer radical, i.e.,  $\text{CH}_3\text{CHO}$  is obtained in the chain reaction along with the main chain degradation (reactions

9-12).



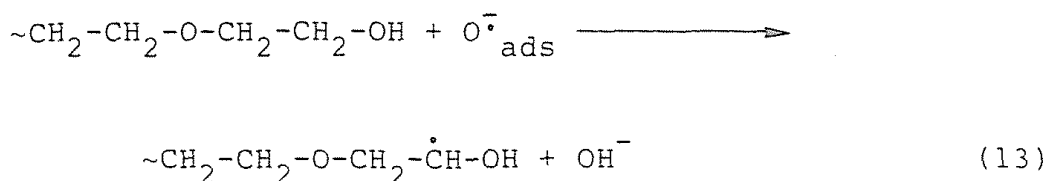
On the other hand, repulsion between the negatively charged surface ( $\equiv\text{Ti}-\text{O}^-$ ) and the ether oxygen in polymer chain appears to be evident in the alkaline suspension. Therefore, the PEO molecule is expected to adsorb on the surface at the end of the polymer chain (i.e., primary alcohol moiety).



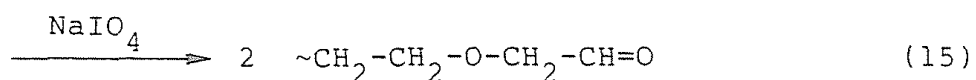
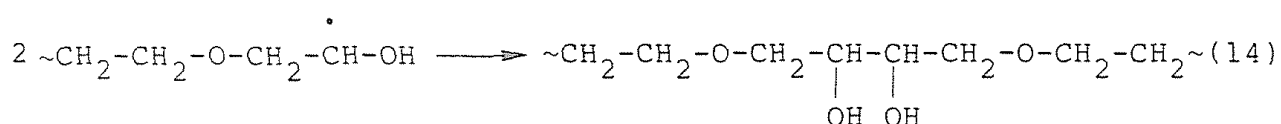
basic—"vertical" adsorption

The "vertical" adsorption causes the hydrogen abstraction from methylene group adjacent to the terminal alcohol moiety, as follows, without degradation (Figure 1).





When the partly lengthened PEO fractions which was obtained by the photocatalytic reaction under the basic conditions (Figure 1, H) were treated with  $\text{NaIO}_4$ , selective oxidant for 1,2-diols and their derivatives,<sup>13</sup> the larger molecular weight peak disappeared (Figure 2, I). These facts suggest that the polymer radicals (reaction 13) and the oxidative cleavage occurred by  $\text{NaIO}_4$  into aldehyde (reaction 15).



Degraded Products in the Photocatalytic Reaction of Poly(ethylene oxide) by  $\text{TiO}_2/\text{Pt}$  Catalyst. Table 1 shows the distribution of the products liberated from the photoirradiated PEO solutions by  $\text{TiO}_2/\text{Pt}$  catalyst. Under neutral and basic conditions (Run 1 and 2, respectively),  $\text{H}_2$  was observed as a sole product in the gas phase of the reaction mixture. Small amounts of  $\text{HCHO}$ ,  $\text{CH}_3\text{CHO}$ , and  $\text{HOCH}_2\text{CH}_2\text{OH}$  were observed in the liquid phase. These results are consistent with the results of the GPC analysis shown in the preceding section (Figure 1).

From the acidic solutions (aqueous  $\text{H}_2\text{SO}_4$  solution, Runs 3 and

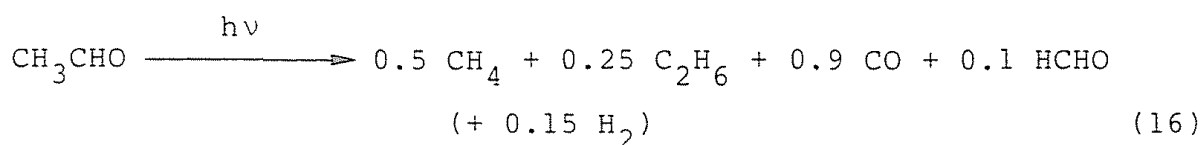
Table 1 Product distribution of photocatalytic degradation of PEO by TiO<sub>2</sub>/Pt.<sup>a</sup>

Run	Condition <sup>b</sup>	Product/ $\mu\text{mol}$						
		H <sub>2</sub>	CH <sub>4</sub>	C <sub>2</sub> H <sub>6</sub>	CO	HCHO	CH <sub>3</sub> CHO	EG <sup>c</sup>
1	H <sub>2</sub> O	7.1	$\approx 0$	$\approx 0$	$\approx 0$	0.3	0.4	0.5
2	1 M NaOH	22.0	$\approx 0$	$\approx 0$	$\approx 0$	0.1	0.5	$\approx 0$
3	0.5 M H <sub>2</sub> SO <sub>4</sub>	11.1	7.2	4.1	11.2	2.7	23.9	6.4
4	2.5 M H <sub>2</sub> SO <sub>4</sub>	7.7	8.3	5.3	14.3	3.0	21.1	8.8
5	0.5 M H <sub>2</sub> SO <sub>4</sub> <sup>d</sup>	8.4	0.5	0.3	$\approx 0$	1.0	19.1	3.4

<sup>a</sup>PEO ( $\bar{M} \approx 600$ , 22 mg) in TiO<sub>2</sub>/Pt (5 wt%, 50 mg) suspended aqueous solution was irradiated by a 400-W high-pressure mercury arc for 20 h at room temperature under Ar. <sup>b</sup>M  $\equiv$  mol dm<sup>-3</sup>. <sup>c</sup>Ethylene glycol (HOCH<sub>2</sub>CH<sub>2</sub>OH). <sup>d</sup>Irradiated only on the solution phase.

4), remarkable formations of  $\text{CH}_4$ ,  $\text{C}_2\text{H}_6$ ,  $\text{CO}$ ,  $\text{HCHO}$ , and  $\text{CH}_3\text{CHO}$  other than  $\text{H}_2$  were observed as the degraded products of PEO. Shielding the gas phase of the reaction mixture against the photoirradiation (Run 5) gave no influence on the yields of  $\text{H}_2$  and  $\text{CH}_3\text{CHO}$ , but decreased those of  $\text{CH}_4$ ,  $\text{C}_2\text{H}_6$ ,  $\text{CO}$ , and  $\text{HCHO}$  to be negligible. Consequently, the latter products (and part of  $\text{H}_2$ ) are accounted for by the successive photolysis, in the gas phase, of a product  $\text{CH}_3\text{CHO}$ .

Figure 2 shows the time course of the product yields from the  $0.5 \text{ mol dm}^{-3} \text{ H}_2\text{SO}_4$  suspension. The  $\text{CH}_4$ ,  $\text{C}_2\text{H}_6$ , and  $\text{CO}$  formations were accelerated by the photoirradiation, due to the accumulation of  $\text{CH}_3\text{CHO}$ . Figure 3 illustrates the material balance of these products; sum of  $\text{CH}_4$  and twice of  $\text{C}_2\text{H}_6$  was plotted against sum of  $\text{CO}$  and  $\text{HCHO}$ . These results indicate that the product yields practically agreed with the stoichiometry of the photolysis of  $\text{CH}_3\text{CHO}$ , as follows.



Photolysis of  $\text{CH}_3\text{CHO}$ . In order to confirm the role of photodecomposition of intermediate  $\text{CH}_3\text{CHO}$ , photoinduced reaction of  $\text{CH}_3\text{CHO}$  in aqueous solution was investigated as shown in Table 2. Significant formations of  $\text{CH}_4$ ,  $\text{C}_2\text{H}_6$ , and  $\text{CO}$  were observed (Runs 1-3) except for the case of alkaline solution (Run 4). These gas evolutions are attributable to the photolysis of  $\text{CH}_3\text{CHO}$ , because no gas formations were observed in the dark (Run 5) and also because the presence of  $\text{TiO}_2/\text{Pt}$  catalyst (Runs 6-8) did not give apparently no influence on

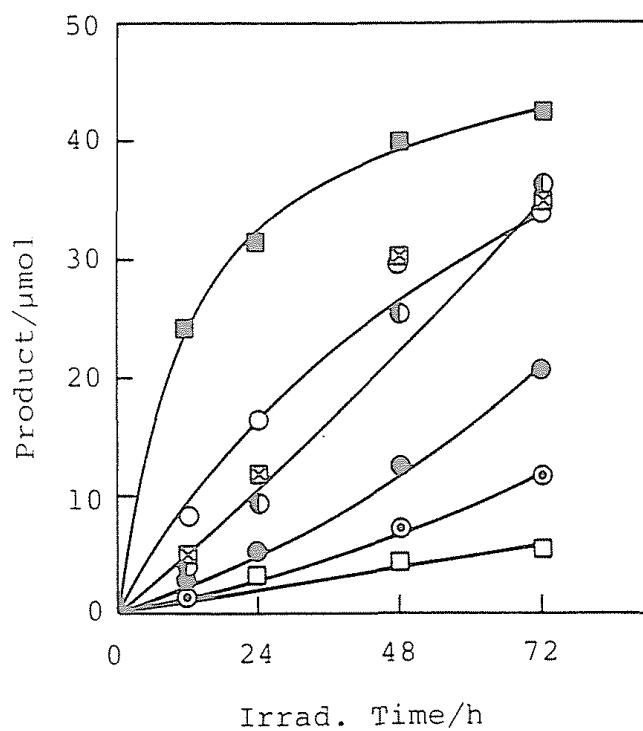


Figure 2 Time course of the photocatalytic formation of H<sub>2</sub> (○), CH<sub>4</sub> (●), C<sub>2</sub>H<sub>6</sub> (⊙), CO (◐), HCHO (□), CH<sub>3</sub>CHO (■), and HOCH<sub>2</sub>CH<sub>2</sub>OH (⊠) by TiO<sub>2</sub>/Pt (50 mg) suspended in a 0.5 M H<sub>2</sub>SO<sub>4</sub> solution (5.0 cm<sup>3</sup>) of PEO (22 mg).

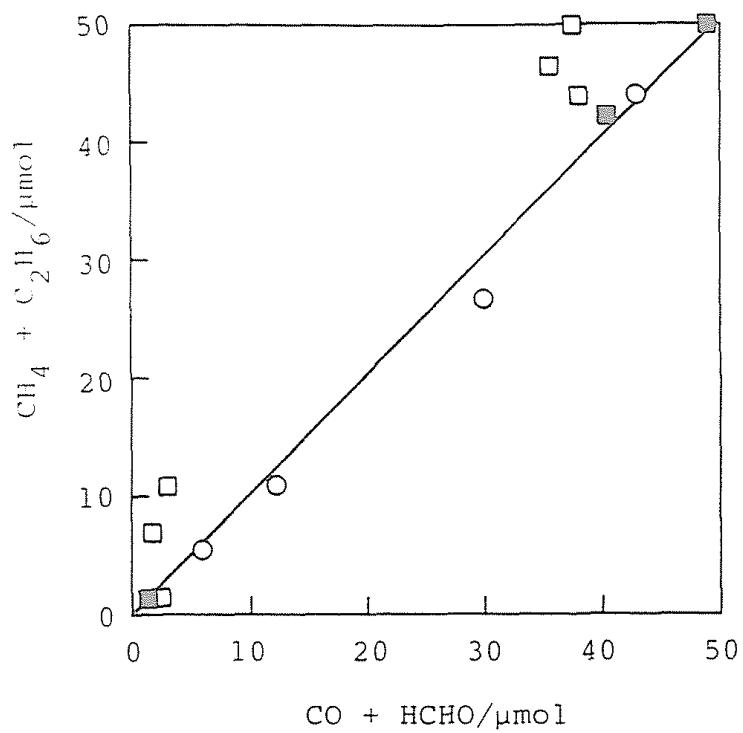
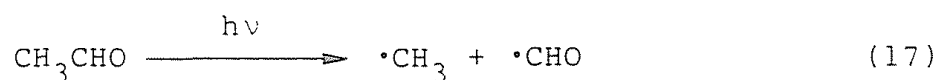


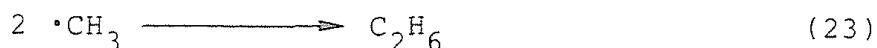
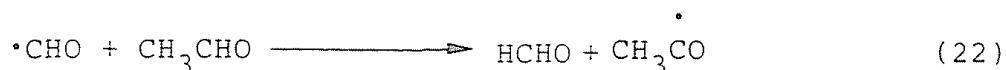
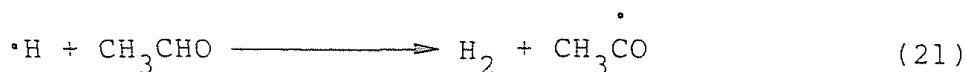
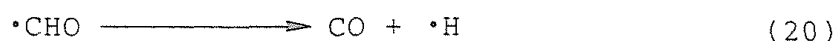
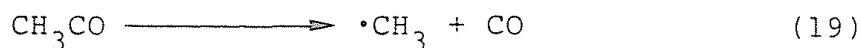
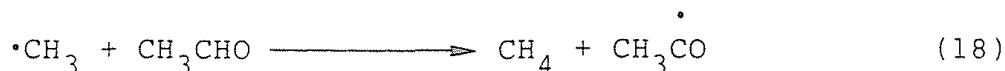
Figure 3 Material balance in the  $\text{TiO}_2/\text{Pt}$  photocatalytic reaction of PEO (○) and in the photolysis of  $\text{CH}_3\text{CHO}$  in the presence (■) and absence (□) of  $\text{TiO}_2/\text{Pt}$ . Data were obtained from Figure 2 and Table 1.

the product yields.

When the photoirradiation was performed only on the liquid phase, the yields of gaseous products decreased drastically (Runs 9 and 10). Therefore, most part of the photolysis of  $\text{CH}_3\text{CHO}$  occurred in the gas phase. The photolysis is initiated by photoabsorption ( $\lambda_{\text{ex}} > 300 \text{ nm}$ , (see Figure 4) corresponds to energy  $< 97 \text{ kcal mol}^{-1}$ ) to decompose into  $\cdot\text{CH}_3$  and  $\cdot\text{CHO}^{14}$  (this reaction is more likely than the process to give  $\cdot\text{H}$  and  $\text{CH}_3\text{CO}$  because of the smaller dissociation energy ( $71\text{-}75 \text{ kcal mol}^{-1} < 88 \text{ kcal mol}^{-1}$  for the latter)).



Following reactions proceed to produce  $\text{CH}_4$ ,  $\text{C}_2\text{H}_6$ ,  $\text{CO}$ ,  $\text{H}_2$ , and  $\text{HCHO}$ .



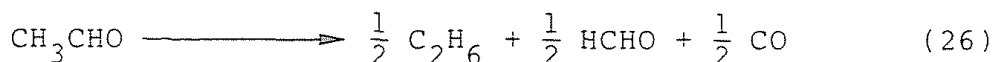
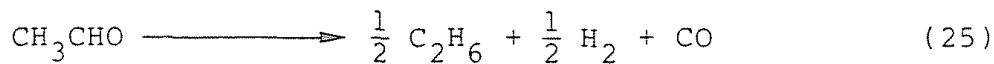
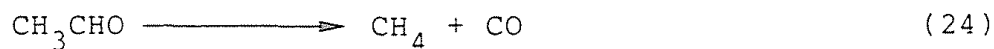
As shown in Figure 3, these reactions satisfy the following

Table 2 Photoinduced decomposition of acetaldehyde in the presence and absence of TiO<sub>2</sub>/Pt catalyst.<sup>a</sup>

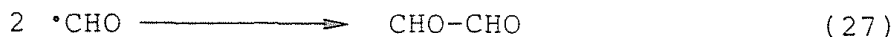
Run	TiO <sub>2</sub> /Pt /mg	Solvent	Irrad. <sup>b</sup>	Product/ $\mu$ mol				
				H <sub>2</sub>	CH <sub>4</sub>	C <sub>2</sub> H <sub>6</sub>	CO	HCHO
1	0	H <sub>2</sub> O	L + G	2.0	26.4	10.2	34.3	1.5
2	0	2.5 M H <sub>2</sub> SO <sub>4</sub>	L + G	4.9	21.1	11.9	37.5	0.7
3	0	0.5 M H <sub>2</sub> SO <sub>4</sub>	L + G	3.3	26.2	12.0	36.1	1.6
4	0	1.0 M NaOH	L + G	0.1	0.5	0.5	2.0	0.6
5	0	H <sub>2</sub> O	None	$\approx$ 0	$\approx$ 0	$\approx$ 0	$\approx$ 0	$\approx$ 0
6	50	H <sub>2</sub> O	L + G	4.4	20.8	11.0	38.4	2.1
7	50	2.5 M H <sub>2</sub> SO <sub>4</sub>	L + G	10.6	23.3	13.3	47.7	1.5
8	50	1.0 M NaOH	L + G	2.7	0.8	0.3	1.3	$\approx$ 0
9	0	H <sub>2</sub> O	L	0.2	10.2	0.4	2.9	0.5
10	0	2.5 M H <sub>2</sub> SO <sub>4</sub>	L	2.8	5.5	0.8	1.2	0.3

<sup>a</sup>Acetaldehyde (500  $\mu$ mol) and solvent (5.0 cm<sup>3</sup>) were placed in a glass tube and irradiated with a 400-W high-pressure mercury arc for 20 h under Ar at room temperature. <sup>b</sup>L + G: irradiated on both liquid and gas (ca. 30 cm<sup>3</sup>) phase, None: not irradiated, and L: irradiated only on liquid phase.

stoichiometries, among which reaction (24) proceeds predominantly.



Small deviation from the linear relation in the photolysis in the absence of  $\text{TiO}_2/\text{Pt}$  (Figure 3) is attributable to the other reaction process in the liquid phase, because the deviation was observed even when only the liquid phase was photoirradiated. The possible process is recombination of  $\cdot\text{CHO}$  to produce dialdehyde which could not be detected at present.



Since the  $\text{TiO}_2$  suspension absorbs the light of wavelength  $< \text{ca. } 400 \text{ nm}$  almost completely under the present conditions (see Chapter 1), light absorption by  $\text{CH}_3\text{CHO}$  in the liquid phase shown in Figure 4 is prevented in the  $\text{TiO}_2/\text{Pt}$  suspension. Therefore, the yield ratio of the liquid-phase photolysis of  $\text{CH}_3\text{CHO}$  in the presence of  $\text{TiO}_2/\text{Pt}$  decreases by this "filter" effect of  $\text{TiO}_2$ .

The smaller yield from the alkaline solution (Run 4) is accounted for by the hydration which prevents vaporization of  $\text{CH}_3\text{CHO}$  into gas phase.



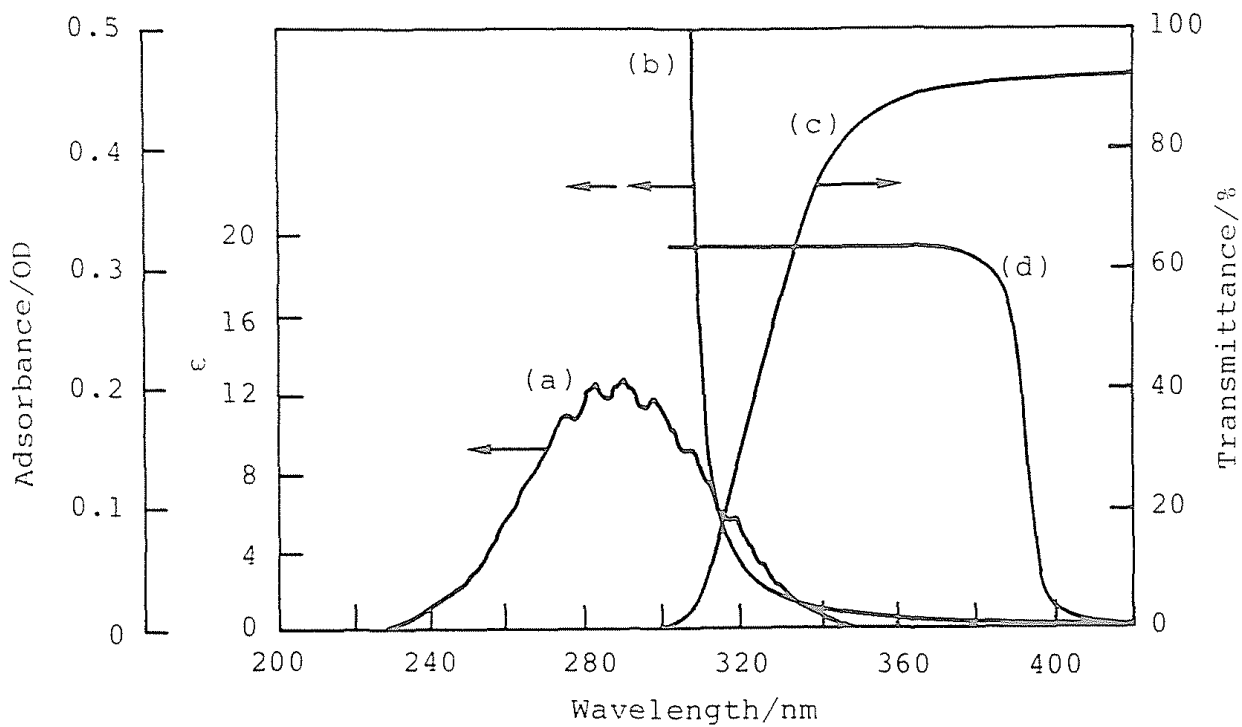
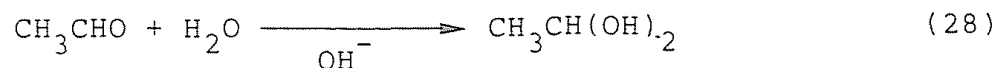


Figure 4 Absorption spectra of acetaldehyde in vapor phase (a) and in aqueous solution ( $2.2 \text{ mol dm}^{-3}$ ) (b), transmission spectrum of a reaction vessel (18 mm $\phi$   $\times$  180 mm glass tube) (c) and action spectrum of photocatalytic dehydrogenation of 2-propanol by aqueous  $\text{TiO}_2/\text{Pt}$  suspension (see Chapter 1) (d).



Nevertheless, the predominant reactions (24) and (25) produced  $\text{CH}_4$ ,  $\text{C}_2\text{H}_6$ , and  $\text{CO}$  in the ratio of ca. 4 : 2 : 7, similar to that obtained in the  $\text{TiO}_2/\text{Pt}$  photocatalyzed degradation of PEO under the acidic conditions.

pH-Dependent Behavior of the Photocatalytic Reaction of PEO in Aqueous Solution. Figure 5 shows the pH-dependent yields of the degraded products. The  $\text{CH}_3\text{CHO}$  formation became significant at  $\text{pH} < 4$ , accompanied by the gaseous products due to the photolysis in the gas phase.

On the other hand, the  $\text{H}_2$  formation was not so enhanced by the pH decrease. The amount of  $\text{H}_2$  liberated by the photocatalytic action of  $\text{TiO}_2/\text{Pt}$  (reaction (2)) can be estimated, taking the  $\text{CH}_3\text{CHO}$  photolysis (to yield  $\text{H}_2$ ) into consideration (equation (16)), as ( $\text{H}_2 - 0.3 \text{CH}_4$ ). This corrected yield of  $\text{H}_2$  shown in Figure 5 was practically constant regardless of the pH. This fact suggests that essential activity of  $\text{TiO}_2/\text{Pt}$  for the  $\text{H}_2$  formation is not influenced by the pH in the acidic region. Therefore, the enhanced yields of  $\text{CH}_3\text{CHO}$  and the  $\text{CH}_3\text{CHO}$  originated products is attributable to the acid catalyzed degradation of the polymer radical of PEO into  $\text{CH}_3\text{CHO}$  (reaction (9)).

On the basis of the reactions (1), (2), (6), and (8), stoichiometry for the formations of  $\text{H}_2$  and the polymer radical is expressed as,

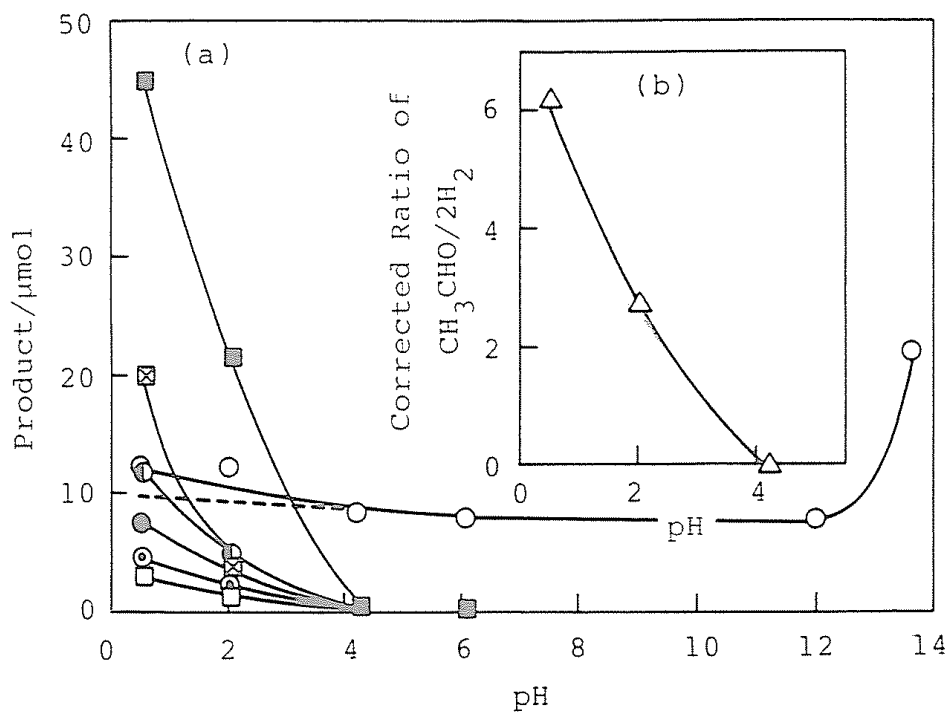
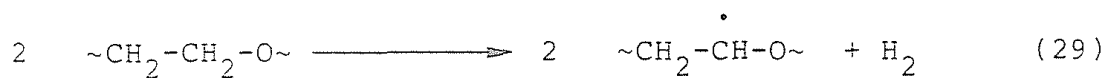
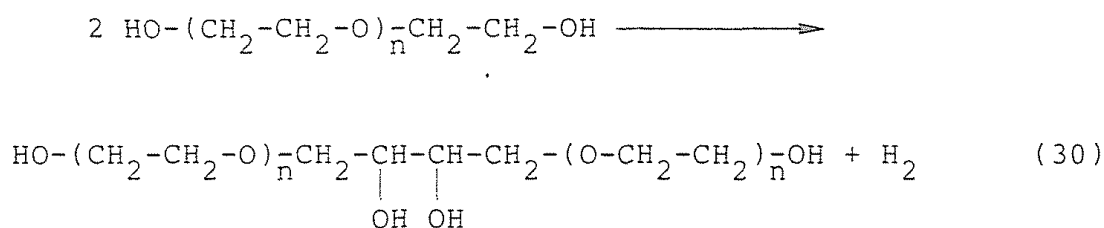


Figure 5 (a) pH dependence of the product yield of  $\text{H}_2$  ( $\circ$ ),  $\text{CH}_4$  ( $\bullet$ ),  $\text{C}_2\text{H}_6$  ( $\odot$ ),  $\text{CO}$  ( $\ominus$ ),  $\text{HCHO}$  ( $\square$ ),  $\text{CH}_3\text{CHO}$  ( $\blacksquare$ ), and  $\text{HOCH}_2\text{-CH}_2\text{OH}$  ( $\boxtimes$ ). Broken line indicates the corrected  $\text{H}_2$  yield (see text). (b) Corrected ratio of  $(\text{CH}_3\text{CHO} / 2 \times \text{H}_2)$ .



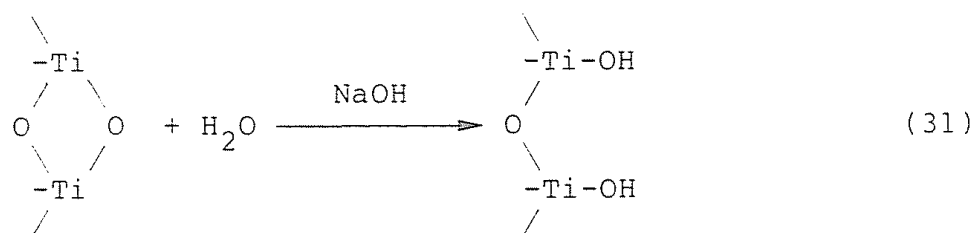
Consequently, the yield ratio of  $\text{CH}_3\text{CHO}$  to twice of  $\text{H}_2$  ( $\text{CH}_3\text{CHO}/2\times\text{H}_2$ ) indicates the efficiency of the chain reaction to produce  $\text{CH}_3\text{CHO}$ . For convenience, total amount of  $\text{CH}_3\text{CHO}$  liberated by the photocatalytic action of  $\text{TiO}_2/\text{Pt}$  was estimated as sum of  $\text{CH}_3\text{CHO}$ ,  $\text{CH}_4$ , and twice of  $\text{C}_2\text{H}_6$  according to the stoichiometry shown in the preceding section (equation (16)). As shown in Figure 5(b), the ratio increased with the pH decrease to attain ca. 6 at  $\text{pH} \approx 0.6$ . These results show that the chain reaction by  $\cdot\text{CH}_2\text{CHO}$  (reaction (11)) produces averagely 6 molecules of  $\text{CH}_3\text{CHO}$  from one polymer radical.

With the increase of pH, the degradation of PEO became less significant. Only  $\text{H}_2$  was observed at  $\text{pH} > 4$ , due to the reduction of  $\text{H}^+$  by the photogenerated electron (reaction (2)). The simultaneously generated hole produced the 1,2-diol, dimeric product, which resembles the dimerization of tert-butyl alcohol (Chapter 2). In this case stoichiometry could be expressed as,



The enhanced  $\text{H}_2$  yield under alkaline conditions ( $\text{pH} \approx 13.6$ ,  $1 \text{ mol dm}^{-3}$   $\text{NaOH}$ ) has also been observed in the  $\text{TiO}_2/\text{Pt}$  photocatalyzed reactions of aliphatic alcohols and amines (Chapters 1-3 and 5, respectively). This behavior may be due to the increased surface

hydroxyl group, as a hole trapping site, induced by the alkaline treatment of the dehydrated TiO<sub>2</sub> surface.



As described above, the pH-dependent modification of the TiO<sub>2</sub> surface, due to the acid-base equilibria of the surface hydroxyl group, gives significant influence not only on the photocatalytic activity but also on the mode of the reaction, degradation or prolongation of PEO chain.

## REFERENCES AND NOTES

- 1 A. J. Bard, *J. Photochem.*, 10, 59 (1979).
- 2 A. J. Nozik, *Annu. Rev. Phys. Chem.*, 29, 189 (1978).
- 3 M. S. Wrighton, P. T. Wolczanski, and A. B. Ellis, *J. Solid. State Chem.*, 22, 17 (1977).
- 4 T. Kawai and T. Sakata, *Chem. Lett.*, 81 (1981).
- 5 T. Sakata and T. Kawai, *Nouv. J. Chim.*, 5, 279 (1981).
- 6 P. Pichat, J.-M. Herrmann, J. Disdier, H. Courbon, and M.-N. Mozzanega, *Nouv. J. Chim.*, 5, 627 (1981).
- 7 S. Teratani, J. Nakamichi, K. Taya, and K. Tanaka, *Bull. Chem. Soc. Jpn*, 55, 1688 (1982).
- 8 K. Domen, S. Naito, T. Onishi, and K. Tamaru, *Chem. Lett.*, 555 (1982).
- 9 S. Nishimoto, B. Ohtani, A. Sakamoto, and T. Kagiya, *Nippon Kagaku Kaishi*, 246 (1984).
- 10 S. Arimitsu and T. Imafuku, *Symposium on Photochemistry 1981, Sapporo Japan*, IIIA 103.
- 11 Japan Industrial Standard K 102 (1974).
- 12 D. J. Edge, B. C. Gilbert, R. O. C. Norman, and P. R. West, *J. Chem. Soc. (B)*, 189 (1971).
- 13 E. L. Jackson, "Organic Reactions," vol.2, Wiley, New York (1957).
- 14 J. G. Calvert and J. N. Pitts Jr., "Photochemistry," Wiley, New York (1967).

## Chapter 5

### Photocatalytic Deaminoalkylation and Cyclization of Aliphatic Amines by Aqueous Suspension of Platinized TiO<sub>2</sub>

#### ABSTRACT

Photoirradiation ( $\lambda_{\text{ex}} > 300 \text{ nm}$ ) of a powdered mixture of anatase TiO<sub>2</sub> with platinum black (5 wt%, TiO<sub>2</sub>/Pt) suspended in an aqueous solution of aliphatic amines has been carried out under Ar at room temperature. Amines of the form RCH<sub>2</sub>NH<sub>2</sub> dissolved in distilled water were converted to symmetrical secondary amines along with liberation of ammonia (NH<sub>3</sub>) and hydrogen (H<sub>2</sub>), while were converted to corresponding primary alcohols and aldehydes in the NaOH solution. Increase of the concentration of NaOH and the amount of Pt loaded on TiO<sub>2</sub> enhanced the photocatalytic deamino-oxidation of propylamine. Deuterium labeling pattern of dipropylamine obtained from propylamine in distilled water was in accord with the mechanism of the photocatalytic deamino-N-alkylation involving in situ hydrogenation of a Schiff base intermediate.  $\alpha$ -Substituted primary amines, such as isopropylamine, were converted to the corresponding ketones and secondary alcohols in both distilled water and NaOH solutions. The increase of the concentration of NaOH and the amount of Pt also enhanced this photocatalytic deamino-oxidation of isopropylamine, and changed the selectivity. As an extensive studies on the deamino-N-alkylation, new photocatalytic reactions were performed to synthesize secondary amines, such as cyclic secondary amines from polymethylene- $\alpha,\omega$ -diamines.

## INTRODUCTION

A number of studies concerning the photocatalytic reaction of semiconductor materials, especially n-type  $\text{TiO}_2$  and related composites, have focused on the utilization of solar energy to produce hydrogen ( $\text{H}_2$ ) from water.<sup>1</sup> In most of the photocatalytic reactions by platinized  $\text{TiO}_2$  powder, organic compounds, such as alcohols, are dehydrogenated into corresponding carbonyl derivatives with the evolution of  $\text{H}_2$  under deaerated conditions as described in Chapters 1-3 of this thesis. More recently several attempts have been made to extend heterogeneous photocatalysis with dispersed semiconductors to synthetic chemistry.<sup>2-7</sup> However, reaction of organic compounds in these photocatalytic systems are apparently limited to the oxidation to yield carbonyl or hydroxylated derivatives, which is essentially identical to anodic process on a photoirradiated semiconductor electrode. The platinized  $\text{TiO}_2$  particle can be regarded as a short-circuited photoelectrochemical cell;  $\text{TiO}_2$  anode being in contact with platinum cathode. In this respect, it is expected that combined photoinduced reaction, not observable in the conventional photoelectrochemical cell, including both oxidation at  $\text{TiO}_2$  surface and subsequent reduction at platinum side occurs effectively on the platinized  $\text{TiO}_2$  particle by the use of photogenerated positive hole and electron, respectively.

This chapter concerns a photocatalytic process of synthesizing secondary amines from primary amines, which is not simple oxidation or reduction process, in aqueous solution by the use of a powdered mixture of  $\text{TiO}_2$  with platinum black. These reactions proceeded efficiently at ambient temperature, in contrast to thermal processes



by homogeneous ruthenium<sup>8</sup> and heterogeneous palladium<sup>9</sup> catalysts.

## EXPERIMENTAL

Materials. Anatase TiO<sub>2</sub> powder was supplied by Merck and ground with 5 wt% of platinum black (Nakarai Chemicals) to prepare catalyst (TiO<sub>2</sub>/Pt). The aqueous suspension of TiO<sub>2</sub>/Pt was made up with ion exchanged distilled water. Deuterized water (D<sub>2</sub>O) was obtained from CEA (99.85 %) and used without further purification. The other materials were obtained commercially and used as received.

Photoirradiation. A suspension of 50 mg of the TiO<sub>2</sub>/Pt catalyst in 5.0 cm<sup>3</sup> of water or NaOH aq. in a glass tube (18 mmφ × 180 mm, transparent for the light of wavelength > 300 nm) was purged by Ar for 30 min and sealed off with a rubber stopper. Substrate aliphatic amine (60-1000 μmol) was injected through the cap by a micro syringe. Photoirradiation was performed using a merry-go-round apparatus equipped with a 400-W or 500-W high-pressure mercury arc (Eiko-sha 400 or 500) under magnet stirring at room temperature.

Product Analysis. After the irradiation, a portion of gaseous products liberated in the gas phase of the reaction mixture was collected by a micro syringe and analyzed by gas chromatography (Shimadzu GC 4A equipped with a TCD and a Molecular Sieves 5A column). The suspension was centrifuged to separate the catalyst and the aqueous solution was analyzed by gas chromatography, <sup>13</sup>C NMR, and gas chromatography-mass spectroscopy (GC-MS). Products were identified by comparison with authentic samples. The typical conditions of the gas chromatographic analysis are as follows; a Shimadzu GC 6A equipped with an FID and a Chromosorb 103 or 20 % Polyethylene Glycol 20M

on Celite 545 column (3 mmφ × 3 m).  $^{13}\text{C}$  NMR spectra were recorded on JEOL JNM FX-100 (25.0 MHz; spectral width, 6 kHz; acquisition time, 0.4096 s; data points, 4096; pulse width 5 μs (45.0 °); pulse interval 1.0 s; number of transients, 2000-10000). The spectra were measured at room temperature, using a  $\text{H}_2\text{O}/\text{D}_2\text{O}$  solution with 1,4-dioxane as an internal standard. The  $^{13}\text{C}$  chemical shift of 1,4-dioxane was 67.4 ppm downfield from tetramethylsilane. Ammonia ( $\text{NH}_3$ ) liberated in the reaction mixture was determined by the indophenol blue method.<sup>10</sup> Gas chromatographic analysis of the gas phase of the reaction mixture revealed that most part (> 98 %) of ammonia liberated during the photoreaction remained in the aqueous solution. The GC-MS measurement was performed using a Hitachi M 80 with ionization potential 70 eV.<sup>11</sup>

## RESULTS AND DISCUSSION

Photocatalytic Deamino-N-alkylation and Oxidation of Aliphatic Amines by Aqueous Suspension of Platinized  $\text{TiO}_2$ . Photoirradiation ( $\lambda_{\text{ex}} > 300 \text{ nm}$ ) on aqueous suspension of  $\text{TiO}_2/\text{Pt}$  powder in aqueous alkylamine solutions under an Ar atmosphere led to the hydrogen ( $\text{H}_2$ ) and ammonia ( $\text{NH}_3$ ) liberations. Table 1 shows the main products other than  $\text{H}_2$  and  $\text{NH}_3$  obtained from a series of alkylamines in distilled water ( $\text{H}_2\text{O}$ ) or 6 mol  $\text{dm}^{-3}$  NaOH solution. Both  $\text{H}_2$  and  $\text{NH}_3$  yields from these alkylamines in 6 mol  $\text{dm}^{-3}$  were 2-10 times as much as those in distilled water, showing the photoinduced reaction could be enhanced under the alkaline conditions.

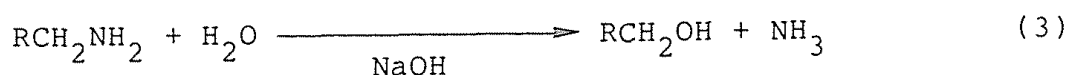
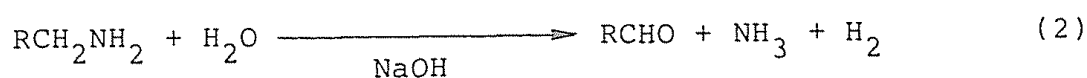
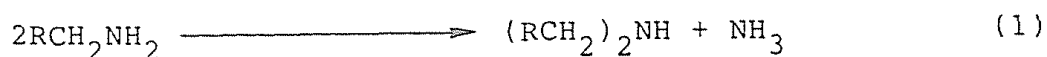
The product distributions were also considerably influenced by the solution conditions. Under the neutral conditions, primary

Table 1 Products observed in the photocatalytic reaction of aliphatic amines in aqueous solution (5.0 cm<sup>3</sup>) by TiO<sub>2</sub>/Pt (50 mg) catalyst.<sup>a</sup>

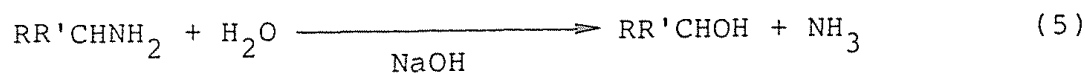
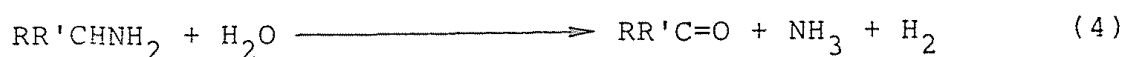
Run	Substrate <sup>b</sup>	Hg arc/W	in H <sub>2</sub> O			in 6 mol dm <sup>-3</sup> NaOH				
			Irrad. /h	Organic Product	/μmol H <sub>2</sub> NH <sub>3</sub>	Irrad. /h	Organic Product	/μmol H <sub>2</sub> NH <sub>3</sub>		
1	CH <sub>3</sub> CH <sub>2</sub> NH <sub>2</sub>	500	41	(CH <sub>3</sub> CH <sub>2</sub> ) <sub>2</sub> NH	41	101	16	CH <sub>3</sub> CH <sub>2</sub> OH	466	255
2	CH <sub>3</sub> CH <sub>2</sub> CH <sub>2</sub> NH <sub>2</sub>	500	21	(CH <sub>3</sub> CH <sub>2</sub> CH <sub>2</sub> ) <sub>2</sub> NH <sup>c</sup> CH <sub>3</sub> CH <sub>2</sub> CH <sub>2</sub> OH CH <sub>3</sub> CH <sub>2</sub> CHO	26	52	14	CH <sub>3</sub> CH <sub>2</sub> CH <sub>2</sub> OH CH <sub>3</sub> CH <sub>2</sub> CHO	305	135
3	CH <sub>3</sub> CH <sub>2</sub> CH <sub>2</sub> CH <sub>2</sub> NH <sub>2</sub>	500	41	(CH <sub>3</sub> CH <sub>2</sub> CH <sub>2</sub> CH <sub>2</sub> ) <sub>2</sub> NH <sup>c</sup>	88	199	16	CH <sub>3</sub> CH <sub>2</sub> CH <sub>2</sub> CH <sub>2</sub> OH	264	118
4	(CH <sub>3</sub> ) <sub>2</sub> CHNH <sub>2</sub>	400	42	(CH <sub>3</sub> ) <sub>2</sub> C=O	133	165	8	(CH <sub>3</sub> ) <sub>2</sub> C=O (CH <sub>3</sub> ) <sub>2</sub> CHOH	345	359
5	CH <sub>3</sub> CH <sub>2</sub> (CH <sub>3</sub> )CHNH <sub>2</sub>	500	41	CH <sub>3</sub> CH <sub>2</sub> (CH <sub>3</sub> )C=O	103	123	16	CH <sub>3</sub> CH <sub>2</sub> (CH <sub>3</sub> )C=O CH <sub>3</sub> CH <sub>2</sub> (CH <sub>3</sub> )CHOH	272	215
6	(CH <sub>3</sub> CH <sub>2</sub> ) <sub>2</sub> NH	400	41	(CH <sub>3</sub> CH <sub>2</sub> ) <sub>3</sub> N CH <sub>3</sub> CH <sub>2</sub> NH <sub>2</sub>	26	11	16	CH <sub>3</sub> CH <sub>2</sub> NH <sub>2</sub>	442	72
7	(CH <sub>3</sub> CH <sub>2</sub> CH <sub>2</sub> ) <sub>2</sub> NH	400	41	CH <sub>3</sub> CH <sub>2</sub> CH <sub>2</sub> NH <sub>2</sub>	20	6	16	CH <sub>3</sub> CH <sub>2</sub> CH <sub>2</sub> NH <sub>2</sub>	166	9
8	(CH <sub>3</sub> CH <sub>2</sub> ) <sub>3</sub> N	400	41	(CH <sub>3</sub> CH <sub>2</sub> ) <sub>2</sub> NH	19	0	16	(CH <sub>3</sub> CH <sub>2</sub> ) <sub>2</sub> NH	226	9
9	(CH <sub>3</sub> CH <sub>2</sub> CH <sub>2</sub> ) <sub>3</sub> N	400	41	(CH <sub>3</sub> CH <sub>2</sub> CH <sub>2</sub> ) <sub>2</sub> NH	49	8	16	(CH <sub>3</sub> CH <sub>2</sub> CH <sub>2</sub> ) <sub>2</sub> NH	98	2

<sup>a</sup>Confirmed by gas chromatography and GC-MS. <sup>b</sup>1.0 mmol. <sup>c</sup>Also confirmed by <sup>13</sup>C NMR.

amines such as ethylamine (Run 1), propylamine (Run 2), and butylamine (Run 3) preferably gave symmetrical secondary amines, while these primary amines were converted into the corresponding primary alcohols and aldehydes under the alkaline conditions. These reactions of the primary amines are given tentatively as follows.

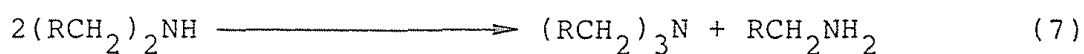
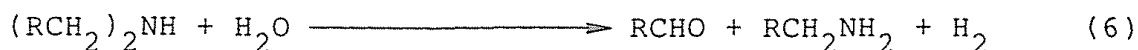


On the other hand,  $\alpha$ -substituted primary amines such as isopropylamine (Run 4) or sec-butylamine (Run 5) gave corresponding ketones in distilled water and both the ketones and secondary alcohols in 6 mol dm<sup>-3</sup> NaOH, although corresponding secondary amines could not be detected in these cases. The predominant reactions are expressed as follows.



These reactions of the primary amines could be observed neither in the dark nor in the absence of the TiO<sub>2</sub>/Pt catalyst. Moreover, negligible amount of the products were obtained when TiO<sub>2</sub> alone, without Pt, was used as photocatalyst.

From the aqueous suspension of secondary amines, such as diethylamine (Run 6) and dipropylamine (Run 7), both primary and tertiary amines were obtained by the photoirradiation in the presence of  $\text{TiO}_2/\text{Pt}$ . In these cases, overall reaction scheme would be given as follows.



Small amount of  $\text{NH}_3$  is attributable to the photocatalytic decomposition of the product primary amine ( $\text{RCH}_2\text{NH}_2$ ).

In the case of tertiary amines, triethylamine (Run 8) and tributylamine (Run 9), secondary amines were detected along with the  $\text{H}_2$  and  $\text{NH}_3$  formation while the amount of  $\text{NH}_3$  was negligibly small in both distilled water and NaOH solution.



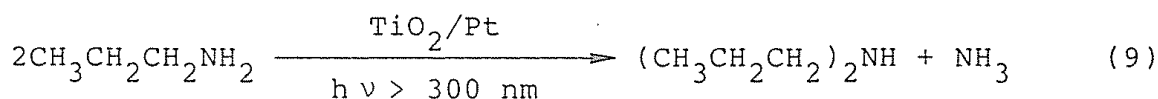
The rate of such dealkylation of the secondary and tertiary amines was relatively small compared with those of the primary amines. The yields of  $\text{H}_2$  and  $\text{NH}_3$  in distilled water were in the order: (tertiary)  $\leq$  (secondary)  $\ll$  (primary)  $<$  ( $\alpha$ -substituted primary). In the NaOH solutions a similar order was also observed.

Although both  $\text{TiO}_2/\text{Pt}$  and the photoirradiation were indispensable for the  $\text{H}_2$  formation, the dealkylation of the secondary and tertiary amines could be observed in the dark at ca. 50 °C, indicating

the products are attributable to both photocatalytic reaction by  $\text{TiO}_2/\text{Pt}$  and thermal reaction in the case of the secondary and tertiary amines.

Photocatalytic Secondary Amine Formation from Propylamine in Distilled Water by Platinized  $\text{TiO}_2$ . Figure 1(a) shows the time-course of photoinduced reaction of propylamine in distilled water by the  $\text{TiO}_2/\text{Pt}$  catalyst. The amount of propylamine decreased monotonously along with the irradiation to result in the formation of photocatalytic products, dipropylamine, propionaldehyde, 1-propanol,  $\text{H}_2$ , and  $\text{NH}_3$ , suggesting that the deamination of propylamine took place efficiently. Among the carbon-containing products, dipropylamine was mainly produced but rather decreased by the prolonged irradiation.

As shown in Figure 1(b), the consumption of propylamine in a series of the above described experiments was practically identical to the total amount of dipropylamine and ammonia formed during the irradiation, indicating the reasonable balance for nitrogen. Figure 1(b) also shows the material balance for carbon; sum of carbon-containing products, dipropylamine, 1-propanol, and propionaldehyde was plotted against the propylamine consumption. A reasonable linear relation was observed by the photoirradiation up to 20 h. On the basis of these results, the photocatalytic reaction of propylamine proceeds predominantly as follows.



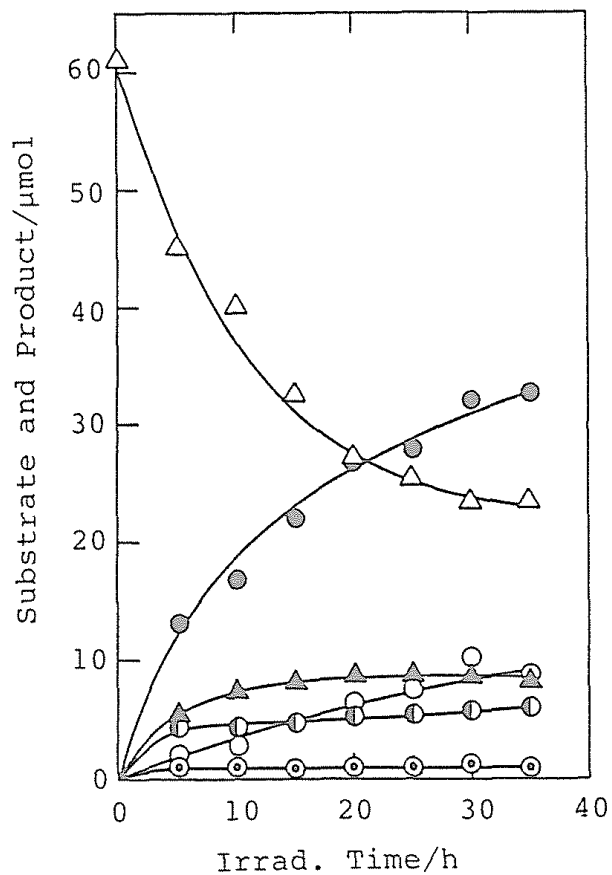


Figure 1 (a) Time course of the photocatalytic reaction of propylamine in distilled water by  $\text{TiO}_2/\text{Pt}$  catalyst;  $\triangle$   $\text{CH}_3\text{CH}_2\text{CH}_2\text{NH}_2$ ,  $\bullet$   $\text{NH}_3$ ,  $\blacktriangle$   $(\text{CH}_3\text{CH}_2\text{CH}_2)_2\text{NH}$ ,  $\ominus$   $\text{CH}_3\text{CH}_2\text{CH}_2\text{OH}$ ,  $\circ$   $\text{H}_2$ , and  $\odot$   $\text{CH}_3\text{CH}_2\text{CHO}$ . Irradiation was performed using a 400-W high-pressure mercury arc.

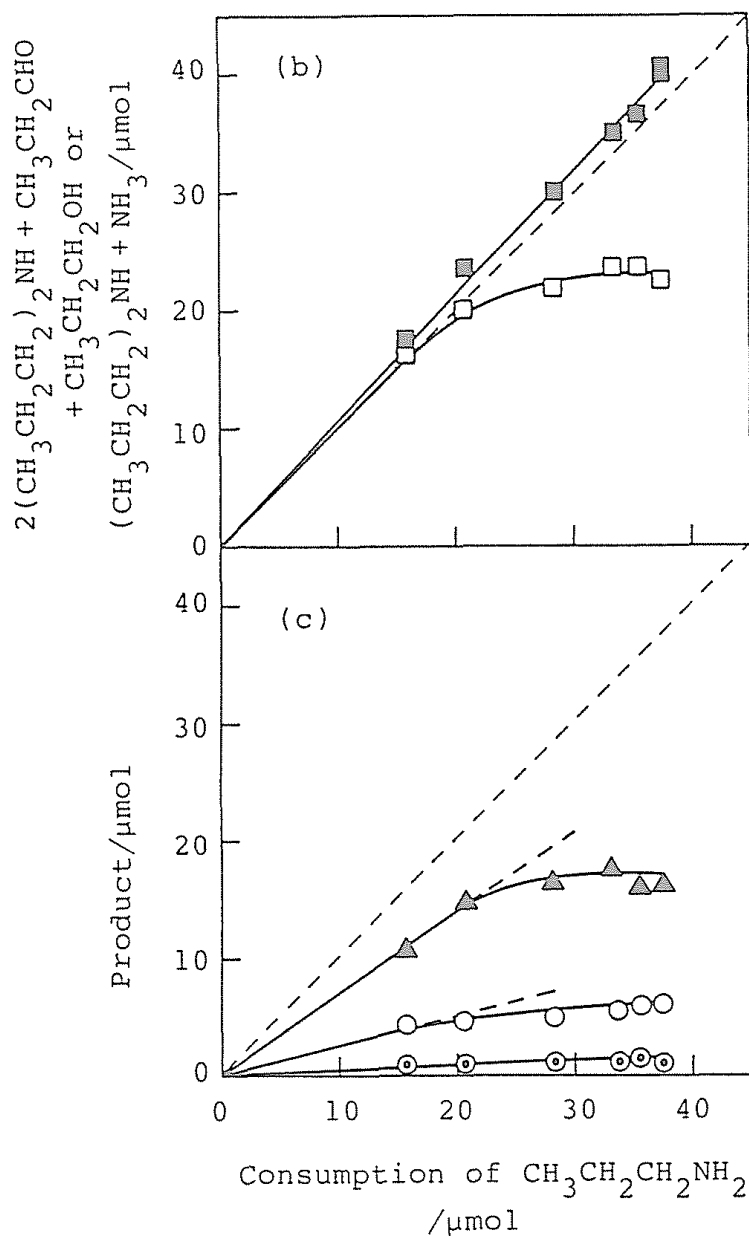
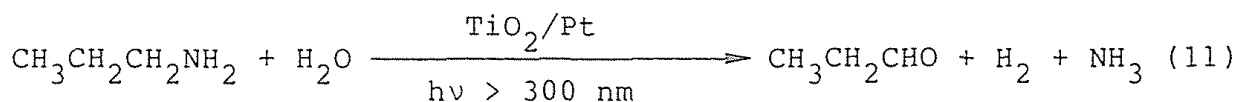
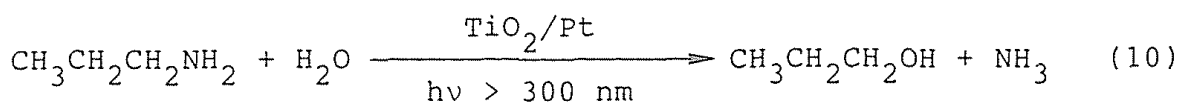


Figure 1 (b)Material balance for nitrogen ( $(\text{CH}_3\text{CH}_2\text{CH}_2)_2\text{NH} + \text{NH}_3$ , ■ ) and carbon ( $2(\text{CH}_3\text{CH}_2\text{CH}_2)_2\text{NH} + \text{CH}_3\text{CH}_2\text{CH}_2\text{OH} + \text{CH}_3\text{CH}_2\text{CHO}$ , □ ), and (c)product distribution in the photocatalytic reaction of propylamine in distilled water. Symbols are same as in Figure 1(a).





The yield ratio of reaction (9)-(11) in distilled water was obtained as 71 : 23 : 5 on the basis of the propylamine consumption as shown in Figure 1(c).

Deviation from the straight line by > 20 h irradiation shows the formation of another product, such as propionic acid which is oxidized product of propionaldehyde or 1-propanol and could be detected qualitatively in the present experiments.

Photocatalytic Alcohol and Aldehyde Formations from Propylamine in Aqueous NaOH Solution by Platinized TiO<sub>2</sub>.

In the aqueous NaOH solution the reaction of propylamine changed drastically compared with that in the distilled water. Figure 2(a) shows the time course of the photocatalytic reaction of propylamine in 1 mol dm<sup>-3</sup> NaOH by the TiO<sub>2</sub>/Pt catalyst. The overall conversion of propylamine, estimated from the NH<sub>3</sub> yield in respect that reactions (9)-(11) involves the NH<sub>3</sub> formation, increased ca. 2.5 times (in the NaOH solution) compared with that in distilled water as shown in Figure 2(d) (the difference is ambiguous by the comparison between Figures 1(a) and 2(a) because of the different photoirradiation conditions). The increased rate of the propylamine consumption is possibly due to the increased oxidation sites, the surface hydroxyl, induced by the alkaline treatment, as is discussed in the following section.

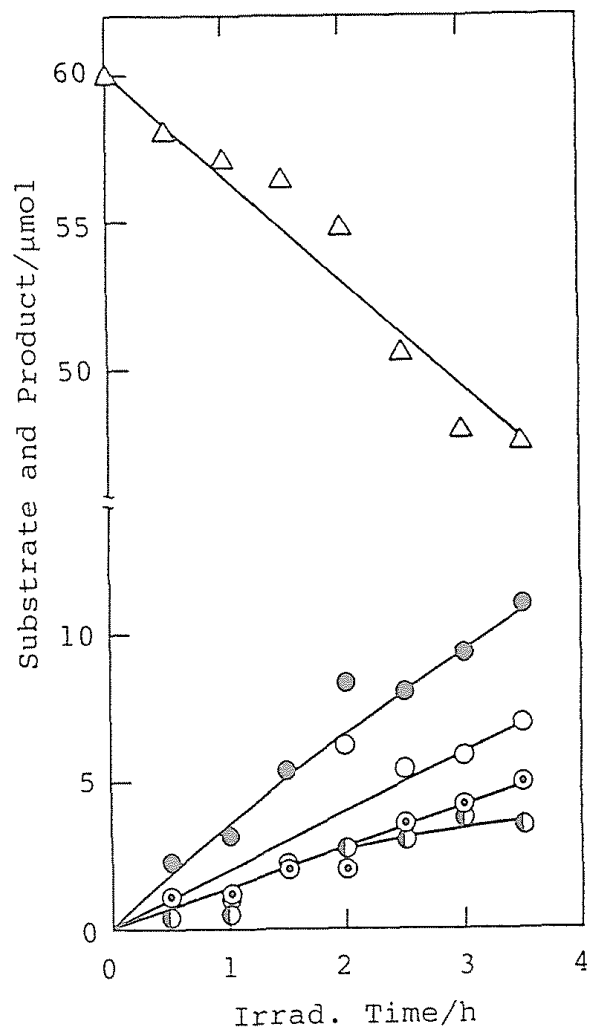


Figure 2 (a) Time course of the photocatalytic reaction of propylamine in  $1 \text{ mol dm}^{-3}$  NaOH by  $\text{TiO}_2/\text{Pt}$  catalyst;  $\Delta$   $\text{CH}_3\text{CH}_2\text{CH}_2\text{NH}_2$ ,  $\bullet$   $\text{NH}_3$ ,  $\circ$   $\text{H}_2$ ,  $\oplus$   $\text{CH}_3\text{CH}_2\text{CH}_2\text{OH}$ , and  $\odot$   $\text{CH}_3\text{CH}_2\text{CHO}$ . Irradiation was performed using a 500-W high-pressure mercury arc.

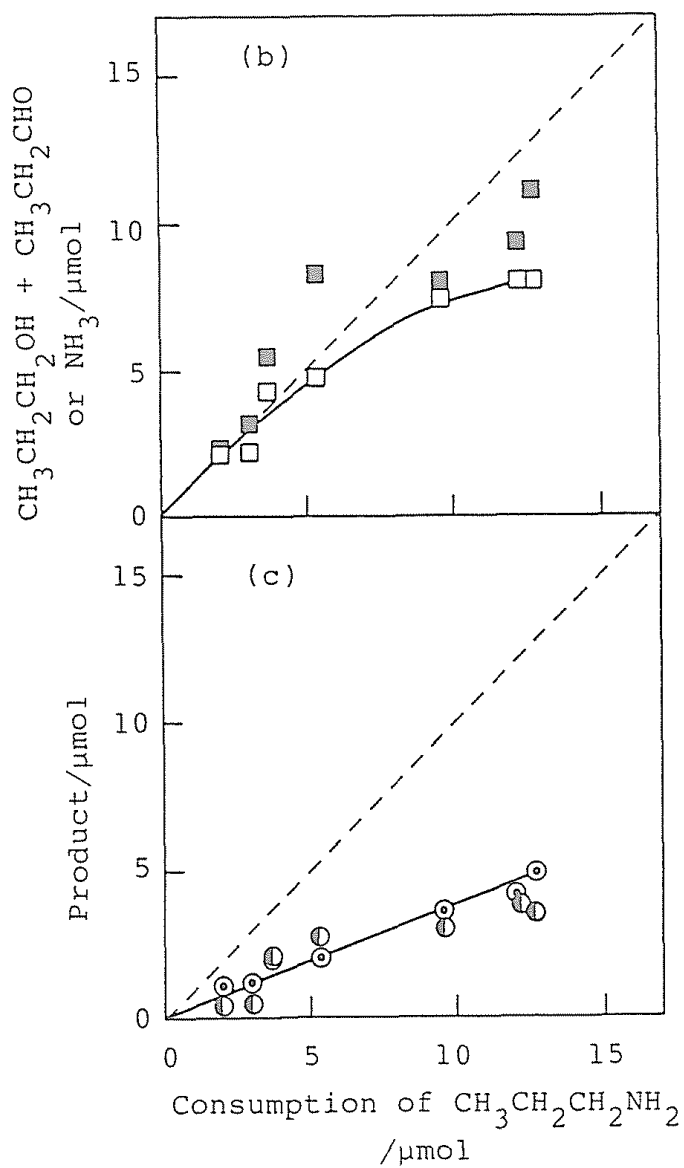


Figure 2 (b)Material balance for nitrogen ( $\text{NH}_3$ ,  $\blacksquare$ ) and carbon ( $\text{CH}_3\text{CH}_2\text{CH}_2\text{OH} + \text{CH}_3\text{CH}_2\text{CHO}$ ,  $\square$ ) and (c) product distribution in the photocatalytic reaction of propylamine in  $1 \text{ mol dm}^{-3}$  NaOH. Symbols are same as in Figure 2(a).

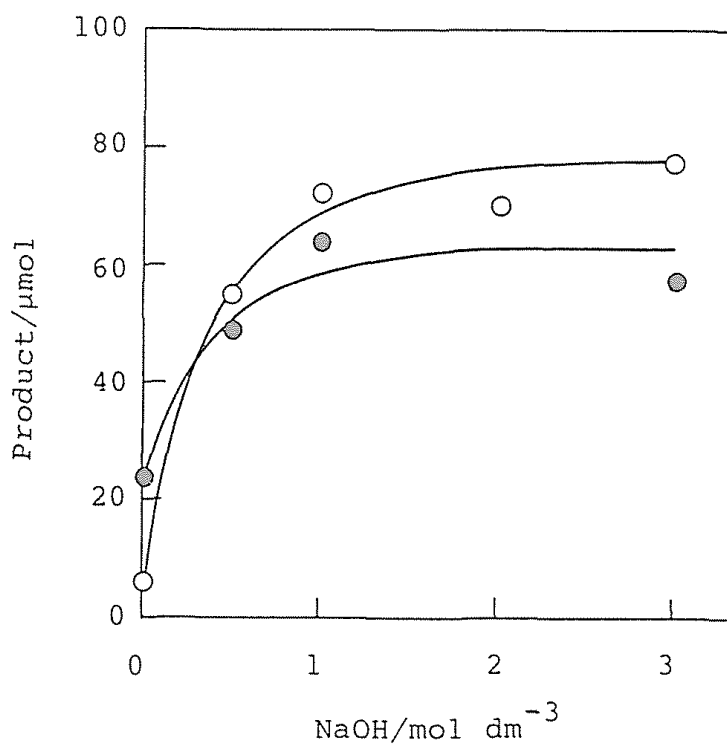


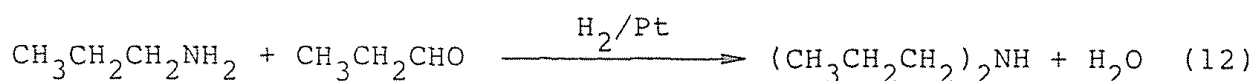
Figure 2 (d) Effect of concentration of NaOH on the yields of products in the photocatalytic reaction of propylamine. Propylamine (1.0 mmol) in 5.0 cm<sup>3</sup> of solvent was irradiated with a 500-W high pressure mercury arc for 12 h in the presence of TiO<sub>2</sub>/Pt (50 mg). ○, H<sub>2</sub> and ●, NH<sub>3</sub>.

In the NaOH solution, dipropylamine, which is the major product in the distilled water as described in the preceding section, could be obtained negligibly; propionaldehyde, 1-propanol,  $\text{NH}_3$  and  $\text{H}_2$  were liberated as main products. As shown in Figure 2(b), total amount of nitrogen- and carbon-containing products ( $\text{NH}_3$  and sum of 1-propanol and propionaldehyde, respectively) was plotted against the propylamine consumption. Practically linear relations between consumed substrate and products in the respect of both nitrogen and carbon balances were obtained. Product distribution shown in Figure 2(c) shows that almost identical amount of propylamine was consumed in the reactions (9) and (10). Deviation from the linear relation by the prolonged irradiation is accounted for by the propionic acid formation by further oxidation of propionaldehyde or 1-propanol. Moreover, the basic condition facilitates the thermal decomposition of the aldehyde (base-induced decomposition has been suggested in Chapter 4 of this thesis).

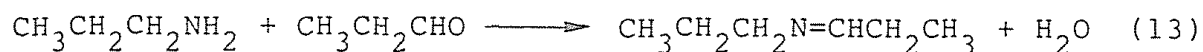
Thus, propylamine undergoes oxidative deamination to yield propionaldehyde and 1-propanol in aqueous NaOH solution (reactions (10) and (11)), while deamino-N-alkylation in distilled water (reaction (9)). The mechanism of these photocatalytic reactions is discussed in the following sections.

Deamino-N-alkylation of Propylamine into Dipropylamine by Platinized  $\text{TiO}_2$  via Schiff Base Intermediate. It has been known that secondary amines are derived experimentally by the hydrogenation of mixture of primary amine and aldehyde.<sup>12</sup> It is, therefore, presumed that similar process gives dipropylamine from the by-product propionaldehyde and the substrate propylamine. In order to clarify the mechanism

of this deamino-N-alkylation, reactions of propylamine were studied in the presence of additives as shown in Table 2. Addition of 1-propanol or propionaldehyde, the by-products, to the photocatalytic system of propylamine under Ar rather reduced the dipropylamine yield. H<sub>2</sub> atmosphere in the absence of additive or in the presence of 1-propanol gave also no influence on the yield of the photocatalytic reaction. Drastic enhancement could be observed in the presence of both propionaldehyde and Pt under H<sub>2</sub> atmosphere to give ca. 3-4 times greater yield of dipropylamine than in the original photocatalytic system (Run 6). The enhanced yield was not affected by the presence of TiO<sub>2</sub> powder (Run 7), and was obtained regardless of whether the system was photoirradiated or in the dark. These observations suggest the mechanism of the formation of final product dipropylamine from propionaldehyde and propylamine in the presence of H<sub>2</sub> and Pt in the dark, as follows.



Most probable intermediate in this hydrogenation is a Schiff base, N-propylidenepropylamine (PPA), derived by intermolecular dehydration of propionaldehyde and propylamine.



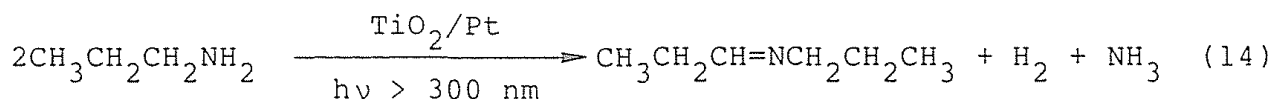
In fact, in a comparative experiment, photocatalytic reaction (10 h) of propylamine (699 μmol) in acetonitrile (5.0 cm<sup>3</sup>, not dehydrated) gave the Schiff base, PPA, (m/e 99 (M<sup>+</sup>, relative intensity 7.1

Table 2 Effect of additive (120-125  $\mu\text{mol}$ ), atmosphere, and catalyst on the yield of dipropylamine.<sup>a</sup>

Run	Additive	Catalyst	Atmosphere	Dipropylamine Yield/% <sup>b</sup>
1	None	TiO <sub>2</sub> /Pt	Ar	10.0
2	CH <sub>3</sub> CH <sub>2</sub> CH <sub>2</sub> OH	TiO <sub>2</sub> /Pt	Ar	5.8
3	CH <sub>3</sub> CH <sub>2</sub> CHO	TiO <sub>2</sub> /Pt	Ar	1.0
4	None	TiO <sub>2</sub> /Pt	H <sub>2</sub>	8.6
5	CH <sub>3</sub> CH <sub>2</sub> CH <sub>2</sub> OH	TiO <sub>2</sub> /Pt	H <sub>2</sub>	9.1
6	CH <sub>3</sub> CH <sub>2</sub> CHO	TiO <sub>2</sub> /Pt	H <sub>2</sub>	34.5 (39.2) <sup>c</sup>
7	CH <sub>3</sub> CH <sub>2</sub> CHO	TiO <sub>2</sub>	H <sub>2</sub>	0.2 (1.6) <sup>c</sup>
8	CH <sub>3</sub> CH <sub>2</sub> CHO	Pt	H <sub>2</sub>	40.9 (41.6) <sup>c</sup>

<sup>a</sup>Propylamine (122  $\mu\text{mol}$ ), catalyst (TiO<sub>2</sub>/Pt 50.0 mg, TiO<sub>2</sub> 47.5 mg, or Pt 2.5 mg), water 5.0 cm<sup>3</sup> were placed in a glass tube and irradiated for 20 h by a 500-W high-pressure mercury arc. <sup>b</sup>Based on the initial amount of propylamine. <sup>c</sup>In the dark.

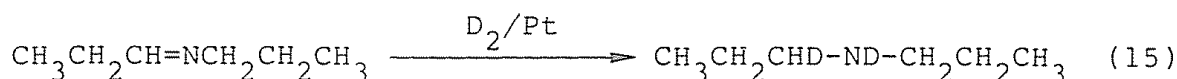
%), 84 ((M - CH<sub>3</sub>)<sup>+</sup>, 3.9 %), 70 ((M - CH<sub>3</sub>CH<sub>2</sub>)<sup>+</sup>, 100 %) along with dipropylamine (2 %), propionaldehyde (3 %), and H<sub>2</sub> (7 %).



Post addition of 5.0 cm<sup>3</sup> of water to the acetonitrile solution decreased the imine to a negligible amount and increased the overall yield of the propionaldehyde to 8 %. These facts indicate that the Schiff base is easily hydrated to yield propionaldehyde and propylamine (reverse reaction of (13)).

In order to clarify the mechanism of the characteristic deamino-N-alkylation of primary amines, isotope distribution in the product dipropylamine obtained in the D<sub>2</sub>O solution was investigated by GC-MS, as shown in Figure 3. In contrast to the mass spectrum of dipropylamine produced in H<sub>2</sub>O (m/e 101 (M<sup>+</sup>, relative intensity 5.6 %), 72 ((M - CH<sub>3</sub>CH<sub>2</sub>)<sup>+</sup>, 44 %), 30 ((M - CH<sub>3</sub>CH<sub>2</sub> - CH<sub>3</sub>CH=CH<sub>2</sub>)<sup>+</sup>, 100 %)), the distribution of deuterium-labeled M<sup>+</sup> signals was observed for dipropylamine from the D<sub>2</sub>O solution: i.e., d<sub>0</sub> (m/e 101, unlabeled) : d<sub>1</sub> (102) : d<sub>2</sub> (103) : d<sub>3</sub> (104) : d<sub>4</sub> (105) : d<sub>5</sub> (106) = 3 : 17 : 23 : 37 : 17 : 3.

Assuming the hydrogenation of PPA in the TiO<sub>2</sub>/Pt photocatalytic reaction of propylamine, the Pt-catalyzed hydrogenation of PPA leads to the d<sub>2</sub> product in D<sub>2</sub>O because D<sub>2</sub> is mainly obtained as the reduction product.





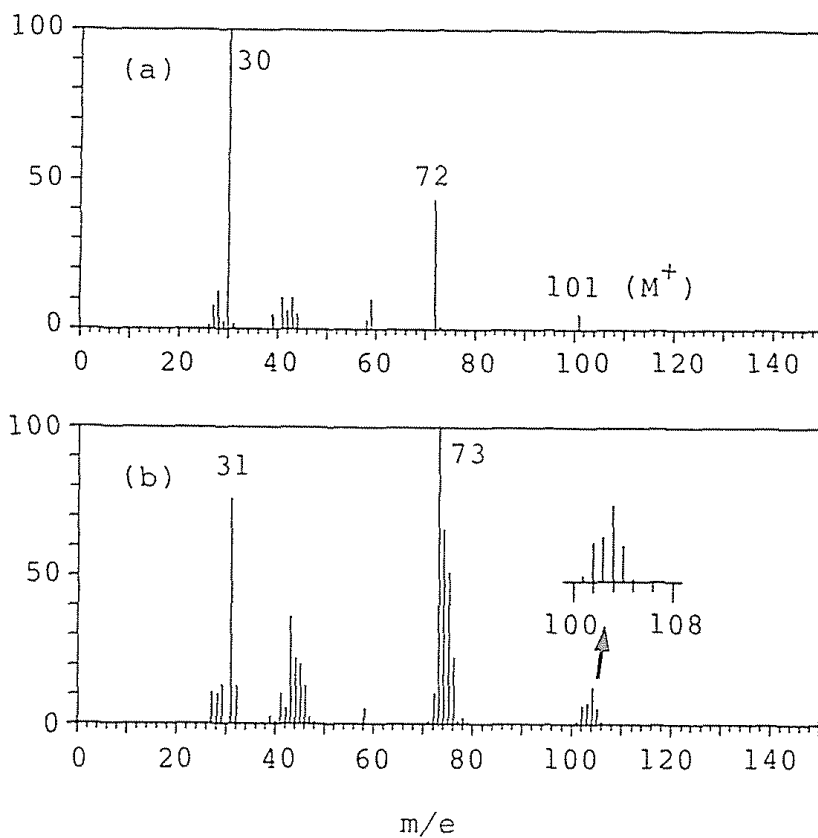
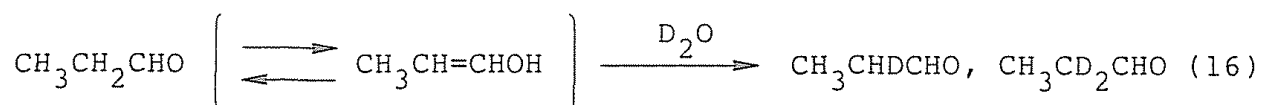


Figure 3 Mass spectra of dipropylamine liberated in the photoinduced reaction of propylamine by TiO<sub>2</sub>/Pt catalyst in (a) H<sub>2</sub>O and in (b) D<sub>2</sub>O.

Additional ( $\geq 3$ ) deuterium incorporation can be accounted for by the keto-enol tautomerisms of propionaldehyde.



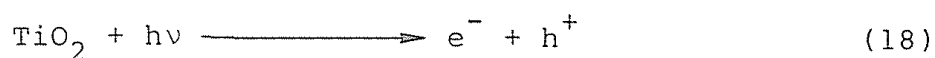
On the basis of these assumptions, the maximum number of deuterium incorporation in dipropylamine molecule is 4 (corresponds to  $\text{CH}_3\text{CD}_2\text{CHD-ND-CH}_2\text{CH}_2\text{CH}_3$ ), which is practically in agreement with the result of GC-MS studies described above. Further deuterized product ( $M^+ 106$ ) could be accounted for by  $\text{CH}_3\text{CD}_2\text{CDO}$  derived through re-oxidation of  $\text{CH}_3\text{CD}_2\text{CDHOD}$ ,  $\text{D}_2$ -reduced product of propionaldehyde, though the amount was relatively small.

Upon raising the pH, the concentration of PPA would decrease because the Schiff base intermediate undergoes base-catalyzed hydrolysis,<sup>13</sup> which would be responsible for the decreased yield of final product, dipropylamine under the alkaline conditions.

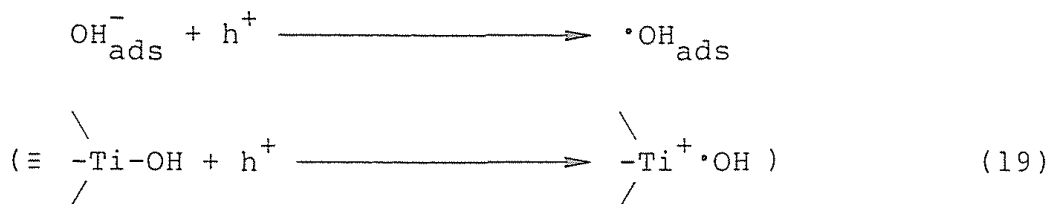


Therefore, in the alkaline solutions propionaldehyde (reaction 11) and 1-propanol (reaction 10) were yielded mainly.

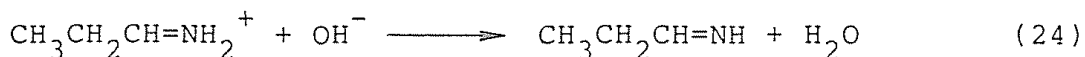
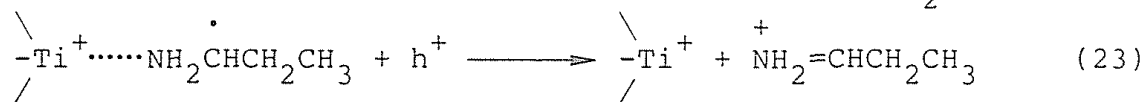
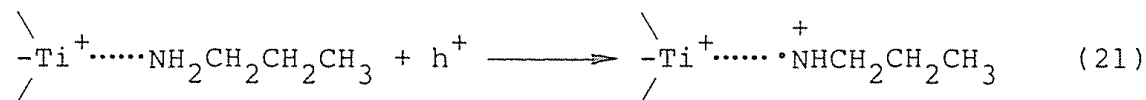
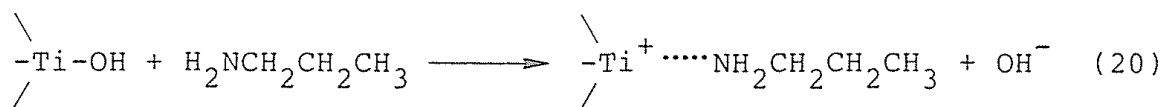
The precursor of the Schiff base, propionaldehyde, is derived by photocatalytic reaction of propylamine, which is initiated by the photoinduced formation of electron ( $e^-$ )-positive hole ( $h^+$ ) pair in  $\text{TiO}_2$ .



The positive hole in the bulk  $\text{TiO}_2$  would migrate to the surface and be trapped by the surface absorbates, such as a surface hydroxyl ( $\text{OH}_{\text{ads}}^-$ ) to give an adsorbed hydroxyl radical ( $\cdot\text{OH}_{\text{ads}}$ ), which abstracts hydrogen from the alcohols as shown in Chapter 1 and 2.

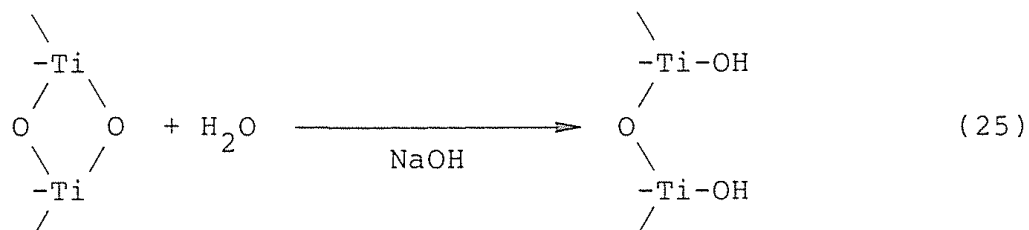


However, in the present system the substrate propylamine, which is much adsorptive on the acid site of the oxide surface and undergoes one-electron oxidation, could trap  $h^+$  directly to form aminium cation radical.



The increased conversion of propylamine in NaOH solution is accounted for by the increasing amount of the adsorption site,  $\text{OH}_{\text{ads}}^-$

which desorbed in exchange with the amine (reaction 20), by the alkaline treatment of the dehydrated  $\text{TiO}_2$  surface, as has been reported previously.<sup>14</sup>

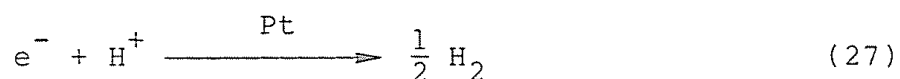


Furthermore, the basic condition would favor the deprotonation of the intermediates, the aminium cation radical (reaction 22) and the iminium cation (reaction 23).

The imine derived as above is unstable in water to undergo hydrolysis into propionaldehyde and  $\text{NH}_3$ .



On the other hand,  $e^-$  generated simultaneously reduces  $\text{H}^+$  on the Pt site as described in the following section.



#### Effect of Pt Loading on the Photocatalytic Reaction of Propylamine.

Figure 4(a) shows the dependence, of the product yields in the photocatalytic reaction of propylamine, on the amount of Pt loaded on  $\text{TiO}_2$ . Negligible amount of products was obtained in the absence of Pt. Along with the increase of Pt amount, the  $\text{NH}_3$  yield, which corresponds to the amount of propylamine oxidized by  $\text{h}^+$  (reaction

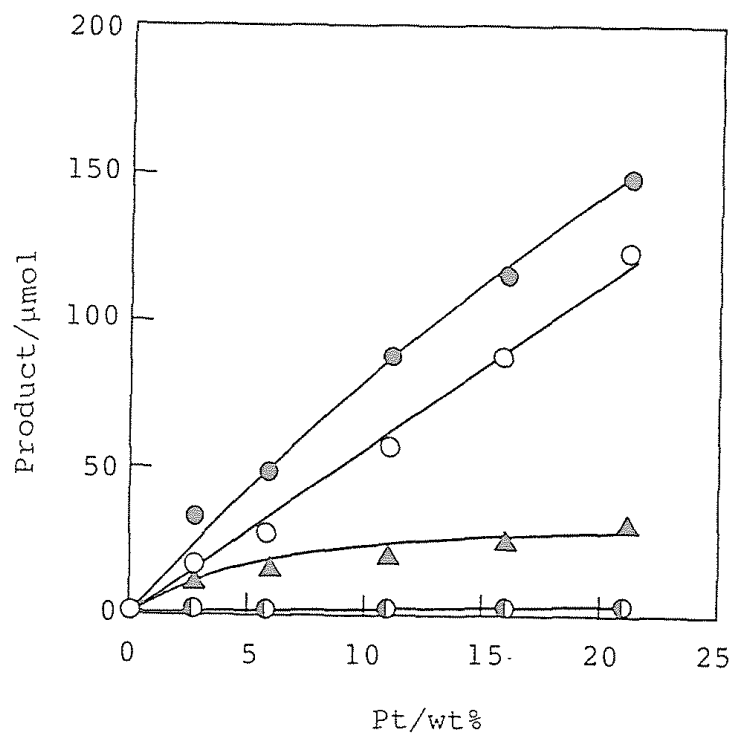


Figure 4 (a) Effect of Pt loading on the yields of products in the photocatalytic reaction of propylamine in distilled water. ● NH<sub>3</sub>, ○ , H<sub>2</sub>, ▲ (CH<sub>3</sub>CH<sub>2</sub>CH<sub>2</sub>)<sub>2</sub>NH, ○ CH<sub>3</sub>CH<sub>2</sub>CH<sub>2</sub>OH. Propylamine (1 mmol) in water (5.0 cm<sup>3</sup>) with TiO<sub>2</sub>/Pt (50 mg) was irradiated with a 500-W high-pressure mercury arc for 20 h.

21) as described above, increased linearly. The behavior seems to be different from that of  $\text{TiO}_2/\text{Pt}$  photocatalyzed dehydrogenation of 2-propanol as described later.

As shown in Figure 4(b), reasonable material balance between sum of  $\text{NH}_3$  and dipropylamine, which corresponds to the consumption of propylamine, and sum of  $\text{H}_2$ , dipropylamine, and 1-propanol was observed. These facts show that reactions (9)-(11) proceed also in this case, on the assumption that the amount of propionaldehyde liberated during the reaction was identical to that of  $\text{H}_2$ . The  $\text{H}_2$  yield (reaction (11)) was practically identical to that of dipropylamine in the Pt amount range ( $\leq 5.7$  wt%), and increased with the increasing Pt amount to be twice larger than that of dipropylamine by 21 wt% Pt loaded  $\text{TiO}_2$ . However, the amount of propionaldehyde could not be determined quantitatively because the aldehyde undergoes successive decomposition under basic conditions, induced by the large amount ( $\approx 1$  mmol,  $\text{pH} \approx 12-13$ ) of starting amine, in the dark without  $\text{TiO}_2/\text{Pt}$  (though the process has not been clarified at present).

Assuming that propionaldehyde was liberated equimolar to  $\text{H}_2$  (reaction (9)) as described above, the yield ratio of reaction (9)-(11) based on the propylamine consumption (Figure 4(b)) was 50 : 9 : 41 (at Pt 5.7 wt%), which indicates that the proportion of dipropylamine and 1-propanol decreased compared with the results shown in Figure 1(c). These facts show that the dipropylamine formation and the decomposition proceed competitively under these conditions and, thereby, practically negligible amount of the aldehyde remained in the reaction mixture. Furthermore, the facts suggest that 1-pro-

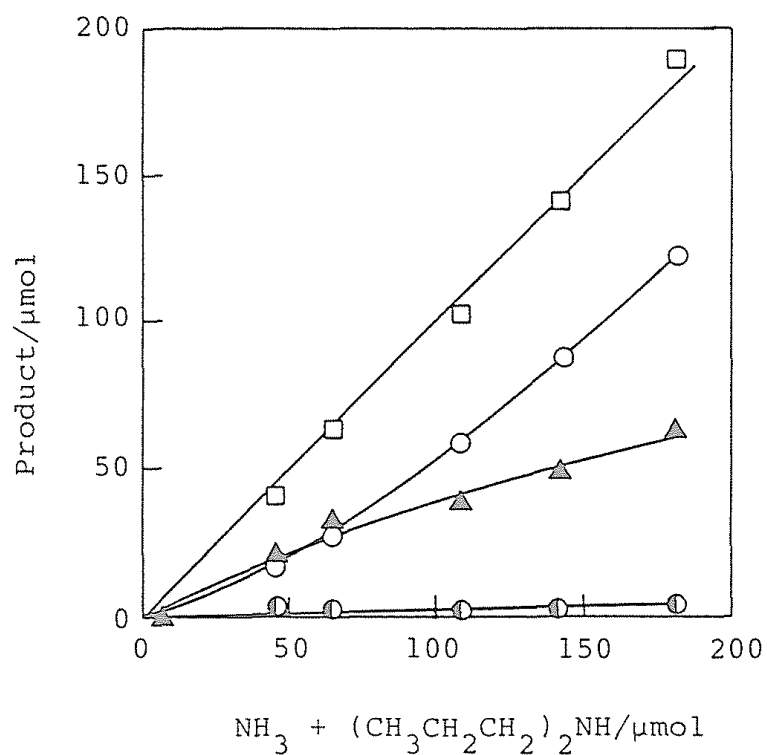
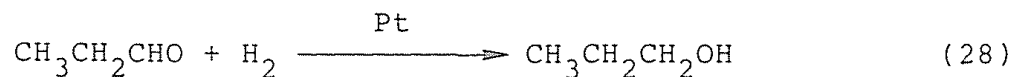
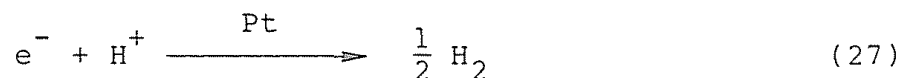


Figure 4 (b) Product distribution in the photocatalytic reaction of propylamine based on the propylamine consumption (see text). ○ H<sub>2</sub>, ▲ 2 (CH<sub>3</sub>CH<sub>2</sub>CH<sub>2</sub>)<sub>2</sub>NH, ○ CH<sub>3</sub>CH<sub>2</sub>CH<sub>2</sub>OH, and □ sum of these products.

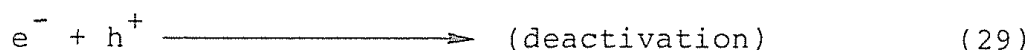
propanol is derived from propionaldehyde by the hydrogenation on the Pt surface, which is similar to the dipropylamine formation, as follows (see also Table 3).



Thus, the increasing yield of propionaldehyde (although disappeared easily), along with the H<sub>2</sub> formation, by the increasing amount of the loaded Pt could be attributable to the enhanced formation of H<sub>2</sub> by the photoexcited electron on the Pt site.



The enhanced reduction facilitates the oxidation of substrate by simultaneously generated positive hole as a result of prevention of electron-hole recombination.



The successive product, dipropylamine and 1-propanol, increased with the increasing amount of the precursor, propionaldehyde, and of catalyst Pt.

As is discussed in Chapters 9 and 10, in the case of the TiO<sub>2</sub>/Pt photocatalyzed dehydrogenation of alcohol (such as 2-propanol to give H<sub>2</sub> and acetone), the yield dependence on the amount of Pt loading was considerably different from that in the present system; the acetone and H<sub>2</sub> yields increased with the increasing amount of Pt



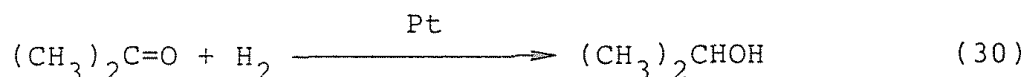
Table 3 Thermal hydrogenation of propionaldehyde and acetone (125  $\mu\text{mol}$ ) in aqueous solution catalyzed by  $\text{TiO}_2/\text{Pt}$  (50 mg).<sup>a</sup>

Run	Substrate	Solvent	Atmos- phere	Product	/ $\mu\text{mol}$
1	$\text{CH}_3\text{CH}_2\text{CHO}$	$\text{H}_2\text{O}$	$\text{H}_2$	$\text{CH}_3\text{CH}_2\text{CH}_2\text{OH}$	2.6
2	$\text{CH}_3\text{CH}_2\text{CHO}$	1 M NaOH	Ar	$\text{CH}_3\text{CH}_2\text{CH}_2\text{OH}$	$\approx 0$
3	$\text{CH}_3\text{CH}_2\text{CHO}$	1 M NaOH	$\text{H}_2$	$\text{CH}_3\text{CH}_2\text{CH}_2\text{OH}$	4.1
4	$(\text{CH}_3)_2\text{C}=\text{O}$	$\text{H}_2\text{O}$	$\text{H}_2$	$(\text{CH}_3)_2\text{CHOH}$	1.5
5	$(\text{CH}_3)_2\text{C}=\text{O}$	1 M NaOH	Ar	$(\text{CH}_3)_2\text{CHOH}$	0.8
6	$(\text{CH}_3)_2\text{C}=\text{O}$	1 M NaOH	$\text{H}_2$	$(\text{CH}_3)_2\text{CHOH}$	42.7

<sup>a</sup>Substrate,  $\text{TiO}_2/\text{Pt}$  (50 mg), and solvent ( $5.0 \text{ cm}^3$ ) were placed in a glass tube under Ar or  $\text{H}_2$  atmosphere and permitted to stand for 20 h.

up to approximately 5 wt%, but was practically constant in the region > 5 wt%.

It is easily expected that Pt, in the present system platinum black, also catalyzes the hydrogenation of acetone by photocatalytically produced H<sub>2</sub>.



The photocatalytic dehydrogenation of 2-propanol proceeds more efficiently along with the increasing amount of Pt. However, the back reaction (hydrogenation of acetone) would be enhanced simultaneously. Consequently, the behavior of Pt loading is possibly interpreted: the acetone and H<sub>2</sub> yields increase with the increasing Pt amount but is constant over the Pt amount region at which back reaction between the products acetone and H<sub>2</sub> proceeds efficiently on the Pt site.

On the other hand, the overall rate of the photocatalytic reaction of propylamine increases along with the increasing amount of Pt, because the photocatalytic reaction of propylamine involving deamination is irreversible, i.e., hydrogenation of product, aldehyde or dipropylamine could give no starting amine.

Photocatalytic Deamino-oxidation of Isopropylamine by Aqueous Suspension of Platinized TiO<sub>2</sub>. Figure 5(a) shows the time course of photocatalytic reaction of isopropylamine, α-substituted primary amine, in distilled water under Ar in the presence of TiO<sub>2</sub>/Pt. Acetone, NH<sub>3</sub>, H<sub>2</sub> and small amount of 2-propanol were obtained along with the consumption of isopropylamine. Note that negligible amount

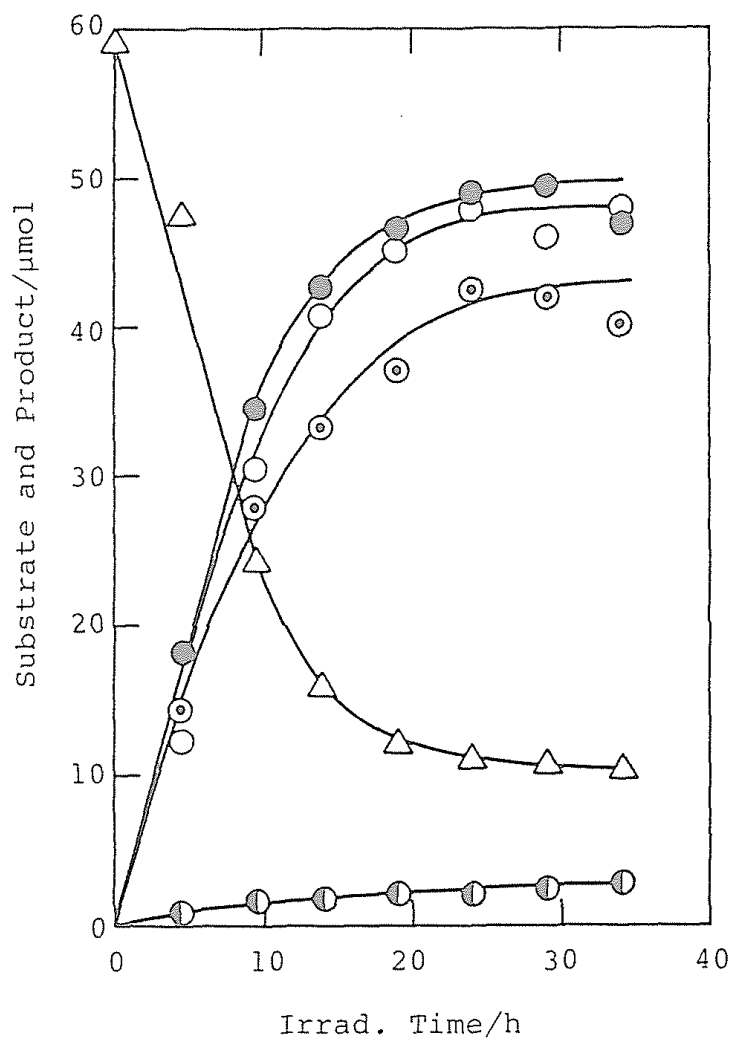
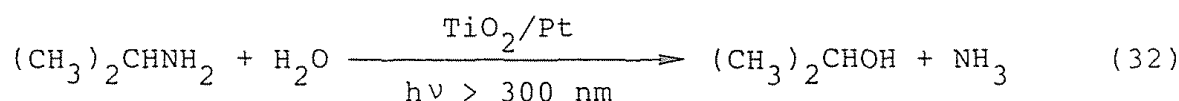
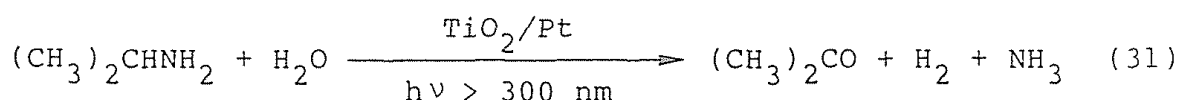


Figure 5 (a) Time course of the photocatalytic reaction of isopropylamine in distilled water by  $\text{TiO}_2/\text{Pt}$  catalyst;  $\Delta$   $(\text{CH}_3)_2\text{CHNH}_2$ ,  $\bullet$   $\text{NH}_3$ ,  $\circ$   $\text{H}_2$ ,  $\odot$   $(\text{CH}_3)_2\text{CO}$ , and  $\ominus$   $(\text{CH}_3)_2\text{CHOH}$ . Irradiation was performed using a 400-W high-pressure mercury arc.

of diisopropylamine, which is expected to be observed on the basis of the result on the propylamine system demonstrated above, was obtained in this case even in the distilled water.

Figure 5(b) is replot of the data in Figure 5(a), demonstrating a reasonable material balance for carbon and nitrogen. Furthermore, as clearly seen in Figure 5(a), amount of H<sub>2</sub> liberated was apparently identical to that of acetone, except for the case of prolonged irradiation > 20 h. Therefore, the stoichiometry of the present photocatalytic reaction is expressed as follows.



The yield ratio of these reactions (31) and (32) was estimated to be 94 : 6 from the product distribution shown in Figure 5(c) (although only reaction (31) proceed photocatalytically and the 2-propanol formation is attributable to the thermal hydrogenation of acetone, as described below).

Figure 6(a) shows the time course of the TiO<sub>2</sub>/Pt photocatalyzed reaction of isopropylamine in 1 mol dm<sup>-3</sup> NaOH. The reaction rate was ca. 5 times larger than that in distilled water, which is similar to the case of propylamine. This behavior is interpreted by the increasing amount of the surface OH<sup>-</sup>, the oxidation site with h<sup>+</sup>, by the alkaline treatment. In this case, acetone, NH<sub>3</sub>, and H<sub>2</sub> were obtained as the major products with small amount of 2-propanol.

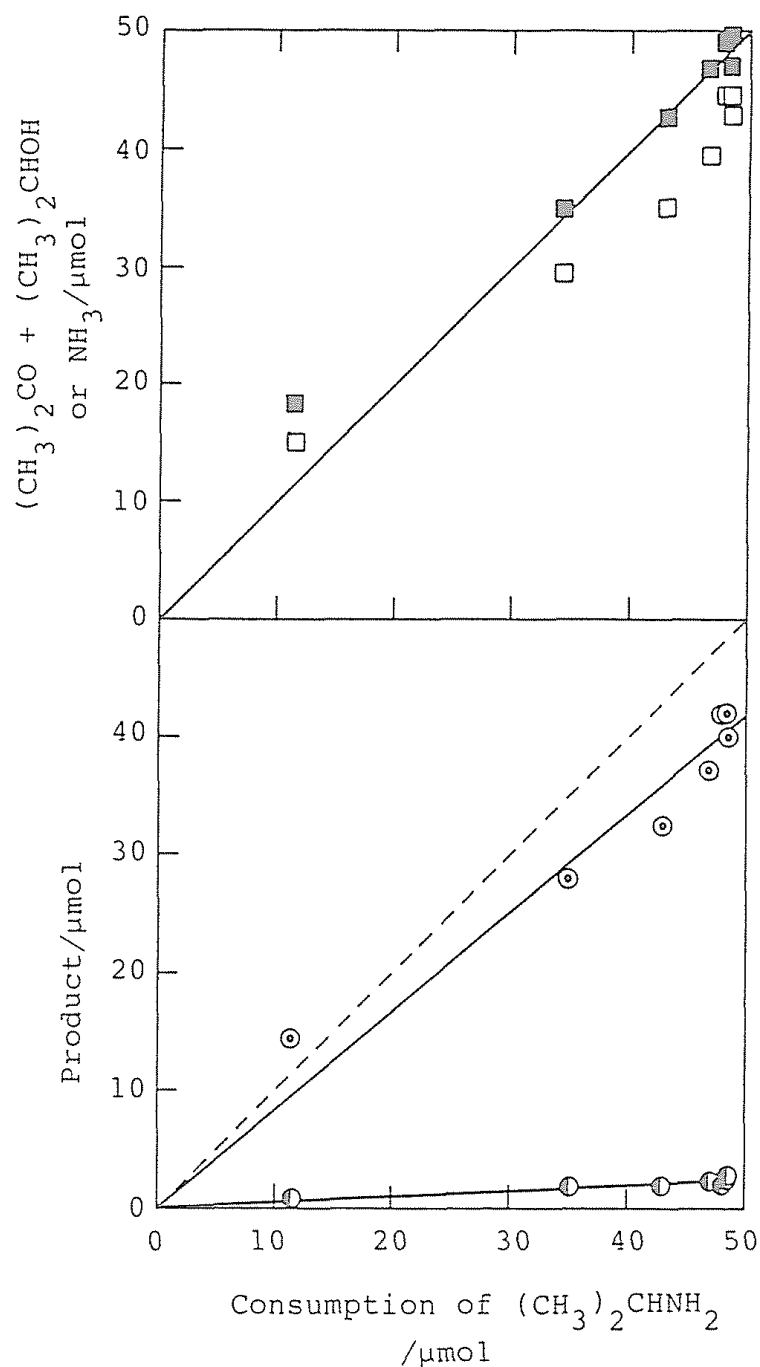


Figure 5 (b)Material balance for nitrogen ( $\text{NH}_3$ , ■ ) and carbon ( $(\text{CH}_3)_2\text{CO} + (\text{CH}_3)_2\text{CHOH}$ , □ ), and (c)product distribution of the photocatalytic reaction of isopropylamine in distilled water: ⊕  $(\text{CH}_3)_2\text{CO}$ , ⊙  $(\text{CH}_3)_2\text{CHOH}$ .

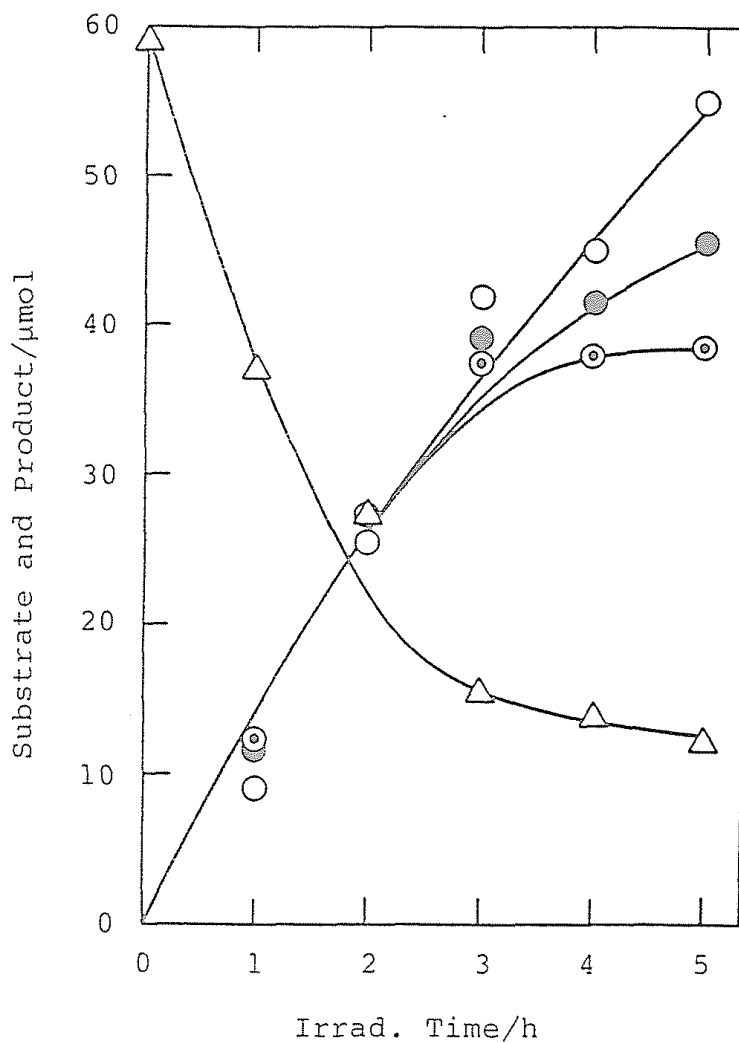
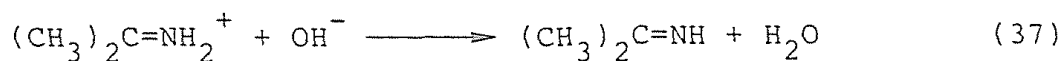
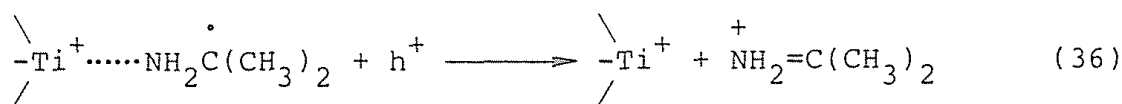
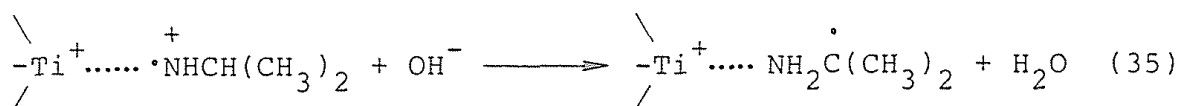
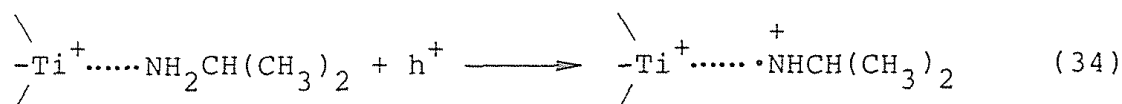
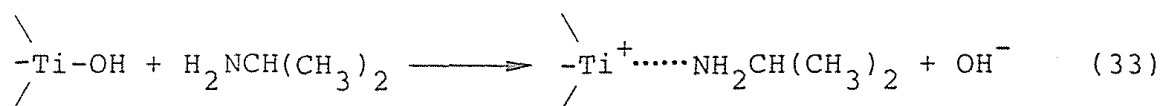


Figure 6 (a) Time course of the photocatalytic reaction of isopropylamine in  $1 \text{ mol dm}^{-3}$  NaOH by  $\text{TiO}_2/\text{Pt}$  catalyst;  $\Delta$   $(\text{CH}_3)_2\text{CHNH}_2$ ,  $\bullet$   $\text{NH}_3$ ,  $\odot$   $(\text{CH}_3)_2\text{CO}$ , and  $\circ$   $\text{H}_2$ . Irradiation was performed with a 400-W high-pressure mercury arc.

These products were identical to those obtained in the distilled water and the linear relation between the consumption of isopropylamine and yield of carbon- and nitrogen-containing products was also observed in this case (see Figure 6(b)). Consequently, reactions (31) and (32) proceed in the ratio of 88 : 12 in the NaOH solution, as shown in Figure 6(c).

Figure 7 shows the dependence of the consumption of isopropylamine, which is estimated as the sum of acetone and 2-propanol yields, on the concentration of NaOH. The conversion at a given photoirradiation period increased with the increase of the NaOH concentration, which is possibly accounted for by the increased amount of the amine adsorption site (reaction 25) and enhanced deprotonation of the oxidaton intermediates, aminium cation radical and iminium cation (reactions (35) and (37), respectively).



The imine would undergo hydrolysis into acetone and  $\text{NH}_3$ , as observed in the propylamine system.

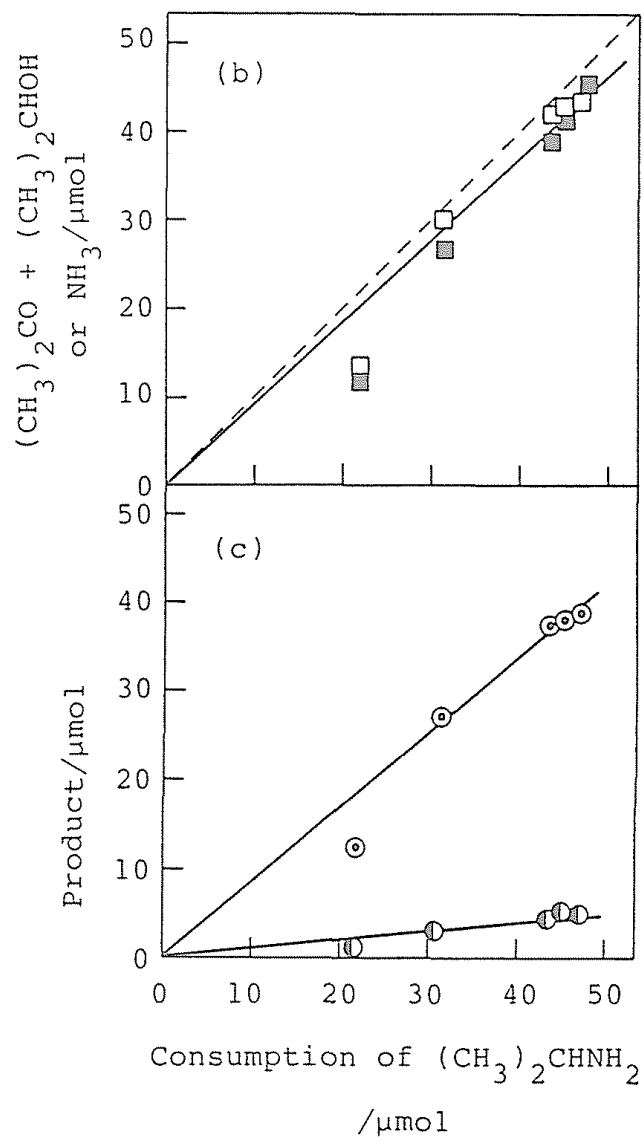
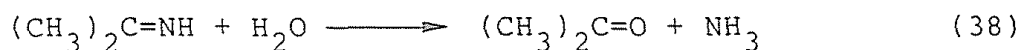
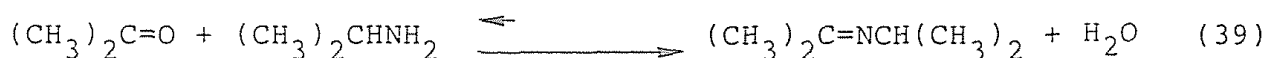


Figure 6 (b)Material balance for nitrogen ( $\text{NH}_3$ , ■ ) and carbon ( $(\text{CH}_3)_2\text{CO} + (\text{CH}_3)_2\text{CHOH}$ , □ ), and (c)product distribution of the photocatalytic reaction of isopropylamine in  $1 \text{ mol dm}^{-3}$  NaOH solution: ⊙  $(\text{CH}_3)_2\text{CO}$ , ⊖  $(\text{CH}_3)_2\text{CHOH}$ .





However diisopropylamine could not be obtained from the product acetone, because of the very low equilibrium constant of the Schiff base formation compared with that of aldehydes, even under the neutral conditions.



The 2-propanol yield increased with the increasing NaOH concentration. The selectivity of the 2-propanol formation ( $100 \times (\text{CH}_3)_2\text{CO} / ((\text{CH}_3)_2\text{CHOH} + (\text{CH}_3)_2\text{CO})$ ) was also shown in Figure 7; the selectivity increased from about zero to 33 % with the increasing NaOH concentration.

Table 3 shows the results of thermal hydrogenation of propionaldehyde and acetone by  $\text{TiO}_2/\text{Pt}$  in the dark. The rate of hydrogenation of acetone to give 2-propanol in  $1 \text{ mol dm}^{-3}$  NaOH solution (Run 6) was ca. 10 times larger than that of the aldehyde to 1-propanol (Run 3), and was ca. 30 times larger than that in distilled water (Run 4). These results lead to the conclusion that the enhanced 2-propanol formation by the increasing NaOH concentration is caused by the Pt catalyzed hydrogenation of acetone with  $\text{H}_2$  produced in reaction (31).



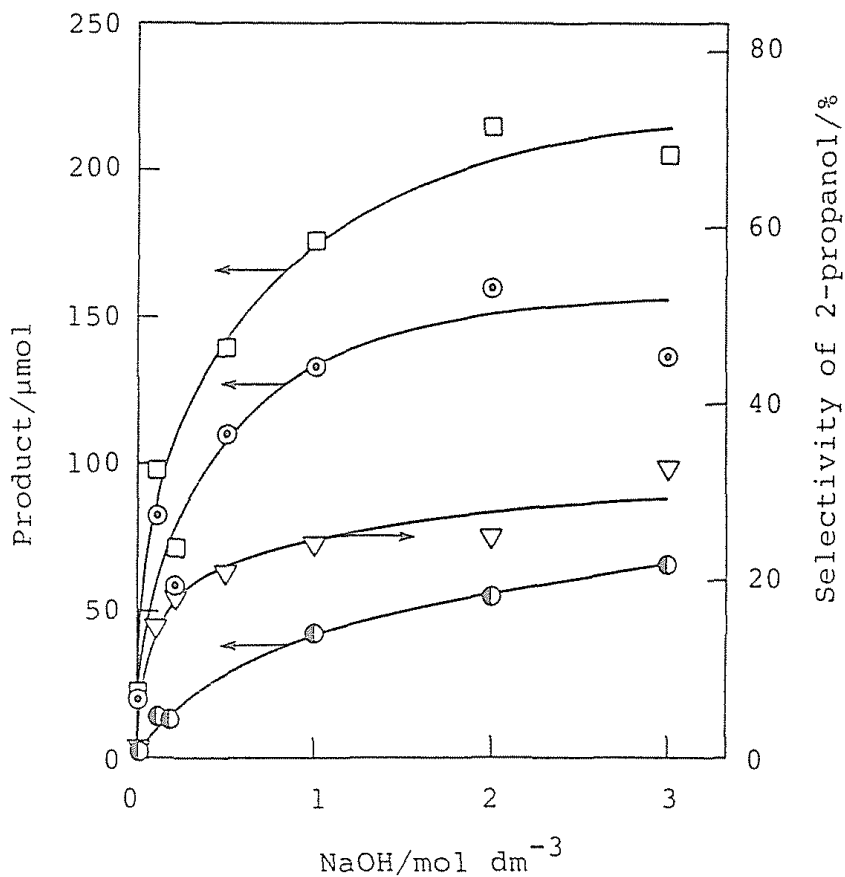


Figure 7 Effect of concentration of NaOH on the yields of products in the photocatalytic reaction of isopropylamine. ⊙ (CH<sub>3</sub>)<sub>2</sub>CO, ⊖ (CH<sub>3</sub>)<sub>2</sub>CHOH, □ sum of (CH<sub>3</sub>)<sub>2</sub>CO and (CH<sub>3</sub>)<sub>2</sub>CHOH, and ▽ selectivity of (CH<sub>3</sub>)<sub>2</sub>CHOH. Irradiation was performed using a 400-W high-pressure mercury arc for 6.0 h.

Thus, the 2-propanol formation (reaction (32)) proceeds not directly but via thermal hydrogenation of the photocatalytic product acetone and H<sub>2</sub>.

Effect of Pt Loading on the Photocatalytic Deamino-oxidation of Isopropylamine. Figure 8(a) shows the effect of Pt loading on the product yields in the isopropylamine reaction in distilled water. The overall consumption of isopropylamine as indicated by the NH<sub>3</sub> yield increased with the increasing amount of Pt loading, which is attributable to the reduction with the photoexcited electron enhanced by the increase in the amount of Pt as a reduction site, as in the case of propylamine (Figure 3).

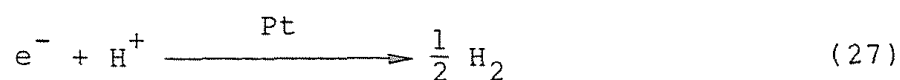


Figure 8(c) shows relationships between the products. The amount of the liberated NH<sub>3</sub> was practically identical to the sum of acetone and 2-propanol, and the acetone yield to the H<sub>2</sub> yield, indicating that reaction (31) and (32) proceed in this region of Pt amount. In this respect, selectivity of the 2-propanol ( $100 \times (\text{CH}_3)_2\text{CHOH} / ((\text{CH}_3)_2\text{CHOH} + (\text{CH}_3)_2\text{CO})$ ) was estimated and shown in Figure 8(b) as a function of the Pt amount. The selectivity increased along with the Pt amount. Figure 8(d) shows the 2-propanol yield as a function of the product of the Pt amount and the acetone yield. Assuming that H<sub>2</sub> is sufficiently liberated, the amount of active H<sub>2</sub> (Pt-H) for the hydrogenation would be predominantly in proportion to the amount of Pt. The linear relation shown in Figure 8(d) confirm the idea that 2-propanol is derived from acetone and H<sub>2</sub> catalyzed by

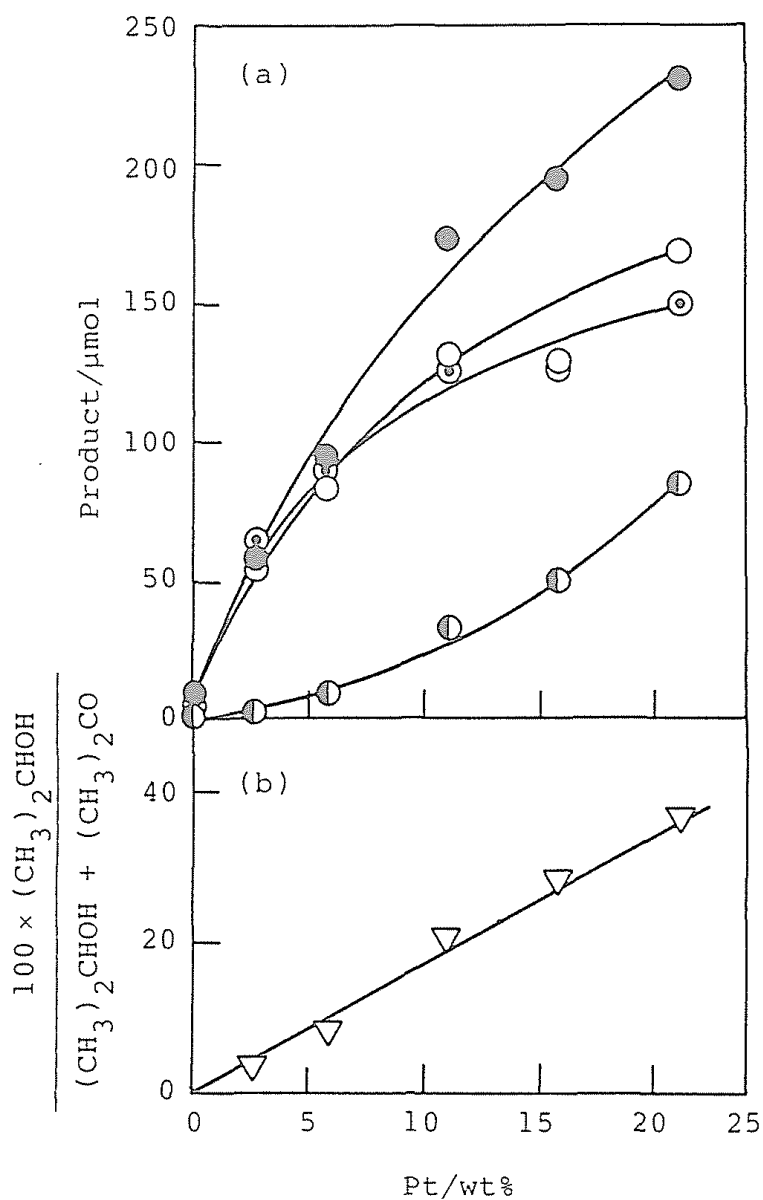


Figure 8 (a) Effect of Pt loading on the yields of products in the photocatalytic reaction of isopropylamine in distilled water;  $\odot$ ,  $(\text{CH}_3)_2\text{CO}$ ,  $\ominus$ ,  $(\text{CH}_3)_2\text{CHOH}$ ,  $\bullet$   $\text{NH}_3$ , and  $\circ$   $\text{H}_2$ , and (b) on the selectivity of 2-propanol formation (see text). Isopropylamine (1 mmol), water (5.0  $\text{cm}^3$ ), and catalyst (50 mg) were placed in a test tube and irradiated for 22 h with a 400-W high-pressure mercury arc under Ar.

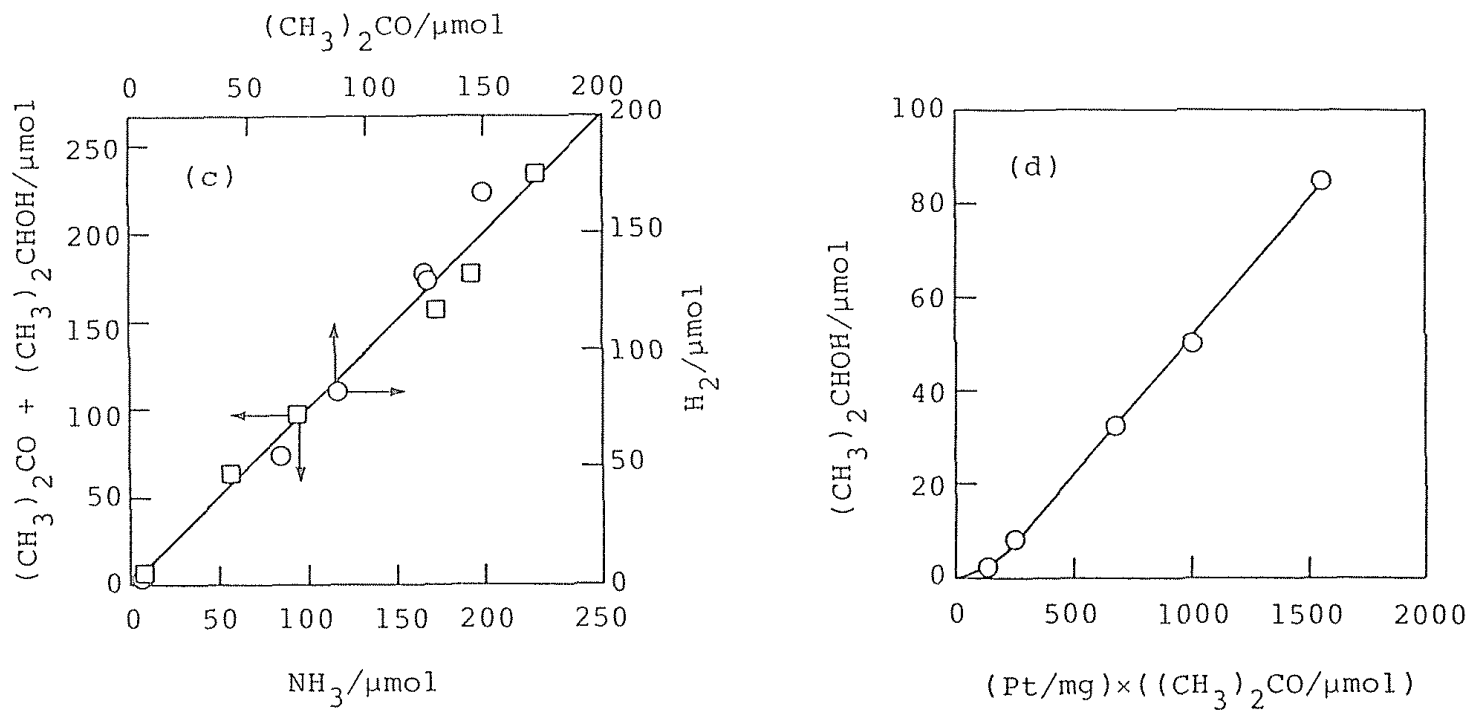
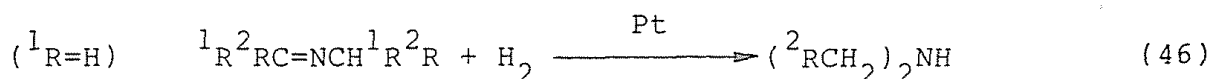
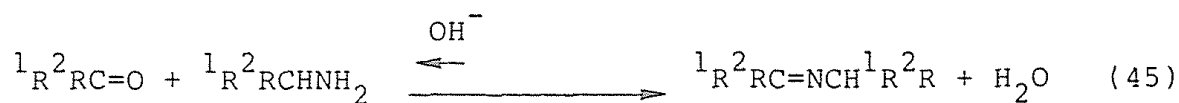
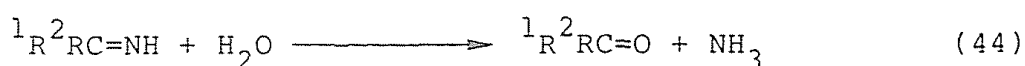
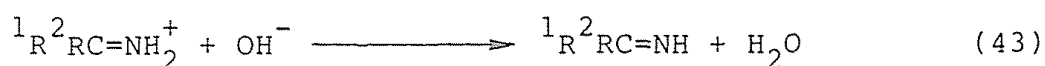
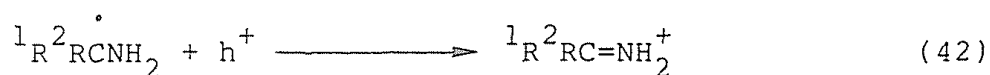
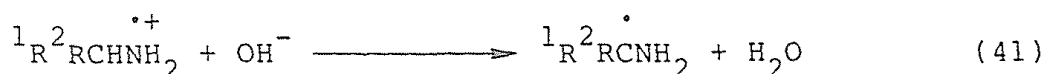
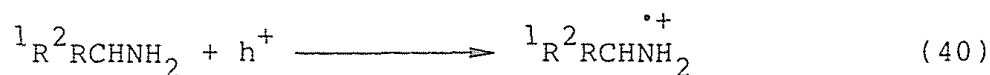
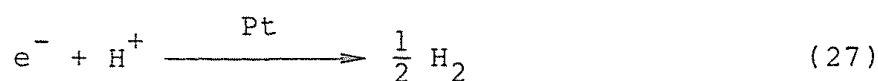
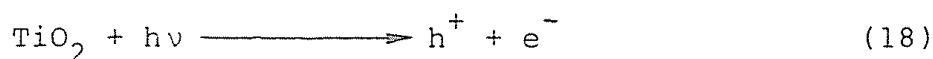


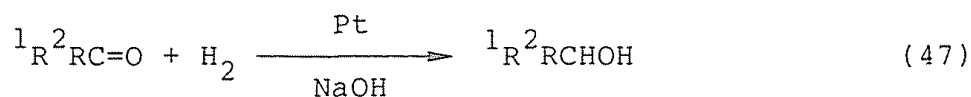
Figure 8 (c) Relations between the product yields;  $\text{NH}_3$  and  $(\text{CH}_3)_2\text{CO} + (\text{CH}_3)_2\text{CHOH}$ , and  $\text{H}_2$  and  $(\text{CH}_3)_2\text{CO}$ . (d) Relation between the yield of  $(\text{CH}_3)_2\text{CHOH}$  and the product of the Pt amount and the  $(\text{CH}_3)_2\text{CO}$  yield.

Pt.

Photocatalytic Deamino-N-alkylation and Deamino-N-cyclization of Primary Straight-chain Amines by Aqueous Suspension of Platinized

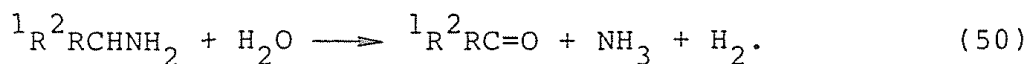
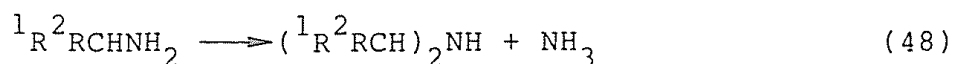
TiO<sub>2</sub>. On the basis of the above mentioned results, it was proved that primary straight-chain amines give symmetrical secondary amines via following intermediates.





As a further extension of the photocatalytic reaction, synthesis of some unsymmetrical secondary amines from two different aliphatic alkylamines and some heterocyclic amines from  $\alpha,\omega$ -aliphatic diamines are accomplished.

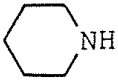
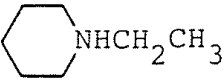
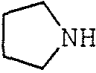

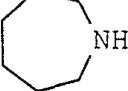

Table 4 shows the results of these extensions. From the detailed studies described above, the net reactions involves are summarized as follows:



Thus, in these reactions  $NH_3$  was produced in amounts equimolar with secondary amine, alcohol, or aldehyde. In this light, the molar ratio of secondary amine to ammonia was listed in Table 4.

A equimolar mixture of ethylamine and propylamine (Run 3) led to unsymmetrical N-ethylpropylamine (12 %) accompanied by symmetrical diethylamine (9 %) and dipropylamine (7 %). The sum of selectivity of these secondary amines achieved to be 70 %, showing the efficient deamino-N-alkylation proceeds also in this system. Similarly, an equimolar mixture of piperidine and ethylamine gave not only symmetrical secondary amine, diethylamine, but also cross N-alkylation

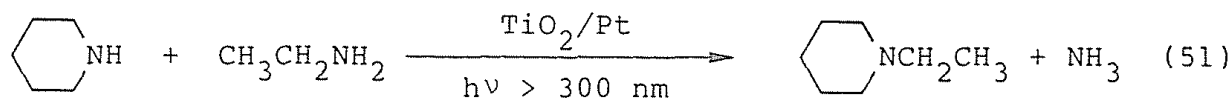
Table 4 Products of photocatalytic reactions of primary monoamines and diamines by the TiO<sub>2</sub>/Pt catalyst in distilled water.<sup>a</sup>

Run	Substrate	Product	Yield <sup>b</sup> /%	Selectivity <sup>c</sup> /%
1	CH <sub>3</sub> CH <sub>2</sub> NH <sub>2</sub>	(CH <sub>3</sub> CH <sub>2</sub> ) <sub>2</sub> NH	33	68
2	CH <sub>3</sub> CH <sub>2</sub> CH <sub>2</sub> NH <sub>2</sub>	(CH <sub>3</sub> CH <sub>2</sub> CH <sub>2</sub> ) <sub>2</sub> NH	24	55
3	CH <sub>3</sub> CH <sub>2</sub> NH <sub>2</sub>	(CH <sub>3</sub> CH <sub>2</sub> ) <sub>2</sub> NH	9	22
	CH <sub>3</sub> CH <sub>2</sub> CH <sub>2</sub> NH <sub>2</sub>	(CH <sub>3</sub> CH <sub>2</sub> CH <sub>2</sub> ) <sub>2</sub> NH	7	18
		CH <sub>3</sub> CH <sub>2</sub> NHCH <sub>2</sub> CH <sub>2</sub> CH <sub>3</sub>	12	30
4	CH <sub>3</sub> CH <sub>2</sub> NH <sub>2</sub>	(CH <sub>3</sub> CH <sub>2</sub> ) <sub>2</sub> NH	8	30
			5	22
5	H <sub>2</sub> N(CH <sub>2</sub> ) <sub>4</sub> NH <sub>2</sub>		67	93
6	H <sub>2</sub> N(CH <sub>2</sub> ) <sub>5</sub> NH <sub>2</sub>		33	87
7	H <sub>2</sub> N(CH <sub>2</sub> ) <sub>6</sub> NH <sub>2</sub>		20	67
8	(NH <sub>2</sub> (CH <sub>2</sub> ) <sub>2</sub> ) <sub>2</sub> NH		8	16

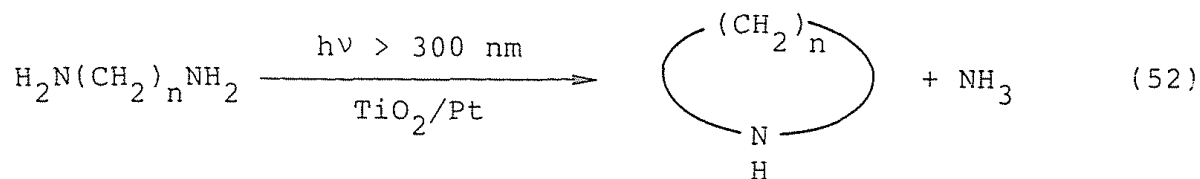
<sup>a</sup>On irradiation of Ar-purged suspensions of TiO<sub>2</sub>/Pt (50 mg) in aqueous amine solutions (60-120 μmol, 5.0 cm<sup>3</sup>) for 20 h at λ<sub>ex</sub> > 300 nm and room temperature. <sup>b</sup>Yields estimated by GC analysis based on starting amines. <sup>c</sup>Molar ratio of product amines to liberated NH<sub>3</sub>.



product, N-ethylpiperidine.



Several cyclic secondary amines could be derived from polymethylene- $\alpha,\omega$ -diamines (Runs 5-8).



Clearly, the present photocatalytic method is more favorable for intramolecular conversion, at room temperature, of primary diamines to cyclic secondary amines (ca. 70-90 % selectivity) when compared with the reported thermal process by homogeneous ruthenium and heterogeneous palladium catalysts. For example, reaction of 1,3-butanedi-amine (100  $\mu\text{mol}$ ) in the presence of  $\text{RuCl}_2(\text{Ph}_3\text{P})_3$  (2  $\mu\text{mol}$ ) in 5.0  $\text{cm}^3$  of THF (26 h at 30  $^\circ\text{C}$  under Ar) resulted in a negligible amount of pyrrolidine (< 1  $\mu\text{mol}$ ). At much higher temperature a good yield has been achieved.<sup>8</sup>

Figure 9 shows the GC-MS patterns of piperidine liberated in the photocatalytic reaction of 1,5-pentanediamine by  $\text{TiO}_2/\text{Pt}$  (see Table 4) in  $\text{H}_2\text{O}$  and  $\text{D}_2\text{O}$ . While characteristic  $\text{M}^+$  signal at  $m/e$  85 was observed in  $\text{H}_2\text{O}$  system, deuterized  $\text{M}^+$  signals were distributed mainly in the range of  $m/e$  85-90 ( $d_0 - d_5$ , and small amount of  $d_6$ ). These facts confirm the mechanism including a cyclic Schiff base intermediate which is similar to that assumed in the propylamine system.

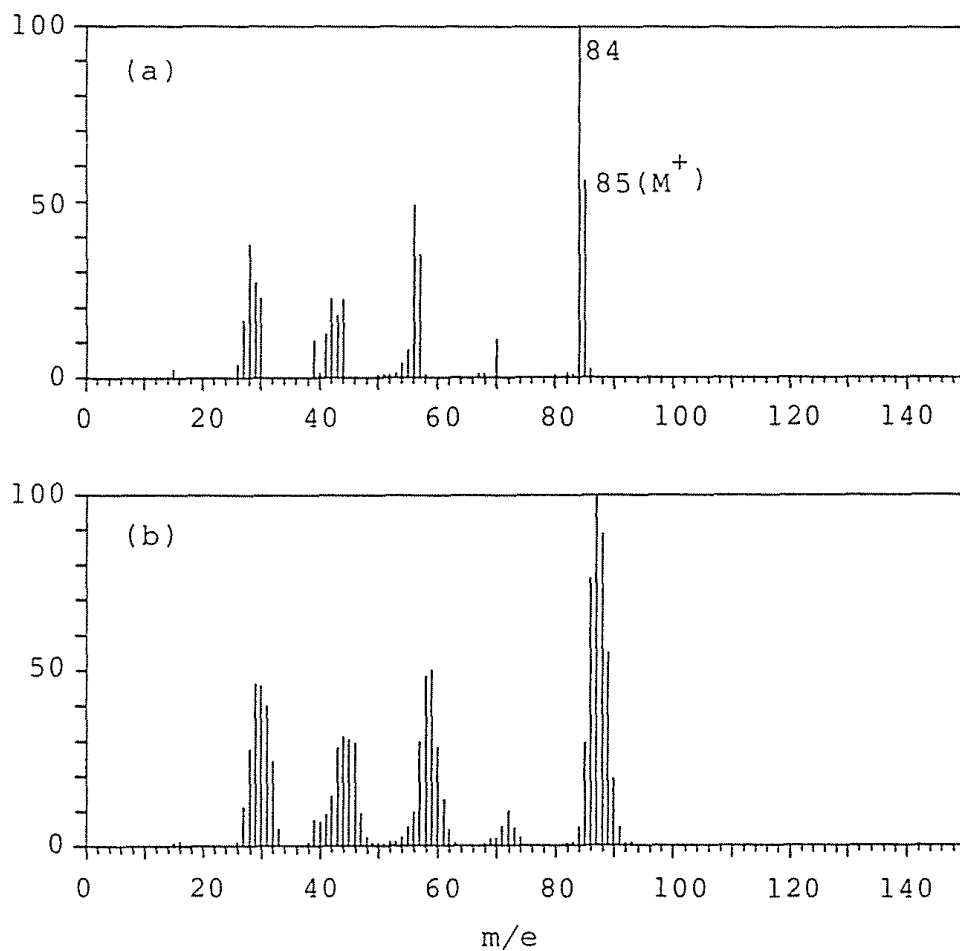
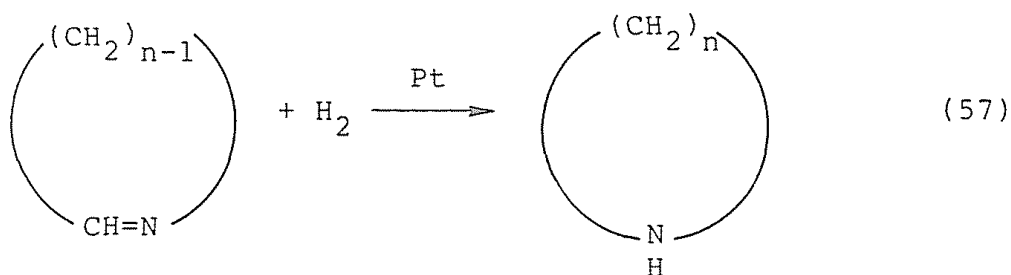
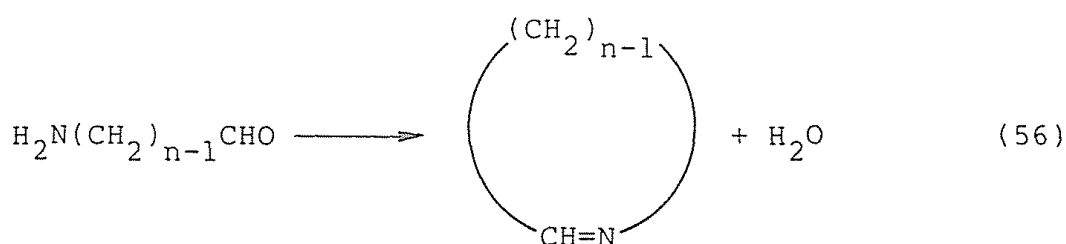
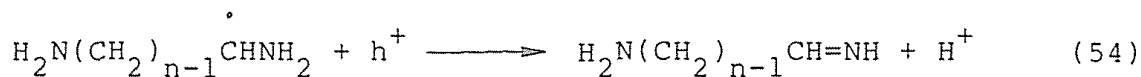
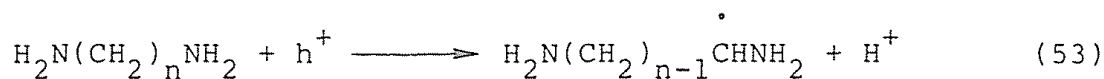
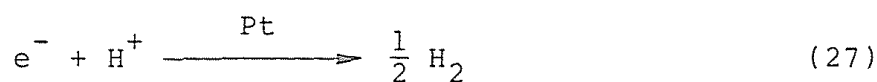
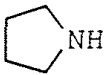
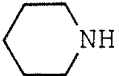
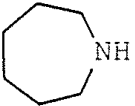
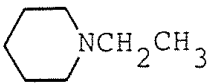
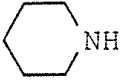



Figure 9 Mass spectra of piperidine formed in the photoinduced reaction by  $\text{TiO}_2/\text{Pt}$  catalyst suspended in (a)  $\text{H}_2\text{O}$  and (b)  $\text{D}_2\text{O}$ .



It is obvious that the conversion of primary amine to secondary amine depends on a dual function of the  $TiO_2/Pt$  catalyst which has oxidizing and reducing sites acting as short-circuited electrode systems. Bard and co-workers have previously demonstrated the analogous property of partially metallized semiconductor photocatalysts in the Kolbe reaction,<sup>2</sup> but these results provide a potentially new mode of photocatalytic synthetic application.

Table 5  $^{13}\text{C}$  NMR chemical shift of the photocatalytic products from aliphatic amines by the  $\text{TiO}_2/\text{Pt}$  catalyst in distilled water (see Table 4)

Product	Substrate	/ppm			
		Observed		Authentic	
$(\text{CH}_3\text{CH}_2)_2\text{NH}$	$\text{CH}_3\text{CH}_2\text{NH}_2$	43.33	13.62	43.51	14.50
$(\text{CH}_3\text{CH}_2\text{CH}_2)_2\text{NH}$	$\text{CH}_3\text{CH}_2\text{CH}_2\text{NH}_2$	51.20	22.19	51.40	22.69
		11.96		12.09	
$\text{CH}_3\text{CH}_2\text{NHCH}_2\text{CH}_2\text{CH}_3$	$\text{CH}_3\text{CH}_2\text{NH}_2$	50.96	43.92	50.96	43.68
	$\text{CH}_3\text{CH}_2\text{CH}_2\text{NH}_2$	21.96	13.62	22.43	14.09
		11.74		11.96	
	$\text{H}_2\text{N}(\text{CH}_2)_4\text{NH}_2$	46.46	25.66	43.68	25.66
	$\text{H}_2\text{N}(\text{CH}_2)_5\text{NH}_2$	46.38	25.71	46.26	25.48
		24.31		24.19	
	$\text{H}_2\text{N}(\text{CH}_2)_6\text{NH}_2$	48.03	28.77	48.26	29.71
		27.24		27.24	
		53.78	52.72	53.78	52.72
	$\text{CH}_3\text{CH}_2\text{NH}_2$	25.71	24.31	25.60	24.31
		11.27		11.27	
	$(\text{NH}_2(\text{CH}_2)_2)_2\text{NH}$	45.68		45.68	

## REFERENCES AND NOTES

- 1 (a) A. J. Bard, *J. Photochem.*, 10, 59 (1979) (b) A. J. Bard, *Science* (Washington, D. C.), 207, 139 (1980) (c) A. J. Bard, *J. Phys. Chem.*, 86, 172 (1982) (d) A. J. Nozik, *Annu. Rev. Phys. Chem.*, 29, 189 (1978) (e) M. S. Wrighton, P. T. Wolczanski, and A. B. Ellis, *J. Solid State Chem.*, 22, 17 (1977).
- 2 (a) B. Kraeutler and A. J. Bard, *J. Am. Chem. Soc.*, 100, 2239 (b) B. Kraeutler and A. J. Bard, *J. Am. Chem. Soc.*, 100, 5985.
- 3 I. Izumi, W. W. Dunn, K. O. Wilbourn, F. F. Fan, and A. J. Bard, *J. Phys. Chem.*, 84, 3207 (1980).
- 4 T. Kanno, T. Oguchi, H. Sakuragi, and K. Tokumaru, *Tetrahedron Lett.*, 21, 467 (1980).
- 5 (a) M. A. Fox and C. C. Chen, *J. Am. Chem. Soc.*, 103, 6757 (1981) (b) M. A. Fox and M.-J. Chen, *J. Am. Chem. Soc.*, 105, 4497 (1983).
- 6 J. W. Pavlik and S. Tantayanon, *J. Am. Chem. Soc.*, 103, 6755 (1981).
- 7 M. Fujihira, Y. Sato, and T. Osa, *Bull. Chem. Soc. Jpn*, 55, 666 (1982).
- 8 (a) B.-T. Khai, C. Concilio, and G. Porzi, *J. Organometal. Chem.*, 208, 269 (1981). (b) B.-T. Khai, C. Concilio, and G. Porzi, *J. Org. Chem.*, 46, 1756 (1981).
- 9 N. Yoshimura, I. Moritani, T. Shimamura, and S.-I. Murahashi, *J. Am. Chem. Soc.*, 95, 3038 (1973).
- 10 Japan Industrial Standard K 0102 (1974).
- 11 The author thanks Dr. Toshimi Sawano and Dr. Koichi Sakano

(Nippon Shokubai Kagaku Kogyo Co.) for the GC-MS measurement of the photocatalytic products.

- 12 K. N. Campbell, A. H. Sommers, and B. K. Campbell, J. Am. Chem. Soc., 66, 82 (1966).
- 13 E. H. Cordes and W. P. Jencks, J. Am. Chem. Soc., 84, 832 (1962).
- 14 S. Okazaki and T. Kanto, Nippon Kagaku Kaishi, 404 (1976).

PART II

Photocatalytic Oxidations of 2-Propanol and Water Along  
with Silver Metal Deposition by  $\text{TiO}_2$  Suspension

## Chapter 6

### Photocatalytic Oxygen Formation and Silver Metal Deposition by TiO<sub>2</sub> Suspension in Aqueous Solution of Various Silver Salts

#### ABSTRACT

The photocatalytic reaction of Ar-purged aqueous solutions containing various silver salts and TiO<sub>2</sub> powder in suspension was studied at room temperature. Photoirradiation ( $\lambda_{\text{ex}} > 300$  nm) resulted in O<sub>2</sub> formation and deposition of Ag metal on the TiO<sub>2</sub> particle. The reaction rate depended on the kind of anion of the silver salt and increased in the order; ClO<sub>4</sub><sup>-</sup> < NO<sub>3</sub><sup>-</sup> ≈ SO<sub>4</sub><sup>2-</sup> < F<sup>-</sup> (≈ PO<sub>4</sub><sup>3-</sup>). The sensitizing activity of the rutile (TiO<sub>2</sub>(R)) was comparable to that of the anatase (TiO<sub>2</sub>(A)). The molar ratio of deposited Ag metal to liberated O<sub>2</sub>, which was independent of the reaction rate, was equal to ca. 5 except for the case of TiO<sub>2</sub>(A)/AgClO<sub>4</sub>. The pH of the reaction mixture decreased with irradiation time, resulting in deactivation of TiO<sub>2</sub>. Although O<sub>2</sub> formation and Ag-metal deposition did not occur at pH < 2, the photosensitizing activity of the TiO<sub>2</sub> powder was recovered by the addition of NaOH. The addition of 2-propanol to the deactivated acidic suspension of TiO<sub>2</sub> was also effective for Ag-metal deposition but not for O<sub>2</sub> formation.



## INTRODUCTION

The photoinduced decomposition of water to produce  $H_2$  and  $O_2$  has been achieved using certain powdered semiconductors, such as  $TiO_2$ ,<sup>1-4</sup> with favourable band energies. Currently, successful modifications of the quantum efficiency for the  $TiO_2$ -photosensitized reactions have been made with electron donors,<sup>5-10</sup> such as alcohols, for the reduction of water to  $H_2$  and electron acceptors,<sup>11-14</sup> such as metal cations, for the oxidation of water to  $O_2$ . The oxidation of water has also been studied from the viewpoint of its application to photoimaging processes<sup>15-17</sup> or the photochemical preparation of metal-loaded catalysts.<sup>18,19</sup>

In the present work, the photoinduced reaction of an aqueous  $TiO_2$  suspension containing silver ion is described. The characteristics of the reaction are discussed on the basis of the results concerning the effects of the form of  $TiO_2$  crystal and of the anion of silver salt. Particular emphasis is placed on the deactivation of the  $TiO_2$  photocatalytic activity for the  $O_2$  formation and Ag metal deposition, due to the decrease of pH of the reaction mixture.

## EXPERIMENTAL

Materials. Anatase titanium dioxide ( $TiO_2(A)$ ) was obtained as a white powder (purity, 99 %;  $SO_4^{2-}$ , 0.05 %;  $Cl^-$ , 0.01 %) from Merck. The slightly ivory-colored powder of rutile  $TiO_2$  ( $TiO_2(R)$ ) was prepared by heating  $TiO_2(A)$  in air for 10 h at 1200 °C. The quantitative conversion of  $TiO_2(A)$  into  $TiO_2(R)$  by this treatment was confirmed by comparison of their X-ray diffraction patterns;<sup>20</sup> e.g. the principal anatase peak at  $25.3^\circ$   $2\theta$  ( $3.52 \overset{\circ}{\text{Å}}$ ) disappeared

completely to give an intense peak characteristic of rutile at  $27.3^\circ 2\theta$  ( $3.25 \text{ \AA}$ ) upon heating. Water ( $\text{H}_2\text{O}$ ) was passed through an ion-exchange resin and distilled immediately before use.  $\text{H}_2^{18}\text{O}$  was obtained from CEA (97.3 %). Silver sulphate ( $\text{Ag}_2\text{SO}_4$ ), silver fluoride ( $\text{AgF}$ ), silver perchlorate ( $\text{AgClO}_4$ ), silver nitrate ( $\text{AgNO}_3$ ), silver phosphate ( $\text{Ag}_3\text{PO}_4$ ) and 2-propanol were of reagent grade and used as received.

Method. X-ray diffraction patterns were obtained using a Rigaku Geigerflex 2013 diffractometer (Cu target, Ni filter, 35 kV, 20 mA, at a scanning rate of  $1^\circ \text{ min}^{-1}$ ). Mass spectra were recorded using a Shimadzu Maspeq 070 spectrometer ( $V_e = 80 \text{ V}$ ;  $I_e = 0.1 \text{ A}$ ). Gas chromatography was performed with Shimadzu GC 4A (for  $\text{O}_2$ , equipped with a TCD, column 60-80 mesh Molecular Sieve 5A ( $3 \text{ m} \times 3 \text{ mm}$ ), Ar carrier at  $130^\circ \text{C}$ ) and GC 6A (for 2-propanol and acetone, equipped with an FID, column 20 % Polyethylene Glycol 20M on 60-80 mesh Celite 545 ( $3 \text{ m} \times 3 \text{ mm}$ ),  $\text{N}_2$  carrier at  $70^\circ \text{C}$ ) gas chromatographs. The pH value of the solution was determined with a Hitachi-Horiba F-5 pH meter. Atomic adsorption analysis was performed with a Jarrel-Ash AA 780 or 8200 spectrometer.

In a typical run, a suspension of a finely ground  $\text{TiO}_2$  powder (50 mg) in  $5.0 \text{ cm}^3$  of aqueous silver salt solution (250  $\mu\text{mol}$  of  $\text{Ag}^+$ ) was placed in a glass tube (15 mm diameter, cut-off wavelengths  $< 300 \text{ nm}$ ), purged for 30 min with Ar and then sealed off with a rubber cap prior to irradiation. Irradiation was performed at room temperature using a merry-go-round apparatus equipped with a 400 or 500 W high-pressure mercury arc (Eiko-sha 400 or 500). The distance between the sample and the light source was 5 cm. The Ar-purged

solution was stirred magnetically throughout the irradiation.

After the appropriate irradiation, the amount of  $O_2$  liberated into the gas phase was determined by gas chromatography. The suspension was then centrifuged to separate the  $TiO_2$  powder from the aqueous solution which was normally subjected to pH measurement and which was additionally subjected to gas chromatography in experiments in which 2-propanol was used. The separated  $TiO_2$  powder was washed with distilled water, dried overnight at  $70^\circ C$  and treated with  $HNO_3$  ( $13 \text{ mol dm}^{-3}$ ;  $1.0 \text{ cm}^3$ ). The resulting suspension of bleached  $TiO_2$  was diluted with distilled water and centrifuged. The aqueous  $Ag^+$  solution was subjected to atomic absorption spectroscopy. The reproducibility of the yield of Ag determined by this procedure was within  $\pm 5 \text{ } \mu\text{mol}$ .

In an experiment with  $H_2O$  containing  $H_2^{18}O$  (4.6 mol%), a suspension of  $TiO_2$  powder (50 mg) in  $2.1 \text{ cm}^3$  of  $Ag_2SO_4$  solution (100  $\mu\text{mol}$  of  $Ag^+$ ) was prepared in a glass tube (15 mm $\phi$ ) equipped with a stopcock, deaerated by repeated freeze-pump-thaw cycles under reduced pressure ( $< 40 \text{ mPa}$ ), and then sealed off. Irradiation was performed under conditions similar to those above. After the irradiation, a portion of the gas phase of the sample was transferred to a gas cell ( $21.4 \text{ cm}^3$ ) on a vacuum line and was subjected to mass spectroscopy for the determination of oxygen isotope distribution.

## RESULTS AND DISCUSSION

Photoreaction of Aqueous Silver Salt Solutions in the Presence of Suspended  $TiO_2$ . Table 1 shows the results of the photoirradiation ( $\lambda_{\text{ex}} > 300 \text{ nm}$ ) under Ar. During the irradiation the dispersed  $TiO_2$

Table 1 Oxygen formation and silver metal deposition in the photo-irradiated system of TiO<sub>2</sub>/silver salt.<sup>a</sup>

Silver Salt	TiO <sub>2</sub> (A)			TiO <sub>2</sub> (R)		
	O <sub>2</sub> /μmol	Ag /μmol	Ag /O <sub>2</sub>	O <sub>2</sub> /μmol	Ag /μmol	Ag /O <sub>2</sub>
AgClO <sub>4</sub>	2.0	18.2	9.0	11.6	64.1	5.5
AgNO <sub>3</sub>	7.0	39.9	5.7	24.5	117.7	4.8
Ag <sub>2</sub> SO <sub>4</sub>	9.3	53.7	5.8	23.0	115.9	5.0
AgF	35.4	181.3	5.1	37.1	182.6	4.9
Ag <sub>3</sub> PO <sub>4</sub> <sup>b</sup>	(44.4)	(218.2)	(4.9)	(41.1)	(182.2)	(4.4)

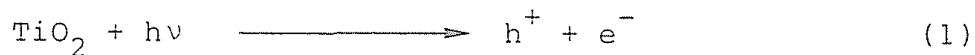
<sup>a</sup>TiO<sub>2</sub> 50 mg, silver salt (containing 250 μmol of silver ion) and water 5.0 cm<sup>3</sup> were placed in a test tube and irradiated with a 500-W high-pressure mercury arc under Ar for 5 h. <sup>b</sup>Partially dissolved.

powder turned grey in  $\text{AgClO}_4$ ,  $\text{AgNO}_3$  and  $\text{Ag}_2\text{SO}_4$  solutions and brown in  $\text{AgF}$  solution and  $\text{Ag}_3\text{PO}_4$  suspension. The X-ray diffraction patterns of the coloured  $\text{TiO}_2(\text{A})$  powders, which were separated from the  $\text{Ag}_2\text{SO}_4$  and  $\text{AgF}$  solutions, involved new diffraction lines assigned to Ag metal<sup>21</sup> in addition to those of  $\text{TiO}_2$ . This observation demonstrates that the  $\text{Ag}^+$  ion is deposited on  $\text{TiO}_2$  particles during the irradiation.<sup>22</sup> Mass spectroscopic measurement showed the formation of oxygen ( $m/e = 32 (\text{M}^+)$ ) in the gas phase together with the Ag-metal deposition. No other volatile products were observed.

Neither  $\text{O}_2$  formation nor Ag-metal deposition occurred in the dark. Irradiation of the suspension of  $\text{TiO}_2(\text{A})$  in  $\text{Ag}_2\text{SO}_4$  solution at  $\lambda_{\text{ex}} > 390$  nm (Toshiba L-42 glass filter) led to the formation of negligible amount of  $\text{O}_2$ . Furthermore, the irradiation of both  $\text{TiO}_2(\text{A})$  and  $\text{TiO}_2(\text{R})$  suspensions in Ar-purged water without a silver salt produced negligible amount of  $\text{O}_2$ ; e.g. the yield was  $< 0.01$   $\mu\text{mol}$  after 10 h irradiation. In the analogous experiments without  $\text{TiO}_2$  powder, none of the aqueous solutions except  $\text{Ag}_3\text{PO}_4$  yielded  $\text{O}_2$  on irradiation at  $\lambda_{\text{ex}} > 300$  nm. When  $\text{Ag}_3\text{PO}_4$  (250  $\mu\text{mol}$  of  $\text{Ag}^+$ ), which is less soluble brown powder, was dispersed in water (5.0  $\text{cm}^3$ ) and irradiated for 5 h, 8.0  $\mu\text{mol}$  of  $\text{O}_2$  could be detected, while the yield was increased by a factor of 5.6 in the presence of  $\text{TiO}_2$  powder (Table 1). The presence of non-semiconductor silicon oxide ( $\text{SiO}_2$ , 50 mg) in the  $\text{Ag}_3\text{PO}_4$  suspension led to a comparable yield of  $\text{O}_2$  (8.2  $\mu\text{mol}$ ) with negligible Ag-metal deposition ( $< 2$   $\mu\text{mol}$ ) on the oxide.

In view of these results,  $\text{O}_2$  formation and Ag-metal deposition are attributable to the well known photocatalytic property of

semiconductor particle of  $\text{TiO}_2$ , which can photochemically generate hole-electron pair, i.e.,

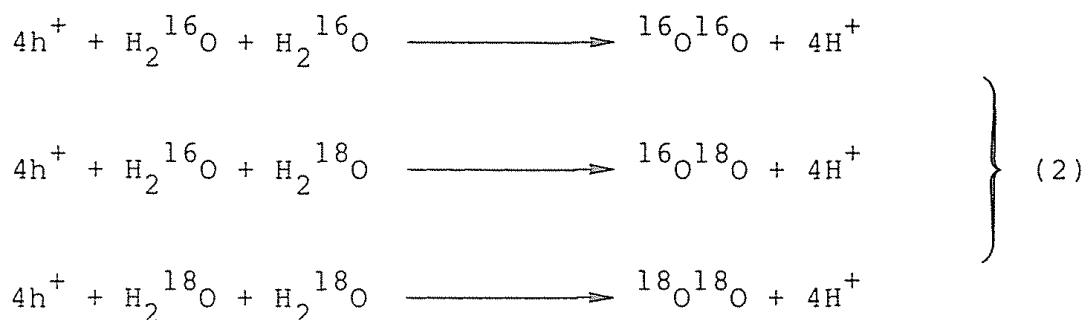


It is seen from Table 1 that the activities of powdered  $\text{TiO}_2$  for photoinduced  $\text{O}_2$  formation and Ag deposition are affected by the kind of anion in the silver salt, increasing in the order  $\text{ClO}_4^- < \text{NO}_3^- \approx \text{SO}_4^{2-} < \text{F}^- (= \text{PO}_4^{3-}$ , the activity cannot be compared directly since this salt was less soluble than the others). Particularly, the yield of  $\text{O}_2$  varied over the range 2.0-44.4  $\mu\text{mol}$  for  $\text{TiO}_2(\text{A})$ , while the activities of the  $\text{TiO}_2(\text{R})$  suspensions were relatively less sensitive to the variation of anion. In a given solution of  $\text{AgClO}_4$ ,  $\text{AgNO}_3$  or  $\text{Ag}_2\text{SO}_4$ ,  $\text{TiO}_2(\text{R})$  was more than twice as active as  $\text{TiO}_2(\text{A})$  for both  $\text{O}_2$  formation and Ag-metal deposition. In contrast, almost identical activities were obtained with  $\text{AgF}$  or  $\text{Ag}_3\text{PO}_4$ .

$\text{O}_2$  Formation via Photoinduced Decomposition of Water. In order to clarify the source of the molecular oxygen, the isotope distribution in the oxygen molecules was determined by mass spectroscopy for an aqueous silver salt solution containing  $\text{H}_2^{18}\text{O}$ .  $\text{TiO}_2(\text{A})$  or  $\text{TiO}_2(\text{R})$  powder (50 mg) was suspended in a mixture of 95.4 mol%  $\text{H}_2^{16}\text{O}$  and 4.6 mol%  $\text{H}_2^{18}\text{O}$  (2.1  $\text{cm}^3$ ) containing  $\text{Ag}_2\text{SO}_4$  (100  $\mu\text{mol}$  of  $\text{Ag}^+$ ) and irradiated for 5 h. Table 2 indicates that  $^{18}\text{O}$  in  $\text{H}_2^{18}\text{O}$  is liberated photochemically to form molecular oxygen as  $^{16}\text{O}^{18}\text{O}$  and  $^{18}\text{O}^{18}\text{O}$  in both systems.

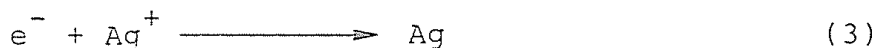
Assuming that water undergoes oxidative decomposition by the hole ( $h^+$ ), which is generated photochemically on the  $\text{TiO}_2$  particles,

the following three processes are possible:



The distribution of  ${}^{16}O^{16}O$  :  ${}^{16}O^{18}O$  :  ${}^{18}O^{18}O$  under the present conditions can be calculated as shown in Table 2 on the assumption that the reactivities of  $h^+$  toward  $H_2^{16}O$  and  $H_2^{18}O$  are identical. This is in good agreement with the observed distributions in both  $TiO_2(A)$  and  $TiO_2(R)$  systems. From these facts it is concluded that photochemical  $O_2$  formation originates from water oxidation. The decomposition of either the  $TiO_2$  lattice or the  $SO_4^{2-}$  ion does not occur to produce  $O_2$ .

It is also likely that Ag-metal deposition occurs via reduction of the  $Ag^+$  ion by the electron ( $e^-$ )<sup>15-17</sup> generated simultaneously with the hole ( $h^+$ ) (reaction (1)), i.e.

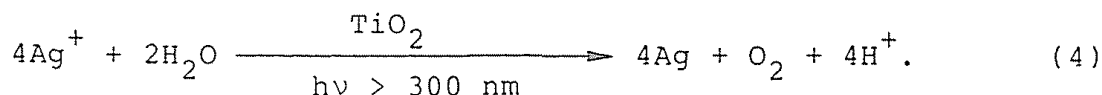


The overall photoredox reaction leading to  $O_2$  formation and Ag-metal deposition, which would occur on the same  $TiO_2$  particle,<sup>23</sup> is as follows:

Table 2 Oxygen isotope distribution observed in the photoinduced reaction system  $\text{TiO}_2/\text{Ag}_2\text{SO}_4$ .

	distribution (%)		
	$^{16}\text{O}^{16}\text{O}$	$^{16}\text{O}^{18}\text{O}$	$^{18}\text{O}^{18}\text{O}$
observed for $\text{TiO}_2(\text{A})$	91.6	8.2	0.2
observed for $\text{TiO}_2(\text{R})$	91.9	7.9	0.2
calculated	91.0	8.8	0.2





As is seen from Table 1, the observed molar ratio of deposited Ag metal to liberated O<sub>2</sub> is close to 5, almost independent of the crystal structure of TiO<sub>2</sub> and the anion of the silver salt. As an exception, the Ag : O<sub>2</sub> ratio (= 9.1) in the TiO<sub>2</sub>(A)/AgClO<sub>4</sub> system was nearly twice those in the other systems. Apparently the observed value of ca. 5 is larger than the stoichiometric value of 4 in reaction (4). The discrepancy would be due to the photoadsorption of O<sub>2</sub> leading to the formation of O<sub>2</sub><sup>-</sup> on TiO<sub>2</sub> surface.<sup>13,14,24-26</sup>

Time-course of the Photoinduced Reaction. Figure 1(a) illustrates the time course of photoinduced O<sub>2</sub> formation from a TiO<sub>2</sub>(A) or TiO<sub>2</sub>(R) suspension in Ar-purged Ag<sub>2</sub>SO<sub>4</sub> and AgF solutions. The amount of O<sub>2</sub> increased with the irradiation time and attained its maximum value in all cases. As shown in Figure 2, the amount of the deposited Ag was ca. 5 times larger than that of O<sub>2</sub>; the ratio was independent of the irradiation time.

In each system of TiO<sub>2</sub>(A)/Ag<sub>2</sub>SO<sub>4</sub>, AgClO<sub>4</sub> or AgNO<sub>3</sub>, the maximum yield of the deposited Ag, in the range 10-20 % based on the amount of Ag<sup>+</sup> ion, was obtained within 2 h (see Table 1). In contrast, the amount of O<sub>2</sub> and Ag metal in the TiO<sub>2</sub>(R)/Ag<sub>2</sub>SO<sub>4</sub> system increased continuously even after the 2 h irradiation, up to the maximum yields (ca. 40 μmol of O<sub>2</sub> and ca. 200 μmol of Ag, 80 % yield based on the amount of Ag<sup>+</sup> ion) for 24 h irradiation. Irradiation of the AgF solution with either TiO<sub>2</sub>(A) or TiO<sub>2</sub>(R) powder produced O<sub>2</sub> at a greater rate than that observed with Ag<sub>2</sub>SO<sub>4</sub> solutions, i.e. more than 80

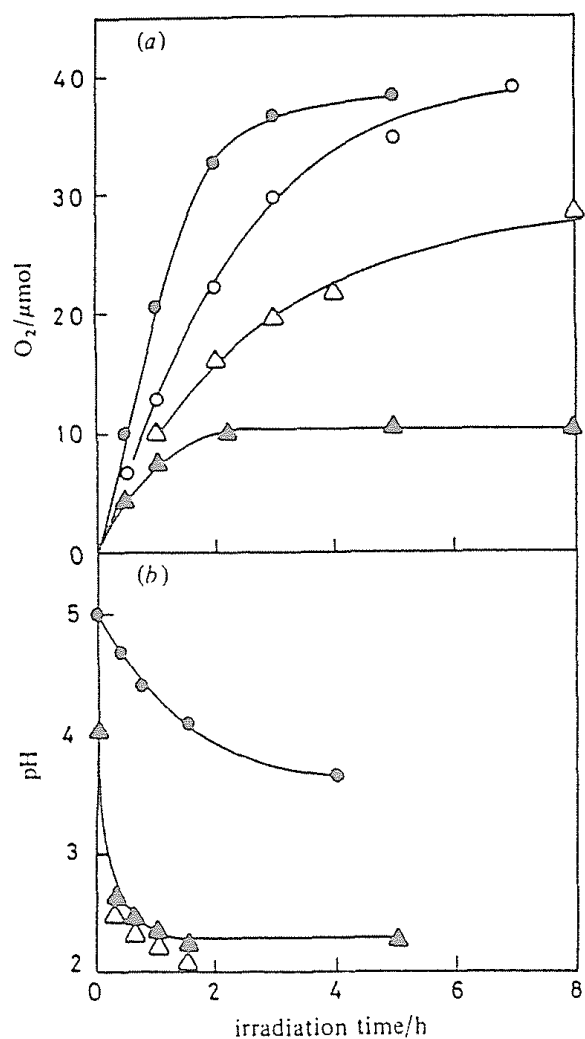


Figure 1 Variation in (a)  $O_2$  yield and (b) pH as a function of time of irradiation ( $\lambda_{\text{ex}} > 300 \text{ nm}$ ) on Ar-purged aqueous suspensions ( $5.0 \text{ cm}^3$ ):  $\blacktriangle$ ,  $\text{TiO}_2(\text{A})/\text{Ag}_2\text{SO}_4$ ;  $\triangle$ ,  $\text{TiO}_2(\text{R})/\text{Ag}_2\text{SO}_4$ ;  $\bullet$ ,  $\text{TiO}_2(\text{A})/\text{AgF}$ ;  $\circ$ ,  $\text{TiO}_2(\text{R})/\text{AgF}$  (50 mg of  $\text{TiO}_2$ ; 250  $\mu\text{mol}$  of  $\text{Ag}^+$ ).

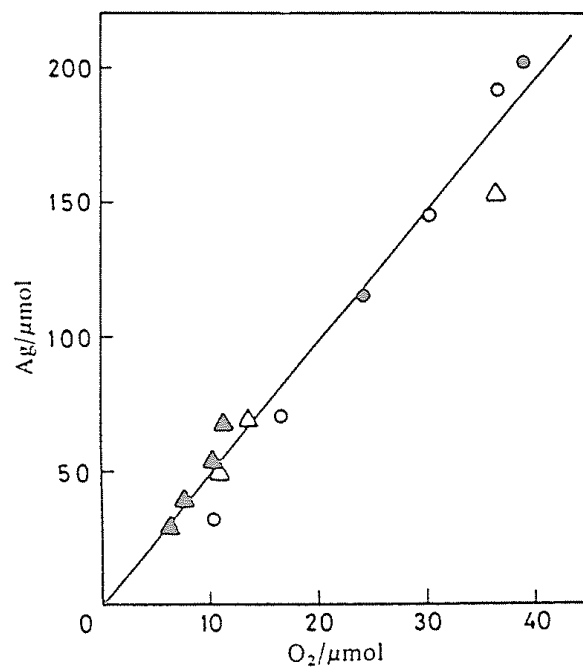


Figure 2 Variation in the yield of Ag metal as a function of the yield of O<sub>2</sub>; ▲, TiO<sub>2</sub>(A)/Ag<sub>2</sub>SO<sub>4</sub>; △, TiO<sub>2</sub>(R)/Ag<sub>2</sub>SO<sub>4</sub>; ●, TiO<sub>2</sub>(A)/AgF; ○, TiO<sub>2</sub>(R)/AgF.

3 of the  $\text{Ag}^+$  ion were photoreduced within 5 h.

As shown in Figure 1(b), the pH value of the reaction mixture decreased rapidly in the  $\text{TiO}_2(\text{A})$  or  $\text{TiO}_2(\text{R})/\text{Ag}_2\text{SO}_4$  system and slowly in the  $\text{TiO}_2(\text{A})/\text{AgF}$  system by the irradiation. The amount of proton ( $\text{H}^+$ ) released in the reaction system at a given time during the irradiation was estimated for convenience from the pH and is plotted against the corresponding yield of  $\text{O}_2$  in Figure 3. The  $\text{H}^+/\text{O}_2$  ratio of ca. 3 was obtained for the  $\text{TiO}_2(\text{A})$  or  $(\text{R})/\text{Ag}_2\text{SO}_4$  system from the slope of these linear plots. This is near to the theoretical value of 4 in reaction (4). However, the  $\text{H}^+/\text{O}_2$  ratio for the AgF system was nearly zero. It appears that most of the  $\text{H}^+$  generated in the AgF solution associates with  $\text{F}^-$ , which was released as the result of the Ag deposition, to form HF because of its extremely small acid-base equilibrium constant ( $\text{pK}_a = 3.45$ )<sup>27</sup> when compared with that of  $\text{H}_2\text{SO}_4$ . It is reasonable to predict that both the  $\text{AgNO}_3$  and  $\text{AgClO}_4$  systems produce highly dissociative acids of  $\text{HNO}_3$  and  $\text{HClO}_4$ , respectively, analogously to the  $\text{Ag}_2\text{SO}_4$  system.

pH Dependence of the Photocatalytic Activity of  $\text{TiO}_2$ . The rate of  $\text{O}_2$  formation ( $R_{\text{O}_2}$ ) at a given time over the irradiation period was estimated from the slope of the  $\text{O}_2$  yield against time curve (see Figure 1(a)). Figure 4 shows the plots of  $R_{\text{O}_2}$  against pH of the aqueous phase of the reaction mixture at the corresponding time. The rate of  $\text{O}_2$  formation in the  $\text{TiO}_2(\text{A})/\text{Ag}_2\text{SO}_4$  system was reduced gradually as the pH value decreased to ca. 3.

In the pH range from 3 to 2, however, a very rapid decrease in  $R_{\text{O}_2}$  by a factor of ca. 10 (corresponding to a maximum factor because the  $R_{\text{O}_2}$  values were uncorrected for the decreased concentration of

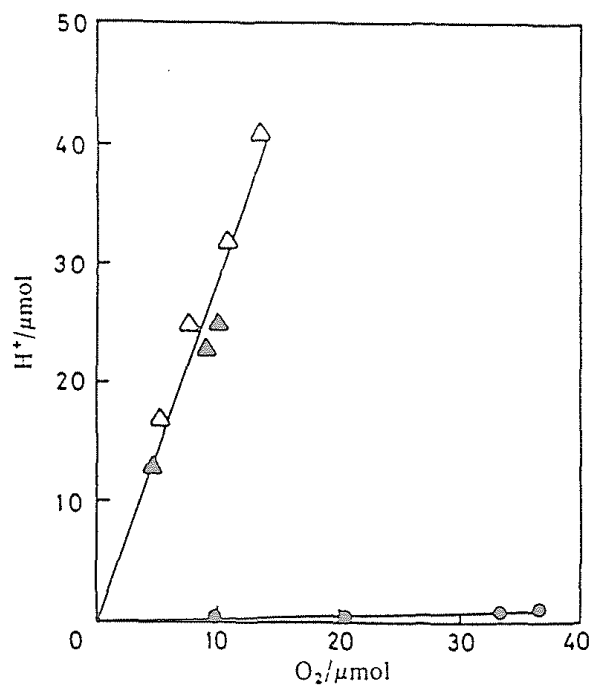


Figure 3 Variation in the increase of  $H^+$  as a function of the yield of  $O_2$ :  $\blacktriangle$ ,  $TiO_2(A)/Ag_2SO_4$ ;  $\triangle$ ,  $TiO_2(R)/Ag_2SO_4$ ;  $\bullet$ ,  $TiO_2(A)/AgF$ .

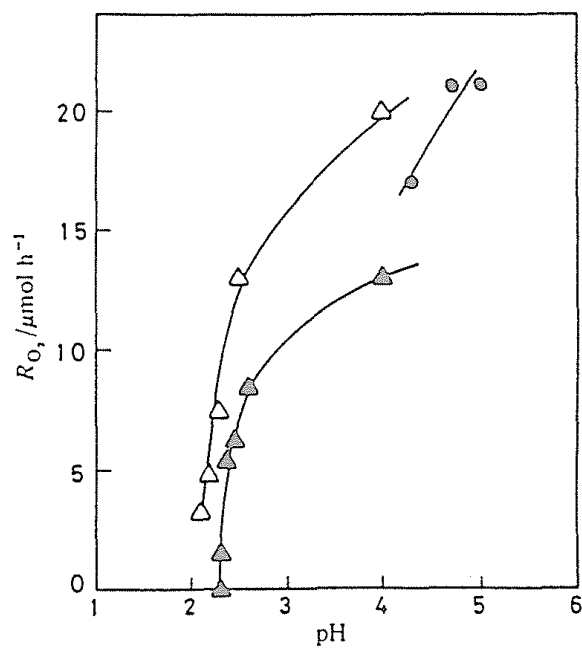


Figure 4 pH Dependence of the rate of O<sub>2</sub> formation (R<sub>O<sub>2</sub></sub>): ▲, TiO<sub>2</sub>(A)/Ag<sub>2</sub>SO<sub>4</sub>; △, TiO<sub>2</sub>(R)/Ag<sub>2</sub>SO<sub>4</sub>; ●, TiO<sub>2</sub>(A)/AgF. The data points were derived from Figure 1 (see text).

$\text{Ag}^+$  ions (see also Figure 2)) occurred. In agreement with this behaviour, neither  $\text{O}_2$  formation nor Ag-metal deposition could be detected on irradiation of a  $\text{TiO}_2(\text{A})$  (50 mg) suspension in Ar-purged  $\text{AgNO}_3$  solution (250  $\mu\text{mol}$  of  $\text{Ag}^+$ ; 5.0  $\text{cm}^3$ ), which was adjusted to pH 1.5 with  $\text{HNO}_3$  prior to irradiation.

The characteristic of the pH-dependent deactivation of  $\text{TiO}_2(\text{R})$  in  $\text{Ag}_2\text{SO}_4$  solution was essentially identical with that of  $\text{TiO}_2(\text{A})$ , but significant deactivation occurred under more acidic conditions. Similarly, the rates of the photocatalytic  $\text{O}_2$  formation by  $\text{TiO}_2(\text{A})$  suspended in AgF solution decreased with decreasing pH, although the pH change during the irradiation was very small. Such a pH effect can account for the observed trend for the silver salts (see Table 1); i.e. salts of weak acids such as AgF and  $\text{Ag}_3\text{PO}_4$  give greater yields than those of strong acids because  $\text{F}^-$  and  $\text{PO}_4^{3-}$  cause smaller pH decrease during the photoreaction. The activity of  $\text{TiO}_2$  in  $\text{AgClO}_4$  solution is due to the lowest initial pH value ( $< 3$ ). Similarly,  $\text{TiO}_2(\text{R})$  shows higher activity than  $\text{TiO}_2(\text{A})$  in the  $\text{AgClO}_4$ ,  $\text{AgNO}_3$  and  $\text{Ag}_2\text{SO}_4$  solutions because of its lower sensitivity to decreasing pH, but comparable activities are observed with AgF or  $\text{Ag}_3\text{PO}_4$  leading to a smaller decrease in pH during the photoreaction.

Further experiments were performed to find out whether the  $\text{TiO}_2$ , which is deactivated in acidic solutions, retains its original activity. For example,  $\text{TiO}_2(\text{A})$  powder (250 mg) was suspended in an  $\text{Ag}_2\text{SO}_4$  solution (1.25 mmol of  $\text{Ag}^+$ ; 25.0  $\text{cm}^3$ ) and irradiated for 20 h under Ar.  $\text{TiO}_2(\text{A})$  powder covered with Ag metal deposit (ca. 50  $\mu\text{mol}$  of Ag on 50 mg of the powder) was recovered and then suspended in freshly prepared  $\text{Ag}_2\text{SO}_4$  or AgF solution (250  $\mu\text{mol}$  of  $\text{Ag}^+$ ; 5.0

cm<sup>3</sup>) and irradiated under similar conditions. Figure 5 shows the variations of O<sub>2</sub> yield with irradiation time, indicating that the recovered TiO<sub>2</sub>(A) powder retains its original activity in Ag<sub>2</sub>SO<sub>4</sub> solution on the second irradiation, while the activity in AgF solution is reduced to ca. 70 %.

In a similar experiment, a suspension of powdered TiO<sub>2</sub>(A) (50 mg) in Ag<sub>2</sub>SO<sub>4</sub> solution (250 μmol of Ag<sup>+</sup>; 5.0 cm<sup>3</sup>) was neutralized by adding 0.1 cm<sup>3</sup> portions of aqueous NaOH solution (1.0 mol dm<sup>-3</sup>) at appropriate times during the irradiation when the rate of O<sub>2</sub> formation fell to nearly zero. The results show that the addition of an alkaline solution can keep the activity of semiconductor TiO<sub>2</sub> at the level required to produce O<sub>2</sub> via photo-oxidative decomposition of water.

On the other hand, although the TiO<sub>2</sub>(A) suspension in Ag<sub>2</sub>SO<sub>4</sub> solution after 20 h irradiation could no longer produce O<sub>2</sub> and Ag metal because of the decreased pH value of the reaction mixture, it was still able to oxidize 2-propanol. In a typical run, irradiation of pre-exposed (20 h) TiO<sub>2</sub>(A)/Ag<sub>2</sub>SO<sub>4</sub> system (the liberated O<sub>2</sub> was purged by Ar prior to the second irradiation) for 2 h in the presence of 2-propanol (500 μmol, 38 mm<sup>3</sup>) yielded 22 μmol of acetone and 51 μmol of deposited Ag metal.

These results clearly demonstrate that the photosensitizing activity of TiO<sub>2</sub> powder for the oxidative decomposition of water to O<sub>2</sub> is promoted by the reduction of the Ag<sup>+</sup> ion as an electron acceptor to Ag metal, but is reduced significantly due to a lowering of the pH of the reaction system during irradiation. Optimum pH control of the aqueous reaction system would enable to obtain the highest



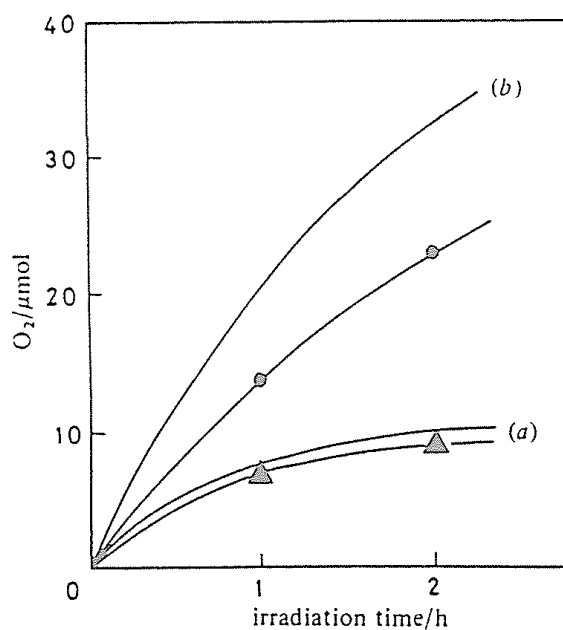
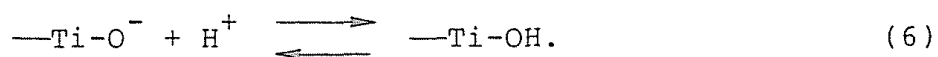
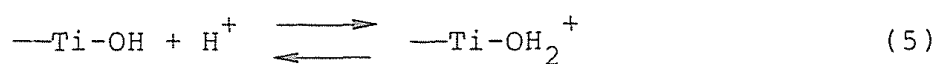


Figure 5 Variation in O<sub>2</sub> yield as a function of time of irradiation ( $\lambda_{\text{ex}} > 300$  nm) of suspension of TiO<sub>2</sub>(A) powder (50 mg), which was recovered from a pre-irradiated (20 h) suspension in Ag<sub>2</sub>SO<sub>4</sub> solution (see text), in Ar-purged aqueous solutions of  $\blacktriangle$ , Ag<sub>2</sub>SO<sub>4</sub> and  $\bullet$ , AgF (250  $\mu\text{mol}$  of Ag<sup>+</sup>; 5.0 cm<sup>3</sup>). The solid lines (a) and (b) denote the time-dependent O<sub>2</sub> yields in Ag<sub>2</sub>SO<sub>4</sub> and AgF, respectively, with a fresh TiO<sub>2</sub>(A) powder.

activity of semiconductor  $\text{TiO}_2$ .

In view of the results of electrochemical studies of the  $\text{TiO}_2$  electrode,<sup>28</sup> the relative potential of  $\text{TiO}_2$  powder with respect to the oxidation of water should be constant regardless of pH, assuming that  $\text{TiO}_2$  powder shows the same behaviour as in the electrode. Therefore, the reversible change in the  $\text{TiO}_2$  activity shown above should be attributable to a pH-dependent modification of the  $\text{TiO}_2$  surface. It is possible that OH groups on the  $\text{TiO}_2$  surface protonate or deprotonate according to the following acid-base equilibria:<sup>29</sup>



The known  $\text{pK}_a$  values<sup>30</sup> of anatase  $\text{TiO}_2$  were 4.98 and 7.80 for equilibria (5) and (6), respectively. It follows that the OH groups on the  $\text{TiO}_2$  used in this work are partly protonated at the initial pH of the photoreaction systems (ca. 4 to 5, see Figure 1). As the reaction proceeds, the pH decreases, resulting in entire protonation of the surface OH groups and the deactivation of the  $\text{TiO}_2$  powder. Thus, the protonated, *i.e.* positively charged, surface would be less favourable for the photoinduced reaction. Similar behaviour of the  $\text{TiO}_2$  activity has been reported by Mills and Porter.<sup>14</sup>

Adsorption of the  $\text{Ag}^+$  ion on the  $\text{TiO}_2$  surface has been reported.<sup>15,17</sup> Such  $\text{Ag}^+$  adsorption to release  $\text{H}^+$  would become less significant with decreasing pH, *i.e.* increase in the protonated surface,

resulting in  $\text{TiO}_2$  deactivation. However, another explanation for the deactivation is also possible, in that the probability of the water oxidation by the photogenerated positive hole to form  $\text{O}_2$  is decreased with increasing protonation of the surface. Among these possibilities, the former likely accounts for the pH dependent activity of  $\text{TiO}_2$ ; the amount of adsorbed  $\text{Ag}^+$  decreases with the pH decrease and thereby decreases the  $\text{TiO}_2$  photocatalytic activity, as has been described in Chapter 11 of this thesis.

In conclusion, it is clarified in this chapter that (1)  $\text{TiO}_2$  photocatalytic activity for the  $\text{O}_2$  formation and Ag metal deposition significantly depends on the pH of the suspension, and (2) the kind of anion in the silver salt influences on the initial pH of the suspension and on the course of the pH decrease during the photoirradiation.

## REFERENCES AND NOTES

- 1 A. V. Bulatov and M. L. Khidekel, *Izv. Acad. Nauk SSSR. Ser. Khim.*, 1902 (1976).
- 2 G. N. Schrauzer and T. D. Guth, *J. Am. Chem. Soc.*, 99, 7189 (1977).
- 3 S. Sato and J. M. White, *Chem. Phys. Lett.*, 72, 83 (1980).
- 4 T. Kawai and T. Sakata, *Chem. Phys. Lett.*, 72, 87 (1980).
- 5 T. Kawai and T. Sakata, *J. Chem. Soc., Chem. Commun.*, 1947 (1970); 694 (1980); *Nature (London)*, 286, 474 (1980); *Chem. Lett.*, 81 (1980).
- 6 S. Sato and J. M. White, *J. Phys. Chem.*, 85, 336 (1981); *Chem. Phys. Lett.*, 70, 131 (1980); *J. Am. Chem. Soc.*, 102, 7206 (1980).
- 7 P. Pichat, J-M. Herrmann, J. Disdier, H. Courbon and M-N. Mozzanega, *Nouv. J. Chim.*, 5, 627 (1981).
- 8 Y. Oosawa, *J. Chem. Soc., Chem. Commun.*, 221 (1982).
- 9 S. Teratani, J. Nakamichi, K. Taya and K. Tanaka, *Bull. Chem. Soc. Jpn*, 55, 1688 (1982).
- 10 K. Domen, S. Naito, T. Ohnishi and K. Tamaru, *Chem. Lett.*, 555 (1982).
- 11 A. A. Krasnovskii and G. P. Brin. *Dokl. Akad. Nauk SSSR*, 139, 142 (1961); 147, 656 (1962); 168, 1100 (1966).
- 12 A. A. Krasnovskii, G. P. Brin and Z. Aliev, *Dokl. Akad. Nauk SSSR*, 199, 952 (1971).
- 13 E. Borgarello, J. Kiwi, M. Grätzel, E. Pelizzeti and M. Visca, *J. Am. Chem. Soc.*, 104, 2996 (1982).

- 14 A. Mills and G. Porter, *J. Chem. Soc., Faraday Trans. 1*, 78, 3659 (1982).
- 15 P. D. Fleischauer, H. K. Alen Kan and J. R. Schepherd, *J. Am. Chem. Soc.*, 94, 283 (1972).
- 16 A. W. Adamson and P. D. Fleischauer, *Concepts of Inorganic Photochemistry* (Wiley, New York, 1975), p. 400.
- 17 H. Hada, Y. Yonezawa and M. Saikawa, *Bull. Chem. Soc. Jpn*, 55, 2010 (1982).
- 18 B. Kraeutler and A. J. Bard, *J. Am. Chem. Soc.*, 100, 4317 (1978).
- 19 H. Reiche, W. W. Dunn and A. J. Bard, *J. Phys. Chem.*, 83, 2248 (1979).
- 20 Joint Committee on Powder Diffraction Standards, *Powder Diffraction File* (Swarthmore, 1974), set 21, no. 1272 (anatase) and set 21, no. 1276 (rutile).
- 21 Joint Committee on Powder Diffraction Standard, *Powder Diffraction File* (Swarthmore, 1974), set 4, no. 0783.
- 22 A. Goetz and E. C. Y. Inn, *Rev. Mod. Phys.*, 20, 131 (1948).
- 23 A. J. Bard, *J. Photochem.*, 10, 59 (1979).
- 24 A. H. Boonstra and C. A. H. A. Mutsaers, *J. Phys. Chem.*, 79, 1694 (1975).
- 25 G. Munuera, V. Rives-Arnau and A. Saucedo, *J. Chem. Soc., Faraday Trans. 1*, 75, 736 (1979).
- 26 A. R. Gonzalez-Elipse. G. Munuera and J. Soria, *J. Chem. Soc. Faraday Trans. 1*, 75, 748 (1979).
- 27 D. Dobos, *Electrochemical Data* (Elsevier, Amsterdam, 1975), p. 149.

- 28 E. C. Dutoit, F. Cardon and W. P. Gomes, Ber. Bunsenges. Phys. Chem., 80, 475 (1976).
- 29 H. P. Boehm, Discuss. Faraday Soc., 52, 264 (1971).
- 30 P. W. Schindler and H. Gamsjager, Discuss. Faraday Soc., 52, 286 (1971).
- 31 The author thanks Professor Dr. Satohiro Yoshida for his valuable advice on mass spectroscopic and X-ray diffraction measurements.
- 32 The author thanks Dr. Eiichiro Nakayama of the Instrumental Analyses Research Center of Kyoto University for his kind advice on atomic absorption measurements.

## Chapter 7

### Photocatalytic Oxidations of 2-Propanol and Water by TiO<sub>2</sub> Suspension in Aqueous Solution of Various Silver Salts

#### ABSTRACT

The effects of 2-propanol and counter anion of a series of silver salts on the photoreaction ( $\lambda_{\text{ex}} > 300 \text{ nm}$ ) catalyzed by a suspension of TiO<sub>2</sub>, anatase (TiO<sub>2</sub>(A)) or rutile (TiO<sub>2</sub>(R)), in aqueous solution were studied at room temperature under Ar. The oxidative decomposition of water to form O<sub>2</sub> was depressed by the addition of 2-propanol as a result of competitive oxidation of the 2-propanol to acetone. The presence of 2-propanol enhanced the reduction of Ag<sup>+</sup> ion to Ag metal in the TiO<sub>2</sub>(A) system. Both the oxidation rates of water and 2-propanol increased with increasing the pK<sub>a</sub> of conjugate acids for the counter anion of the silver salt. In the CH<sub>3</sub>COOAg solution the decarboxylation of acetate ion to liberate CO<sub>2</sub> occurred simultaneously, for which TiO<sub>2</sub>(A) was more active than TiO<sub>2</sub>(R).

## INTRODUCTION

Previously, the photocatalytic action of powdered  $\text{TiO}_2$ , either anatase ( $\text{TiO}_2(\text{A})$ ) or rutile ( $\text{TiO}_2(\text{R})$ ), that gives rise to the oxidation of water to liberate  $\text{O}_2$  and reduction of  $\text{Ag}^+$  ion to deposit Ag metal onto the  $\text{TiO}_2$  particle in aqueous suspension containing silver salt has been reported in the preceding chapter of this thesis.<sup>1</sup> This mode of photocatalytic reaction did not proceed in the pH range below 2, while the  $\text{TiO}_2$  was still able to induce oxidation of 2-propanol to acetone under photoirradiation.

The present study characterizes further details of the  $\text{TiO}_2$  catalyzed photoreaction in aqueous solution of several silver salts containing 2-propanol. In this chapter the effects of the 2-propanol and the series of the counter anions of silver salts on the photoreaction characteristics are described. The difference in photocatalytic activity between  $\text{TiO}_2(\text{A})$  and  $\text{TiO}_2(\text{R})$  is discussed on the basis of these results.

## EXPERIMENTAL

Materials. Anatase powder of  $\text{TiO}_2$  ( $\text{TiO}_2(\text{A})$ ) was supplied by Merck and rutile powder ( $\text{TiO}_2(\text{R})$ ) was prepared by heating the  $\text{TiO}_2(\text{A})$ . The characterization of these powders was carried out as reported.<sup>1</sup> Water was passed through an ion-exchange resin and distilled immediately prior to use. Silver salts ( $\text{AgClO}_4$ ,  $\text{AgNO}_3$ ,  $\text{Ag}_2\text{SO}_4$ ,  $\text{AgF}$ ,  $\text{Ag}_3\text{PO}_4$ , and  $\text{CH}_3\text{COOAg}$ ) and 2-propanol were of reagent grade and used without further purification.

Photoirradiation. A finely ground  $\text{TiO}_2$  powder (50 mg) was suspended in  $5.0 \text{ cm}^3$  of aqueous silver salt solution (250  $\mu\text{mol}$  of  $\text{Ag}^+$ ), which



was freshly prepared in a glass tube (15 mm $\phi$   $\times$  180 mm, transmits wavelengths  $>$  300 nm of the light), purged for 30 min with Ar and then sealed off with a rubber cap. After injection of 2-propanol (38 mm<sup>3</sup>, 500  $\mu$ mol), the Ar-purged and magnetically stirred aqueous TiO<sub>2</sub> suspension was irradiated at room temperature using a merry-go-round apparatus equipped with a 400-W high-pressure mercury arc (Ei-ko-sha 400).

Product Analysis. The procedures for the analyses of liberated O<sub>2</sub>, acetone, and deposited Ag were the same as reported previously.<sup>1</sup> In the experiments with CH<sub>3</sub>COOAg, carbon dioxide liberated into the gas phase of the sealed sample was analyzed by a Shimadzu GC 4A gas chromatograph equipped with a TCD (column Chromosorb 103 (3 mm $\phi$   $\times$  3 m), Ar carrier at 100 °C).

## RESULTS AND DISCUSSION

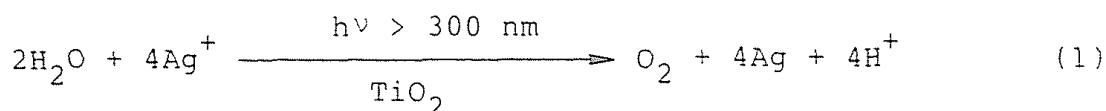
Effect of 2-Propanol on the TiO<sub>2</sub> Catalyzed Photoredox Reaction in Aqueous Solution of Inorganic Silver Salts. Table 1 summarizes the product distribution observed upon photoirradiation ( $\lambda_{\text{ex}} >$  300 nm) of a suspension of powdered TiO<sub>2</sub> in Ar-purged aqueous solution containing inorganic silver salt and 2-propanol. Typically, the Ag<sub>2</sub>SO<sub>4</sub> solution without 2-propanol (pH  $\approx$  4.0 before irradiation) led to O<sub>2</sub> formation and Ag-metal deposition (Runs 1 and 2). The molar ratio of liberated O<sub>2</sub> to deposited Ag metal was ca. 0.20, almost independent of the crystal structure of TiO<sub>2</sub>. These characteristics of the photocatalytic reaction are in accord with the previous observation (see Chapter 6).<sup>1</sup> Thus, the overall photoredox reaction is given as follows:

Table 1 Photocatalytic reaction by  $\text{TiO}_2$  in aqueous solution of inorganic silver salts with and without 2-propanol.<sup>a</sup>

Run	$\text{TiO}_2$ <sup>b</sup>	Silver Salt	Product/ $\mu\text{mol}$			S <sup>c</sup> %	Initial pH
			$\text{O}_2$	Acetone	Ag		
1	A	$\text{Ag}_2\text{SO}_4$ <sup>d</sup>	10.0	—	50	—	4.0
2	R	$\text{Ag}_2\text{SO}_4$ <sup>d</sup>	19.9	—	95	—	4.0
3	A	$\text{AgClO}_4$	0.4	41	94	98	2.7
4	A	$\text{AgNO}_3$	0.7	46	100	97	3.8
5	A	$\text{Ag}_2\text{SO}_4$	0.9	46	107	96	4.0
6	A	$\text{AgF}$	3.3	64	161	91	5.0
7	A	$\text{Ag}_3\text{PO}_4$ <sup>e</sup>	5.0	66	(210) <sup>f</sup>	87	— <sup>g</sup>
8	R	$\text{AgClO}_4$	4.1	29	79	78	2.7
9	R	$\text{AgNO}_3$	3.5	32	82	82	3.8
10	R	$\text{Ag}_2\text{SO}_4$	4.1	35	87	81	4.0
11	R	$\text{AgF}$	6.6	47	126	78	5.0
12	R	$\text{Ag}_3\text{PO}_4$ <sup>e</sup>	5.9	36	(215) <sup>f</sup>	75	— <sup>g</sup>

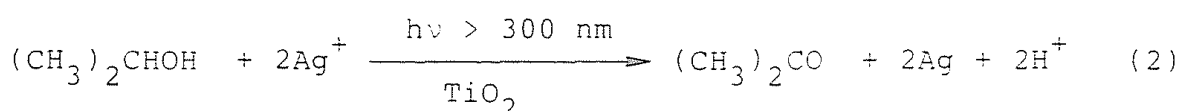
<sup>a</sup> $\text{TiO}_2$  (50 mg) suspension in aqueous solution ( $5.0 \text{ cm}^3$ ) containing 250  $\mu\text{mol}$  of  $\text{Ag}^+$  ion and 500  $\mu\text{mol}$  of 2-propanol in a test tube was irradiated with 400-W high-pressure mercury arc under Ar for 3.0 h.

<sup>b</sup>A and R refer to  $\text{TiO}_2(\text{A})$  and  $\text{TiO}_2(\text{R})$ , respectively. <sup>c</sup>Selectivity of 2-propanol oxidation (see text). <sup>d</sup>Without 2-propanol. <sup>e</sup>Partly dissolved. <sup>f</sup>Contained undissolved  $\text{Ag}_3\text{PO}_4$ . <sup>g</sup>Not determined.



The discrepancy of the observed  $\text{O}_2 : \text{Ag}$  ratio (= 0.20) from the stoichiometric value (= 0.25) indicated by equation (1) is attributable to partial photoadsorption of  $\text{O}_2$  on the  $\text{TiO}_2$  surface.<sup>2-6</sup> It is clear in Table 1 that for the formation of  $\text{O}_2$  and Ag metal in the  $\text{Ag}_2\text{SO}_4$  solution the apparent photocatalytic activity of  $\text{TiO}_2(\text{R})$  is approximately twice greater than that of  $\text{TiO}_2(\text{A})$ .

The presence of 2-propanol (500  $\mu\text{mol}$ ) in  $\text{Ag}_2\text{SO}_4$  solution (Runs 5 and 10) depressed the  $\text{O}_2$  formation by a factor of ca. 5, regardless of the irradiation of  $\text{TiO}_2(\text{A})$  or  $\text{TiO}_2(\text{R})$  suspension, giving rise to an alternative oxidation of the 2-propanol to acetone. Similar formations of  $\text{O}_2$  and acetone were observed together with the Ag-metal deposition in aqueous solution of a series of inorganic silver salts containing 2-propanol. These results show that the following mode of photoredox reaction proceeds in competition with the process as in equation (1).

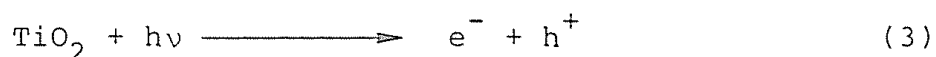


In accord with equations (1) and (2) which involve release of proton, the significant pH decrease during the irradiation was observed with  $\text{AgClO}_4$ ,  $\text{Ag}_2\text{SO}_4$ , or  $\text{AgNO}_3$ . In the  $\text{AgF}$  solution, however, such a pH decrease was exceptionally slow as a result of efficient association of the photochemically released proton with  $\text{F}^-$  ion.<sup>1</sup>

In order to characterize the photocatalytic activities of  $\text{TiO}_2(\text{A})$

and  $\text{TiO}_2(\text{R})$  in a given inorganic silver salt solution containing 2-propanol, the yield of individual products by these photocatalytic reactions is shown in Figure 1. The  $\text{TiO}_2(\text{R})$  is seen to produce larger amount of  $\text{O}_2$ , by 2-10 times depending on the kind of counter anion of the silver salt, compared with the  $\text{TiO}_2(\text{A})$ . In contrast, the yields of acetone and Ag metal by the  $\text{TiO}_2(\text{A})$  are 1.4 and 1.3 times, respectively, as large as those by the  $\text{TiO}_2(\text{R})$ . Moreover, these yield ratios 1.4 and 1.3 are almost independent of the kind of counter anion.

On the basis of these results, a possible scheme for the photocatalytic actions of  $\text{TiO}_2(\text{A})$  and  $\text{TiO}_2(\text{R})$  is outlined as follows. In the initial step an electron-hole pair is created by the excitation of the electron of semiconductor  $\text{TiO}_2$  powder, from the valence band into the conduction band, with light of energy greater than the band gap (3.23 eV for  $\text{TiO}_2(\text{A})$  and 3.02 eV for  $\text{TiO}_2(\text{R})$ ).<sup>7,8</sup>



Trapping of the electron and hole at the  $\text{TiO}_2$  surface accounts for the charge separation of such an electron-hole pair.

It is presumed that oxidation sites of the  $\text{TiO}_2$  photocatalyst surface which trap holes are conveniently classified into two groups i.e., one group has oxidizing ability sufficient to cleave adsorbed water and produce  $\text{O}_2$  (termed an  $h^+_{\text{I}}$  site), while the other group is not responsible for the water decomposition because of the lower oxidizing ability (termed an  $h^+_{\text{II}}$  site).

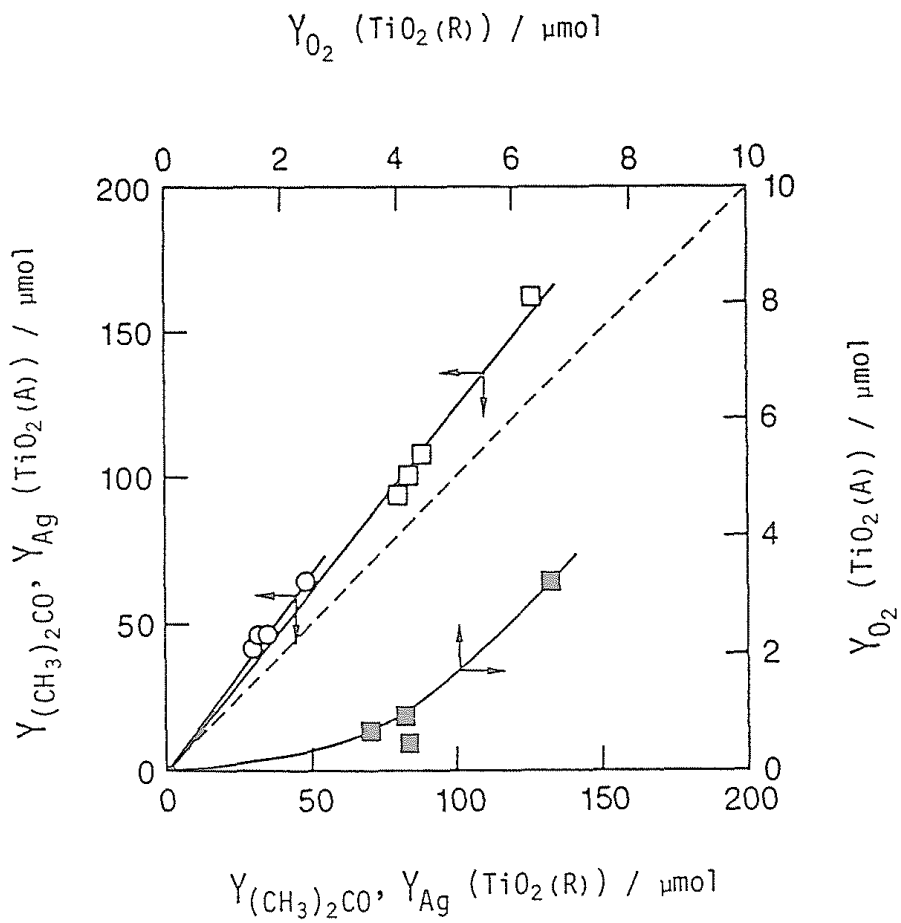
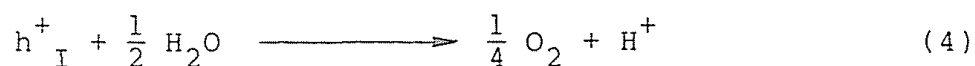


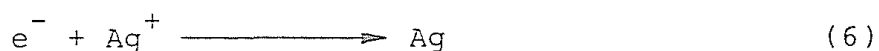
Figure 1 Relationships between the product yields (Y) by  $\text{TiO}_2(\text{A})$  and  $\text{TiO}_2(\text{R})$  powders: acetone (○), Ag (□), and  $\text{O}_2$  (■).



This classification implies that the reactivity of the trapped hole is strongly dependent on the structure of  $\text{TiO}_2$  surface. In addition, it was presumed that not only the  $h^+_{\text{I}}$  site but also the  $h^+_{\text{II}}$  site leads to oxidation of adsorbed 2-propanol to acetone.



On the other hand, the trapped electron on  $\text{TiO}_2$  surface can be a reduction site toward adsorbed  $\text{Ag}^+$  ion to form Ag metal.



Following the above scheme, the ratio of  $\text{O}_2$  yields by  $\text{TiO}_2(\text{R})$  and  $\text{TiO}_2(\text{A})$  (= 2.0) in  $\text{Ag}_2\text{SO}_4$  solution without 2-propanol (Runs 1 and 2) shows that the  $\text{TiO}_2(\text{R})$  surface has larger amount of  $h^+_{\text{I}}$  site than the  $\text{TiO}_2(\text{A})$  surface to oxidize adsorbed water. This is also the cases for the  $\text{AgClO}_4$  (the corresponding  $\text{O}_2$  yield ratio is 5.8, see Table 1 of Chapter 6) and  $\text{AgNO}_3$  (3.5) solution.<sup>1</sup> In the  $\text{AgF}$  (1.0) solution, however, the amount of the  $h^+_{\text{I}}$  site of  $\text{TiO}_2(\text{A})$  and  $\text{TiO}_2(\text{R})$  would be equal.<sup>1</sup> The depression of water oxidation by the addition of 2-propanol is attributable to competitive adsorptions between 2-propanol and water on the  $h^+_{\text{I}}$  site. Since the  $\text{O}_2$  yield ratios between the  $\text{TiO}_2(\text{R})$  and  $\text{TiO}_2(\text{A})$  systems increase by 1.4-2.3 times in the presence of 2-propanol (Table 1), it is also

expected that the adsorption of 2-propanol relative to water occurs to larger extent on the  $h^+_{\text{I}}$  site of  $\text{TiO}_2(\text{A})$  compared with  $\text{TiO}_2(\text{R})$  in these silver salt solutions.

Furthermore, the adsorption of 2-propanol on the  $h^+_{\text{II}}$  site is responsible for the oxidative formation of acetone (equation (5)). The  $\text{TiO}_2(\text{A})$  system probably involves this type of 2-propanol oxidation and thereby promotes reduction of  $\text{Ag}^+$  ion to by the trapped  $e^-$  (equation (6)), because the yield of Ag metal by the  $\text{TiO}_2(\text{A})$  is enhanced in the presence of 2-propanol. In the absence of 2-propanol the hole trapped at the  $h^+_{\text{II}}$  site of  $\text{TiO}_2(\text{A})$ , which can not oxidize water, should neutralize part of the electron so that the efficiency of Ag-metal decreases. On the other hand, the irradiated  $\text{TiO}_2(\text{R})$  would not effectively form such  $h^+_{\text{II}}$  site, because the yield of Ag metal by the  $\text{TiO}_2(\text{R})$  is little affected by the addition of 2-propanol in contrast to the  $\text{TiO}_2(\text{A})$  system. The Ag-metal yield relationship in Figure 1 also suggests that the total amount of oxidation site,  $h^+_{\text{I}}$  and  $h^+_{\text{II}}$ , on the  $\text{TiO}_2(\text{A})$  surface is 1.3 times as much as that of  $h^+_{\text{I}}$  on the  $\text{TiO}_2(\text{R})$  in a given silver salt solution under these conditions.

According to the stoichiometries in equations (1) and (2), one may expect the following relationship between the yields of total oxidation product,  $\text{O}_2$  ( $Y_{\text{O}_2}$ ) plus acetone ( $Y_{(\text{CH}_3)_2\text{CO}}$ ), and reduction product Ag ( $Y_{\text{Ag}}$ ).

$$4Y_{\text{O}_2} + 2Y_{(\text{CH}_3)_2\text{CO}} = Y_{\text{Ag}} \quad (7)$$

As plotted in Figure 2, the data for both the  $\text{TiO}_2(\text{A})$  and  $\text{TiO}_2(\text{R})$

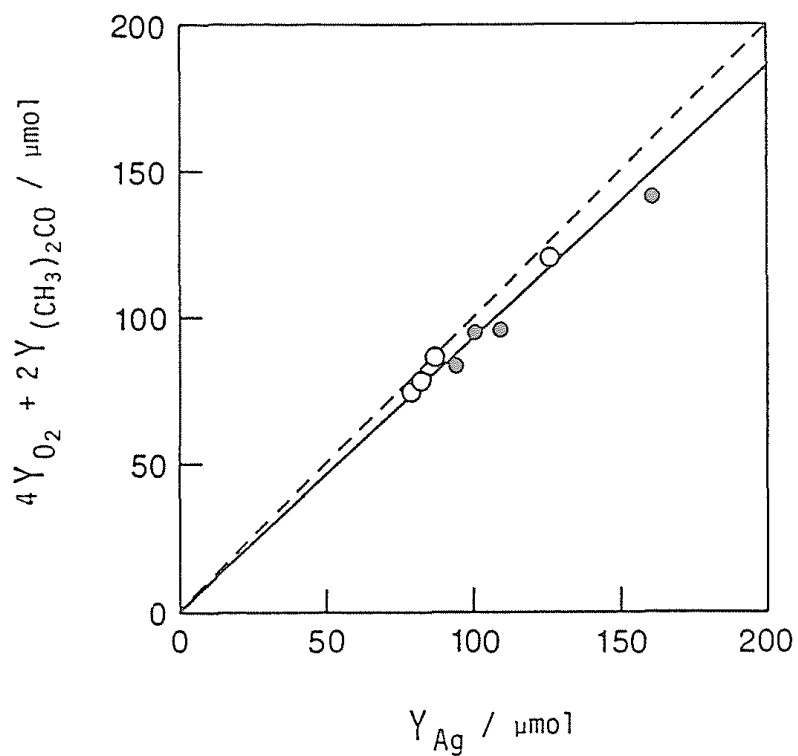


Figure 2 Linear plot of the yield of reduction product versus that of oxidation product in the  $\text{TiO}_2(\text{A})$  (●) and  $\text{TiO}_2(\text{R})$  (○) systems, following the relationships in eqn. (3) (see text).



systems listed in Table 1 are seen to satisfy this relationship. In this light, we defined the selectivity of 2-propanol oxidation (S) by

$$S/\% = 2Y_{(\text{CH}_3)_2\text{CO}} \times 100 / (4Y_{\text{O}_2} + 2Y_{(\text{CH}_3)_2\text{CO}}) \quad (8)$$

Table 1 shows that the selectivities S thus evaluated are in the range of 87-91 % with  $\text{TiO}_2(\text{A})$  (Runs 3-7) and 75-82 % with  $\text{TiO}_2(\text{R})$  (Runs 8-12), respectively. Such high selectivities indicate that the predominant adsorption of 2-propanol at  $0.1 \text{ mol dm}^{-3}$  occurs on the  $\text{h}^+_{\text{I}}$  sites of both  $\text{TiO}_2(\text{A})$  and  $\text{TiO}_2(\text{R})$ . Moreover, the adsorption of 2-propanol on the  $\text{h}^+_{\text{II}}$  site in the  $\text{TiO}_2(\text{A})$  system partly accounts for the fact that the selectivity of acetone formation is greater than that in the  $\text{TiO}_2(\text{R})$  system without the effective  $\text{h}^+_{\text{II}}$  site.

Effect of Counter Anion on the  $\text{TiO}_2$  Catalyzed Photoredox Reaction in Aqueous Solution of Inorganic Silver Salts. The initial pH of aqueous silver salt solution, before irradiation, depended on the counter anions and decreased in the order  $\text{F}^- > \text{SO}_4^{2-} > \text{NO}_3^- > \text{ClO}_4^-$  (Table 1). Table 1 also shows a trend that the yield of Ag metal as a measure of the net photocatalytic activity increases with lowering the initial pH.

From the  $\text{pK}_a$  value (ca. 6) of  $\text{TiO}_2(\text{A})$  in the following acid - base equilibrium,<sup>1,9,10</sup>



it is expected that OH groups on the  $\text{TiO}_2(\text{A})$  surface prior to irradiation will be partly protonated in AgF solution (initial pH 5.0) and the extent of such a protonation will increase with varying the counter anions in the order  $\text{F}^- < \text{SO}_4^{2-} < \text{NO}_3^- < \text{ClO}_4^-$ . Accordingly, the photocatalytic activity of  $\text{TiO}_2(\text{A})$  as measured by the yield of Ag metal is suggested to increase with decreasing the extent of the surface protonation. This means that the formation of positively charged surface by protonation is responsible for the deactivation of both  $\text{h}^+_{\text{I}}$  and  $\text{h}^+_{\text{II}}$  sites and thereby depresses the oxidations of water and 2-propanol. Under such conditions the neutralization between electron and hole would become more effective, so that the reduction of  $\text{Ag}^+$  ion is also depressed.

Since the  $\text{pK}_a$  values of  $\text{HClO}_4$  (-8),  $\text{H}_2\text{SO}_4$  (-3), and  $\text{HNO}_3$  (-1.64) are negative,<sup>11</sup> most of the proton released by the photocatalytic reactions (equations (1) and (2)) should not associate with counter anions in aqueous solution of  $\text{AgClO}_4$ ,  $\text{Ag}_2\text{SO}_4$ , and  $\text{AgNO}_3$ . Alternatively, the photo-released proton could associate with surface hydroxyl group of  $\text{TiO}_2(\text{A})$  or  $\text{TiO}_2(\text{R})$  to deactivate the oxidation site. The smaller pH decrease during the irradiation in AgF solution is related to the positive  $\text{pK}_a$  value (= 3.18)<sup>11</sup> of the conjugate acid HF, i.e., the  $\text{F}^-$  ion is much more associative with the photo-released proton, compared with the  $\text{ClO}_4^-$ ,  $\text{SO}_4^{2-}$ , and  $\text{NO}_3^-$  ions. In this case, therefore, the deactivation of oxidation site of  $\text{TiO}_2$  photocatalyst by the surface protonation during irradiation is relatively minor.<sup>1</sup>

For convenience, the yields of  $\text{O}_2$  and acetone in the series of inorganic silver salt solutions are plotted in Figures 3 and 4,

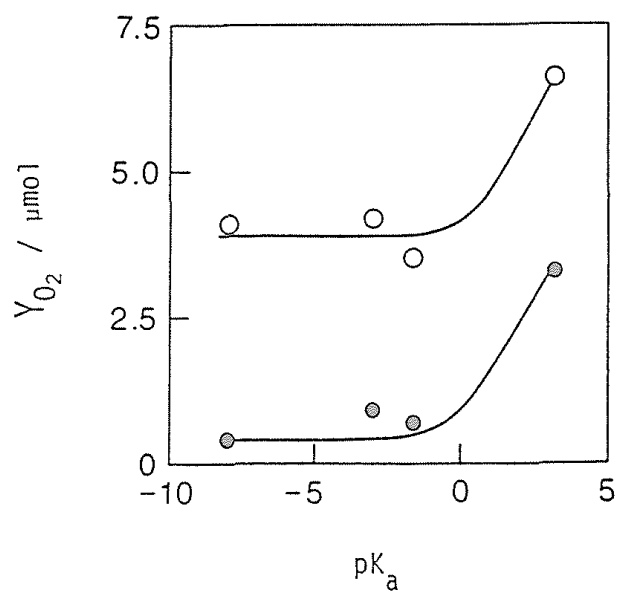


Figure 3 Variation of the O<sub>2</sub> yield (Y<sub>O<sub>2</sub></sub>) as a function of pK<sub>a</sub> of conjugated acids for the anions of several inorganic silver salts: TiO<sub>2</sub>(A) ( ● ), TiO<sub>2</sub>(R) ( ○ ).

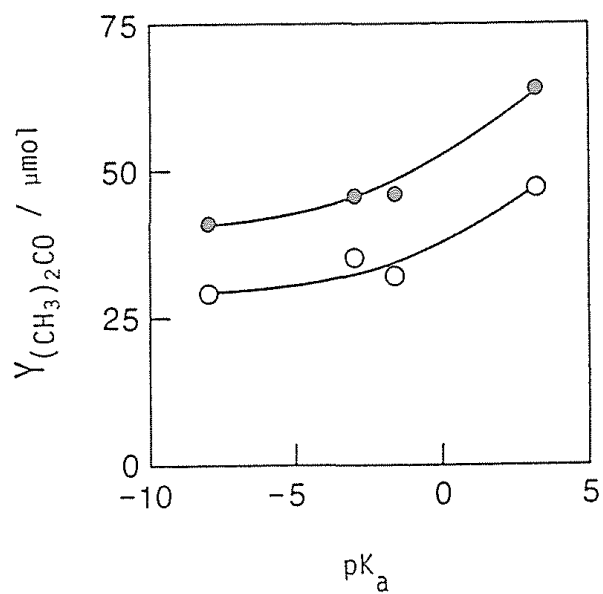


Figure 4 Variation of the acetone yield ( $Y_{(\text{CH}_3)_2\text{CO}}$ ) as a function of  $\text{pK}_a$  of conjugate acids for the anions of several inorganic silver salts:  $\text{TiO}_2(\text{A})$  (●),  $\text{TiO}_2(\text{R})$  (○).

respectively, as a function of  $pK_a$  of the corresponding conjugate acid as above. The  $O_2$  yield little changes under conditions where the  $pK_a$  of conjugate acid for the counter anion of the silver salt is negative. In the positive  $pK_a$  region, however, the  $O_2$  yield increases rapidly upon increasing the  $pK_a$ . Although the characteristics of  $pK_a$  dependences in the  $TiO_2(A)$  and  $TiO_2(R)$  systems are very similar (Figure 3), the  $TiO_2(R)$  is able to produce 2-10 times larger amount of  $O_2$  than the  $TiO_2(A)$  as described above (Figure 1). In the case of acetone formation the yield increases gradually with increasing the  $pK_a$ , in which the  $TiO_2(A)$  is 1.4 times more active than the  $TiO_2(R)$  (Figure 1).

$TiO_2$  Catalyzed Photoredox Reaction in the  $CH_3COOAg$  System. The

$CH_3COOAg$  solution (initial pH 6.2) showed several features of the photocatalytic redox reaction, which are distinct from those in the inorganic silver salts systems. Thus, not only the  $O_2$  formation and Ag-metal deposition, as was observed with a series of inorganic silver salts, but also liberation of  $CO_2$  occurred during the irradiation without 2-propanol (Table 2). This reaction was confirmed not to proceed in the dark. It is therefore probable that the following photoredox reaction occurs in competition with the similar process in equation (1).

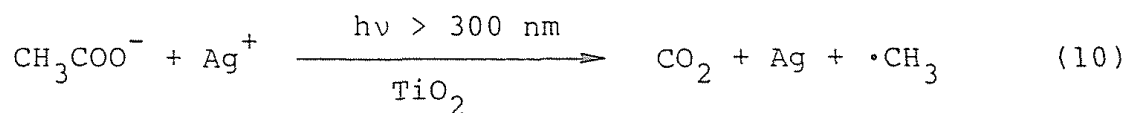


Table 2 shows that the  $TiO_2(A)$  is 5 times more active over the  $TiO_2(R)$  for the oxidative decomposition of acetate ion into  $CO_2$ . It is worth noting that the ratio of  $O_2$  yield by  $TiO_2(R)$  and  $TiO_2(A)$  (=

Table 2  $\text{TiO}_2$  Catalyzed photoredox reactions in aqueous  $\text{CH}_3\text{COOAg}$  solutions with or without 2-propanol.<sup>a</sup>

Run	$\text{TiO}_2^b$	Products/ $\mu\text{mol}$			
		$\text{O}_2$	$\text{CO}_2$	Acetone	Ag
13 <sup>c</sup>	A	12.7	17	—	176
14 <sup>c</sup>	R	6.9	3.3	—	65
15	A	5.2	2.3	68	188
16	R	3.0	3.0	37	93

<sup>a</sup> $\text{TiO}_2$  (50 mg) suspension in aqueous solution ( $5.0 \text{ cm}^3$ ) containing 250  $\mu\text{mol}$  of  $\text{Ag}^+$  and 500  $\mu\text{mol}$  of 2-propanol in a test tube was irradiated with 400-W high-pressure mercury arc under Ar for 3.0 h.

<sup>b</sup>A and R refer to  $\text{TiO}_2(\text{A})$  and  $\text{TiO}_2(\text{R})$ , respectively. <sup>c</sup>Without 2-propanol.

0.5) is smaller than unity, contrary to the inorganic silver salt systems. From the initial pH values it is expected that OH groups on the  $\text{TiO}_2$  surface are largely deprotonated in the  $\text{CH}_3\text{COOAg}$  solution (pH 6.2) whereas partly protonated in the inorganic silver salt solutions (pH  $\leq$  5.0). Thus, without the deactivation effect due to surface protonation in the lower pH region, larger amount of  $h^+_{\text{I}}$  sites is available for the water oxidation with the  $\text{TiO}_2(\text{A})$  rather than the  $\text{TiO}_2(\text{R})$ . Nevertheless, the  $h^+_{\text{I}}$  site of  $\text{TiO}_2(\text{A})$  would be protonated and deactivated more rapidly than that of  $\text{TiO}_2(\text{R})$  with decreasing the pH of aqueous silver salt solution.

Previously, Kraeutler and Bard have reported the photocatalytic Kolbe reaction of acetate ion by an aqueous suspension of platinumized  $\text{TiO}_2$  that produces  $\text{CO}_2$  and  $\text{CH}_4$  as the major products.<sup>8</sup> They also observed the significant depression of the  $\text{CH}_4$  formation in the presence of  $\text{O}_2$ .<sup>8</sup> In accord with these results, we could detect only negligible amounts of hydrocarbon products ( $\text{CH}_4 < 1 \mu\text{mol}$ ,  $\text{C}_2\text{H}_6 < 0.5 \mu\text{mol}$ ) and methanol ( $< 1 \mu\text{mol}$ ) in the  $\text{CH}_3\text{COOAg}$  system involving the  $\text{O}_2$  formation. It is reasonable to presume that the intermediate  $\cdot\text{CH}_3$  radical reacts with  $\text{O}_2$  to give methanol,<sup>8,12</sup> which should readily undergo secondary photocatalytic oxidation to  $\text{CO}_2$  via formaldehyde and formic acid.<sup>13</sup>

The presence of 2-propanol with  $\text{TiO}_2(\text{A})$  depressed both the liberations of  $\text{O}_2$  and  $\text{CO}_2$  due to the efficient acetone formation as an alternative oxidation process (Run 15). In contrast to the  $\text{Ag}_2\text{SO}_4$  solution, the reduction of  $\text{Ag}^+$  ion to Ag metal in the  $\text{CH}_3\text{COOAg}$  solution was not appreciably promoted by the acetone formation. It is presumable that the acetate ion adsorbed on not only  $h^+_{\text{I}}$  but also

$h^+_{II}$  sites of the  $TiO_2(A)$  surface undergo oxidation, similar to 2-propanol, and release  $CO_2$ .



Under these conditions, therefore, the competitive oxidation of 2-propanol should no longer enhance the Ag-metal deposition.

In summary, the present study have demonstrated that the oxidizing ability of powdered  $TiO_2$  photocatalyst in aqueous silver salt solution depends on not only the crystal structure but also the extent of protonation of the surface OH group.



## REFERENCES AND NOTES

- 1 S. Nishimoto, B. Ohtani, H. Kajiwara, and T. Kagiya, *J. Chem. Soc., Faraday Trans. 1*, 79, 2685 (1983).
- 2 E. Borgarello, J. Kiwi, M. Grätzel, E. Pelizzetti, and M. Visca, *J. Am. Chem. Soc.*, 104, 2996 (1982).
- 3 A. Mills and G. Porter, *J. Chem. Soc., Faraday Trans. 1*, 78, 3659 (1982).
- 4 A. H. Boonstra and C. A. H. A. Mutsaers, *J. Phys. Chem.*, 79, 1694 (1975).
- 5 G. Munuera, V. Rives-Arnau, and A. Saucedo, *J. Chem. Soc., Faraday Trans. 1*, 75, 736 (1979).
- 6 A. R. Gonzalez-Elipe, G. Munuera, and J. Soria, *J. Chem. Soc., Faraday Trans. 1*, 75, 748 (1979).
- 7 V. N. Pak and N. G. Ventov, *Russ. J. Phys. Chem. (Engl. Trans.)*, 49, 1489 (1975).
- 8 B. Kraeutler and A. J. Bard, *J. Am. Chem. Soc.*, 100, 5985 (1978).
- 9 Detailed characterization of the  $\text{TiO}_2(\text{A})$  and (R) surface is given in Chapter 11 of this thesis. Total amount of surface hydroxyl on  $\text{TiO}_2(\text{A})$  is larger than that on  $\text{TiO}_2(\text{R})$ .
- 10 (a) P. W. Schindler and H. Gamsjager, *Discuss. Faraday Soc.*, 52, 286 (1971) (b) H. P. Boehm, *Discuss. Faraday Soc.*, 52, 264 (1971).
- 11 A. Albert and E. P. Serjeant, *Ionization Constants of Acids and Bases*, Wiley, New York, 1962, p. 151.
- 12 J. E. Barry, M. Finkelstein, E. A. Mayeda, and S. D. Ross, *J.*

Am. Chem. Soc., 98, 8098 (1976).

13 T. Kawai and T. Sakata, J. Chem. Soc., Chem. Commun., 694  
(1980).

## Chapter 8

### Effect of the Concentrations of 2-Propanol and Silver Sulfate on Photocatalytic Oxidations of 2-Propanol and Water Along with Silver Metal Deposition by $\text{TiO}_2$ Suspension

#### Abstract

Redox reactions catalyzed by the suspensions of powdered  $\text{TiO}_2$ , anatase ( $\text{TiO}_2(\text{A})$ ) and rutile ( $\text{TiO}_2(\text{R})$ ), under photoirradiation ( $\lambda_{\text{ex}} > 300 \text{ nm}$ ) in Ar-purged aqueous solution of  $\text{Ag}_2\text{SO}_4$  and 2-propanol have been investigated at room temperature. Quantum yields for oxidation of 2-propanol to acetone and for reduction of  $\text{Ag}^+$  ion to Ag metal deposit increased and asymptotically reached their individual saturation limits, whereas that for the oxidation of water to  $\text{O}_2$  decreased monotonously upon increasing the concentration of 2-propanol. The enhanced acetone formation with increasing  $\text{Ag}^+$  concentration was also observed until a saturation yield was attained. The maximum activity of  $\text{TiO}_2(\text{A})$  photocatalyst, that was available at the concentrations of 2-propanol and  $\text{Ag}^+$  ion over certain limits, was 1.5-fold greater than the corresponding activity of  $\text{TiO}_2(\text{R})$ . The observation of these behavior is discussed in terms of adsorptions of 2-propanol and  $\text{Ag}^+$  ion on the  $\text{TiO}_2$  surface, both following Langmuir isotherm, and of trapping of the photogenerated hole and electron by the surface adsorbates.

## INTRODUCTION

Suspension of  $\text{TiO}_2$  particles is operative as heterogeneous photocatalyst for several types of redox-related reactions, commonly resulting in characteristics of an electrochemical process because of the semiconducting property of this material under illumination.<sup>2</sup> While numerous studies<sup>3-16</sup> concerning the formation of products by the irradiated  $\text{TiO}_2$  suspensions or overall efficiency of the process have been performed from the viewpoint of either solar energy storage or synthetic application, a few efforts have been recently made to characterize the behavior of reactants at the irradiated  $\text{TiO}_2$  surface. In particular, a better understanding of trapping of the photogenerated electron in the  $\text{TiO}_2$  by solution species such as transition metal ions<sup>17,18</sup> and methyl viologen dication<sup>19</sup> is now available.

The preceding chapter<sup>1</sup> in this thesis have described the deposition of Ag metal on the  $\text{TiO}_2$  photocatalyst, either anatase ( $\text{TiO}_2$  (A)) or rutile ( $\text{TiO}_2$  (R)), upon the irradiation in aqueous suspension containing several silver salts. This process involved concomitant oxidation of water or added 2-propanol to produce  $\text{O}_2$  or acetone, respectively. In the present work photocatalytic activities of the  $\text{TiO}_2$  (A) and  $\text{TiO}_2$  (R) suspensions in  $\text{Ag}_2\text{SO}_4$  solution that are enhanced upon increasing concentrations of 2-propanol and  $\text{Ag}^+$  ion are reported, and the effect of surface adsorptions of the reactants on the trapping of hole and electron photogenerated within the particle is discussed.

## EXPERIMENTAL

Materials. Anatase  $\text{TiO}_2$  ( $\text{TiO}_2(\text{A})$ ) powder was supplied by Merck and rutile analog ( $\text{TiO}_2(\text{R})$ ) was prepared by heating  $\text{TiO}_2(\text{A})$  in air at  $1200^\circ\text{C}$  for 10 h. The characterization of these materials were reported in Chapter 6 of this thesis.<sup>1</sup> Reagent grade 2-propanol and  $\text{Ag}_2\text{SO}_4$  were used as received. Ion-exchanged water was distilled immediately prior to use.

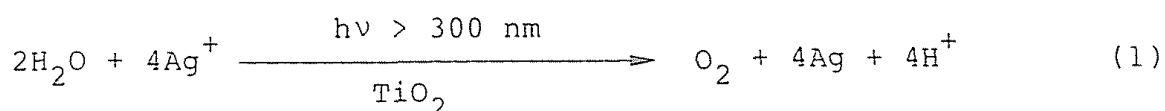
Photoirradiation. A suspension of finely powdered  $\text{TiO}_2$  (50 mg) in  $5.0\text{ cm}^3$  of water or aqueous solution of  $\text{Ag}_2\text{SO}_4$  (over a wide range of  $\text{Ag}^+$  concentration up to 50 mM ( $M \equiv \text{mol dm}^{-3}$ )) was prepared in a glass tube (18 mm $\phi$   $\times$  180 mm, transparent for wavelengths above 300 nm of the exciting light), purged for 30 min with Ar, and then sealed off with a rubber cap. The Ar-purged and magnetically stirred suspension, after injection of 0-260 mM 2-propanol, was irradiated at room temperature using a merry-go-round apparatus equipped with a 400-W high-pressure mercury arc (Eiko-sha 400). The light source emitted quanta effective for excitation of the suspension (300-400 nm) at a rate of  $5 \times 10^{-6}$  einstein  $\text{cm}^{-2} \text{min}^{-1}$  (total quanta  $1.8 \times 10^5$  einstein  $\text{min}^{-1}$ ) which was estimated by the integration of the calibrated emission spectrum. Since the quantum yield should at least depend upon size and number density of the  $\text{TiO}_2$  particles, is only obtained minimum quantum yield. The quantum yield for a given product formation was derived from the corresponding product yield over the initial period less than 30 min of irradiation. Under these conditions, the conversion of neither 2-propanol nor  $\text{Ag}^+$  ion usually exceeded 10 % and the yields of  $\text{O}_2$ , acetone, and Ag metal deposit increased linearly with irradiation time. In a

series of experiments at less than 1 mM of  $\text{Ag}^+$  ions, a maximum conversion of the  $\text{Ag}^+$  ion to Ag metal was estimated as ca. 30 % from the material balance with the oxidation of 2-propanol to acetone. Direct measurement of the yields of Ag metal from such dilute solutions of  $\text{Ag}^+$  failed to be achieved with a satisfactory reproducibility.

The analyses of the photocatalytic products were carried out following the reported procedures described in Chapter 6.<sup>1</sup>

## RESULTS AND DISCUSSION

Effect of 2-Propanol on Photocatalytic Activity. In accord with the previous study,<sup>1</sup> upon irradiation ( $\lambda_{\text{ex}} > 300 \text{ nm}$ ) of a suspension of  $\text{TiO}_2(\text{A})$  or  $\text{TiO}_2(\text{R})$  in Ar-purged  $\text{Ag}_2\text{SO}_4$  solution (50 mM  $\text{Ag}^+$ ) without 2-propanol, the liberation of  $\text{O}_2$  by oxidative cleavage of water and the deposition of Ag metal onto the  $\text{TiO}_2$  surface as a result of reduction of  $\text{Ag}^+$  ion were observed. The net redox reaction is given as follows.<sup>1</sup>



Under these conditions the photocatalytic activities of  $\text{TiO}_2(\text{A})$  and  $\text{TiO}_2(\text{R})$ , as measured by the corresponding quantum yields of Ag (see also Figure 1), were of approximately comparable levels.

Upon addition of 2-propanol to the same  $\text{Ag}_2\text{SO}_4$  solution, the oxidation to produce acetone occurred simultaneously with the  $\text{O}_2$  liberation and Ag deposition. Figure 1 illustrates that the quantum yields of  $\text{O}_2$  ( $\phi(\text{O}_2)$ ), acetone ( $\phi(\text{acetone})$ ), and Ag ( $\phi(\text{Ag})$ ) vary

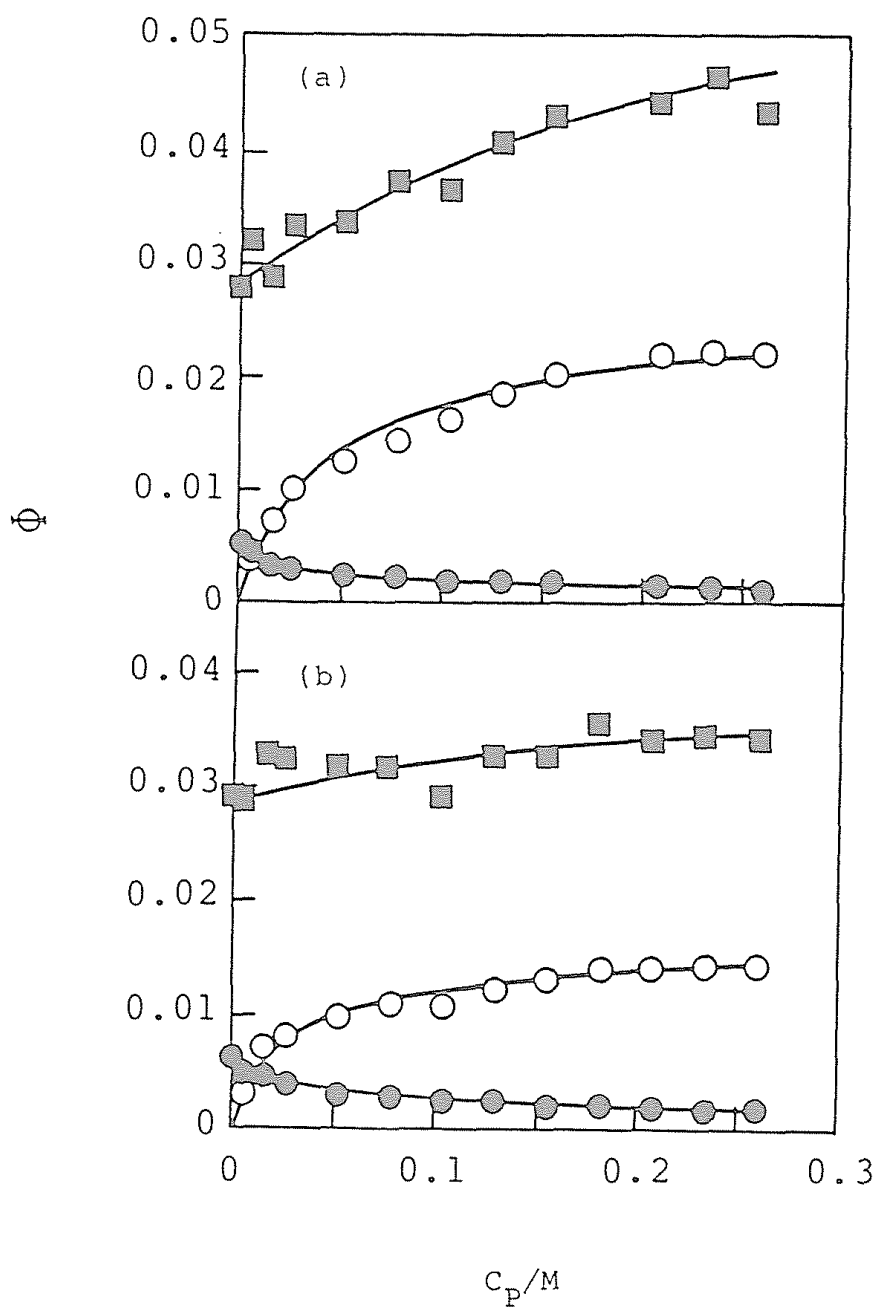


Figure 1 Variation in the quantum yields ( $\phi$ ) of Ag deposit (■), acetone (○), and  $O_2$  (●) with 2-propanol concentration ( $C_p$ ), observed in the photoredox reaction catalyzed by  $TiO_2(A)$  (a) and  $TiO_2(R)$  (b) suspension in aqueous  $Ag_2SO_4$  (50 mM  $Ag^+$ ) solution.

significantly as a function of the concentration of added 2-propanol ( $C_p$ ). Thus, both the  $\phi(\text{acetone})$  and  $\phi(\text{Ag})$  first increased and then asymptotically approached their individual saturation limits as  $C_p$  increased up to 260 mM at a fixed concentration of  $\text{Ag}^+$  ions ( $C_A = 50$  mM). The limiting values  $\phi_\infty(\text{acetone}) = 0.022$  and  $\phi_\infty(\text{Ag}) = 0.050$  at  $C_p \rightarrow \infty$ , which were estimated for  $\text{TiO}_2(\text{A})$  by extrapolation, were greater than those ( $\phi_\infty(\text{acetone}) = 0.015$ ,  $\phi_\infty(\text{Ag}) = 0.036$ ) obtained for  $\text{TiO}_2(\text{R})$  by the factor of 1.5-1.6. In contrast, the  $\phi(\text{O}_2)$  decreased monotonously in such a manner that it will reach zero at  $C_p \rightarrow \infty$  ( $\phi_\infty(\text{O}_2) = 0$ ). It is also evident from the behavior in Figure 1 that 2-propanol exerts greater effect on the photocatalytic action of  $\text{TiO}_2(\text{A})$  rather than  $\text{TiO}_2(\text{R})$ , thus giving rise to more enhanced quantum yields of acetone and Ag deposit. Instead, the oxidation of water to  $\text{O}_2$  by  $\text{TiO}_2(\text{A})$  is more markedly depressed in the presence of 2-propanol.

Figure 2 shows that the enhanced value of  $\phi(\text{acetone})$  with increasing  $C_p$  is responsible for the decrement of  $\phi(\text{O}_2)$  relative to  $\phi_0(\text{O}_2)$  at  $C_p = 0$ ; i.e.,  $-\Delta\phi(\text{O}_2) = \phi(\text{O}_2) - \phi_0(\text{O}_2)$ . Another feature involved in Figure 2 is that each plot curves upward and extent of the curvature is more pronounced for the  $\text{TiO}_2(\text{A})$  system. This behavior must be associated with the evidence that the photocatalytic reduction of  $\text{Ag}^+$  ions to Ag metals becomes more efficient as  $C_p$  increases, particularly when  $\text{TiO}_2(\text{A})$  is used. These results are consistent with a scheme that the following mode of net redox reaction competes with analogous process as in eq 1.



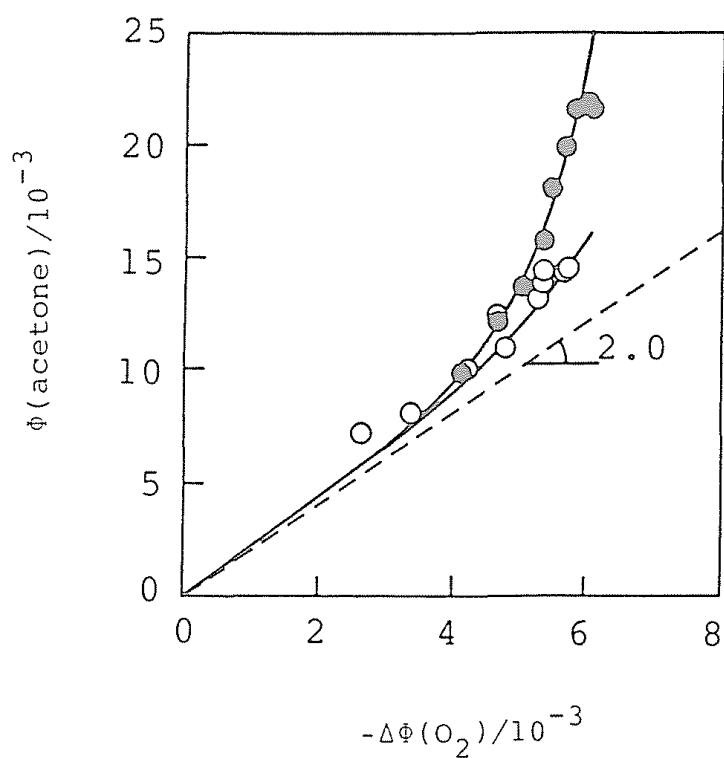
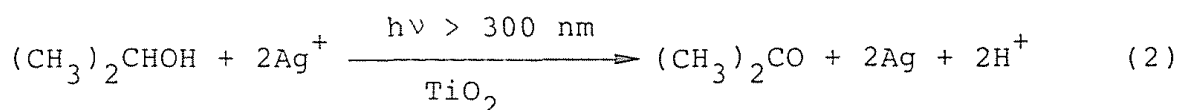


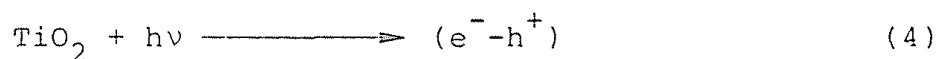
Figure 2 Relationships between  $\phi(\text{acetone})$  and  $-\Delta\phi(\text{O}_2)$  ( $= \phi(\text{O}_2) - \phi_0(\text{O}_2)$ ) in the photoredox reaction catalyzed by  $\text{TiO}_2(\text{A})$  (●) and  $\text{TiO}_2(\text{R})$  (○) suspensions in aqueous  $\text{Ag}_2\text{SO}_4$  (50 mM  $\text{Ag}^+$ ) solution with varying concentrations of 2-propanol.



The competitive redox reactions (eqs 1 and 2) as above require a stoichiometric relationship to hold between the formal quantum yields of total oxidation product  $\text{O}_2$  plus acetone and reduction product Ag; i.e.,

$$4\phi(\text{O}_2) + 2\phi(\text{acetone}) = \phi(\text{Ag}) \quad (3)$$

Indeed, the plot of data for both  $\text{TiO}_2(\text{A})$  and  $\text{TiO}_2(\text{R})$  according to eq 3 provided a common, reasonably straight line that agrees with the expected stoichiometry (Figure 3). Following an electrochemical model for the semiconductor photocatalysis,<sup>2</sup> this linear relationship in turn implies a condition of electric neutrality that identical amounts of hole and electron participated in the reaction of solution species; these charges were initially generated as electron hole ( $e^-h^+$ ) pair in the irradiated bulk  $\text{TiO}_2$  surface.



Activities of  $\text{TiO}_2$  suspensions is the efficient trapping of photo-generated holes, so that the extent of recombination of ( $e^-h^+$ ) pair is decreased and the quantum yields for both reactions of hole and electron solution species are enhanced.

Effect of Silver Ion on Photocatalytic Activity. Trapping of photogenerated electron in the  $\text{TiO}_2$  by reducible agents, like hole

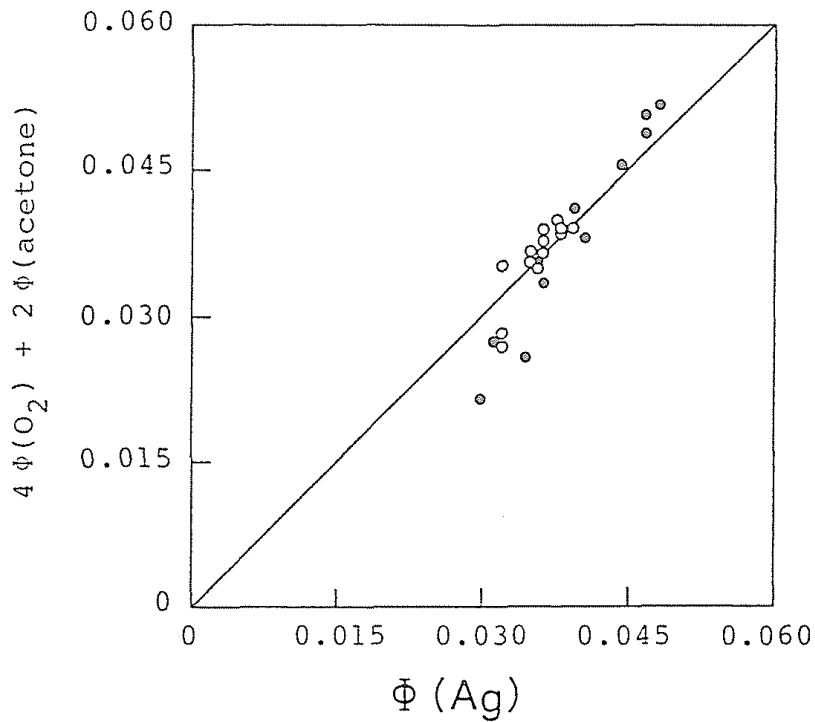


Figure 3 Linear plot of  $\phi(\text{Ag})$  vs.  $2\phi(\text{acetone}) + 4\phi(\text{O}_2)$  for the  $\text{TiO}_2(\text{A})$  (●) and  $\text{TiO}_2(\text{R})$  (○) systems, following the relationship in eq 3. The data are derived from Figure 1.

trapping by oxidizable agents as is presumable in the case of 2-propanol, must diminish the extent of unfavorable electron-hole recombination. Evidence for such an effect has been obtained with  $\text{Cu}^{2+}$ ,  $\text{Fe}^{3+}$ , and methyl viologen dication which are effective for enhancement of anodic photocurrent in  $\text{TiO}_2$  suspensions.<sup>18,19</sup> It is now clear that the photodeposition of Ag metal onto the  $\text{TiO}_2$  in  $\text{Ag}_2\text{SO}_4$  solution originates from similar electron trapping by  $\text{Ag}^+$  ion.

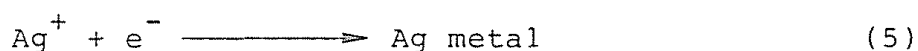


Figure 4 shows that the quantum yield  $\phi(\text{acetone})$  in  $\text{Ag}_2\text{SO}_4$  solution containing 100 mM 2-propanol increased dramatically upon increasing  $C_A$  up to 10 mM, although only negligible amount of acetone could be obtained in the absence of  $\text{Ag}^+$  ion. Further increases of  $C_A$  no more enhanced the value of  $\phi(\text{acetone})$ . The saturation limit  $\phi_\infty(\text{acetone})$  possibly corresponds to a maximum quantum yield of separated hole that is derived from electron trapping by  $\text{Ag}^+$  ions under these conditions. The  $\phi_\infty(\text{acetone})$  value (0.022 by extrapolation) observed for  $\text{TiO}_2(\text{A})$  was 1.5-fold greater than that (0.015) for  $\text{TiO}_2(\text{R})$ . This factor 1.5 is an indication of difference in a critical activity at  $C_A \rightarrow \infty$  between these photocatalysts. In relation to this finding, it is worth noting that identical limiting value of  $\phi_\infty(\text{acetone})$  for each photocatalyst can also be obtained when excess amount of 2-propanol is added at a fixed  $C_A$ , as described above. These results suggest the presence of a limiting rate for the photogeneration of available holes and electrons in each  $\text{TiO}_2$  particle, which is possibly dependent on exciting light

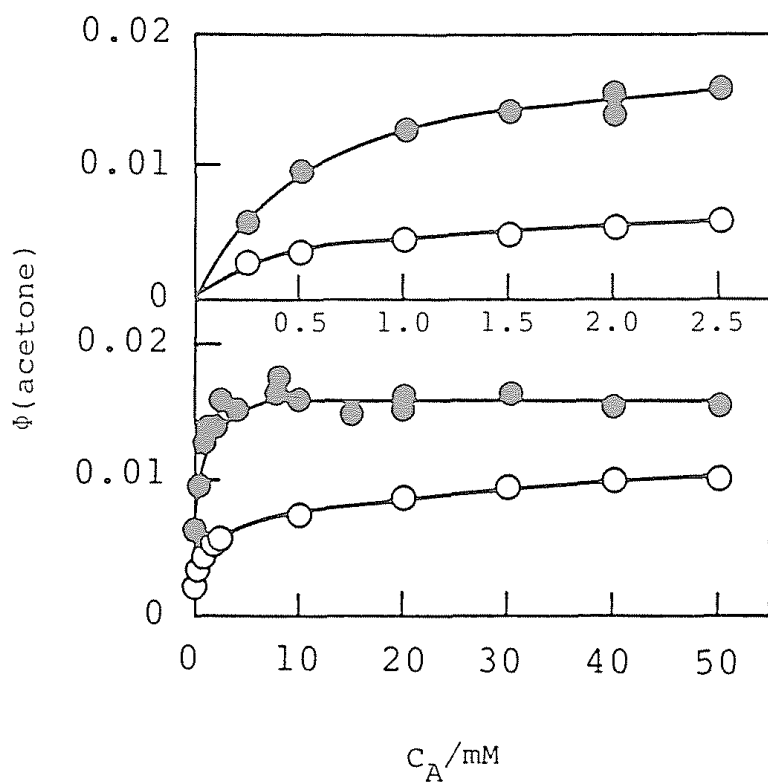
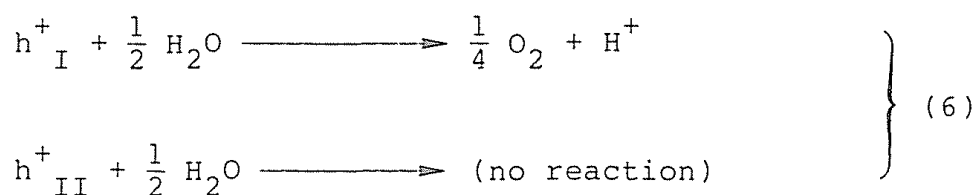


Figure 4 Variation in the quantum yield of acetone ( $\phi(\text{acetone})$ ) as a function of  $\text{Ag}^+$  ion concentration ( $C_A$ ), as observed in the photo-redox reaction catalyzed by  $\text{TiO}_2(\text{A})$  (●) and  $\text{TiO}_2(\text{R})$  (○) suspensions in aqueous  $\text{Ag}_2\text{SO}_4$  solution containing 100 mM 2-propanol.

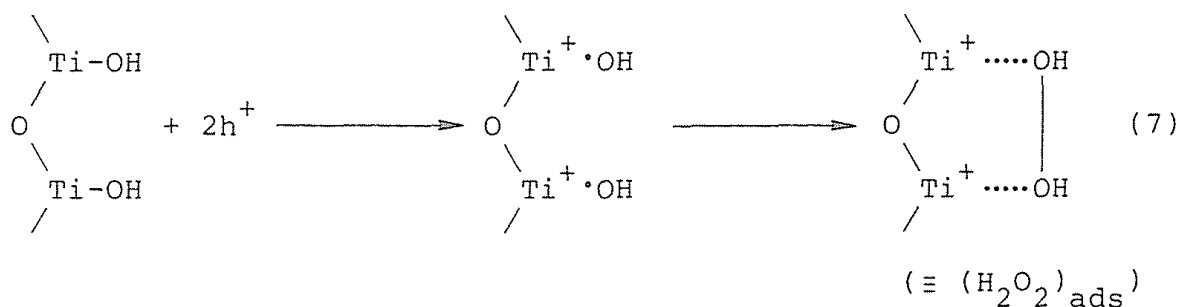
intensity. This is in accord with the previous conclusion by Ward and Bard.<sup>18</sup>

Mechanism of Trapping of Photogenerated Charges by Surface Adsorbates.

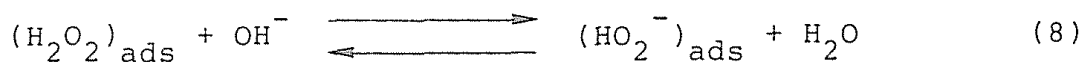
Characterization of the above mentioned results concerning the competitive oxidations of 2-propanol and water to yield acetone and O<sub>2</sub> leads to the assumption on the nature of the oxidation sites on the TiO<sub>2</sub> surface at which the photogenerated positive hole reacts with adsorbed substrates: two different types of oxidation sites adsorb and oxidize 2-propanol and water. One of the sites, termed an h<sup>+</sup><sub>I</sub> site, has oxidizing ability sufficient to cleave adsorbed water and produce O<sub>2</sub>, while the other group is not responsible for the water decomposition because of the lower oxidizing ability (termed an h<sup>+</sup><sub>II</sub>).



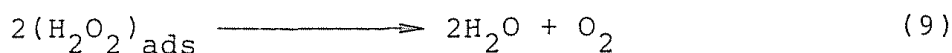
This classification interprets that the reactivity of the positive hole trapped on the surface is strongly dependent on the structure of TiO<sub>2</sub> surface. Most probable chemical structure for the h<sup>+</sup><sub>I</sub> site is hydroxyl group on the TiO<sub>2</sub> surface, as has been suggested in Chapter 11 of this thesis. The positive hole reacts with the hydroxyl to surface-adsorbed hydroxyl radical to recombine into hydrogen peroxide adsorbed on the surface ((H<sub>2</sub>O<sub>2</sub>)<sub>ads</sub>).



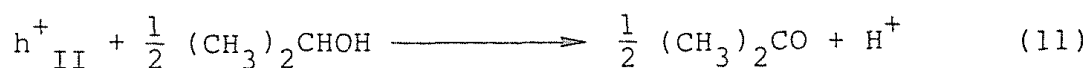
Following reactions could lead to the  $\text{O}_2$  formation from  $\text{H}_2\text{O}_2$  on the  $\text{TiO}_2$  surface in the dark.



These reactions are formally summarized, as follows, and are consistent with the stoichiometry of the photocatalytic reaction (equation (1)).



In addition, it was presumed that not only the  $h^+_{\text{I}}$  site but also the  $h^+_{\text{II}}$  site leads to oxidation of adsorbed 2-propanol to acetone.



These assumptions are supported by the findings that in the absence of silver salt 2-propanol could be dehydrogenated into acetone and  $H_2$  while negligible amount of water could oxidized to  $O_2$  in the photoirradiated suspension of the platinized  $TiO_2$ , as has been described in Chapter 1 of this thesis.

Following the above scheme, the increment of the acetone yield ( $\phi(\text{acetone})$ ) shown in Figures 1 and 2 is attributable to the oxidation at both  $h^+_{II}$  (instead of water) and  $h^+_{II}$  sites. The increment by the oxidation at the  $h^+_{II}$  site is presented by the deviation from the straight line in Figure 2, i.e., the straight line indicates that identical amount of positive hole reacts with 2-propanol and water, alternatively, at the  $h^+_{II}$  site regardless of  $C_P$ . Figure 5 shows the quantum yield of acetone formation at  $h^+_{II}$  ( $\phi^{II}(\text{acetone})$ ) obtained on the basis of this derivation. The yield is apparently half of that of corresponding reduction process which could be obtained from the difference between  $\phi(\text{Ag})$  and  $\phi_0(\text{Ag})$ , clearly indicating the reasonable fit to equation (2) in both cases of  $TiO_2(A)$  and  $TiO_2(R)$ .

Replots of these data as a function of  $C_P$  clarify the nature of  $h^+_{II}$  on both  $TiO_2$  powders, as shown in Figure 6. The limiting quantum yield for the  $h^+_{II}$  site on  $TiO_2(A)$  was 2-3 times as large as that on  $TiO_2(R)$ . Reciprocal plots of the data in Figure 6 lead to linear relationships for the quantum yield ( $\phi^{II}(\text{acetone})$ ) by both  $TiO_2(A)$  and  $TiO_2(R)$ , which are represented by

$$\phi^{II}(\text{acetone}) = \phi^{II}_{\text{lim}}(\text{acetone}) K_L C_P / (1 + K_L C_P) \quad (12)$$



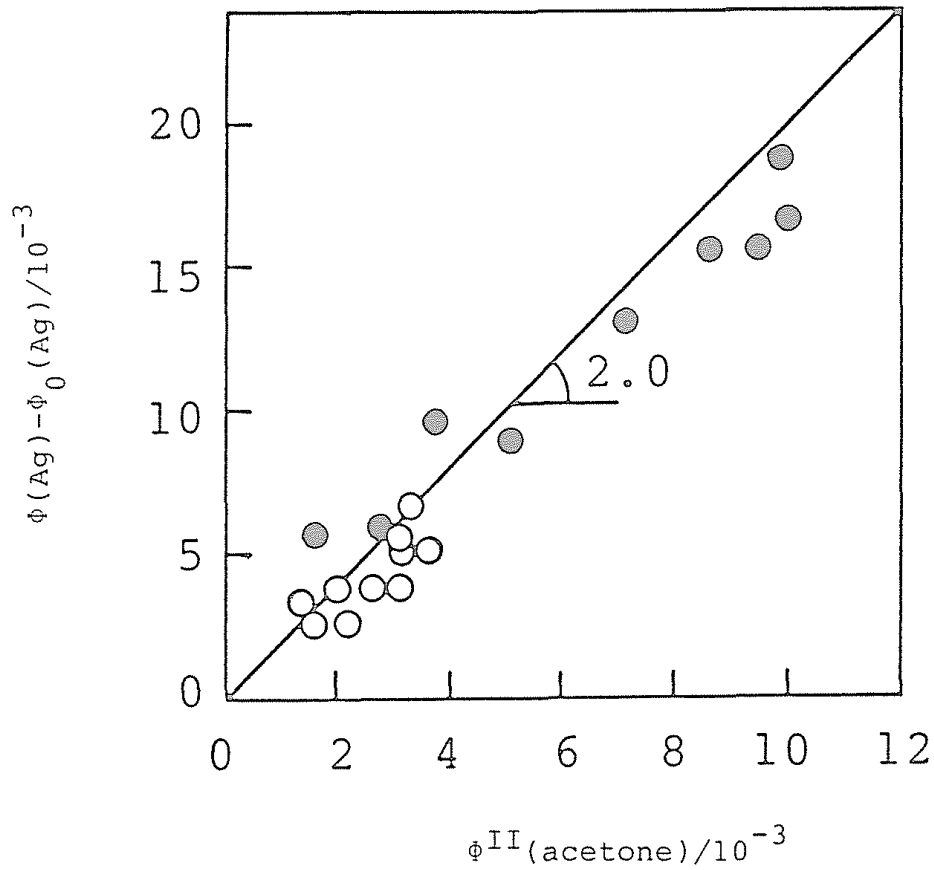


Figure 5 Linear relation between the quantum yield of acetone at  $h^+_{\text{II}}$  site ( $\phi^{\text{II}}(\text{acetone})$ ) and increment in that of Ag metal ( $\phi(\text{Ag}) - \phi_0(\text{Ag})$ ) observed in the  $\text{TiO}_2(\text{A})$  (●) and  $\text{TiO}_2(\text{R})$  (○) suspensions.

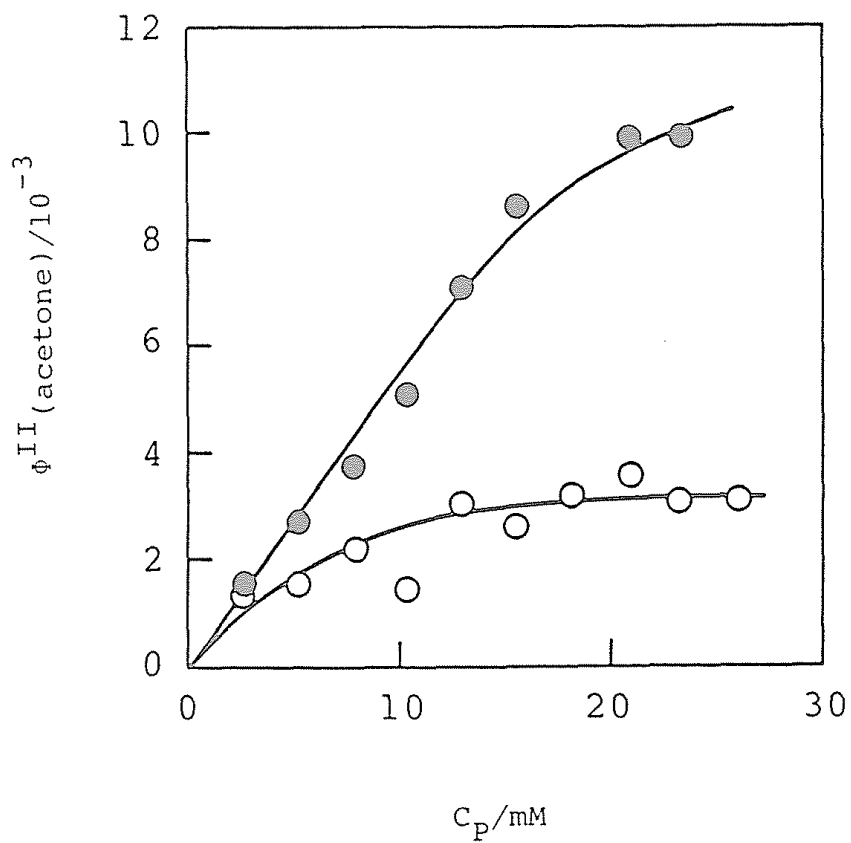


Figure 6 Dependence of the quantum yield of acetone formation at  $h^+_{II}$  site ( $\phi^{II}(\text{acetone})$ ) on the 2-propanol concentration ( $C_P$ ) of  $\text{TiO}_2(\text{A})$  (●) and  $\text{TiO}_2(\text{R})$  (○) suspensions.

where  $\phi_{lim}^{II}(\text{acetone})$  and  $K_L$  represent the limiting quantum yield of acetone formation at the  $h^+_{II}$  site and a Langmuir adsorption constant, respectively. Values derived from the slopes and intercepts of the straight lines in Figure 7 are listed in Table 1.

On the other hand, the quantum yield of acetone formation at the  $h^+_I$  site ( $\phi^I(\text{acetone})$ ) is responsible to the decrement of that of  $O_2$  formation by the addition of 2-propanol, as follows.

$$\phi^I(\text{acetone}) = 2 (\phi^0(O_2) - \phi(O_2)) \quad (13)$$

Figure 8 illustrates that  $\phi^I(\text{acetone})$  for both  $TiO_2(A)$  and  $TiO_2(R)$  also significantly depends on  $C_P$ . Also in this case, the reciprocal plots of  $\phi^I(\text{acetone})$  and  $C_P$  gave linear relationships which is similar to equation (12), as shown in Figure 9.

$$\phi^I(\text{acetone}) = \phi_{lim}^I(\text{acetone}) K_L C_P / (1 + K_L C_P) \quad (14)$$

The linear plots in Figures 9 and 10 are now strong implication that competitive adsorptions of 2-propanol and water on the  $TiO_2$  surface determine the extent of hole trapping as a key step leading to acetone and  $O_2$ , because equations (12) and (14) have the forms characteristic of a Langmuir isotherm.

The reported observations are rationalized as follows. At thermal equilibrium in the dark the oxidation sites of  $TiO_2$  photocatalyst, at which hole reactions (or anodic oxidations) proceed when irradiated, are expected to be hydrated (adsorption of molecular water) or hydroxylated (dissociative adsorption of water into two

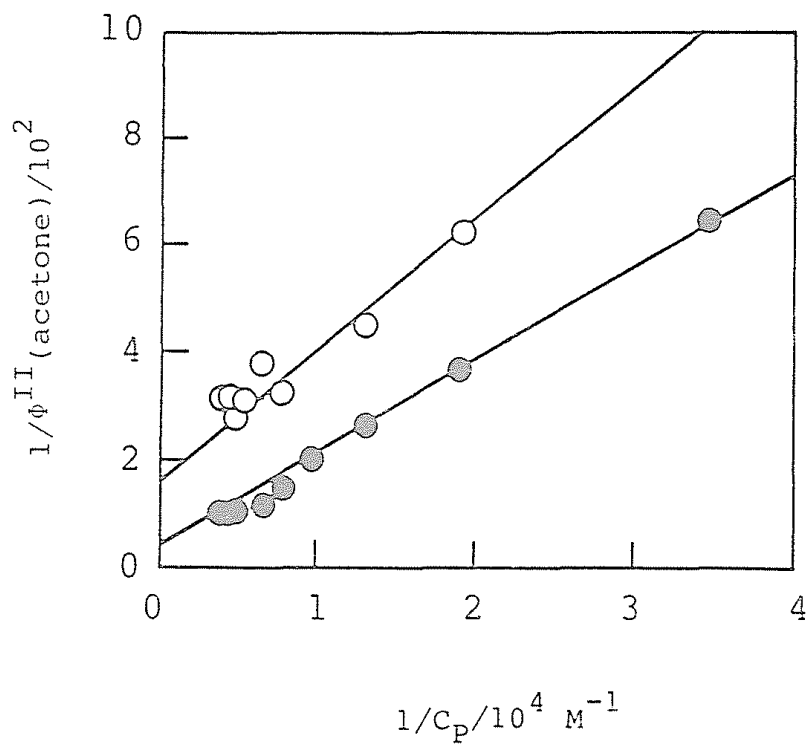


Figure 7 Reciprocal plots between  $\phi^{II}(\text{acetone})$  and  $C_p$ . The data are derived from Figure 6. Symbols are same as in Figure 6.

Table 1 Kinetic data for  $\text{TiO}_2$  photocatalytic reaction in  $\text{Ag}_2\text{SO}_4$  solution

$\phi_{\text{lim}}$ or $K_L$	Site	$\text{TiO}_2(\text{A})$	$\text{TiO}_2(\text{R})$
$\phi_{\text{lim}}(\text{acetone}) : C_P \rightarrow \infty$	I	0.012	0,011
	II	0.023	0.006
$K_L$	I	$6.8 \times 10^4$	$5.6 \times 10^4$
	II	$2.6 \times 10^3$	$6.7 \times 10^3$
$\phi_{\text{lim}}(\text{acetone}) : C_A \rightarrow \infty$		0.020	0.014
	$K_L$	$9.7 \times 10^2$	$2.7 \times 10^2$

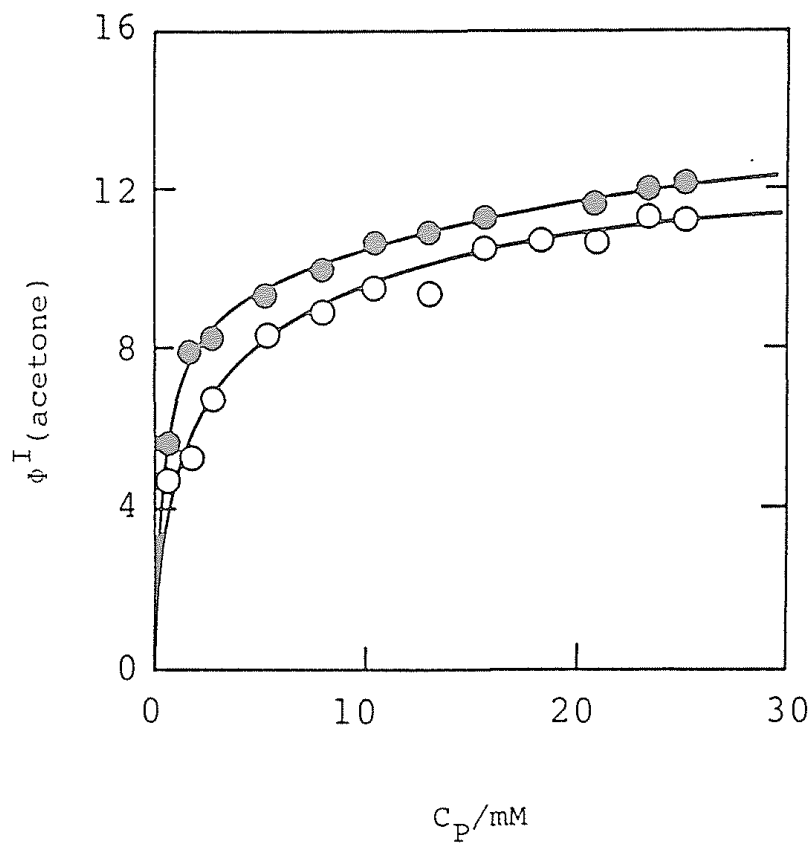


Figure 8 Dependence of the quantum yield of acetone formation at  $h^+_{\text{I}}$  site ( $\phi^{\text{I}}$ (acetone)) on the 2-propanol concentration ( $C_P$ ) of  $\text{TiO}_2(\text{A})$  (●) and  $\text{TiO}_2(\text{R})$  (○) suspensions.

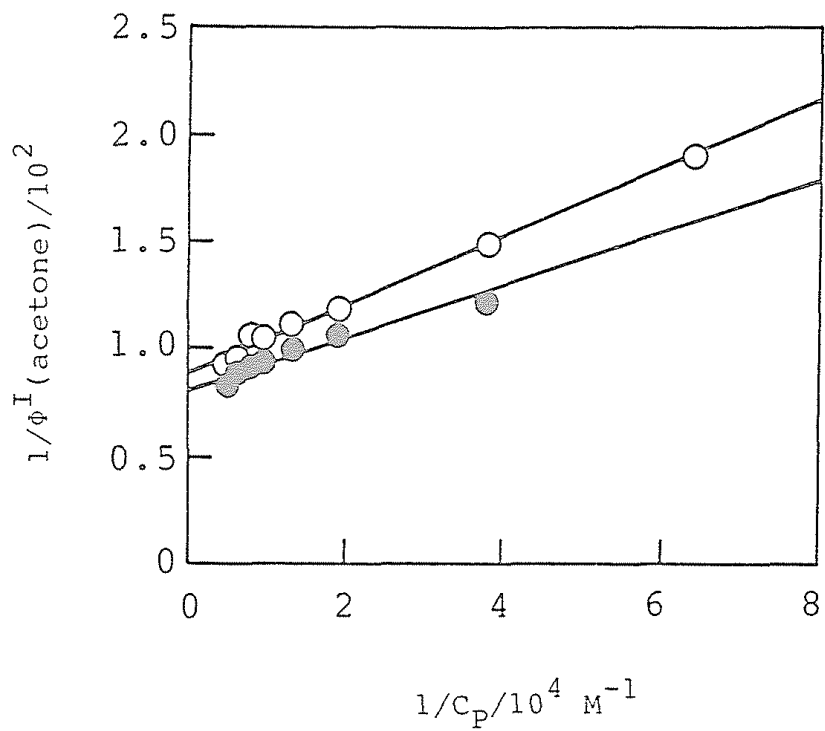
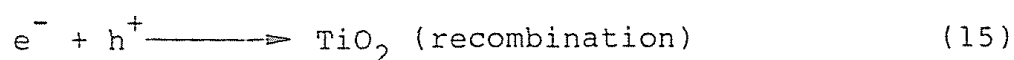


Figure 9 Reciprocal plots between  $\phi^I(\text{acetone})$  and  $C_P$ . The data are derived from Figure 8. Symbols are same as in Figure 8.

surface OH groups) in aquaous media without 2-propanol. Such adsorption characteristics on the surface of  $\text{TiO}_2$  particles have been well documented.<sup>20-25</sup> Relatively small amount of 2-propanol molecules possibly competes with molecular water for the same adsorption sites of  $\text{TiO}_2$ , thus being adsorbed in an undissociated form; e.g., by hydrogen bonding forces.<sup>25</sup> The  $\text{TiO}_2$  surface is also capable of adsorbing 2-propanol dissociatively to form a surface propoxy group.<sup>25</sup> Although several types of models are available for the adsorption isotherm, the results presented here favor the Langmuir conditions for a good approximation. Furthermore, in the photocatalytic reaction system in the absence of silver salt the apparent reaction rate has depended on the amount of adsorbed substrate 2-propanol or 2-methyl-2-propanol adsorbed according to a Langmuir isotherm, as shown in Chapters 1 and 2, respectively (although unique adsorption has been presumed in these cases).

Thus, the observed effect of increasing concentration of 2-propanol at a fixed  $C_A = 50$  mM on the enhancement of apparent photocatalytic activity of  $\text{TiO}_2$  suspensions is attributable mainly to modification of a dynamic process of electron-hole separation in a irradiated  $\text{TiO}_2$  particle that depends upon relative importance among charge trappings by surface adsorbates and a recombination.



The characteristic difference between the activities of  $\text{TiO}_2(\text{A})$  and  $\text{TiO}_2(\text{R})$  is seen in Table 1; the limiting yield at  $h^+_{\text{I}}$  of  $\text{TiO}_2(\text{A})$  is practically identical to that of  $\text{TiO}_2(\text{R})$ , while the yield at  $h^+_{\text{II}}$



of  $\text{TiO}_2(\text{A})$  is 3.7 times as large as that of  $\text{TiO}_2(\text{R})$ . Therefore, the enhanced yield of silver metal deposit on  $\text{TiO}_2(\text{A})$  is attributed to the enhanced oxidation of 2-propanol at  $h^+_{\text{II}}$  site.

The effect of  $\text{Ag}^+$  ion (see Figure 4) is consistent with an electron trapping to decrease the extent of electron-hole recombination. The electron trapping presumably proceeds via adsorption of  $\text{Ag}^+$  on the  $\text{TiO}_2$  surface, from the evidence that the observed dependences (Figure 4) of quantum yield of acetone formation by both  $\text{TiO}_2$  suspensions on the  $\text{Ag}^+$  concentration could fulfil Langmuir isotherms (Figure 10) as,

$$\phi(\text{acetone}) = \phi_{\text{lim}}(\text{acetone}) K_L C_A / (1 + K_L C_A)$$

Fleischauer and coworkers have reported the similar adsorption of  $\text{Ag}^+$  on the single-crystal  $\text{TiO}_2$  in respect of the dependences of quantum efficiency on the concentration of silver salt in the absence of the other substrates.<sup>17a</sup> The constant  $K_L$  observed in this work is in good agreement with their observations. Recently, Hada and coworkers reported the similar photocatalytic reaction by  $\text{TiO}_2$  suspension, though their results failed to agree with Langmuir isotherms.<sup>26</sup> Nevertheless, the present results suggesting the Langmuir adsorption of  $\text{Ag}^+$  ion on the  $\text{TiO}_2$  surface is consistent with the results, which will be shown in Chapter 11, that the actual amount of  $\text{Ag}^+$  adsorbed on the  $\text{TiO}_2$  surface obeys a Langmuir isotherm. Moreover, good agreement of the  $K_L$  values (for  $\text{TiO}_2(\text{A})$   $9.7 \times 10^2$  (see Table 1) and  $6.2 \times 10^2$  (see Table 2 of Chapter 11)) strongly supports the present findings.

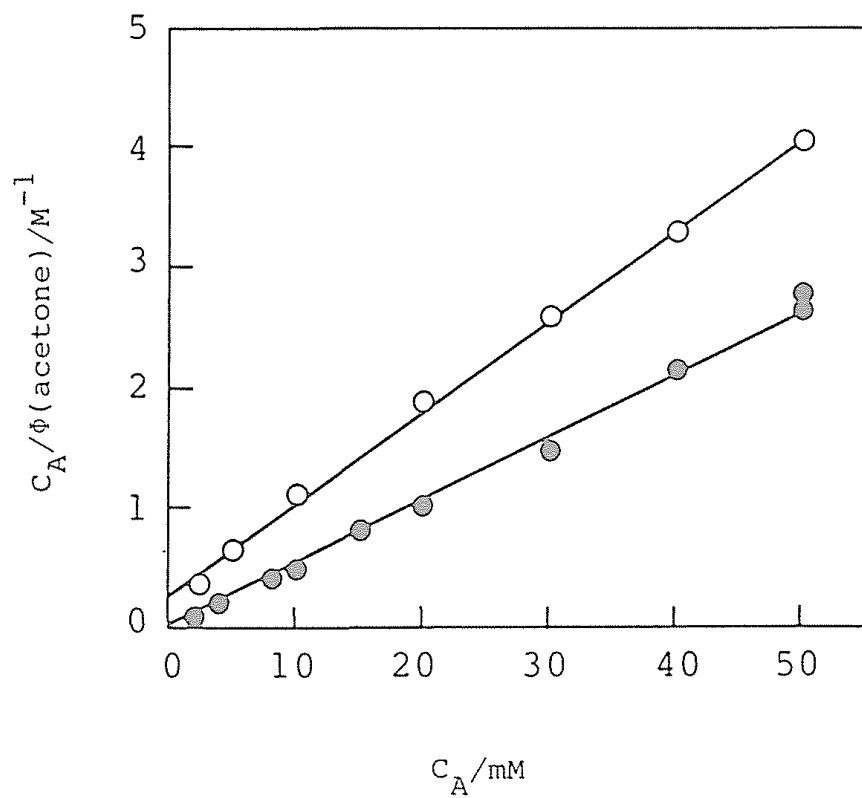


Figure 10 Langmuir plot of  $\phi(\text{acetone})$  in  $\text{TiO}_2(\text{A})$  ( ● ) and  $\text{TiO}_2(\text{R})$  ( ○ ) suspensions as a function of the  $\text{Ag}^+$  concentration ( $C_A$ ). The data are derived from Figure 4.

In summary it was shown that addition of either 2-propanol or  $\text{Ag}^+$  ion can enhance the catalytic activity of irradiated  $\text{TiO}_2$  particles in aqueous suspension. The experimental data derived from photocatalytic reaction of producing acetone,  $\text{O}_2$  and Ag metal deposit are related to adsorption characteristics of both 2-propanol and  $\text{Ag}^+$  ion on the  $\text{TiO}_2$  surface, for which the Langmuir isotherm is a useful model. The observed effects are in accord with competitive hole trappings by adsorbed 2-propanol and water as well as electron trapping by adsorbed  $\text{Ag}^+$ , thereby diminishing the extent of electron hole recombination and increasing trapped charges for net chemical reactions.

## REFERENCES AND NOTES

- 1 S. Nishimoto, B. Ohtani, H. Kajiwara, and T. Kagiya, *J. Chem. Soc., Faraday Trans. 1*, 79, 2685 (1983).
- 2 (a) A. J. Bard, *J. Photochem.*, 10, 59 (1979) (b) A. J. Bard, *Science* (Washington D. C.), 207, 139 (1980) (c) A. J. Bard, *J. Phys. Chem.*, 86, 172 (1982) (d) A. J. Nozik, *Annu. Rev. Phys. Chem.*, 29, 189 (1978) (e) M. S. Wrighton, P. T. Wolczanski, A. B. Ellis, *J. Solid State Chem.*, 22, 17 (1977) (f) M. A. Fox, *Acc. Chem. Res.*, 16, 314 (1983).
- 3 (a) B. Kraeutler and A. J. Bard, *J. Am. Chem. Soc.*, 100, 2239 (1978) (b) B. Kraeutler and A. J. Bard, *J. Am. Chem. Soc.*, 100, 5985 (1978) (c) H. Reiche and A. J. Bard, *J. Am. Chem. Soc.*, 101, 3127 (1979) (d) H. Reiche, W. W. Dunn, K. Wilbourn, F. F.-R. Fan, and A. J. Bard, *J. Phys. Chem.*, 84, 3207 (1980) (e) I. Izumi, F. F.-R. Fan, and A. J. Bard, *J. Phys. Chem.*, 85, 218 (1981) (f) H. Yoneyama, Y. Takao, H. Tamura, and A. J. Bard, *J. Phys. Chem.*, 87, 1417 (1983).
- 4 (a) T. Kawai and T. Sakata, *J. Chem. Soc., Chem. Commun.*, 1047 (1979) (b) T. Kawai and T. Sakata, *J. Chem. Soc., Chem. Commun.*, 694 (1980) (c) T. Kawai and T. Sakata, *Nature* (London), 286, 474 (1980) (d) T. Kawai and T. Sakata, *Chem. Phys. Lett.*, 72, 87 (1980) (e) T. Kawai and T. Sakata, *Chem. Lett.*, 81 (1981) (f) T. Sakata and T. Kawai, *Nouv. J. Chim.*, 5, 279 (1981).
- 5 (a) T. Kanno, T. Oguchi, H. Sakuragi, and K. Tokumaru, *Tetrahedron Lett.*, 21, 467 (1980) (b) Y. Shimamura, H. Misawa, T. Oguchi, T. Kanno, H. Sakuragi, and K. Tokumaru, *Chem. Lett.*,

- 1961 (1983).
- 6 (a) J. Kiwi, E. Borgarello, E. Pelizzetti, M. Visca, and M. Grätzel, *Angew. Chem., Int. Ed. Engl.*, 19, 646 (1980) (b) E. Borgarello, J. Kiwi, E. Pelizzetti, M. Visca, and M. Grätzel, *Nature (London)*, 284, 158 (1981) (c) E. Borgarello, J. Kiwi, E. Pelizzetti, M. Visca, and M. Grätzel, *J. Am. Chem. Soc.*, 103, 6324 (1981) (d) E. Borgarello, J. Kiwi, M. Grätzel, E. Pelizzetti, and M. Visca, *J. Am. Chem. Soc.*, 104, 2996 (1982).
- 7 (a) M. Fujihira, Y. Satoh, and T. Osa, *Nature (London)*, 293, 206 (1981) (b) M. Fujihira, Y. Satoh, and T. Osa, *Chem. Lett.*, 1053 (1981) (c) M. Fujihira, Y. Satoh, and T. Osa, *Bull. Chem. Soc. Jpn*, 55, 666 (1982).
- 8 (a) M. A. Fox and C. C. Chen, *J. Am. Chem. Soc.*, 103, 6757 (1981) (b) M. A. Fox and M.-J. Chen, *J. Am. Chem. Soc.*, 105, 4497 (1983) (c) M. A. Fox and C. C. Chen, *Tetrahedron Lett.*, 24, 547 (1983).
- 9 J. W. Pavlik and S. Tantayanon, *J. Am. Chem. Soc.*, 103, 6755 (1981).
- 10 (a) P. Pichat, J.-M. Herrmann, J. Disdier, H. Courbon, and M.-N. Mozzanega, *Nouv. J. Chim.*, 5, 627 (1981) (b) J.-M. Herrmann, M.-N. Mozzanega, and P. Pichat, *J. Photochem.*, 22, 333 (1983).
- 11 S. Teratani, J. Nakamichi, K. Taya, and K. Tanaka, *Bull. Chem. Soc. Jpn*, 55, 1688 (1982).
- 12 K. Domen, S. Naito, T. Onishi, and K. Tamaru, *Chem. Lett.*, 555 (1982).
- 13 M. R. St. John, A. J. Furgala, A. F. Sammells, *J. Phys. Chem.*, 87, 801 (1983).

- 14 H. L. Chum, M. Ratcliff, F. L. Posey, J. A. Turner, and A. J. Nozik, *J. Phys. Chem.*, 87, 3089 (1983).
- 15 A. Mills, and G. Porter, *J. Chem. Soc., Faraday Trans. 1*, 78, 3659 (1982).
- 16 (a) S. Nishimoto, B. Ohtani, T. Yoshikawa, and T. Kagiya, *J. Am. Chem. Soc.*, 105, 7180 (1983) (b) S. Nishimoto, B. Ohtani, A. Sakamoto, and T. Kagiya, *Nippon Kagaku Kaishi*, 246 (1984).
- 17 (a) P. D. Fleischauer, H. K. Alan Kan, and J. R. Shepherd, *J. Am. Chem. Soc.*, 94, 283 (1972) (b) A. W. Adamson, and P. D. Fleischauer, "Concepts of Inorganic Photochemistry", Wiley, New York, 1975, p. 400.
- 18 M. D. Ward and A. J. Bard, *J. Phys. Chem.*, 86, 3559 (1982).
- 19 M. D. Ward, J. R. White, and A. J. Bard, *J. Am. Chem. Soc.*, 105, 27 (1983).
- 20 D. J. C. Yates, *J. Phys. Chem.*, 65, 746 (1961).
- 21 (a) H. P. Boehm, *Angew. Chem.*, 78, 617 (1966) (b) M. Herrmann and H. P. Boehm, *Z. Anorg. Chem.*, 368, 73 (1969) (c) H. P. Boehm, *Disc. Faraday Soc.*, 52, 264 (1971).
- 22 (a) K. E. Lewis and G. D. Parfitt, *Trans. Faraday Soc.*, 62, 204 (1966) (b) P. Jackson and G. D. Parfitt, *Trans. Faraday Soc.*, 67, 2469 (1971) (c) P. Jackson and G. D. Parfitt, *Trans. Faraday Soc.*, 68, 896 (1972).
- 23 (a) P. Jones and J. A. Hockey, *Trans. Faraday Soc.*, 67, 2669 (1971) (b) P. Jones and J. A. Hockey, *Trans. Faraday Soc.*, 67, 2679 (1971) (c) P. Jones and J. A. Hockey, *Trans. Faraday Soc.*, 68, 907 (1972).
- 24 P. Primet, P. Pichat, and M.-V. Mathieu, *J. Phys. Chem.*, 75,

1216 (1971).

25 R. I. Bickley and R. K. M. Jayanty, *Disc. Faraday Soc.*, 58, 194 (1974).

26 H. Hada, Y. Yonezawa, M. Saikawa, *Bull. Chem. Soc. Jpn*, 55, 2010 (1982).

Part III

Correlation of Photocatalytic Activity of  $\text{TiO}_2$  for  
Redox Reaction in Aqueous 2-Propanol and Silver Salt Solution  
with Crystal Form and Surface Structure of  $\text{TiO}_2$

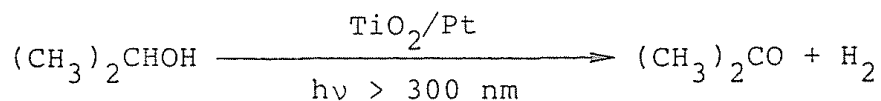


## Chapter 9

### Photocatalytic Activity of TiO<sub>2</sub> Prepared from Titanium Sulfate for Dehydrogenation of 2-Propanol in Aqueous Solution

#### ABSTRACT

A series of TiO<sub>2</sub> powders was prepared by calcining titanium(IV) hydroxide slurry, which was provided by hydrolysis of titanium(IV) sulfate, in the temperature range (T<sub>c</sub>) of 170 up 1000 °C. The content (C<sub>A</sub>) and crystallite size (L<sub>A</sub>) of anatase crystal in the TiO<sub>2</sub> powder increased with increasing T<sub>c</sub> up to 700 °C. The transition from anatase to rutile occurred at 740-830 °C. The residual sulfate ion in the TiO<sub>2</sub> powder decreased linearly with increasing T<sub>c</sub>, disappearing almost completely above 800 °C. The T<sub>c</sub> dependence of the photocatalytic activity of Pt (5 wt%)-loaded TiO<sub>2</sub>, with reference to the above structural characteristics of the TiO<sub>2</sub>, suggested that the anatase, but not the rutile, has a sufficient photocatalytic activity to reduce H<sup>+</sup> and oxidize 2-propanol when loaded with a small amount of platinum black (Pt).



However, in another reaction system consisting of 2-propanol and silver salts, even the rutile TiO<sub>2</sub> without Pt could effectively photocatalyze the reduction of Ag<sup>+</sup> to Ag metal onto the TiO<sub>2</sub> and oxidation of 2-propanol to acetone.

## INTRODUCTION

Recently, photocatalytic reaction of semiconductor materials have focused on the utilization of solar energy to produce chemical one such as hydrogen. Among the semiconductors,  $\text{TiO}_2$  has been used in a number of studies, because of its photostability and favorable band energies for various oxidations and reductions.<sup>1</sup> Moreover, it has been reported that loading of small amount of platinum (Pt) enhanced the photocatalytic activity of  $\text{TiO}_2$  powders for the reaction of water decomposition and dehydrogenation of various organic,<sup>2</sup> and inorganic<sup>3</sup> compounds. However, most of these works were concerned with the efficiency of the commercially available  $\text{TiO}_2$  catalysts and the effect of the metal loading. Little attention has been paid to the correlation between properties of  $\text{TiO}_2$  powders and their photocatalytic activity.<sup>4-6</sup>

$\text{TiO}_2$  has been also known as catalyst or support for gas-phase reaction.<sup>7</sup> In this respect, there have been many reports on the method of preparation, the structure of  $\text{TiO}_2$ , and physicochemical properties. This chapter shows the correlation of the photocatalytic activity with the crystal and surface structure of  $\text{TiO}_2$  prepared from titanium(IV) sulfate.

## EXPERIMENTAL

Preparation of  $\text{TiO}_2$  Powder. Titanium(IV) hydroxide ( $\text{Ti}(\text{OH})_4$ ) slurry prepared from  $\text{Ti}(\text{SO}_4)_2$  was supplied from Ishihara Sangyo Co. Ltd., which contained 0.003 % of Fe and 6.85 % of  $\text{SO}_3$  (wt% with reference to  $\text{TiO}_2$  weight). The slurry was dried at 170 °C for 21 h in air and was subjected to the further calcination in air for 3 h at

various temperature in an electric furnace.

X-Ray Diffraction Analysis of TiO<sub>2</sub> Powder. Crystal structure of these powders was analyzed by X-ray diffraction using Rigaku Geigerflex 2013 diffractometer (target: Cu, filter: Ni, 35 kV, 20 mA, scanning speed 1 ° min<sup>-1</sup>). Contents of anatase and rutile crystals were evaluated from the data obtained by integration of the most intensive peak (2θ, 25.4 ° (d = 0.352 nm, (011) plane) and 27.3 ° (d = 0.325 nm (110) plane), respectively) by reference to that of CaCO<sub>3</sub> as an internal standard.<sup>8</sup> Calibration curves for anatase and rutile crystals were obtained with commercially available anatase TiO<sub>2</sub> (Merck) and rutile TiO<sub>2</sub> prepared by heating the Merck TiO<sub>2</sub> powder at 1200 °C for 10 h in air,<sup>9</sup> respectively, by the same procedure as above. Mean crystallite size (L) of these crystals was determined with the Scherrer equation<sup>10</sup> ( $L = k\lambda / \beta \cos\theta$ , where  $\lambda$  is the radiation wavelength,  $\theta$  the Bragg angle, and  $k = 0.90$ ) from the line broadening ( $\beta$ ) of the most intensive peak in the X-ray diffraction patterns after corrections for K<sub>α</sub> doublet and instrumental broadenings.

Physical Properties of TiO<sub>2</sub> Powder. Specific surface area of TiO<sub>2</sub> was evaluated from nitrogen adsorption at -196 °C based on the BET equation.

IR spectrum of TiO<sub>2</sub> powder before and after treatment with 1.0 mol dm<sup>-3</sup> NaOH or distilled water was measured by KBr disk (KBr 200 mg, TiO<sub>2</sub> 4 mg) method with JASCO A-302 spectrophotometer.

Total amount of hydroxyl group on the TiO<sub>2</sub> surface was estimated by Na<sup>+</sup> ion adsorption from 0.1 mol dm<sup>-3</sup> NaOH (5.0 cm<sup>3</sup>; pH ca. 13) solution on 50 mg of TiO<sub>2</sub>. The amount of adsorbed Na<sup>+</sup> was

determined from the decrease in the  $\text{Na}^+$  concentration using Jarrel Ash AA 8200 atomic absorption spectrophotometer.<sup>22</sup>

Apparatus and Procedure of Photoreaction. The  $\text{TiO}_2$  powders were brayed in an agate mortar with or without platinum black (typically 5 wt%, Nakarai Chemicals) to prepare catalyst. Silver sulfate ( $\text{Ag}_2\text{SO}_4$ ) and 2-propanol were used as received. The aqueous solution was made up with ion-exchanged distilled water.

A finely ground  $\text{TiO}_2$  (or platinum-loaded  $\text{TiO}_2$  ( $\text{TiO}_2/\text{Pt}$ )) powder (50 mg) was suspended in water ( $5.0 \text{ cm}^3$ ) or an aqueous  $\text{Ag}_2\text{SO}_4$  solution ( $0.025 \text{ mol dm}^{-3}$ ;  $5.0 \text{ cm}^3$ ) in a glass tube ( $18 \text{ mm}\phi \times 180 \text{ mm}$ , transparent for the light of wavelength  $> 300 \text{ nm}$ ). In the experiment for the determination of pH-dependent activity of  $\text{TiO}_2$ ,  $\text{H}_2\text{SO}_4$  or  $\text{NaOH}$  solution was used to adjust the pH of the suspension. The tube was purged of air by Ar stream for at least 30 min and sealed off with a rubber cap. 2-Propanol ( $38 \text{ mm}^3$ , 0.50 mmol) was injected through the cap by means of a syringe. The Ar-purged  $\text{TiO}_2$  suspension was irradiated at room temperature with a merry-go-round apparatus equipped with 400-W high-pressure mercury arc (Eiko-sha 400). The irradiation was performed under magnetic stirring.

Product Analysis. Product liberated in the gas phase of the sealed sample, e.g.  $\text{H}_2$  and  $\text{O}_2$ , was analyzed with a Shimadzu GC 4A gas chromatograph equipped with a thermal conductivity detector and a Molecular Sieves 5A column ( $3 \text{ mm}\phi \times 3 \text{ m}$ ) with Ar carrier at  $100 \text{ }^\circ\text{C}$ . 2-Propanol and acetone were analyzed with a Shimadzu GC 6A gas chromatograph equipped with a flame ionization detector and a Polyethylene Glycol 20M on Celite 545 column ( $3 \text{ mm}\phi \times 2 \text{ m}$ ) with  $\text{N}_2$  carrier at  $90 \text{ }^\circ\text{C}$ .

Procedure and apparatus for the determination of the amount of Ag deposition were described in Chapter 6 of this thesis.<sup>21</sup>

## RESULTS AND DISCUSSION

Crystal Structure of Titanium(IV) Oxide. It is well known that three types of  $\text{TiO}_2$  crystal (anatase, rutile, and brookite) can be derived according to the starting materials and the preparation conditions.<sup>2</sup> In this study, variety of  $\text{TiO}_2$  powders could be obtained by the calcination at various temperatures ( $T_c$ ) up to 1000 °C. Figure 1(a) shows the contents of anatase and rutile crystals ( $C_A$  and  $C_R$ , respectively) in the  $\text{TiO}_2$  powders evaluated by the X-ray diffraction analysis. The  $\text{TiO}_2$  powders calcined at  $T_c \leq 700$  °C consisted not rutile but anatase crystal. The  $C_A$  value was ca. 60 % at  $T_c$  170 °C and increased with the elevation of  $T_c$  to attain 100 % at  $T_c$  700 °C. Further elevation of  $T_c$  rather decreased  $C_A$  as a result of crystal transformation into rutile. The  $\text{TiO}_2$  powder obtained at  $T_c \geq 830$  °C only consisted of rutile crystal. It is reasonable that the remainder other than these crystals is amorphous  $\text{TiO}_2$  which does not give X-ray diffraction pattern. The content of the amorphous ( $C_{AM}$ ) was ca. 40 % at  $T_c$  170 °C and decreased drastically to be ca. 10 % at  $T_c$  500 °C and negligible at  $T_c$  830 °C.

Crystallite size of anatase crystal ( $L_A$ ) (Figure 1(b)) increased with the elevating  $T_c$ , especially over 700 °C. The size of rutile crystal ( $T_c \geq 740$  °C) was larger than that of anatase, except for the case of  $T_c$  740 °C, although the exact size could not be measured with the Scherrer equation because the line broadening of the rutile crystal was negligibly small.

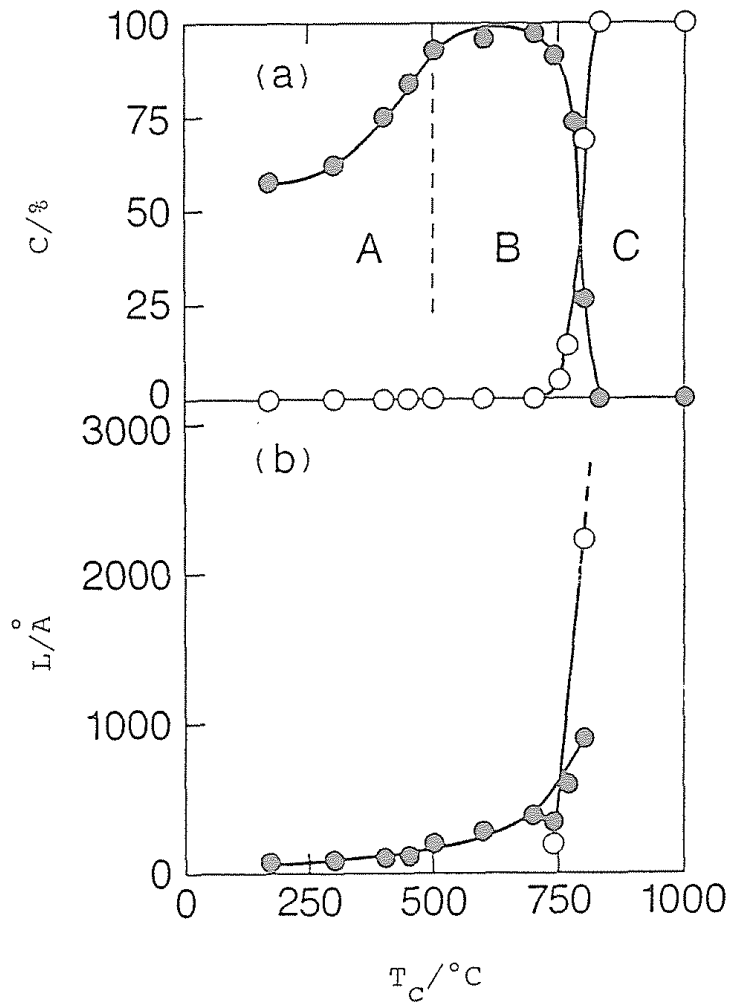


Figure 1 Variations in the crystal content (C) and the crystallite size (L) of  $\text{TiO}_2$  powders with calcination temperature ( $T_c$ ); ● : Anatase, ○ : Rutile.

Thus, the  $\text{TiO}_2$  powders consist of two crystals and amorphous phase of various contents were obtained. They are classified according to the crystal structure into three groups, as follows:

(1)  $\text{TiO}_2$  with poorly-grown anatase, and amorphous, obtained at  $T_c < 500^\circ\text{C}$  (A in Figure 1(a)).

(2)  $\text{TiO}_2$  with well-grown anatase obtained at  $500^\circ\text{C} < T_c \leq 800^\circ\text{C}$  (B in Figure 1(a)).

(3)  $\text{TiO}_2$  with well-grown rutile obtained at  $T_c > 830^\circ\text{C}$  (C in Figure 1(a)).

Specific Surface Area of Titanium(IV) Oxide. Figure 2 shows the relation between  $T_c$  and specific surface area ( $S$ ) of the  $\text{TiO}_2$  powders. The value of  $S$  at  $T_c$   $170^\circ\text{C}$  was ca.  $300\text{ m}^2\text{ g}^{-1}$ , decreased drastically with elevating  $T_c$ , and reached  $60\text{ m}^2\text{ g}^{-1}$  at  $T_c$   $500^\circ\text{C}$ . The value of  $S$  was practically constant over the  $T_c$  range of  $500\text{--}800^\circ\text{C}$  and then decreased by the treatment at higher-temperature to be negligible (ca.  $2\text{ m}^2\text{ g}^{-1}$ ) at  $T_c$   $1000^\circ\text{C}$ .

Compared with the crystal structures described in the preceding section, it is evident that  $S$  is proportional to  $C_{AM}$  as shown in Figure 2. Therefore, the decrease of  $S$  in the  $T_c$  range  $< 500^\circ\text{C}$  is attributable to the decrease of amorphous phase of  $\text{TiO}_2$ , which possesses relatively larger surface area, i.e., dehydration process of  $\text{Ti}(\text{OH})_4$  to yield  $\text{TiO}_2$  was accomplished by the heat-treatment at ca.  $500^\circ\text{C}$ . The further elevation of  $T_c$  led to the growth of anatase crystal. The decrease of  $S$  in the higher  $T_c$  region at ca.  $830^\circ\text{C}$  would be due to the crystal transformation of anatase into rutile, because the rutile crystal has the larger crystallite size (Figure 1).

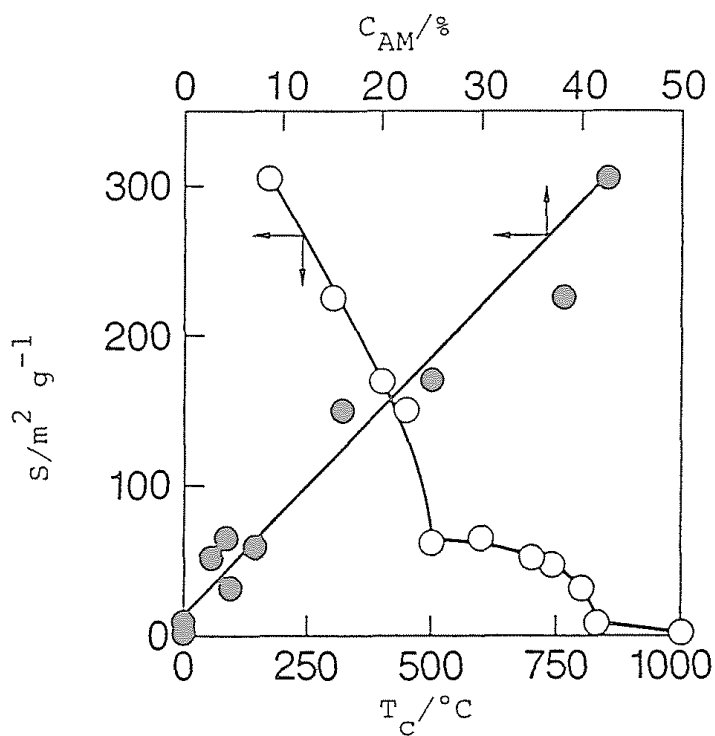


Figure 2 BET surface area ( $S$ ) of  $\text{TiO}_2$  powders vs. calcination temperature ( $T_c$ ) and the content of amorphous  $\text{TiO}_2$  ( $C_{AM}$ ).

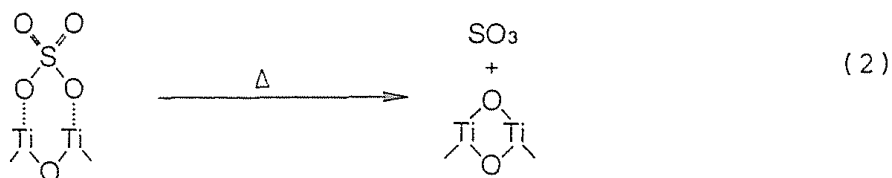


Residual Sulfate Ion on the Titanium(IV) Oxide Powder.

Figure 3

shows part of IR spectra of  $\text{TiO}_2$  powders. Intensive peaks around 1040 and 1140  $\text{cm}^{-1}$  and shoulders at ca. 970 and 1200  $\text{cm}^{-1}$  were observed.<sup>6</sup> These results were essentially identical to that for the similarly derived  $\text{TiO}_2$  powders reported by Kurosaki and Okazaki.<sup>7</sup> By comparing with the IR absorption of sulfate ion in a cobalt complex,<sup>8</sup> it is concluded that the residual sulfate ion is located on the  $\text{TiO}_2$  powder bridging on the two metal (Ti) atoms.

These IR absorptions of the residual sulfate ion were decreased with elevating  $T_c$  without shifting. For example, the absorbance of the peak at ca. 1140  $\text{cm}^{-1}$  decreased linearly with the elevating  $T_c$  up to 800 °C and disappeared almost completely over the  $T_c$  range of 800-1000 °C (Figure 4). This decrease is attributable to the desorption of  $\text{SO}_3$  by the calcination (reaction (2)).



Sulfate anion is expected to retard the transformation of anatase into rutile.<sup>7,9</sup> Actually, in the present study, the transformation could not be observed by the calcination at < 800 °C at which sulfate anion remained on the  $\text{TiO}_2$  surface.<sup>10</sup>

The IR absorption decreased by suspending in distilled water (see Figure 4) and the pH of the suspension also decreased as shown in Figure 5. The pH of the suspension of  $\text{TiO}_2$  calcined at < 500 °C

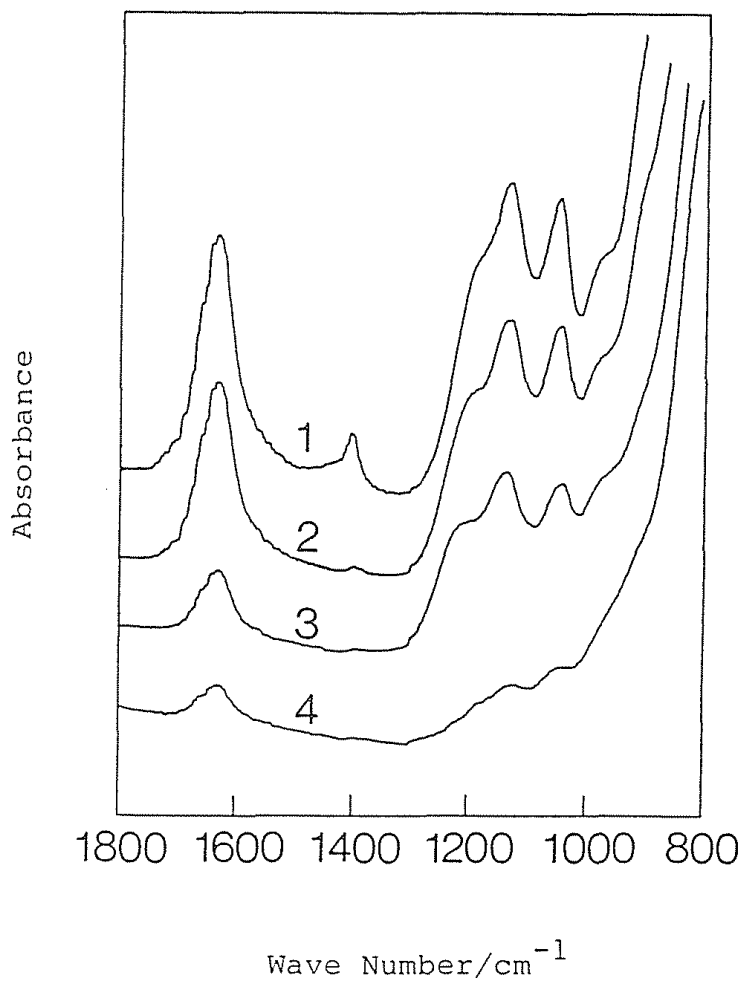


Figure 3 IR spectral change of TiO<sub>2</sub> with calcination temperature of TiO<sub>2</sub>; T<sub>c</sub>/°C 1: 170, 2: 300, 3: 500, 4: 700.

The spectra were recorded by the KBr method and translated for clarify along the absorbance axis.

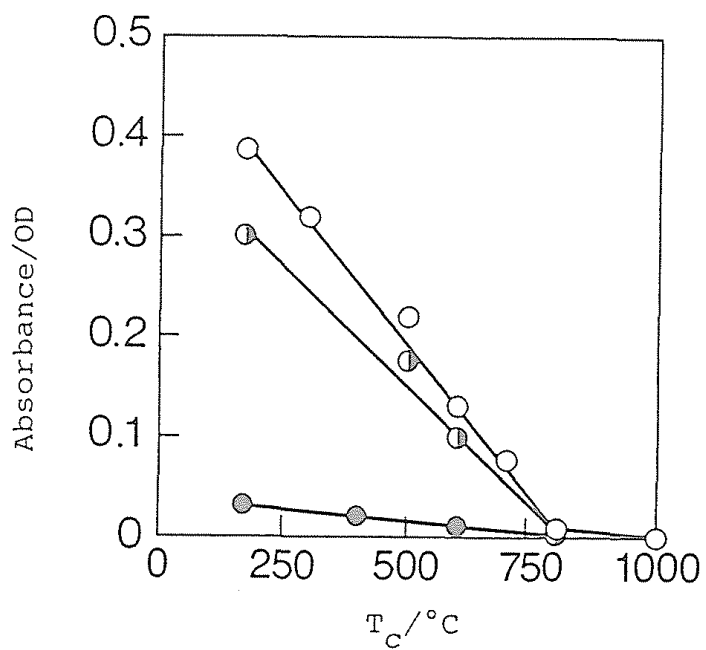
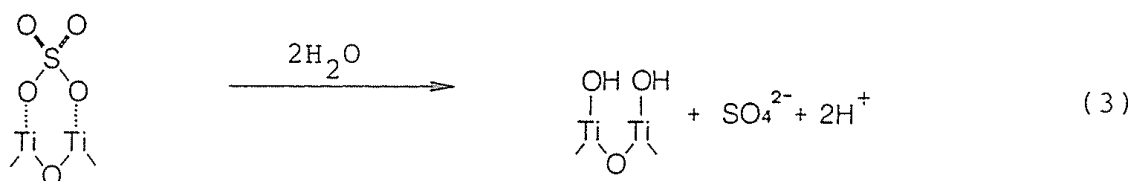


Figure 4 Absorbance of sulfate anion at  $1140\text{ cm}^{-1}$  ○: before and after treatments with ◐: water and ●:  $1.0\text{ mol dm}^{-3}$  NaOH.

was approximately 2.5. Along with the elevation of  $T_c$ , i.e. the decrease in the amount of sulfate anion on the  $TiO_2$  surface, the pH of the suspension increased to attain ca. 5 in the case of  $TiO_2$  calcined at 1000 °C.

It is known that the pH of the suspension of metal oxide powder such as  $TiO_2$  exhibits the specific point of zero charge, as a result of acid-base equilibria of surface hydroxyl groups on the oxide.<sup>11</sup> Therefore, the pH change shown in Figure 5 is attributable to not only the desorption of the sulfate anion but the surface hydroxyl group. From the decrease of IR absorption of the sulfate anion, it is plausible that the pH decrease mainly depends on the desorption of sulfate anion in the form of sulfuric acid by hydrolysis.



Treatment with 1 mol  $\text{dm}^{-3}$  NaOH was also effective to the desorption of the sulfate anion; most part of the IR absorption disappeared by the treatment (Figure 4). Therefore, in the photocatalytic system of 6 mol  $\text{dm}^{-3}$  NaOH as described below, the sulfate anion could be expected to liberate in the solution.

Surface Hydroxyl Group on the  $TiO_2$ . Surface properties of  $TiO_2$  powder suspended in an aqueous solution are strongly dependent on the surface hydroxyl or physically adsorbed water, as in the case in moist atmosphere.<sup>12</sup> In this study,  $\text{Na}^+$  adsorption ( $A_{\text{NaOH}}$ ) from aqueous NaOH solution was measured to evaluate the amount of the surface

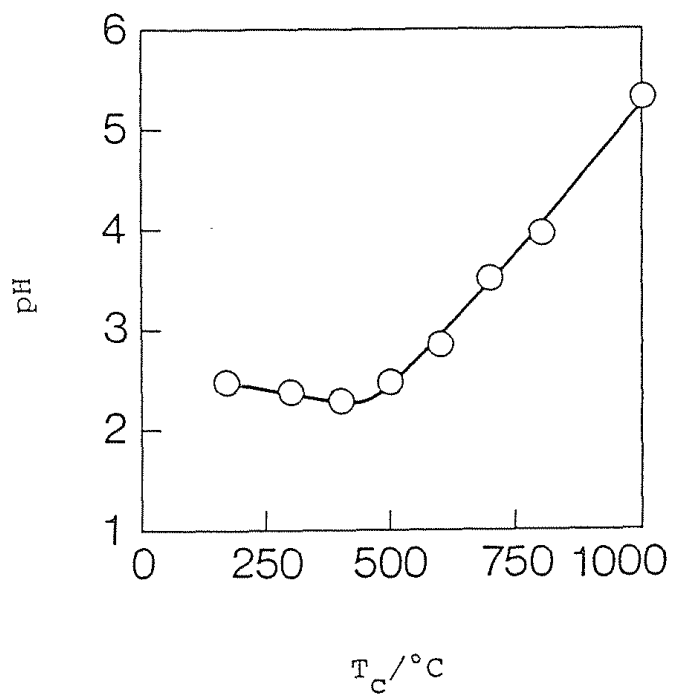


Figure 5 pH of  $\text{TiO}_2$  aqueous suspension vs. calcination temperature ( $T_c$ ).

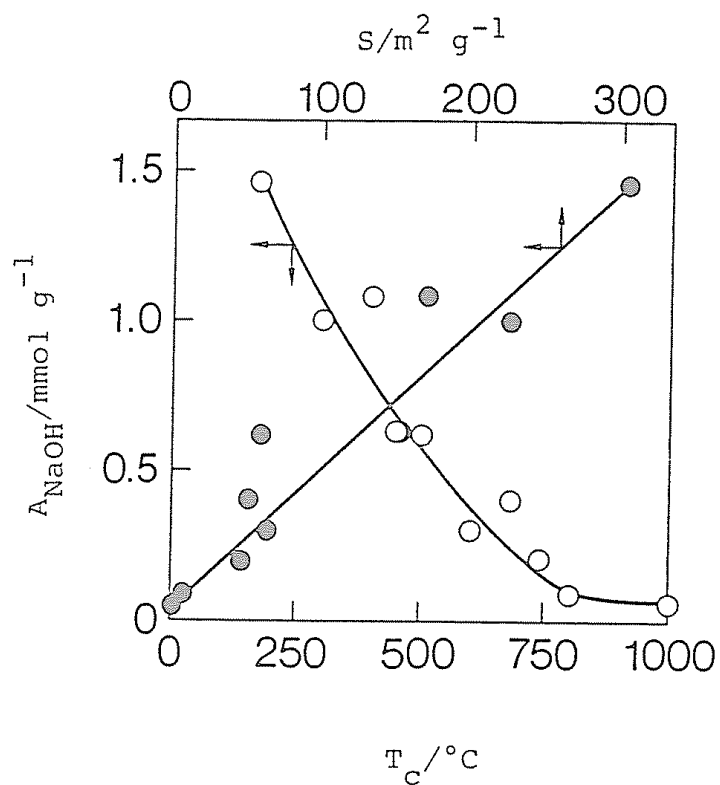


Figure 6 Adsorption of  $\text{Na}^+$  ( $A_{\text{NaOH}}$ ) onto  $\text{TiO}_2$  from  $0.1 \text{ mol dm}^{-3}$  NaOH vs. calcination temperature ( $T_c$ ) and surface area ( $S$ ).

hydroxyl group.<sup>13</sup>

Figure 6 shows the relation between  $A_{\text{NaOH}}$  and  $T_c$ . The value of  $A_{\text{NaOH}}$  was ca.  $1.5 \text{ mmol g}^{-1}$  at  $T_c$   $170^\circ \text{C}$  and decreased monotonously up to  $0.05 \text{ mmol g}^{-1}$  at  $T_c$   $1000^\circ \text{C}$ . This  $\text{Na}^+$  adsorption is accounted for by not the sulfate anion but the surface hydroxyl group,<sup>14</sup> because the sulfate on the  $\text{TiO}_2$  surface liberated almost entirely by the alkaline treatment.<sup>15</sup> The amount of  $A_{\text{NaOH}}$  would include the adsorption on the weakly acidic hydroxyl group, i.e. it exhibits the total amount of hydroxyl group on the  $\text{TiO}_2$  surface. Figure 6 also shows the linear relation between  $A_{\text{NaOH}}$  and specific surface area (S), showing that the density of the surface hydroxyl group is ca. 3 per  $1 \text{ nm}^2$  regardless of  $T_c$ . Assuming that most part of hydroxyl group evaluated in  $A_{\text{NaOH}}$  belongs to the amorphous phase, the decrease of  $A_{\text{NaOH}}$  along with the decrease of S is reasonable, because S mainly depended on the amount of the amorphous phase (see Figure 2).

#### Photocatalytic Reaction of 2-Propanol in Aqueous Solution by Titanium(IV) Oxide.

Photocatalytic reactions of various organic compounds by  $\text{TiO}_2$  or platinum loaded  $\text{TiO}_2$  have been reported.<sup>1</sup> Especially, alcohols are reactive to undergo dehydrogenation into their carbonyl derivatives. Primary alcohols such as ethanol or methanol give aldehydes, acetaldehyde or formaldehyde respectively, which is successively oxidized into carboxylic acids. Moreover, the carboxylic acids are expected to be decomposed into carbon dioxide and alkanes.<sup>16</sup> On the other hand, secondary alcohols give less reactive ketones by  $\text{TiO}_2$  or platinized  $\text{TiO}_2$  suspension. In these respects, 2-propanol, secondary alcohol, has been employed as a substrate for the photocatalytic reaction by the  $\text{TiO}_2$  powders prepared as above.

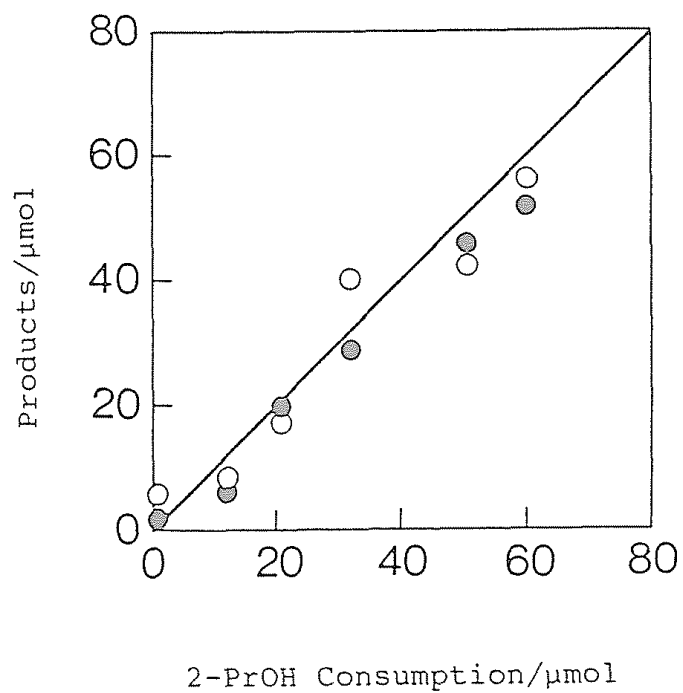
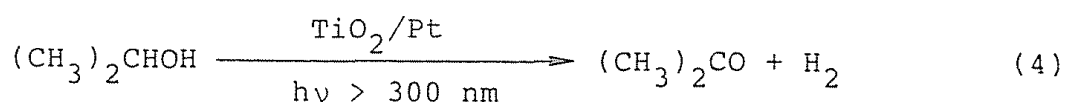


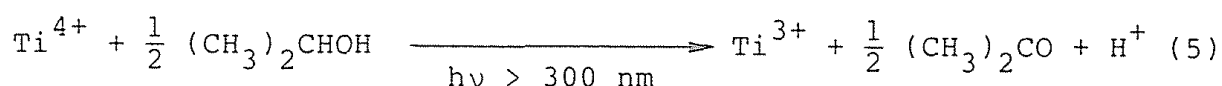
Figure 7 Material balance in the  $\text{TiO}_2/\text{Pt}$  (5 wt%)/2-PrOH aq. photoreaction system (1 h irradiation);  $\circ$  :  $\text{H}_2$ ,  $\bullet$  : Acetone.



Photoirradiation on aqueous TiO<sub>2</sub> or platinum loaded TiO<sub>2</sub> (TiO<sub>2</sub>/Pt) suspension containing 2-PrOH (500 μmol, 0.1 mol dm<sup>-3</sup>) led to H<sub>2</sub> and acetone formations. In the case of TiO<sub>2</sub>/Pt (5 wt%) amount of H<sub>2</sub> and acetone was practically identical to the 2-PrOH consumption regardless of T<sub>c</sub> of TiO<sub>2</sub> powders, as shown in Figure 7, indicating that dehydrogenation of 2-PrOH occurred mainly in this system.



On the other hand, the amounts of H<sub>2</sub> and acetone obtained by TiO<sub>2</sub> suspension without Pt were ca. 100 times smaller than that by TiO<sub>2</sub>/Pt. In this case, the H<sub>2</sub> yield was 2 or 5 times smaller than the acetone yield, inconsistent with the stoichiometric relation of 2-PrOH dehydrogenation (eqn 4). These facts indicate that in the absence of Pt, TiO<sub>2</sub> is reduced photochemically along with oxidation of 2-propanol as follows:



Support of the Ti<sup>3+</sup> formation is that the TiO<sub>2</sub> powder turned blue by the photoirradiation in the 2-PrOH solution. Following experiments were performed by the use of TiO<sub>2</sub>-Pt to avoid the TiO<sub>2</sub> reduction.

Effect of the Amount of Platinum on the Photocatalytic Activity.

Figure 8 shows the initial rate of H<sub>2</sub> formation as a function of the amount of Pt loaded on the anatase TiO<sub>2</sub> powder (T<sub>c</sub> 700 °C). The activity of TiO<sub>2</sub> alone was negligible, but drastically increased by the Pt loading up to 10 wt%. Practically constant activity (ca. 60

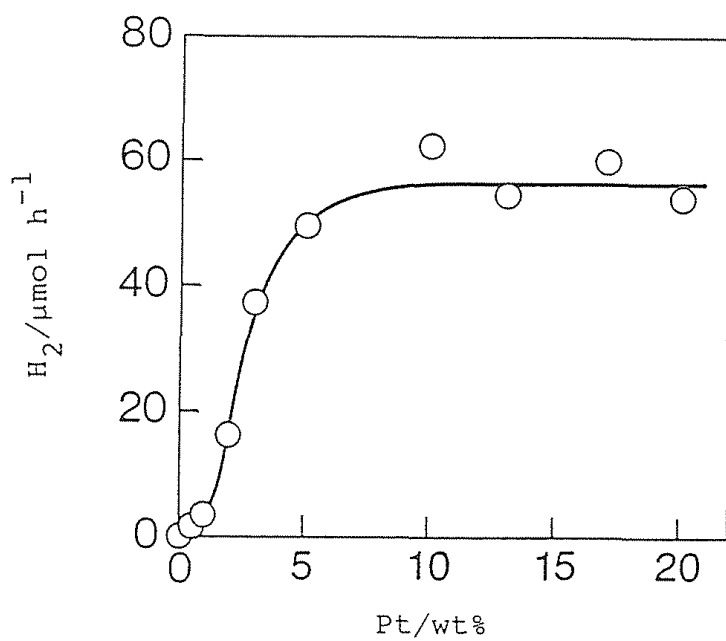


Figure 8 Dependence of the photocatalytic activity of TiO<sub>2</sub> (T<sub>c</sub> = 700 °C) on Pt loading.

$\mu\text{mol h}^{-1}$ ) was observed in the region of 10-20 wt%.

It is expected that Pt facilitates the reduction of  $\text{H}^+$  (i.e. the  $\text{H}_2$  formation) by photogenerated electron ( $\text{e}^-$ ), resulting in the decrease in the deactivation by recombination of  $\text{e}^-$  and hole ( $\text{h}^+$ ). Therefore, the contact between  $\text{TiO}_2$  and Pt, through which  $\text{e}^-$  can migrate, is important in order to maximize the photocatalytic activity. In the present system, however, platinum particles were liberated during the photoirradiation; the contact between  $\text{TiO}_2$  and Pt became poor when > 10 wt% of Pt was loaded. Another problem is the back reaction, hydrogenation of acetone, catalyzed by Pt in the dark.<sup>19</sup> In view of these results, photocatalytic reaction was carried out by the use of  $\text{TiO}_2$ -5 wt% Pt, which showed the maximum activity (Figure 8).

Crystallite size of Pt particle was also evaluated from X-ray diffraction pattern to be ca. 6 nm, which was smaller than that of  $\text{TiO}_2$ , indicating that the Pt particles were well-dispersed on the  $\text{TiO}_2$  particles.

Correlation of Photocatalytic Activity of  $\text{TiO}_2$  Powder with the Calcination Temperature. Figure 9 shows the initial rate of the photocatalytic  $\text{H}_2$  evolution from 2-PrOH solution, with  $\text{TiO}_2$ -Pt, in distilled water or aqueous  $6 \text{ mol dm}^{-3}$  NaOH solution. In distilled water,  $\text{TiO}_2$  of  $T_c$  170 °C exhibited relatively larger activity. The activity increased with the elevating  $T_c$  in the range of 400-800 °C, but decreased drastically at  $T_c$  830 °C to attain negligible. Similar behavior of the  $\text{TiO}_2$  photocatalytic activity was observed when irradiated in  $6 \text{ mol dm}^{-3}$  NaOH solution; the activity increased up to 770 °C and drastically decreased over the  $T_c$  region of 800-1000 °C.

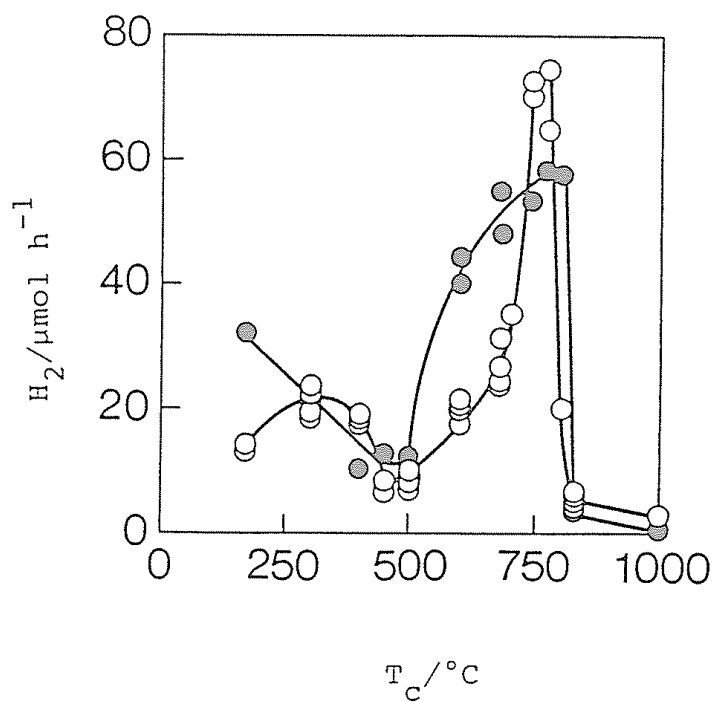


Figure 9 Photocatalytic activities of  $\text{TiO}_2/\text{Pt}(5 \text{ wt}\%)$  in distilled water (●) and  $6 \text{ mol dm}^{-3}$  NaOH (○).

Comparison between the photocatalytic activity and the crystal structure of the  $\text{TiO}_2$  powder leads to the correlation as follows: (1) The activity of  $\text{TiO}_2$  powder which possesses larger amount of amorphous phase ( $T_c < 500^\circ\text{C}$ , A region in Figure 1) is relatively large but decreases with the decreasing amount of the amorphous phase. (2) The activity of  $\text{TiO}_2$  most part of which consists of anatase crystal ( $500^\circ\text{C} \leq T_c < 800^\circ\text{C}$ , B in Figure 1) increases with the crystal growth. (3) The activity of  $\text{TiO}_2$  containing both anatase and rutile crystal ( $T_c \approx 800^\circ\text{C}$ ) is large enough so long as the anatase crystal remains in  $\text{TiO}_2$ . (4) The activity of  $\text{TiO}_2$  consists of only rutile crystal ( $T_c > 830^\circ\text{C}$ , C in Fig. 1) is negligible.

There were apparently some difference in the stability of the suspensions with the crystal structure of the  $\text{TiO}_2$  powders. The  $\text{TiO}_2$  powders calcined at  $T_c < 500^\circ\text{C}$  formed stable suspension in distilled water, while those of rutile crystal precipitated easily. On the other hand, in aqueous  $6 \text{ mol dm}^{-3}$  NaOH solution, these  $\text{TiO}_2$  powders did not form stable suspension to result in the sedimentation within several minutes under these conditions, regardless of  $T_c$ . These facts suggest that number of photons absorbed by  $\text{TiO}_2$  powder in the  $6 \text{ mol dm}^{-3}$  NaOH suspension is smaller than that in distilled water. Therefore, the activity of the  $\text{TiO}_2$  powders obtained in the  $T_c$  region of  $700\text{--}770^\circ\text{C}$  is unambiguously enhanced under the strongly alkaline conditions compared with that under neutral conditions, which is consistent with the results that well-grown anatase powders which obtained commercially shows higher activity in the alkaline suspension as reported previously.<sup>20</sup>

It is expected that the residual sulfate anion on the  $\text{TiO}_2$

powders is liberated almost entirely in the aqueous NaOH solution, and partly in the distilled water under the conditions of the photocatalytic reaction. Comparison between the amount of the residual sulfate anion (Figure 4) and the photocatalytic activity (Figure 9) could not elucidate the effect of residual sulfate at present.<sup>10</sup> Moreover, dependences of the photocatalytic activity on the surface area of TiO<sub>2</sub> (Figure 2) or the amount of surface hydroxyl group (Figure 6) were ambiguous; the activity of the anatase TiO<sub>2</sub> powders (500 < T<sub>c</sub> < 700 °C) rather decreased with the increase of the surface area or the amount of surface hydroxyl group.

On the basis of these results, it is concluded that most influential property of TiO<sub>2</sub> powder in the photocatalytic activity for the 2-PrOH dehydrogenation is the crystal structure, and the activity increases with the crystal growth of anatase.

Photocatalytic Activity of Titanium(IV) Oxide for 2-Propanol Oxidation in the Presence of Silver Salt. The photocatalytic activity of TiO<sub>2</sub> consists of only rutile was extremely smaller than that of TiO<sub>2</sub> contains anatase crystal. This fact could be accounted for by the relatively lower energy of the conduction band of rutile TiO<sub>2</sub> compared with that of anatase TiO<sub>2</sub> which is disadvantageous for the reduction of H<sup>+</sup> by photoexcited electron (e<sup>-</sup>).<sup>16</sup> In order to demonstrate this explanation experimentally, photocatalytic reaction was carried out in the presence of silver salt.

Photoirradiation of aqueous TiO<sub>2</sub> suspension containing silver salt (Ag<sub>2</sub>SO<sub>4</sub> 125 μmol) and 2-PrOH (500 μmol) led to the deposition of Ag metal on the TiO<sub>2</sub> powder and the formation of acetone. Simultaneous O<sub>2</sub> formation was observed from the rutile TiO<sub>2</sub> suspension

Table 1 Photocatalytic reaction of  $\text{TiO}_2/\text{Ag}_2\text{SO}_4$  aq./2-PrOH systems.

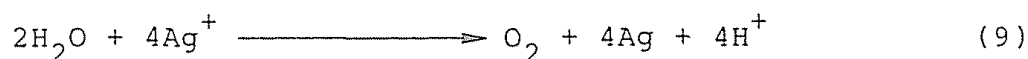
$T_c/^\circ\text{C}$	Ag/ $\mu\text{mol}$	Acetone/ $\mu\text{mol}$	$\text{O}_2/\mu\text{mol}$
500	94	44	$\approx 0$
700	87	40	$\approx 0$
800	218	90	7
1000	148	55	7

$\text{TiO}_2$  50 mg,  $\text{Ag}_2\text{SO}_4$  aq. (5.0  $\text{cm}^3$ ;  $\text{Ag}^+$ , 250  $\mu\text{mol}$ ), and 2-PrOH 500  $\mu\text{mol}$  were placed in a test tube and irradiated for 2 h with a 400-W high pressure mercury arc under Ar.

(Table 1).<sup>21</sup> Negligible amount of H<sub>2</sub> was obtained and the Pt loading gave practically no effect on the product distributions. Stoichiometries of these photoinduced reactions are expressed as follows.



and



Thus, photoirradiated suspension of TiO<sub>2</sub> reduced Ag<sup>+</sup> ion instead of H<sup>+</sup> in the silver salt solution, since the redox potential of Ag<sup>+</sup>/Ag couple is sufficiently positive (E<sup>0</sup> = + 0.799 V) enough to be reduced by the photoexcited electron (e<sup>-</sup>). The resulting Ag metal yield of rutile TiO<sub>2</sub> (T<sub>c</sub> 1000 °C) was comparable or a little smaller than those of anatase TiO<sub>2</sub>, demonstrating that the influence of the drastic decrease in the surface area at T<sub>c</sub> ≈ 830 °C is apparently negligible in these systems. The result that even rutile TiO<sub>2</sub> could oxidize 2-PrOH in the presence of silver salt confirms the idea that rutile TiO<sub>2</sub> has lower-energy conduction band disadvantageous for the H<sup>+</sup> reduction (eqn 7).



## REFERENCES AND NOTES

- 1 Chemical Society of Japan Ed., "Inorganic Photochemistry", Gak-kai Shuppan Center, Tokyo, Japan (1983), p. 118 and references therein.
- 2 A. Ozaki Ed., "Shokubai Chosei Kagaku", Kodansha, Tokyo, Japan (1980), p. 209.
- 3 R. A. Spurr, H. Meyers, Anal. Chem., 29, 761 (1957).
- 4 H. Klug, L. E. Alexander, "X-ray Diffraction Procedures", 2nd Ed. John Wiley and Sons, Inc., New York (1974), p. 618.
- 5 T. Kawai and T. Sakata, Nature, 286, 474 (1980).
- 6 Absorption at ca.  $1600\text{ cm}^{-1}$  could be assigned to be physically adsorbed water on the  $\text{TiO}_2$  surface.
- 7 A. Kurosaki and S. Okazaki, Nippon Kagaku Kaishi, 1816 (1976).
- 8 995, 1050-1060, 1105, 1170  $\text{cm}^{-1}$ : K. Nakamoto, J. Fujita, S. Tanaka, M. Kobayashi, J. Am. Chem. Soc., 79, 4904 (1957).
- 9 K. Funaki and Y. Saeki, Kogyo Kagaku Zasshi, 59, 1291 (1956).
- 10 The transformation of anatase into rutile crystal was observed at ca.  $600\text{ }^\circ\text{C}$  when titanium(IV) tetra-2-propoxide was used as a starting material: (see Chapter 10) S. Nishimoto, B. Ohtani, H. Kajiwara, T. Kagiya, 2nd Meeting on Catalytic Chemistry of Solar Energy Conversion, p. 22 (1983); J. Chem. Soc., Faraday Trans. 1, 80, (1984), in press.
- 11 M. A. Butler, D. S. Ginley, J. Electrochem. Soc., 125, 228 (1978).
- 12 H. P. Boehm, Angew. Chem., 78, 617 (1966).
- 13 H. P. Boehm, Disc. Faraday Soc., 52, 264 (1971).

- 14 It is expected that the influence of liberated sulfate anion on the measurement of  $\text{Na}^+$  adsorption is negligible because the amount of  $\text{Na}^+$  adsorption was evaluated from the decrease of  $\text{Na}^+$  in the solution.
- 15  $-\text{Ti}-\text{OH} + \text{NaOH} \longrightarrow -\text{Ti}-\text{O}^-\text{Na}^+ + \text{H}_2\text{O}$
- 16 B. Kraeutler, A. J. Bard, J. Am. Chem. Soc., 100, 5985 (1978).
- 17 S. Teratani, J. Nakamichi, K. Taya, K. Tanaka, Bull. Chem. Soc. Jpn., 55, 1688 (1982).
- 18 A. D. Buss, M. A. Malati, R. Atkinson, J. Oil. Col. Chem. Assoc., 59, 369 (1976).
- 19 S. Teratani, H. Ikuo, I. Anazawa, K. Tanaka, 2nd Meeting on Catalytic Chemistry of Solar Energy Conversion, p. 1 (1983).
- 20 T. Kawai, T. Sakata, Chem. Lett., 81 (1981).
- 21 Photoirradiation of aqueous  $\text{TiO}_2$  suspension in silver salt solution without 2-PrOH led to the  $\text{O}_2$  formation as a result of oxidative decomposition of water and the deposition of silver metal on the  $\text{TiO}_2$  surface (eqn 9): (see Chapter 6) S. Nishimoto, B. Ohtani, H. Kajiwara, T. Kagiya, J. Chem. Soc., Faraday Trans. 1, 79, 2685 (1983).
- 22 The author thanks Professor Dr. Satohiro Yoshida (Kyoto University) for his valuable advice on X-ray diffraction and BET surface area measurements. The author also thanks Dr. Eiichiro Nakayama of the Instrumental Analyses Research Center of Kyoto University for his kind advice on atomic absorption measurement.

## Chapter 10

### Correlation between Crystal Form of $\text{TiO}_2$ Prepared from Titanium Tetra-2-propoxide and Photocatalytic Activity for Redox Reaction in Aqueous 2-Propanol and Silver Salt Solutions

#### ABSTRACT

Titanium dioxide ( $\text{TiO}_2$ ) was prepared by the hydrolysis of titanium tetra-2-propoxide, followed by calcination at various temperatures ( $T_c$ ) up to 1000 °C. The content and crystallite size of anatase crystal in the  $\text{TiO}_2$  powders increased upon elevating  $T_c$  up to 550 °C, without formation of rutile crystal. In the  $T_c$  range of 550-600 °C, a mixture of anatase and rutile crystals was obtained. Further rises of  $T_c$  resulted in the  $\text{TiO}_2$  consisting of only rutile crystal. Photocatalytic activities of these  $\text{TiO}_2$  powders for redox reactions were estimated for the following three systems: (1) aqueous 2-propanol solution, (2) aqueous  $\text{Ag}_2\text{SO}_4$  solution, and (3) aqueous  $\text{Ag}_2\text{SO}_4$  solution containing 2-propanol. The anatase  $\text{TiO}_2$  showed photocatalytic activity in all these systems; the activity increased with the crystal growth. In aqueous 2-propanol solution the activity is dramatically enhanced by partial coverage of the  $\text{TiO}_2$  with platinum black. The photocatalytic activity of the rutile  $\text{TiO}_2$  powder was comparable to or even greater than the anatase analog, so long as the reaction system included the silver salt, but was negligibly small for aqueous 2-propanol solution regardless of the Pt coverage.

## INTRODUCTION

TiO<sub>2</sub>-photocatalyzed reactions such as dehydrogenation of alcohols<sup>1-4</sup> or photo-Kolbe reaction of carboxylic acids<sup>5-9</sup> have been widely investigated. Although various kind of commercially available TiO<sub>2</sub> powders have been hitherto used as a photostable catalyst with sufficient oxidizing and reducing abilities,<sup>10-13</sup> the correlation of the physical properties, e.g., bulk crystal and surface structures of TiO<sub>2</sub> powder with the photocatalytic activity has not yet been well established. In Chapter 9 of this thesis, the photocatalytic activity of TiO<sub>2</sub> powders prepared from Ti(SO<sub>4</sub>)<sub>2</sub> by hydrolysis and calcination at various temperatures was described.<sup>14</sup> The activity of such types of TiO<sub>2</sub> powders, when mixed with platinum black, for dehydrogenation of 2-propanol in aqueous solution turned out to depend mainly on the crystal structures, i.e., the activity of anatase TiO<sub>2</sub> was sufficient whereas that of rutile one was negligible. In this case, a small amount of residual sulfate ions caused considerable lowering of photocatalytic activity of the TiO<sub>2</sub> powders due to the decrease of the pH of the aqueous suspension.<sup>14</sup> In order to characterize the intrinsic photocatalytic activities it is therefore desirable that TiO<sub>2</sub> powder free from such a contamination is prepared by alternative method and is subjected to further investigation.

The present study concerns the preparation of anion-free TiO<sub>2</sub> powders from titanium tetra-2-propoxide (Ti(OPr)<sub>4</sub>) and characterization of their crystal structures by means of X-ray diffraction analysis. In this chapter the photocatalytic activity of aqueous suspensions of these TiO<sub>2</sub> powders is discussed on the basis of the

results for three photoredox reaction systems: (1) dehydrogenation of 2-propanol in aqueous solution,<sup>2-4,14</sup> (2) Ag metal deposition and O<sub>2</sub> formation in aqueous Ag<sub>2</sub>SO<sub>4</sub> solution,<sup>15</sup> and (3) acetone and O<sub>2</sub> formations together with Ag metal deposition in aqueous solution of 2-propanol and Ag<sub>2</sub>SO<sub>4</sub>. The main purpose of this chapter is to clarify the effect of crystal structure of the TiO<sub>2</sub> powder on the photocatalytic activity for redox reactions.

## EXPERIMENTAL

Preparation of TiO<sub>2</sub> Powder. Titanium tetra-2-propoxide (Ti(OPr)<sub>4</sub>) was supplied by Wako Pure Chemicals and distilled before use (b.p. 92.0-94.0 °C, 0.47 kPa). To an ice-cooled mixture of 2-propanol (450 cm<sup>3</sup>) and distilled water (150 cm<sup>3</sup>) a mixture of Ti(OPr)<sub>4</sub> (100 cm<sup>3</sup>, 0.34 mol) and 2-propanol (180 cm<sup>3</sup>) was added dropwise with vigorous stirring. The resulting white precipitate of titanate was filtered off, washed repeatedly with distilled water, and precalcined for 24 h at 120 °C in air. The TiO<sub>2</sub> powder thus obtained was subjected to further calcination in air at various temperatures with an electric furnace equipped with programmed controller (Ohkura EC 53/2 PB). The heating was first performed for 4 h at a constant rate of elevating temperature until a specified temperature (T<sub>c</sub>) was attained, continued for 5 h at the T<sub>c</sub>, and then for 4 h at a constant rate of falling temperature.

X-Ray Diffraction Analysis. Crystal structure of the TiO<sub>2</sub> powder was analyzed by X-ray diffraction method, using a Rigaku Geigerflex 2013 diffractometer (Cu target, Ni filter, 35 kV, 20 mA, scanning speed of 1 ° min<sup>-1</sup>). Contents of anatase and rutile crystals in

the  $\text{TiO}_2$  were evaluated by integration of the most intensive peaks  $2\theta = 25.4^\circ$  ( $d = 0.352$  nm, the (011) plane of anatase) and  $27.3^\circ$  ( $d = 0.325$  nm, the (110) plane of rutile), respectively, by reference to  $\text{CaCO}_3$  as an internal standard.<sup>16</sup> The calibration curves for the anatase and rutile crystals were obtained with the use of commercially available anatase  $\text{TiO}_2$  (Merck) and rutile  $\text{TiO}_2$  (prepared by heating of the Merck  $\text{TiO}_2$  powder at  $1200^\circ\text{C}$  for 10 h in air<sup>15</sup>), respectively. The mean crystallite size ( $L$ ) was determined from broadening ( $\beta$ ) of the most intensive line in the X-ray diffraction pattern, after corrections for  $K_\alpha$  doublet and instrumental broadenings based on the Scherrer equation<sup>17</sup> ( $L = k\lambda / \beta \cos\theta$ , where  $\lambda$  is the radiation wavelength,  $\theta$  is the Bragg angle, and  $k = 0.90$ ).

Photoreaction. A finely ground  $\text{TiO}_2$  powder (50 mg), with or without platinum black (typically 5 wt%, Nakarai Chemicals), was suspended in distilled water ( $5.0\text{ cm}^3$ ) or aqueous  $\text{Ag}_2\text{SO}_4$  solution ( $0.025\text{ mol dm}^{-3}$ ;  $5.0\text{ cm}^3$ ) in a glass tube ( $18\text{ mm}\phi \times 180\text{ mm}$ , transparent for the wavelengths  $> 300\text{ nm}$  of exciting light). The suspension was purged by Ar for at least 30 min and sealed off by a rubber cap. 2-Propanol ( $38\text{ mm}^3$ ,  $0.50\text{ mmol}$ ) was injected through the cap by a syringe. The Ar-purged  $\text{TiO}_2$  suspension was irradiated under magnetic stirring at room temperature with a merry-go-round apparatus equipped with 400-W high-pressure mercury arc (Eiko-sha 400).

Product Analysis. Volatile products such as  $\text{H}_2$  and  $\text{O}_2$  liberated in the gas phase of the sealed sample were analyzed with a Shimadzu GC 4A gas chromatograph equipped with a TCD and a Molecular Sieve 5A column ( $3\text{ mm}\phi \times 3\text{ m}$ ) with Ar carrier at  $100^\circ\text{C}$ . 2-Propanol and acetone were analyzed with a Shimadzu GC 6A gas chromatograph equipped

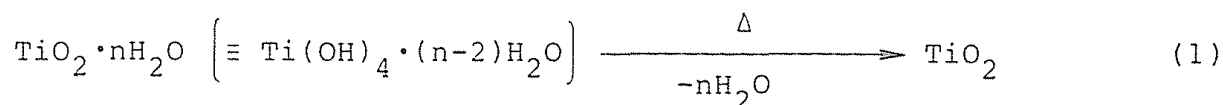
with an FID and a Polyethylene Glycol 20M on Celite 545 column (3 mm $\phi$   $\times$  2m) with N<sub>2</sub> carrier at 90 °C.

The procedure and apparatus for the determination of the amount of Ag deposition were described in Chapter 6 of this thesis.<sup>15</sup>

## RESULTS AND DISCUSSION

### Physical Properties of the TiO<sub>2</sub> Powders Prepared from Ti(OPr)<sub>4</sub>.

Figure 1(a) shows the weight decrease of TiO<sub>2</sub> powders by calcination at a given T<sub>c</sub>, relative to pre-calcination at 120 °C, i.e.,  $W = 100 \times w(T_c) / w(120 \text{ }^\circ\text{C})$  (%). The relative weight decreased with elevating T<sub>c</sub> to attain a constant value of ca. 50 %. This behaviour is in accord with the following dehydration of titanate acid by calcination.



Assuming that the TiO<sub>2</sub> powder calcined at 1000 °C contains no water molecules, one can estimate the mean number of water molecules per one TiO<sub>2</sub> unit (n in eqn 1). As is shown in Figure 1(a), the TiO<sub>2</sub> unit at T<sub>c</sub> 120 °C contained ca. 4 water molecules. The mean number n decreased as T<sub>c</sub> was elevated, becoming less than 0.3 over the T<sub>c</sub> range of above 400 °C.

Figure 1(b) shows the variations in the content of anatase (C<sub>A</sub>) and rutile (C<sub>R</sub>) crystals as a function of T<sub>c</sub>. The TiO<sub>2</sub> powders prepared at T<sub>c</sub>  $\leq$  550 °C contained only anatase crystal, the content of which increased to some extent upon elevating T<sub>c</sub>. A mixture of anatase and rutile crystals was obtained in the T<sub>c</sub> range of 600-650

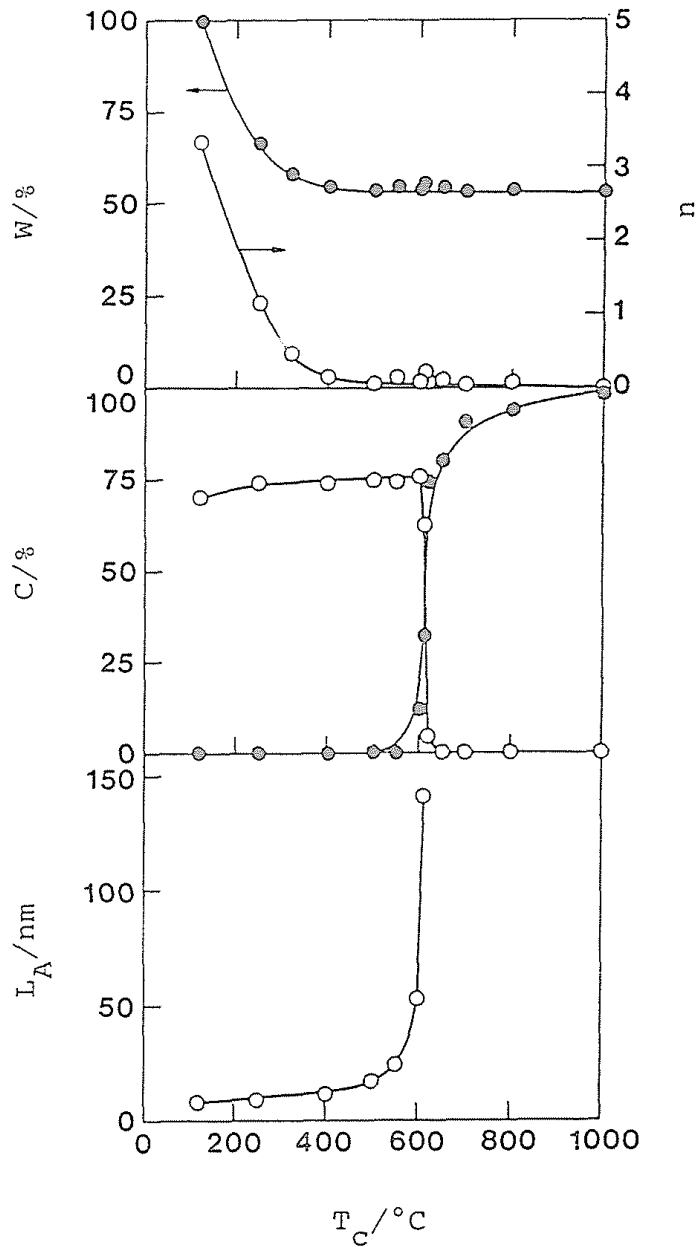


Figure 1 Variation in the physical properties of  $TiO_2$  powders as a function of calcination temperature ( $T_c$ ): (a) relative weight (W, ●) and number of water molecules per one  $TiO_2$  unit (n, ○), (b) contents of anatase ( $C_A$ , ○) and rutile ( $C_R$ , ●) crystals, and (c) mean crystallite size of anatase ( $L_A$ ).



°C, indicating partial transformation of the anatase into rutile. The TiO<sub>2</sub> powders containing only rutile crystal were obtained at T<sub>c</sub> ≥ 650 °C.

The mean crystallite size of the anatase (L<sub>A</sub>) is plotted against T<sub>c</sub> in Figure 1(c). The value of L<sub>A</sub> did not appreciably change at T<sub>c</sub> ≤ 550 °C, but rapidly increased in the narrow T<sub>c</sub> range of 550-610 °C. The mean crystallite size of the rutile crystal obtained at T<sub>c</sub> ≥ 600 °C was estimated to be more than 200 nm, although its exact value was failed to be determined by the Scherrer equation.

The transformation of anatase into rutile by the heat treatment was also observed when TiO<sub>2</sub> was prepared from Ti(SO<sub>4</sub>)<sub>2</sub>,<sup>14</sup> although the corresponding transition temperature (750-800 °C) was considerably higher than that (ca. 550-650 °C) for the present anion-free TiO<sub>2</sub>. This difference is partly attributable to the duration of the heat treatment, i.e., TiO<sub>2</sub> from Ti(OPr)<sub>4</sub> was treated for 5 h at a given T<sub>c</sub>, while TiO<sub>2</sub> from Ti(SO<sub>4</sub>)<sub>2</sub> was for 3 h. However, it is more likely that the residual sulfate anion in the TiO<sub>2</sub> from Ti(SO<sub>4</sub>)<sub>2</sub> depresses the transformation,<sup>18,19</sup> thereby permitting further growth of the anatase crystal in such higher T<sub>c</sub> range.

Photocatalytic Activities of TiO<sub>2</sub> and TiO<sub>2</sub>/Pt in Aqueous 2-Propanol solution.

The TiO<sub>2</sub> powders prepared as above, when suspended in aqueous 2-propanol solution and irradiated at λ<sub>ex</sub> > 300 nm under Ar, produced H<sub>2</sub> and acetone. Figure 2(a) shows that both yields of the H<sub>2</sub> (Y<sub>H<sub>2</sub></sub>) and acetone (Y<sub>(CH<sub>3</sub>)<sub>2</sub>CO</sub>) over the irradiation period of 10 h are strongly dependent on the calcination temperature T<sub>c</sub> of the TiO<sub>2</sub> powders. It is seen in Figure 2(a) that Y<sub>H<sub>2</sub></sub> and Y<sub>(CH<sub>3</sub>)<sub>2</sub>CO</sub> increase with increasing T<sub>c</sub> until the maximum values (Y<sub>H<sub>2</sub></sub> ≈ 7 μmol and

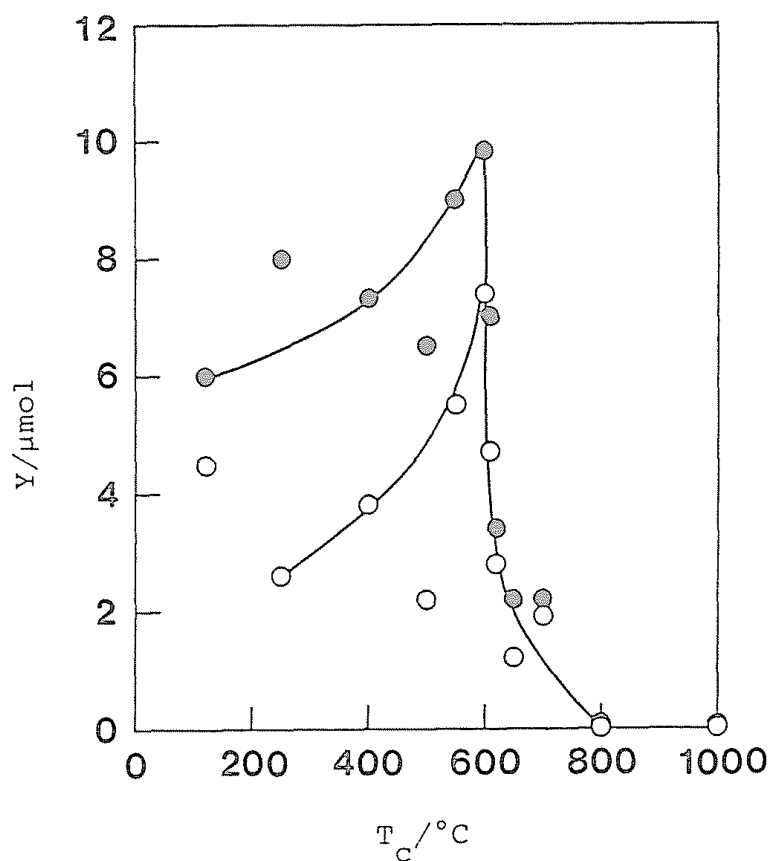


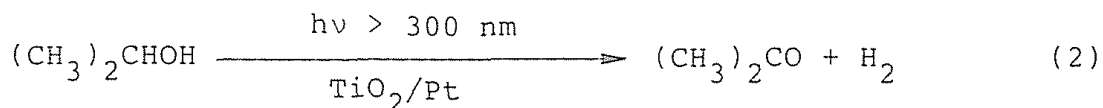
Figure 2(a) Yields of acetone ( $Y_{(\text{CH}_3)_2\text{CO}}$ ,  $\bullet$ ) and  $\text{H}_2$  ( $Y_{\text{H}_2}$ ,  $\circ$ ) by the irradiation (10 h) of  $\text{TiO}_2$  (50 mg) suspended in aqueous 2-propanol ( $38 \text{ mm}^3$ ,  $500 \mu\text{mol}$ ) solution ( $5.0 \text{ cm}^3$ ) under Ar.

$Y_{(\text{CH}_3)_2\text{CO}} \approx 10 \text{ } \mu\text{mol}$ ) are attained at  $T_c$  600 °C. By the treatment at higher  $T_c > 610 \text{ } ^\circ\text{C}$ ,  $Y_{\text{H}_2}$  and  $Y_{(\text{CH}_3)_2\text{CO}}$  decreased to greater extent relative to the maximum values. The  $\text{TiO}_2$  at  $T_c$  1000 °C which consists of only rutile crystal was virtually ineffective for the formation of  $\text{H}_2$  and acetone.

The yield ratio of  $\text{H}_2$  to acetone ( $Y_{\text{H}_2}/Y_{(\text{CH}_3)_2\text{CO}}$ ) was ca. 0.6 regardless of  $T_c$  as shown in Figure 2(b). This fact indicates that reduction other than the liberation  $\text{H}_2$  which should be equimolar to acetone, the reduction of  $\text{TiO}_2$  to form Ti(III) as described below.

Figure 3 shows that partial coverage of the  $\text{TiO}_2$  ( $T_c$  610 °C) with small amount of Pt up to 5 wt% enhances the rate of  $\text{H}_2$  formation ( $R_{\text{H}_2}$ ), as has been well documented.<sup>1-3</sup> A saturation limit of the  $R_{\text{H}_2}$  was observed in the range of Pt coverage of 2.5 to 5.0 wt %, which was 100-fold greater than that without Pt. Figure 4 illustrates the  $T_c$  dependences of  $Y_{\text{H}_2}$  and  $Y_{(\text{CH}_3)_2\text{CO}}$  which were observed upon 1-h photoirradiation of the  $\text{TiO}_2$  powders covered with 5 wt% of Pt ( $\text{TiO}_2/\text{Pt}$ ). The profiles of these  $T_c$  dependences are seen to be essentially identical with those in Figure 2(a), suggesting that the photocatalytic activity of a given  $\text{TiO}_2$  particle is intrinsically determined by the solid properties of the particle and it can be amplified by the surface Pt.

As is plotted in Figure 5, with the use of  $\text{TiO}_2/\text{Pt}$  the yield of  $\text{H}_2$  is practically equal to that of acetone regardless of  $T_c$ . The net photoreaction in this system is therefore represented as follows.



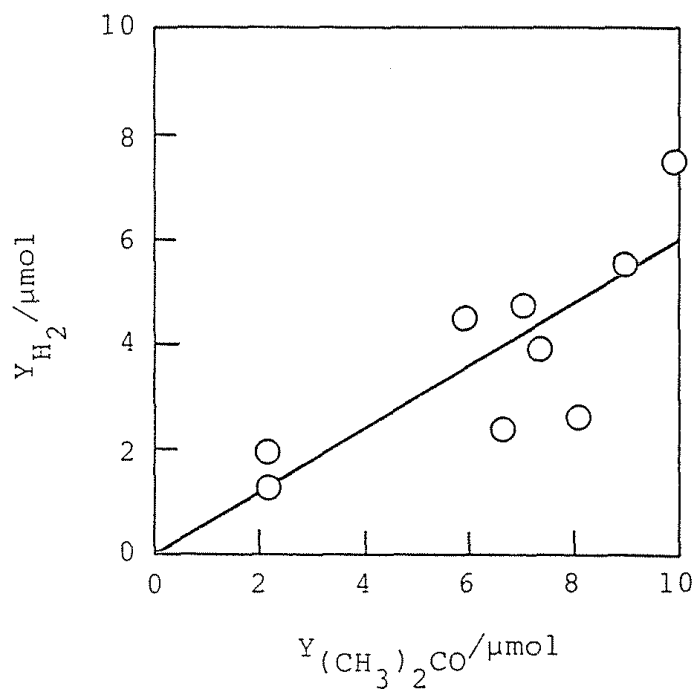


Figure 2(b) Relation between the yields of acetone ( $Y_{(\text{CH}_3)_2\text{CO}}$ ) and  $\text{H}_2$  ( $Y_{\text{H}_2}$ ). The data are derived from Figure 2(a).

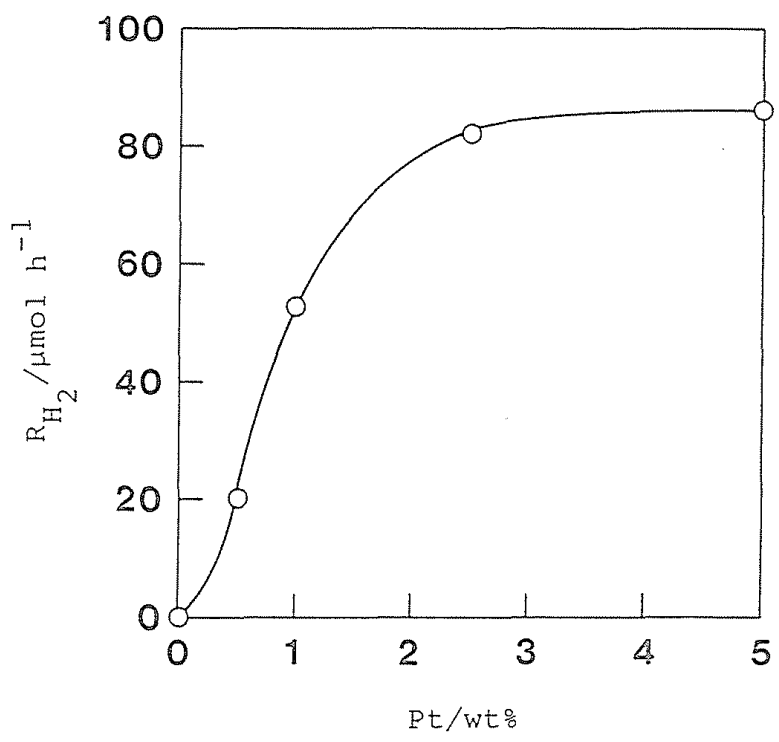
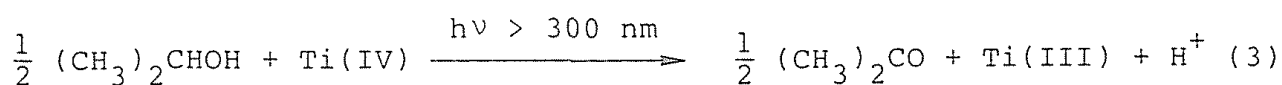


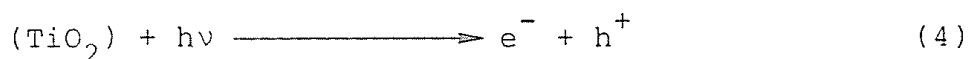
Figure 3 Rate of photocatalytic H<sub>2</sub> formation ( $R_{H_2}$ ) by TiO<sub>2</sub> ( $T_c$  610 °C) as a function of Pt amount.

In the case of  $\text{TiO}_2$  without Pt,  $Y_{\text{H}_2}$  was smaller (about 60 %) than the  $Y_{(\text{CH}_3)_2\text{CO}}$ , as shown in Figure 2(b). The lesser yield of  $\text{H}_2$  in this case is accounted for by the reduction of Ti(IV) on the illuminated  $\text{TiO}_2$  to form Ti(III)<sup>20</sup> as a non-catalytic side reaction, because the white suspension of  $\text{TiO}_2$  was observed to turn grey during the photoirradiation. The mechanism of this 2-propanol oxidation is discussed later.



Thus, in the absence of Pt two types of the photoreactions as in eqns (2) and (3) proceed competitively. Figure 2(b) provides an estimate that maximally 60 % of the photogenerated reducing species, i.e., electron photoexcited to the conduction band of  $\text{TiO}_2$ , would be consumed for the self-reduction of the  $\text{TiO}_2$  with formation of Ti(III).

In contrast, the presence of Pt on the  $\text{TiO}_2$  surface could prevent such an electron trapping by Ti(IV) to yield Ti(III). Moreover, the Pt is responsible for the efficient charge separation of the photogenerated electron-hole pair in the  $\text{TiO}_2$ ,<sup>10</sup> i.e., Pt catalyzes the reduction of proton by the photoexcited "conduction band" electron, thereby promoting the overall reaction of 2-propanol dehydrogenation.



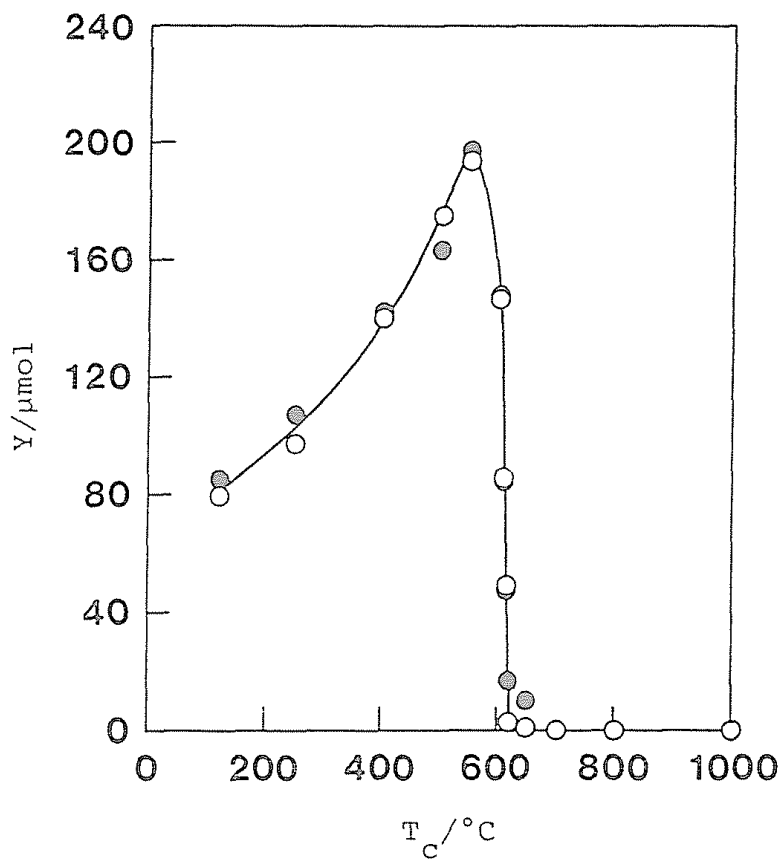


Figure 4 Photocatalytic formation of  $H_2$  ( $Y_{H_2}$ ,  $\bigcirc$ ) and acetone ( $Y_{(CH_3)_2CO}$ ,  $\bullet$ ) by 5 wt%-Pt loaded  $TiO_2$  (50 mg) suspended in aqueous 2-propanol ( $38\text{ mm}^3$ ,  $500\text{ }\mu\text{mol}$ ) solution ( $5.0\text{ cm}^3$ ).

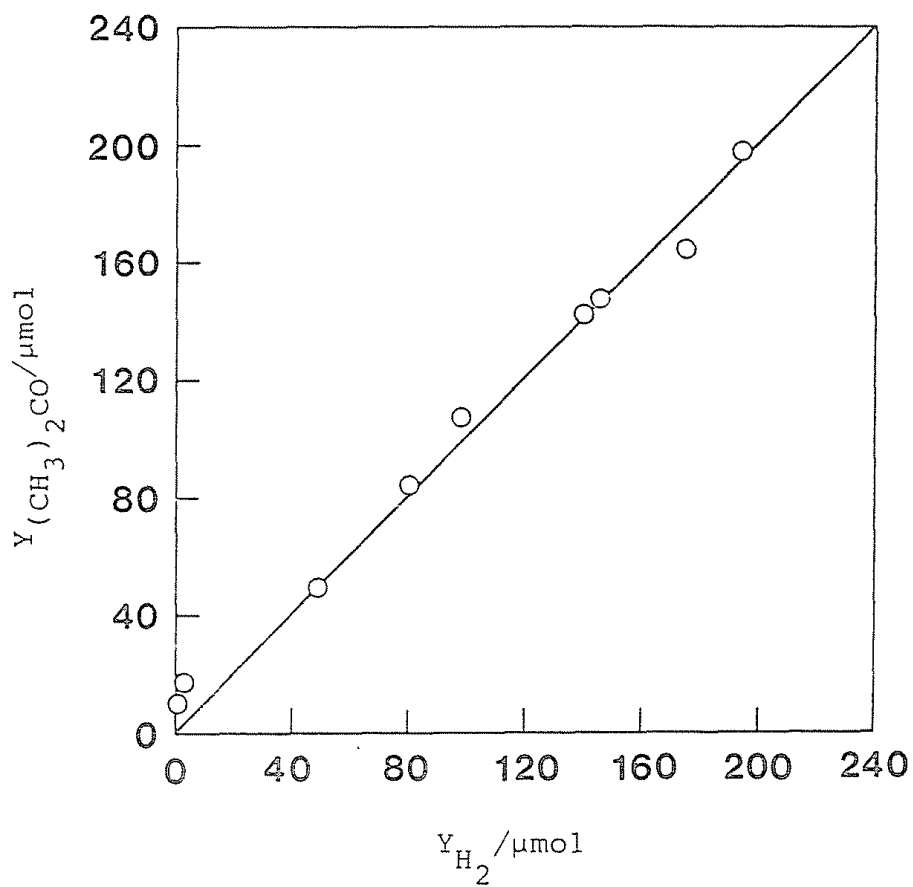
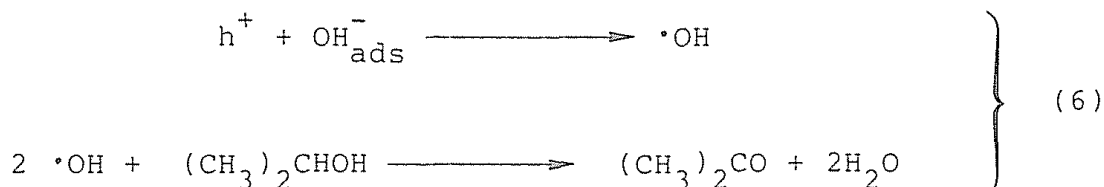


Figure 5 Linear relation between the yields of acetone ( $Y_{(CH_3)_2CO}$ ) and  $H_2$  ( $Y_{H_2}$ ). The data are derived from Figure 4.



Most probable reaction pathway of the 2-propanol oxidation is hydrogen abstraction by  $\cdot\text{OH}$  produced by the oxidation of surface hydroxyl with the photogenerated positive hole ( $h^+$ ), as shown in Chapter 1.



This scheme (reactions (4)-(6)) is in accord with the stoichiometry as in eqn (2).

By reference to the structural evidence in Figure 1, it is clear from Figures 2 and 4 that the  $\text{TiO}_2$  powders containing anatase crystal ( $T_c$  120-620 °C) show sufficient photocatalytic activities to produce  $\text{H}_2$  and acetone, while those containing only rutile crystal ( $T_c \geq 650$  °C) show negligible activities even when covered with Pt. The activity of the anatase-containing  $\text{TiO}_2$  powders increases with increasing the content of anatase crystal  $C_A$ . Concerning the  $\text{TiO}_2$  powders ( $T_c$  600-650 °C) which contain both anatase and rutile crystals, the activity decreases with decreasing  $C_A$  and therefore increasing  $C_R$ . The negligible activity of rutile  $\text{TiO}_2$  in aqueous 2-propanol solution is attributable to the disadvantageous energetics for the reduction of protons to  $\text{H}_2$  compared with anatase  $\text{TiO}_2$ : because a rutile electrode exhibits more positive flat-band potential than an anatase electrode, the energy of photoexcited electrons in the conduction band of rutile  $\text{TiO}_2$  is expected to be lower than that of anatase  $\text{TiO}_2$ .<sup>5,21</sup>

This dependence, on the crystal structure, of the photocatalytic

activity of  $\text{TiO}_2$  powder for the 2-propanol dehydrogenation is essentially identical to the recently reported results with the  $\text{TiO}_2$  derived from  $\text{Ti}(\text{SO}_4)_2$ .<sup>14</sup> The  $\text{TiO}_2$  from  $\text{Ti}(\text{OPr})_4$  ( $T_c$  600 °C,  $L_A$  53 nm) is, however, approximately 3 times as active as the one from  $\text{Ti}(\text{SO}_4)_2$  ( $T_c$  700 °C,  $L_A$  37 nm) having similar crystallite size of anatase, as indicated by the initial rate of hydrogen formation under the conditions of partial Pt coverage (ca. 150 and 50  $\mu\text{mol h}^{-1}$ , respectively). The residual sulfate on the  $\text{TiO}_2$  derived from  $\text{Ti}(\text{SO}_4)_2$  emerged into water phase and decreased the pH of the suspension.<sup>14</sup> On the other hand, the pH of the suspension of  $\text{TiO}_2$  prepared from  $\text{Ti}(\text{OPr})_4$  was almost the same level (ca. 6) as that of distilled water regardless of its calcination temperature. In view of the fact that the  $\text{TiO}_2$  activity depends on the pH of the suspension and shows its maximum under neutral conditions,<sup>22</sup> the seemingly smaller activity of  $\text{TiO}_2$  from  $\text{Ti}(\text{SO}_4)_2$  is at least attributable to the pH-lowering effect of the residual sulfate ion.

#### Photocatalytic Activity of $\text{TiO}_2$ in Aqueous Silver Salt Solution.

Photoirradiation ( $\lambda_{\text{ex}} > 300$  nm) of aqueous suspensions of these  $\text{TiO}_2$  powders containing  $\text{Ag}_2\text{SO}_4$  led to the formation of  $\text{O}_2$  and the Ag metal deposition on the  $\text{TiO}_2$  particles.<sup>14,15</sup> Mechanism of the  $\text{O}_2$  formation including  $\cdot\text{OH}$  formation by the photogenerated  $h^+$  is discussed in Chapter 11 of this thesis. The  $T_c$  dependences of the yields of  $\text{O}_2$  ( $Y_{\text{O}_2}$ ) and Ag deposit ( $Y_{\text{Ag}}$ ) over the irradiation period of 1 h are shown in Figure 6. The linear relationship with a slope of 0.23 between the  $Y_{\text{O}_2}$  and  $Y_{\text{Ag}}$  (Figure 7) is in accord with the following net photoreaction.

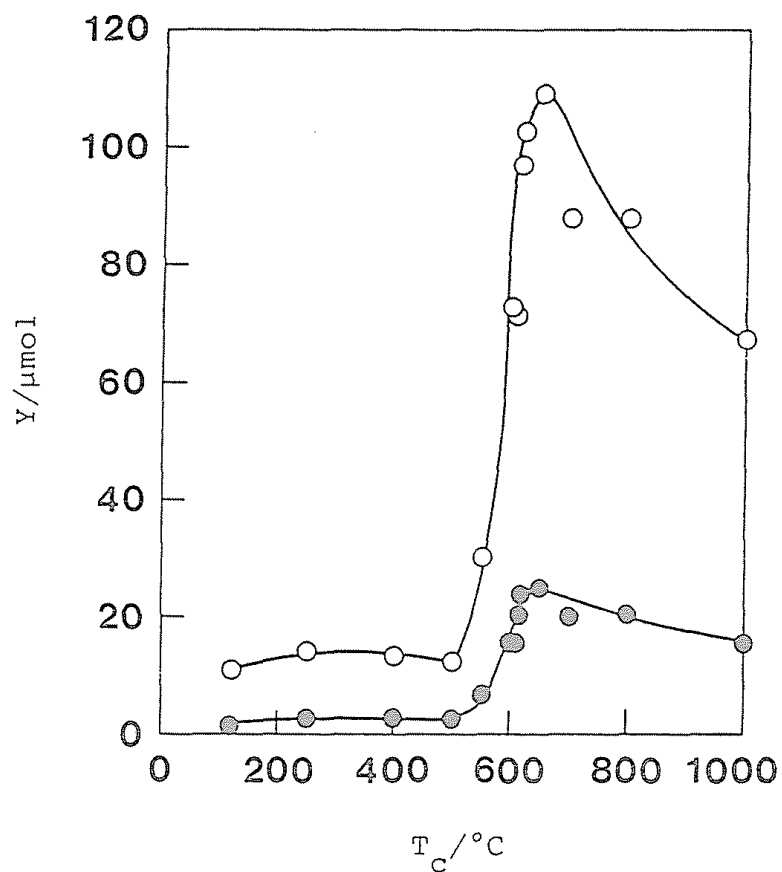


Figure 6 Photocatalytic formation of Ag metal ( $Y_{Ag}$ ,  $\bigcirc$ ) and  $O_2$  ( $Y_{O_2}$ ,  $\bullet$ ) in the aqueous  $TiO_2$  suspension in  $Ag_2SO_4$  solution (250  $\mu\text{mol}$  of  $Ag^+$ ; 5.0  $\text{cm}^3$ ) over the 1-h photoirradiation as a function of calcination temperature ( $T_c$ ) of  $TiO_2$ .

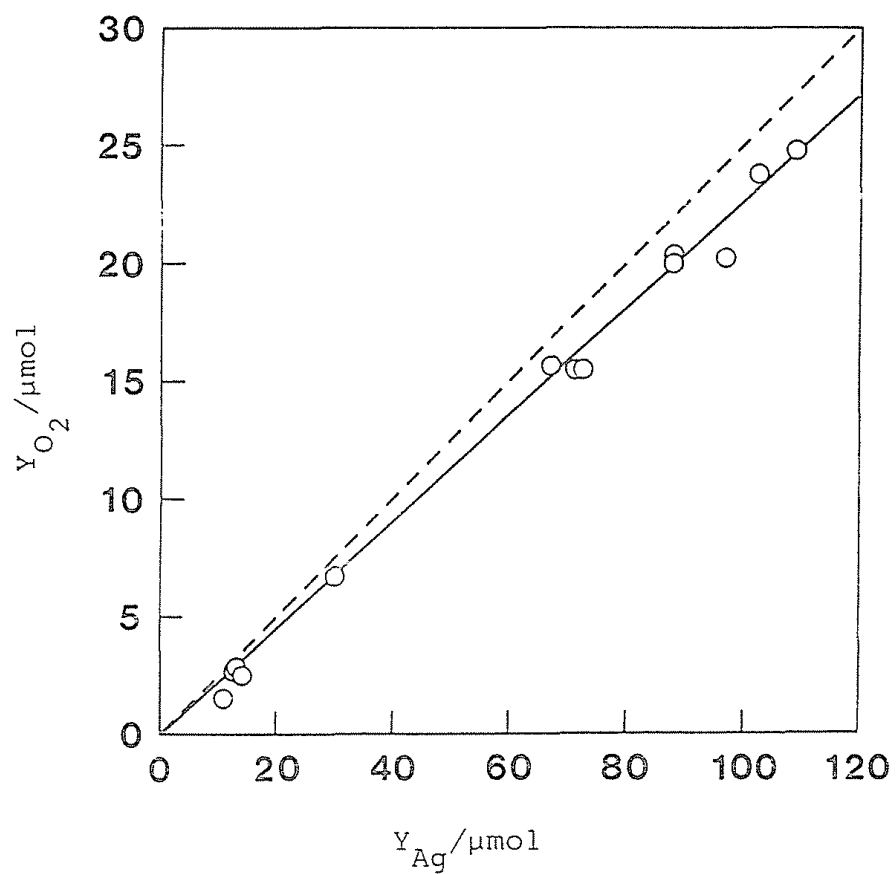
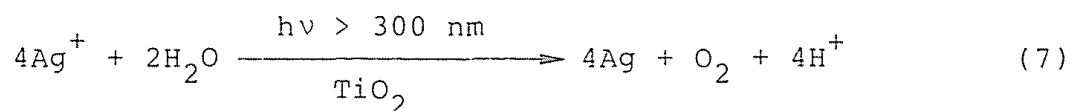


Figure 7 Linear relation between the yields of Ag metal and O<sub>2</sub> observed in the photoreaction of TiO<sub>2</sub>-suspended aqueous Ag<sub>2</sub>SO<sub>4</sub> solution. The data are derived from Figure 6.



Such release of proton in this scheme was supported by the observation of the rapid pH decrease (from ca. 4 to 2) of the suspension during the photoirradiation. A little larger amount of Ag deposit (Figure 7) compared with the stoichiometry in reaction (7) would be attributable to the partial photoadsorption of another product  $\text{O}_2$  on the  $\text{TiO}_2$  surface.<sup>22-26</sup>

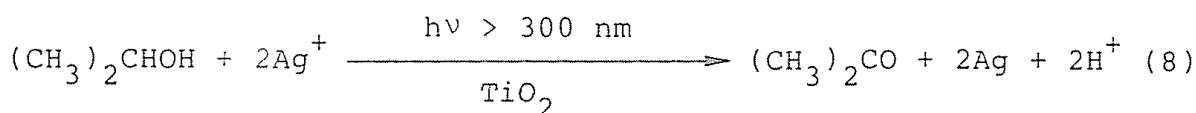
Figure 6 shows that both the  $Y_{\text{Ag}}$  and  $Y_{\text{O}_2}$  are relatively small and even independent of  $T_c$  when  $\text{TiO}_2$  powders prepared in the lower  $T_c$  region (120-550 °C) are used. Upon elevating  $T_c$  from 550 to 600 °C the photocatalytic reaction became more rapid to eventually give maximum values of  $Y_{\text{Ag}} \approx 110 \mu\text{mol}$  and  $Y_{\text{O}_2} \approx 25 \mu\text{mol}$ . The  $Y_{\text{Ag}}$  and  $Y_{\text{O}_2}$  then decreased and reached constant values of 80 and 20  $\mu\text{mol}$ , respectively, in the  $T_c$  range of 800 to 1000 °C. These constant values are likely characteristic of a rutile  $\text{TiO}_2$  (see also Figure 1). It is worth noting that the  $\text{TiO}_2$  powders containing only rutile crystal, which were practically inactive in aqueous 2-propanol solution even with the Pt coverage, showed larger activity than the anatase  $\text{TiO}_2$  ( $T_c < 600$  °C) in the presence  $\text{Ag}^+$ . In particular, the anatase rutile mixed  $\text{TiO}_2$  ( $600$  °C  $\leq T_c \leq 620$  °C) showed the highest activity for the formation of Ag and  $\text{O}_2$  in contrast to the 2-propanol dehydrogenation (Figures 2 and 4). These facts clearly demonstrate that photocatalytic activity of rutile crystal is essentially comparable to that of anatase crystal in certain photoreaction systems, as in the case where more reducible  $\text{Ag}^+$  ion but not proton

can react with the photogenerated electrons of rutile  $\text{TiO}_2$ .<sup>15</sup>

Photocatalytic Activity of  $\text{TiO}_2$  in Aqueous Solution of Silver Salt

and 2-Propanol. Addition of 2-propanol to the above mentioned aqueous suspension of  $\text{TiO}_2$  containing  $\text{Ag}_2\text{SO}_4$  resulted in the oxidation of 2-propanol into acetone together with the  $\text{O}_2$  formation and Ag metal deposition. Figure 8 shows the variations of the product yields  $Y_{\text{Ag}}$ ,  $Y_{\text{O}_2}$ , and  $Y_{(\text{CH}_3)_2\text{CO}}$  over the 1-h photoirradiation as a function of  $T_c$ . The  $\text{O}_2$  formation by the  $\text{TiO}_2$  powders at  $T_c \leq 550$  °C was negligible, while small amount of  $\text{O}_2$  (ca. 5  $\mu\text{mol}$ ) was obtained in the  $T_c$  region of  $\geq 600$  °C. The  $Y_{\text{Ag}}$  and  $Y_{(\text{CH}_3)_2\text{CO}}$  increased with elevating  $T_c$  to attain their maxima of ca. 125 and 50  $\mu\text{mol}$  at  $T_c$  650 °C, and then decreased toward constant values by the further elevation of  $T_c$  ( $> 650$  °C).

Figure 9 shows a plot of the total yield of oxidation products ( $2 Y_{(\text{CH}_3)_2\text{CO}} + 4 Y_{\text{O}_2}$ ) against that of reduction product ( $Y_{\text{Ag}}$ ). It is clear from the linear relationship that the oxidation of both water (eqn 7) and 2-propanol (eqn 8) is involved in the present system, although the proportion of the water oxidation is much smaller than that of acetone. Mechanism of the 2-propanol oxidation is shown in Chapter 1.



It is seen from Figure 8 that the  $\text{TiO}_2$  powders at  $T_c \geq 550$  °C, which consist of anatase crystal but not rutile one, give rise to 2-propanol oxidation almost exclusively according to reaction (8).

In the  $T_c$  range of  $> 600$  °C the profile of the  $T_c$  dependent

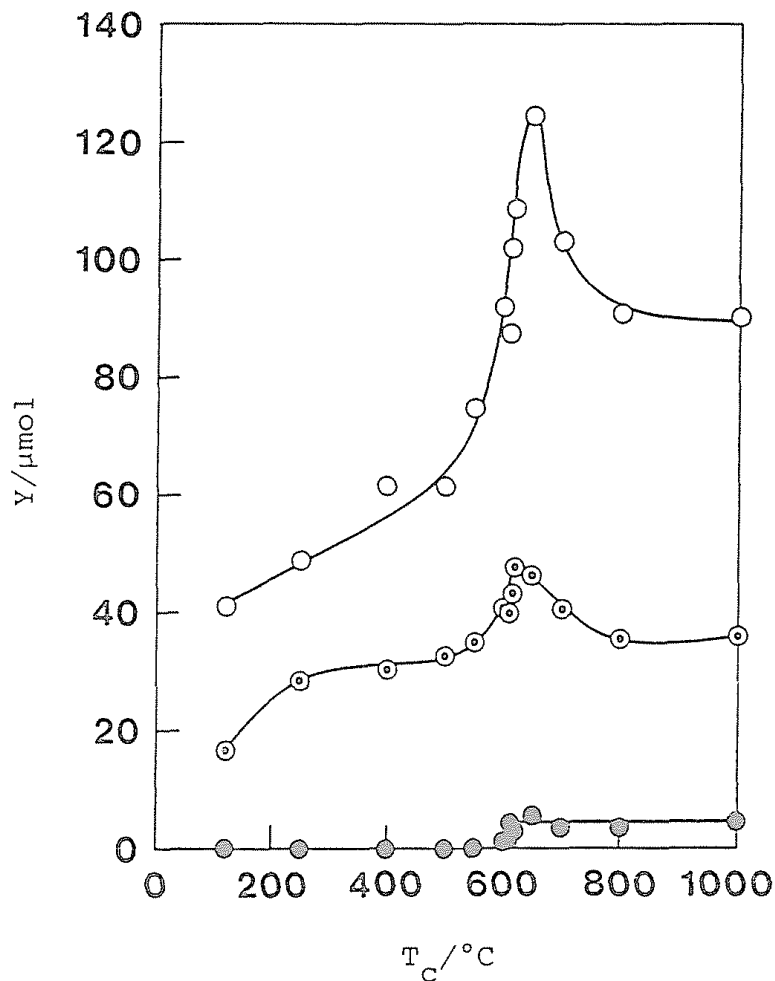


Figure 8 Photocatalytic formation of Ag metal ( $Y_{\text{Ag}}$ , ○), acetone ( $Y_{(\text{CH}_3)_2\text{CO}}$ , ⊙), and  $\text{O}_2$  ( $Y_{\text{O}_2}$ , ●) in the aqueous  $\text{TiO}_2$  (50 mg) suspension containing  $\text{Ag}_2\text{SO}_4$  solution (250  $\mu\text{mol}$  of  $\text{Ag}^+$ ; 5.0  $\text{cm}^3$ ) and 2-propanol (38  $\text{mm}^3$ , 500  $\mu\text{mol}$ ) over the 1-h irradiation, observed as a function of calcination temperature ( $T_c$ ) of  $\text{TiO}_2$ .

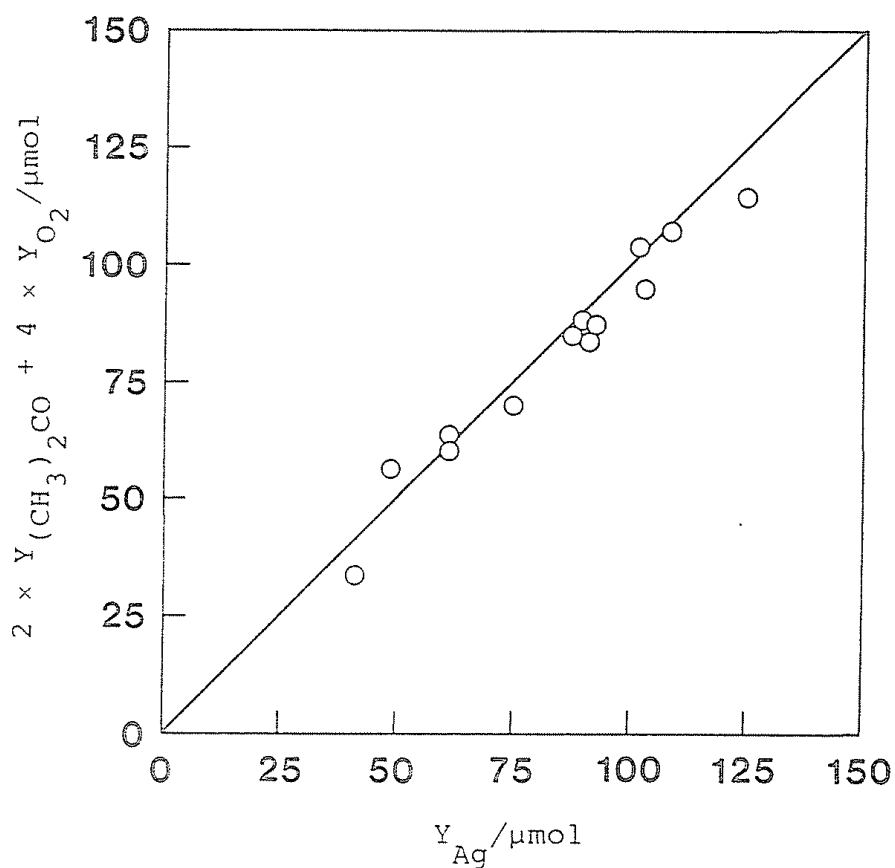


Figure 9 Linear relation between the yields of reduction product ( $Y_{Ag}$ ) and the oxidation products ( $2 Y_{(CH_3)_2CO} + 4 O_2$ ). The data are derived from Figure 8.



activity in this system (Figure 8) is very similar to that without 2-propanol (Figure 6), though 2-propanol predominantly undergoes oxidation instead of water. Since the  $\text{TiO}_2$  powders in this  $T_c$  range contain rutile crystal to much greater extent as the  $T_c$  is elevated (Figure 1), this similarity seems to originate largely from the action of the rutile crystal. In contrast, the apparent photocatalytic activity of the  $\text{TiO}_2$  powders at  $T_c \leq 550$  °C, which contain no rutile but anatase, is at least 3-fold enhanced by the addition of 2-propanol. This fact clearly shows that the oxidation of 2-propanol occurs more readily than that of water, by the photoirradiation on the anatase  $\text{TiO}_2$ .

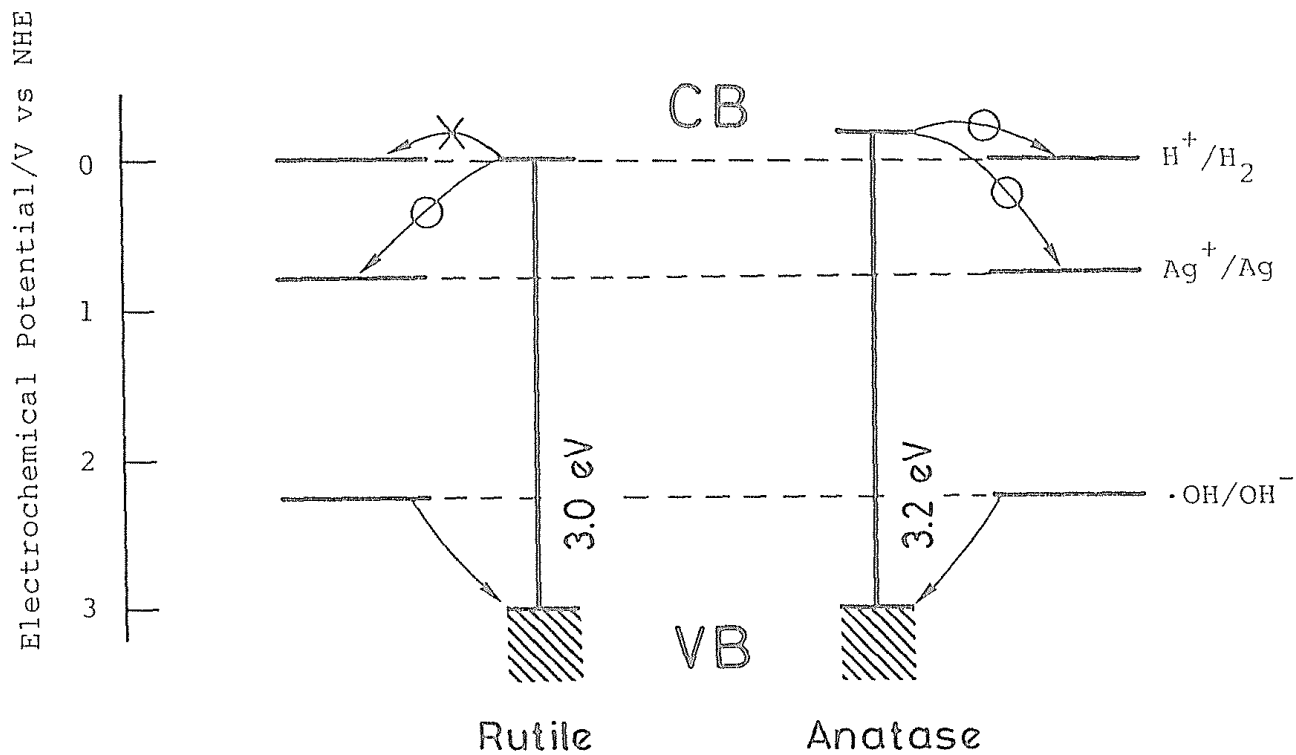
In comparison with the results of  $\text{TiO}_2$  prepared from  $\text{Ti}(\text{SO}_4)_2$ , the activity of  $\text{TiO}_2$  powders from  $\text{Ti}(\text{OPr})_4$  seemed to be a little larger in this photoreaction system:  $Y_{Ag}$  values by the  $\text{TiO}_2$  powders from  $\text{Ti}(\text{OPr})_4$  ( $T_c$  600 °C,  $L_A$  53 nm) and  $\text{Ti}(\text{SO}_4)_2$  ( $T_c$  700 °C,  $L_A$  37 nm)<sup>14</sup> were 73  $\mu\text{mol}$  over 1-h irradiation and 87  $\mu\text{mol}$  over 2-h irradiation, respectively.

Photocatalytic Activity of  $\text{TiO}_2$  Powder for Reduction and Oxidation of Different Species in Solution. As described above, the photocatalytic activity of  $\text{TiO}_2$  powders suspended in aqueous solution depended on both the crystal structure and the kind of substrate to be oxidized or reduced by the photogenerated hole ( $h^+$ ) or electron ( $e^-$ ), respectively. The photocatalytic activities in the three photoreaction systems clearly demonstrate the characteristic nature of oxidation and reduction sites on the photoirradiated  $\text{TiO}_2$  particle.

Almost no reaction occurred by the photoirradiation of aqueous

TiO<sub>2</sub> suspension without 2-propanol or Ag<sup>+</sup> ion. However, addition of 2-propanol to this system led to the formation of small amount of H<sub>2</sub> and acetone, the part of which proceeded by a non-catalytic process, the self-reduction of TiO<sub>2</sub> to form Ti(III). When Pt black was loaded on the TiO<sub>2</sub> powders, the activity increases drastically to yield stoichiometric amounts of H<sub>2</sub> and acetone. These facts show that easily oxidizable species 2-propanol is more effective for the trapping of the photogenerated hole which is little able to oxidize water (in the absence of Ag<sup>+</sup>). In addition, the loaded Pt catalyzes the reduction of H<sup>+</sup> by the photogenerated electron and depresses the self reduction of Ti(IV) to Ti(III) in the TiO<sub>2</sub>. This effect of Pt is evident especially in the case of anatase; rutile TiO<sub>2</sub> shows little activity for the H<sub>2</sub> evolution because of lower energy of the photoexcited electron to reduce H<sup>+</sup> in comparison with that of the anatase TiO<sub>2</sub> (Scheme 1).

The effect of Ag<sup>+</sup> ions was also evident; TiO<sub>2</sub> could oxidize water to O<sub>2</sub>, which could not be observed in the absence of Ag<sup>+</sup> even with the Pt-loaded TiO<sub>2</sub> (without 2-propanol). This results show that Ag<sup>+</sup> adsorbed on the TiO<sub>2</sub> surface effectively traps the photogenerated electron, as described in Chapters 8 and 11, and thereby promoting the oxidation of water. In this case the photocatalytic activity of TiO<sub>2</sub> depends mainly on the amount of the adsorbed Ag<sup>+</sup> (see Chapter 11). Because the redox potential of Ag<sup>+</sup>/Ag lies in the sufficiently positive region compared with the potential of conduction band electron of both anatase and rutile TiO<sub>2</sub> (Scheme 1), effect of the crystal structure of TiO<sub>2</sub>, anatase and rutile, is not so evident, compared with that for the H<sub>2</sub> evolution.



Scheme 1 Potential of conduction (CB) and valence (VB) bands of anatase and rutile TiO<sub>2</sub> evaluated from the electrochemical measurement of the TiO<sub>2</sub> electrodes.

Further enhancement of the photocatalytic activity of  $\text{TiO}_2$  was observed by the addition of both 2-propanol and  $\text{Ag}_2\text{SO}_4$ , particularly with the use of anatase  $\text{TiO}_2$  (see Figures 6 and 8). In this case both electron and positive hole are trapped effectively by the surface-adsorbed  $\text{Ag}^+$  and 2-propanol, respectively.

On the basis of these results, it was concluded in order to prepare the highly active photocatalyst that: (1) photocatalyst to be used in the reaction involving hydrogen evolution, and/or hydrogenation of intermediate species, is desirable to include "anatase" but not "rutile" crystal. (2) for the reaction involving reduction of silver ion, both "anatase" and "rutile" crystal forms are sufficient. (3) platinization is necessary for the catalytic reduction (without self reduction of  $\text{TiO}_2$ ) of proton into  $\text{H}_2$  even in the case of "anatase"  $\text{TiO}_2$ . (4) in both cases of anatase and rutile, it is desirable to adsorb larger amount of substrates, which are oxidized or reduced by the photogenerated positive hole and electron, respectively, on their surface.

## REFERENCES AND NOTES

- 1 T. Kawai and T. Sakata, *J. Chem. Soc., Chem. Commun.*, 694 (1980); *Nature (London)*, 286, 474 (1980); *Chem. Lett.*, 81 (1981).
- 2 P. Pichat, J-M. Herrmann, J. Disdier, H. Courbon and M-N. Mozzanega, *Nouv. J. Chim.*, 5, 627 (1981).
- 3 S. Teratani, J. Nakamichi, K. Taya and K. Tanaka, *Bull. Chem. Soc. Jpn*, 55, 1688 (1982).
- 4 K. Domen, S. Naito, T. Onishi and K. Tamaru, *Chem. Lett.*, 555 (1982).
- 5 B. Kraeutler and A. J. Bard, *J. Am. Chem. Soc.*, 100, 2239 (1978); 100, 5985 (1978).
- 6 H. Reiche and A. J. Bard, *J. Am. Chem. Soc.*, 101, 3127 (1979).
- 7 H. Reiche, W. W. Dunn, K. Wilbourn, F-R. F. Fan and A. J. Bard, *J. Phys. Chem.*, 84, 3207 (1980).
- 8 I. Izumi, F-R. F. Fan and A. J. Bard, *J. Phys. Chem.*, 85, 218 (1981).
- 9 H. Yoneyama, Y. Takao, H. Tamura and A. J. Bard, *J. Phys. Chem.*, 87, 1417 (1983).
- 10 A. J. Bard, *J. Photochem.*, 10, 59 (1979); *Science (Washington D. C.)*, 207, 139 (1980); *J. Phys. Chem.*, 86, 172 (1982).
- 11 A. J. Nozik, *Annu. Rev. Phys. Chem.*, 29, 189 (1978).
- 12 M. S. Wrighton, P. T. Wolczanski and A. B. Ellis, *J. Solid State Chem.*, 22, 17 (1977).
- 13 M. A. Fox, *Acc. Chem. Res.*, 16, 314 (1983).
- 14 S. Nishimoto, B. Ohtani, H. Kajiwara and T. Kagiya, *Nippon*

- Kagaku Kaishi, 246 (1984).
- 15 S. Nishimoto, B. Ohtani, H. Kajiwara and T. Kagiya, *J. Chem. Soc., Faraday Trans. 1*, 79, 2685 (1983).
  - 16 R. A. Spurr, H. Myers, *Anal. Chem.*, 29, 760 (1957).
  - 17 H. Klug, L. E. Alexander, *X-ray Diffraction Procedures*, 2nd Ed. (Wiley, New York, 1974), p. 618.
  - 18 A. Kurosaki and S. Okazaki, *Nippon Kagaku Kaishi*, 1816 (1976).
  - 19 K. Funaki and Y. Saeki, *Kogyo Kagaku Zashi*, 1291 (1956).
  - 20 A. D. Buss, M. A. Malati, R. Atkinson, *J. Oil. Col. Chem. Assoc.*, 59, 369 (1976).
  - 21 M. V. Rao, K. Rajeshwar, V. R. Pai Verneker and J. DuBow, *J. Phys. Chem.*, 84, 1987 (1980).
  - 22 A. Mills and G. Porter, *J. Chem. Soc., Faraday Trans. 1*, 78, 3659 (1982).
  - 23 E. Borgarello, J. Kiwi, M. Grätzel, E. Pelizzetti and M. Visca, *J. Am. Chem. Soc.*, 104, 2996 (1982).
  - 24 A. H. Boonstra and C. A. H. A. Mutsaers, *J. Phys. Chem.*, 79, 1694 (1975).
  - 25 G. Munuera, V. Rives-Arnau and A. Saucedo, *J. Chem. Soc., Faraday Trans. 1*, 75, 736 (1979).
  - 26 A. R. Gonzalez-Elipse, G. Munuera and J. Soria, *J. Chem. Soc., Faraday Trans. 1*, 75, 748 (1979).

## Chapter 11

### Influence of pH on the Photocatalytic Activity of TiO<sub>2</sub> Powders Suspended in Aqueous Silver Nitrate Solution and on Chemical Structure of TiO<sub>2</sub> Surface

#### ABSTRACT

Photocatalytic ( $\lambda_{\text{ex}} > 300 \text{ nm}$ ) activity of anatase and rutile TiO<sub>2</sub> powders suspended in AgNO<sub>3</sub> solution was investigated at room temperature. Initial rate of the photocatalytic reaction to produce O<sub>2</sub> and Ag metal was strongly dependent upon the pH of the reaction system, i.e., the rate decreased with decrease of the pH of the system to be negligible at pH < 2 and 5 in both cases of anatase and rutile TiO<sub>2</sub> powders, respectively. The amount of Ag<sup>+</sup> adsorbed on the TiO<sub>2</sub> surfaces in the dark decreased with the decreasing pH from 8 to 2. The initial rate of the photocatalytic reaction by both anatase and rutile TiO<sub>2</sub> was in proportion to the amount of Ag<sup>+</sup> adsorbed, i.e., the rate was expressed to be 1.18  $\mu\text{mol min}^{-1}$  per unit amount ( $\mu\text{mol}$ ) of the adsorbed Ag<sup>+</sup> under the given reaction conditions. Surface hydroxyl group on the TiO<sub>2</sub> powders was characterized quantitatively by the potentiometric titration of aqueous suspension. Ag<sup>+</sup> adsorbed both on neutral hydroxyl group ( $\equiv\text{Ti-OH}$ , 24 % at pH = 7) and ether oxygen ( $-\text{Ti-O-Ti}-$ , 76 %). Decrease of pH caused the protonation of  $\equiv\text{Ti-OH}$  into  $\equiv\text{Ti-OH}_2^+$  the positive charge of which inhibited the Ag<sup>+</sup> adsorption.

## INTRODUCTION

A great number of studies concerning the photocatalytic reaction of organic or inorganic compounds by aqueous suspension of  $\text{TiO}_2$  or platinum loaded  $\text{TiO}_2$  have been extensively reported.<sup>1</sup> Among these studies, it has been pointed out that the photocatalytic activity of  $\text{TiO}_2$  for various types of reactions strongly depends on the pH of the suspension,<sup>2,3</sup> though the reason is so far ambiguous. In this thesis, the pH dependence of the activity of  $\text{TiO}_2$  catalyst for dehydrogenation of alcohols (Chapters 1-3), degradation or prolongation of poly(ethylene oxide) (Chapter 4), N-alkylation of amines (Chapter 5) has been also clarified. Particularly, significant pH dependence of the reaction rate was demonstrated in the photocatalytic  $\text{O}_2$  evolution and Ag metal deposition from aqueous silver salt solutions, as described in Chapter 6.

In the present work, the pH dependent activity of  $\text{TiO}_2$  catalyst for the Ag metal deposition and  $\text{O}_2$  formation is discussed in connection with the amount of adsorbed  $\text{Ag}^+$  and chemical structure of surface hydroxyl group on the  $\text{TiO}_2$  surface, which are dependent on the pH of the system.

## EXPERIMENTAL

Materials. Anatase and rutile  $\text{TiO}_2$  powders were supplied from Merck and Wako Pure Chemicals, respectively. Another rutile analog used in the measurement of surface hydroxyl group was obtained by the calcination of the anatase  $\text{TiO}_2$  at 1200 °C in air.<sup>3</sup> The other materials were obtained commercially and used without further purification. Water was passed through ion-exchange resin and distilled



before use.

Photocatalytic Reaction. The finely ground  $\text{TiO}_2$  powder (250 mg) was suspended in  $2.00 \times 10^{-3}$  to  $1.00 \times 10^{-2}$   $\text{mol dm}^{-3}$   $\text{AgNO}_3$  aqueous solution ( $5.0 \text{ cm}^3$ , containing  $9 \times 10^{-2}$   $\text{mol dm}^{-3}$   $\text{KNO}_3$ ) in a glass tube ( $18 \text{ mm}\phi \times 130 \text{ mm}$ , transparent for the light of wavelength  $> 300 \text{ nm}$ ). The pH of the suspension was adjusted by adding  $1.00 \times 10^{-1}$   $\text{mol dm}^{-3}$   $\text{NaOH}$  or  $\text{HNO}_3$  ( $< 0.15 \text{ cm}^3$ ). The suspension was sonicated in an ultrasonic cleaning bath for 5 min, purged of air by Ar at least 30 min, and sealed off with a rubber stopper. Irradiation was performed with a 400-W high-pressure mercury arc. The  $\text{TiO}_2$  suspension was magnetically stirred throughout the irradiation. Gaseous product, typically  $\text{O}_2$ , was measured by gas chromatography using Shimadzu GC 4A equipped with Molecular Sieve 5A column ( $3 \text{ mm}\phi \times 2 \text{ m}$ ) and a TCD at  $100 \text{ }^\circ\text{C}$  with Ar carrier. The resulting suspension was centrifuged to separate the catalyst. The silver metal deposited on the  $\text{TiO}_2$  surface was dissolved with concentrated  $\text{HNO}_3$  and the resulting solution was diluted and subjected to the atomic absorption measurement recorded on a Jarrel-Ash AA 8200 spectrophotometer.

$\text{Ag}^+$  Adsorption on  $\text{TiO}_2$ . Amount of  $\text{Ag}^+$  adsorbed on the  $\text{TiO}_2$  surface, under the condition for the measurement of photocatalytic reaction, was measured from the difference between the  $\text{Ag}^+$  concentration before and after addition of  $\text{TiO}_2$  at various pH and concentration of  $\text{AgNO}_3$ . The measurement was carried out in a  $200 \text{ cm}^3$  flat-bottomed pyrex jar equipped with glass and double junction type reference electrodes (Horiba 1026A-06T and 2530A-06T, respectively), thermometer, inlet and outlet for purified  $\text{N}_2$  gas, and microburette.<sup>4,5</sup> The outer and inner chambers of the reference electrode were filled

with  $\text{KNO}_3$  and  $\text{KCl}$  aqueous solutions, respectively, to avoid precipitation of  $\text{AgCl}$ . The cell was kept at a constant temperature ( $25\text{ }^\circ\text{C}$ ) by pumping thermostated water through a jacket around the cell. An  $\text{Ag}^+$  ion selective electrode (Horiba 8011-06T) was used with a Hitachi-Horiba M-8s pH-mV meter calibrated with standard  $\text{AgNO}_3$  solutions ( $10^{-2}$  -  $10^{-5}$  mol  $\text{dm}^{-3}$   $\text{AgNO}_3$  in  $9 \times 10^{-2}$  mol  $\text{dm}^{-3}$   $\text{KNO}_3$ ). The  $\text{TiO}_2$  powder (anatase or rutile, 5.00 g) was added to the  $\text{AgNO}_3$  solution ( $99.50\text{ cm}^3$ ,  $2.00 \times 10^{-3}$  to  $1.00 \times 10^{-2}$  mol  $\text{dm}^{-3}$  in  $0.1$  mol  $\text{dm}^{-3}$   $\text{KNO}_3$ ) in the cell at a constant temperature ( $27.0 \pm 0.2\text{ }^\circ\text{C}$ ). (For the experimental convenience, the  $\text{Ag}^+$  adsorption measurement was carried out in the 20 times larger scale of the photocatalytic reaction.) A small portion ( $0.05$ - $0.15\text{ cm}^3$ ) of  $\text{NaOH}$  or  $\text{HNO}_3$  ( $1.00 \times 10^{-1}$  mol  $\text{dm}^{-3}$ ) was added to the magnetically stirred suspension of  $\text{TiO}_2$  for the pH adjustment. Stirring for ca. 30 min was required to obtain the equilibrium value of pH of the system.

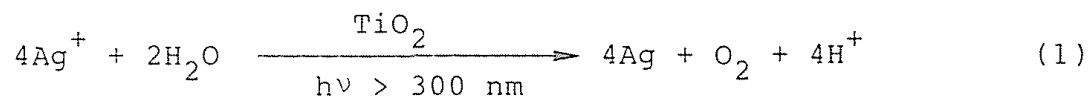
Potentiometric Titration. A  $\text{TiO}_2$  suspension in  $100\text{ cm}^3$  of  $10^{-3}$  mol  $\text{dm}^{-3}$   $\text{KOH}$  was titrated with  $10^{-2}$  mol  $\text{dm}^{-3}$   $\text{HNO}_3$  under nitrogen atmosphere with magnetic stirring, in the cell which is used for the  $\text{Ag}^+$  adsorption measurement described above. In this titration, the anatase powder (Merck) and its rutile analog were used.

## RESULTS AND DISCUSSION

### Photocatalytic Reaction of $\text{TiO}_2$ Suspended in Aqueous $\text{AgNO}_3$ Solution.

Photoirradiation ( $\lambda_{\text{ex}} > 300\text{ nm}$ ) of  $\text{TiO}_2$  suspended in an aqueous  $\text{AgNO}_3$  solution led to the liberation of  $\text{O}_2$  in the gas phase of the reaction mixture and concomitant deposition of silver metal on the  $\text{TiO}_2$  surface, as reported in Chapter 6. The stoichiometry is

given as follows.<sup>3</sup>



According to equation (1) pH of the reaction mixture decreased as the photocatalytic reaction proceeds. This pH decrease is undesirable for the evaluation of pH dependent rate of the photocatalytic reaction. The rate was, therefore, measured within a short period of the irradiation, e.g., 10-30 s, under the conditions of various concentration of  $\text{AgNO}_3$  and pH of the suspension, as shown in Figure 1. In the light of equation (1), the overall rate of the photocatalytic reaction was represented as initial rate of the Ag metal deposition ( $R_{\text{Ag}}^0$ ).

In the case of anatase  $\text{TiO}_2$ , no significant formation of Ag metal could be detected in the pH range  $< 2$ . At pH above 2 the initial rate increased significantly with the increase of pH (2 to 8), regardless of the  $\text{Ag}^+$  concentration ( $2.00 \times 10^{-3} - 1.00 \times 10^{-2} \text{ mol dm}^{-3}$ ). At given pH of the suspension the rate increased with the  $\text{Ag}^+$  concentration. As same as anatase  $\text{TiO}_2$ , photocatalytic activity of rutile  $\text{TiO}_2$  was negligible at  $\text{pH} < 5$  and increased with the pH increase (5-8), though relatively small compared with that of anatase  $\text{TiO}_2$  ( $\text{Ag}^+$  concentration;  $3.00 \times 10^{-3} \text{ mol dm}^{-3}$ ). Further increase of pH ( $> 8$ ) led to the formation of brown precipitate,  $\text{Ag}_2\text{O}$ , and the  $\text{Ag}^+$  concentration in the suspension decreased drastically, in both cases of anatase and rutile  $\text{TiO}_2$  powders.

In order to clarify the cause of this pH dependence of photocatalytic reaction, dependence on pH and  $\text{Ag}^+$  concentration, of the

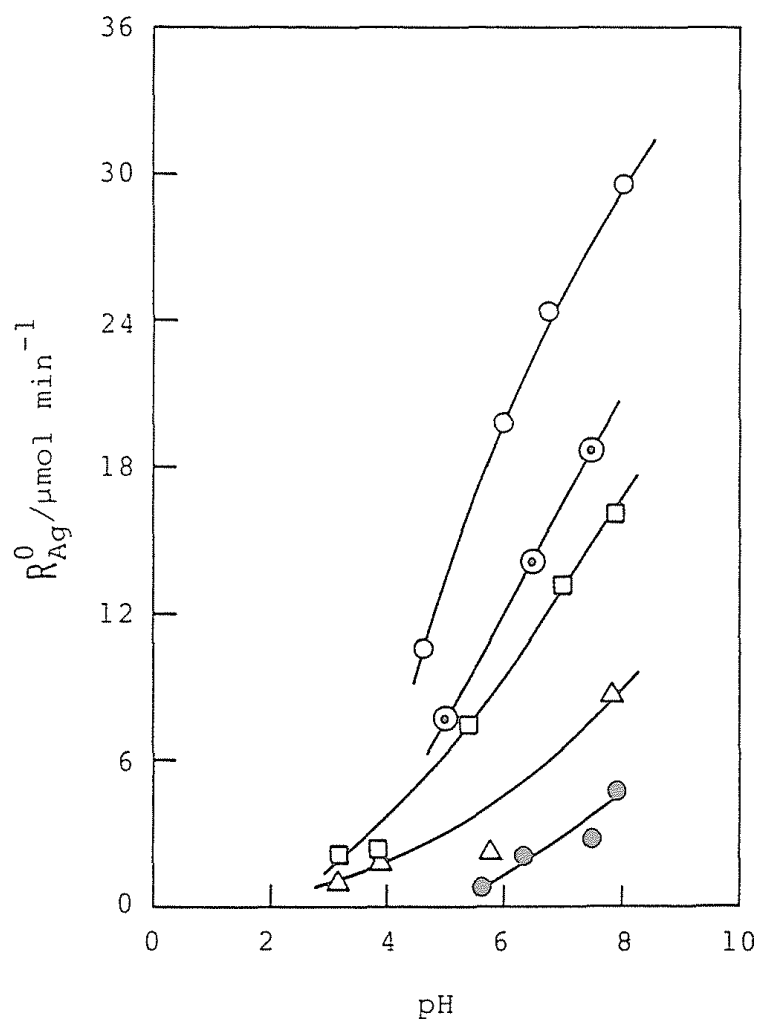


Figure 1 pH dependence of initial rate of photocatalytic Ag metal deposition ( $R_{Ag}^0$ ) from  $\text{AgNO}_3$  solution ( $5.00 \text{ cm}^3$ ). Initial concentration of  $\text{AgNO}_3$   $\circ$   $1.00 \times 10^{-2}$ ,  $\odot$   $5.00 \times 10^{-3}$ ,  $\square$   $3.00 \times 10^{-3}$ ,  $\triangle$   $2.00 \times 10^{-3} \text{ mol dm}^{-3}$  with anatase  $\text{TiO}_2$  (250 mg) and  $\bullet$   $3.00 \times 10^{-3} \text{ mol dm}^{-3}$  with rutile  $\text{TiO}_2$  (250 mg).

Ag<sup>+</sup> adsorption onto the surfaces of anatase and rutile TiO<sub>2</sub> powders was measured in the dark, as shown in Figure 2. The amount of Ag<sup>+</sup> adsorbed on the anatase TiO<sub>2</sub> decreased with the decrease of pH to be negligible at pH < 2. On the other hand, the amount of Ag<sup>+</sup> adsorbed on the rutile TiO<sub>2</sub> was negligible at pH < ca. 5 and increased with the pH increase at pH > 6. In the given pH region (2-6), the amount of Ag<sup>+</sup> adsorbed on the anatase TiO<sub>2</sub> surface was larger than that on the rutile surface. These pH dependences can be correlated to the pH dependent modification of hydroxyl group on the TiO<sub>2</sub> surface, positively and negatively charged in the lower and higher pH region, and is discussed in the following section.

On the basis of these results shown in Figures 1 and 2, the photocatalytic activity of TiO<sub>2</sub> suspended in AgNO<sub>3</sub> solution is expected to depend on the amount of Ag<sup>+</sup> adsorbed on the TiO<sub>2</sub> surface. In fact, the rate of the photocatalytic reaction is proportional to the amount of the adsorbed Ag<sup>+</sup> with both anatase and rutile TiO<sub>2</sub> as shown in Figure 3. Therefore, the initial rate of the photocatalytic reaction is represented as a function of the amount of adsorbed Ag<sup>+</sup>, as follows.

$$R_{Ag}^0 / \mu\text{mol min}^{-1} = 1.18 \times (\text{Ag}^+ \text{ adsorbed} / \mu\text{mol}) \quad (2)$$

Moreover, these facts clearly demonstrate that another pH-dependent nature which is expected to influence on the photocatalytic activity, e.g., protonation and deprotonation equilibria of surface hydroxyl groups (see following section), affects negligibly. For instance, same amount of adsorbed Ag<sup>+</sup> (from different concentration

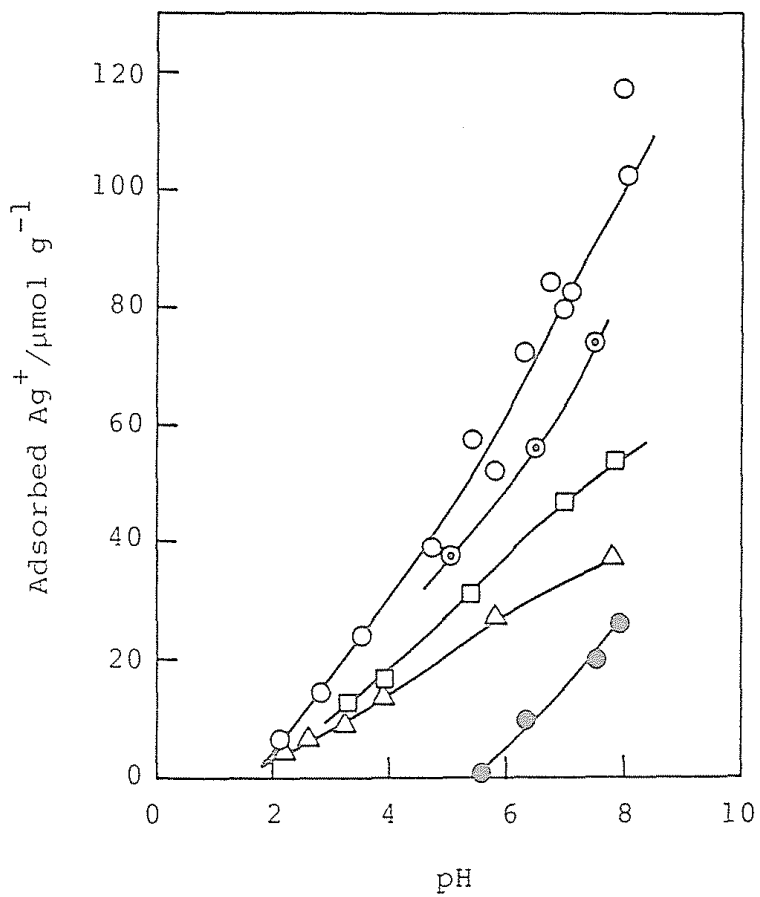


Figure 2 pH dependence of the  $\text{Ag}^+$  adsorption on  $\text{TiO}_2$  surfaces. Symbols are same as in Figure 1.

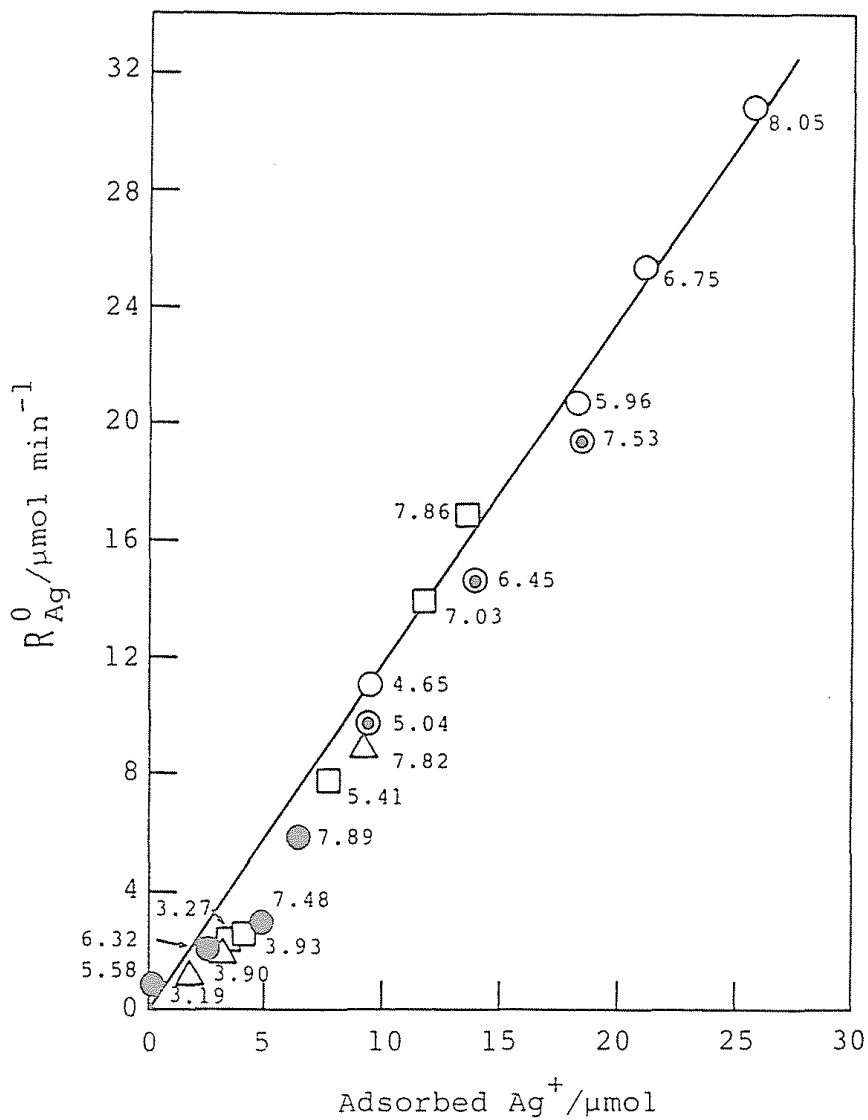
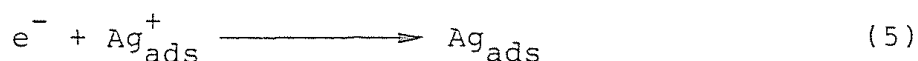
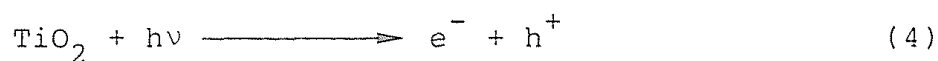
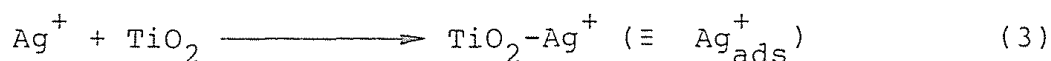


Figure 3 Correlation between the initial rate of photocatalytic Ag metal deposition ( $R_{Ag}^0$ ) and the amount of  $Ag^+$  adsorbed on  $TiO_2$ . Symbols are same as in Figures 1 and 2. Number denotes pH of the suspension.

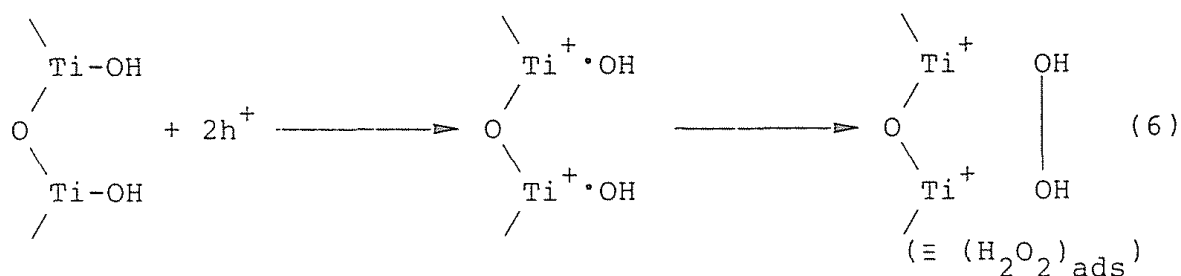
of AgNO<sub>3</sub> solution with appropriate pH) gives practically same rates of Ag metal deposition although the pH values are significantly different (> 3 unit of pH at the amount of adsorbed Ag ≈ 9 μmol on 250 mg of the anatase TiO<sub>2</sub>, see Figure 3).

Fleischauer and coworkers reported the similar photocatalytic action of single crystal/Ag<sup>+</sup> system.<sup>6</sup> They showed the mechanism including Ag<sup>+</sup> adsorption on the TiO<sub>2</sub> surface from the result on the effect of Ag<sup>+</sup> concentration. However, the amount of the adsorbed Ag<sup>+</sup> was not measured in their work. Recently, Hada and coworkers also reported the photocatalytic reaction of TiO<sub>2</sub>/Ag<sup>+</sup> system and discussed the effect of Ag<sup>+</sup> concentration, making no account of the pH influence.<sup>7</sup> The results presented here provide new information of the importance of Ag<sup>+</sup> adsorption on the TiO<sub>2</sub> surface in the photocatalytic reaction of TiO<sub>2</sub>/Ag<sup>+</sup> system. The oxidation step leading to the O<sub>2</sub> generation could proceed smoothly so long as the photoexcited "conduction band" electron is trapped by the surface adsorbed Ag<sup>+</sup>.

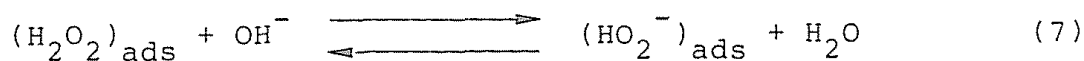


The positive hole (h<sup>+</sup>) left in the bulk of TiO<sub>2</sub> would oxidize surface hydroxyl on TiO<sub>2</sub> to yield H<sub>2</sub>O<sub>2</sub>.

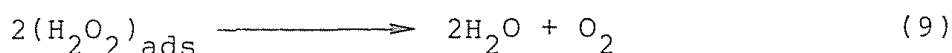




Following reaction to yield  $\text{O}_2$  from  $\text{H}_2\text{O}_2$  on the  $\text{TiO}_2$  surface, in the dark, is expected from the result of electrochemical evolution of  $\text{O}_2$  at the anode surface.<sup>8-11</sup>



These reactions are formally summarized, as follows, and are consistent with the stoichiometry of the photocatalytic reaction (equation (1)).



Characterization of Hydroxyl Group on the  $\text{TiO}_2$  Surface. It has been reported that the surface of metal oxides, such as  $\text{TiO}_2$ , is covered with chemisorbed (i.e., surface hydroxyl group) or physically adsorbed water when suspended in aqueous solution. Measurement of the surface hydroxyl has been carried out by means of acid-base titration,<sup>12</sup> substitution with fluoride anion,<sup>13</sup> or esterification with organic acids.<sup>14</sup> In this chapter, hydroxyl group on the surface

of  $\text{TiO}_2$  powders is characterized in detail.

Figure 4 shows the titration curves for the anatase and rutile  $\text{TiO}_2$  powders suspended in an aqueous KOH solution. A titration curve for the aqueous KOH solution without  $\text{TiO}_2$  is also plotted in Figure 4. As is clearly seen, the pH decreased to 8.3 and 10.0 by the addition of the anatase  $\text{TiO}_2$  ( $\text{TiO}_2(\text{A})$ ) and its rutile analog ( $\text{TiO}_2(\text{R})$ ), prepared by annealing of  $\text{TiO}_2(\text{A})$  (5.0 g each), respectively, in the alkaline solution (initial pH  $\approx$  11.0). These facts show that both  $\text{TiO}_2$  powders have acidic sites to neutralize  $\text{OH}^-$ , and the amount of the acidic sites on  $\text{TiO}_2(\text{A})$  is larger than that on  $\text{TiO}_2(\text{R})$  at a given amount.

On the other hand, the pH of acidic solution was raised from ca. 3.1 (in the absence of  $\text{TiO}_2$ ,  $0.01 \text{ mol dm}^{-3} \text{ HNO}_3$   $15.0 \text{ cm}^3$ ) to 4.4 and 3.6 by the addition of  $\text{TiO}_2(\text{A})$  and  $\text{TiO}_2(\text{R})$  (5.0 g each), respectively. Therefore, the both  $\text{TiO}_2$  powders have also basic sites to neutralize  $\text{H}^+$ . As is clearly seen in Figure 5 the amount of basic sites on the  $\text{TiO}_2(\text{A})$  surface is larger than that on  $\text{TiO}_2(\text{R})$  surface. Therefore, both amounts of acidic and basic sites on  $\text{TiO}_2(\text{A})$  are larger than those of  $\text{TiO}_2(\text{R})$ .

In each system the titration curve became horizontal with the increasing amount of  $\text{TiO}_2$  and these curves intersected each other on an unique point around pH  $\approx$  7. The pH of the intersecting points ( $\text{pH}_{\text{ip}}$ ) are shown in Table 1.

These results seem to be accounted for by the amphoteric character of surface hydroxyl group schematically shown as follows.<sup>12-14</sup>

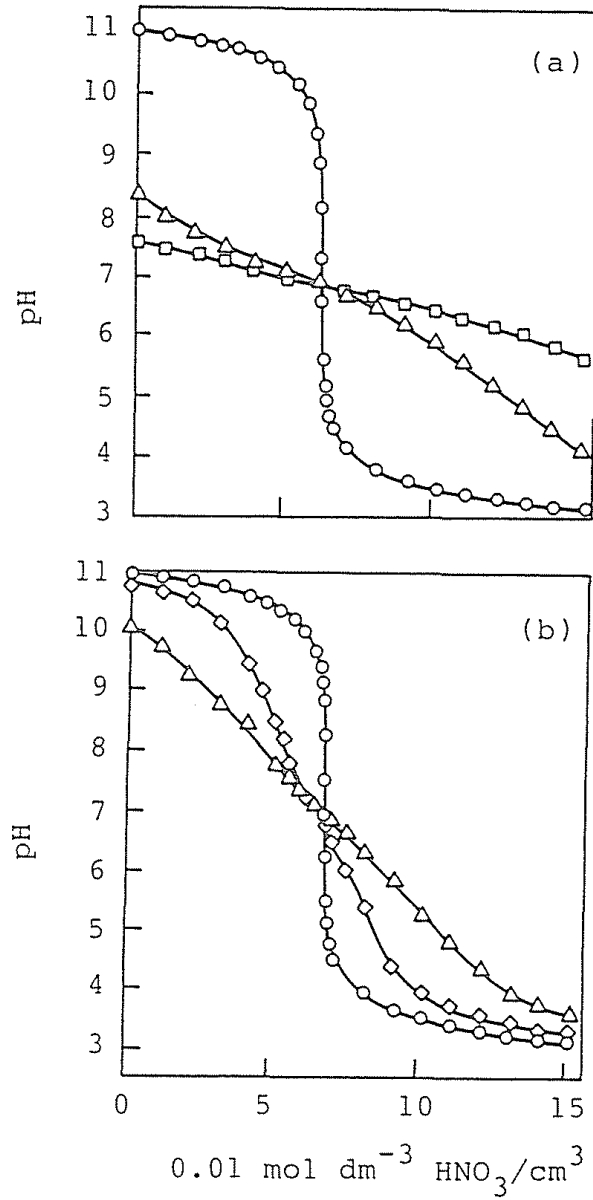
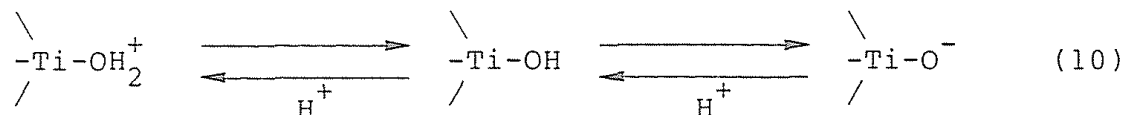


Figure 4 Potentiometric titration curves of (a) TiO<sub>2</sub>(A) and (b) TiO<sub>2</sub>(R) suspensions; ○ : without TiO<sub>2</sub>, ◇ : 2.5 g, △ : 5.0 g, and □ : 10.0 g of TiO<sub>2</sub>.

Table 1 Properties of hydroxyl group on the surface of TiO<sub>2</sub>(A) and TiO<sub>2</sub>(R) obtained by potentiometric titration of the suspensions.

TiO <sub>2</sub>	$T^a$ μmol g <sup>-1</sup>	pK <sub>a1</sub>		pK <sub>a2</sub>		pH <sub>EABP</sub> <sup>b</sup>	pH <sub>ip</sub> <sup>c</sup>
		a	b	c	d		
TiO <sub>2</sub> (A)	21.4	6.29	-52.0	7.49	58.9	6.89	6.89
TiO <sub>2</sub> (R)	13.6	6.47	147	6.93	330.4	7.58	7.46
P-25 <sup>d</sup>	460	4.98	-26.4	7.80	13.1	6.39	6.4

<sup>a</sup>Total amount of surface hydroxyl obtained by extrapolation of plots for  $1/\Gamma_H$  (or  $1/\Gamma_{OH}$ ) vs  $1/C_H$  (or  $1/C_{OH}$ ). <sup>b</sup>pH of equi-acid-base point;  $(a + c) / 2$ , see text.<sup>9</sup> <sup>c</sup>pH of the intersection of the titration curves (Figure 1). <sup>d</sup>Reported values for anatase-rutile mixed TiO<sub>2</sub> (Supplied by Degassa, see reference 8). As clearly seen, the surface area of P-25 is significantly larger than that of TiO<sub>2</sub> used in this study, presumably owing to the smaller particle size  $\approx$  30 nm. The photocatalytic activity of this material was preliminarily examined; the rate of the Ag metal deposition from aqueous AgNO<sub>3</sub> solution (pH  $\approx$  5, see preceding section) was approximately as same as that of TiO<sub>2</sub>(A). The detailed study is now in progress.



On the assumption of these equilibria, difference between the amounts of the protonated ( $\equiv\text{Ti-OH}_2^+$ ) and the deprotonated ( $\equiv\text{Ti-O}^-$ ) hydroxyl groups ( $\Gamma_{\text{H}}$  and  $\Gamma_{\text{OH}}$ , respectively) can be evaluated from the difference in pH of the solution in the presence and absence of  $\text{TiO}_2$ .

$$\Gamma_{\text{OH}} - \Gamma_{\text{H}} = V [(C_{\text{H}} - C_{\text{OH}}) - (C_{\text{H}} - C_{\text{OH}})_{\text{init}}] / m \quad (11)$$

where  $V$  is volume of the suspension,  $m$  is weight of the  $\text{TiO}_2$  powder,  $(C_{\text{H}} - C_{\text{OH}})$  is difference in the concentration between proton and hydroxide ion, and  $(C_{\text{H}} - C_{\text{OH}})_{\text{init}}$  is the difference in the absence of  $\text{TiO}_2$ . Figure 5 shows the plots of  $(\Gamma_{\text{OH}} - \Gamma_{\text{H}})$  as a function of pH of the suspension, showing that the excess amount of hydroxyl ( $\Gamma_{\text{OH}} - \Gamma_{\text{H}}$ ) is independent of the amount of  $\text{TiO}_2$  suspended in the aqueous solution for both  $\text{TiO}_2(\text{A})$  and  $\text{TiO}_2(\text{R})$  powders.

Since except for a small range around the intersecting point the coexistence of  $\equiv\text{Ti-OH}_2^+$  and  $\equiv\text{Ti-O}^-$  groups is unlikely, the following simplifications seems to be justified.

$$\text{if } C_{\text{H}} - C_{\text{OH}} > 0 \quad \text{then} \quad \Gamma_{\text{OH}} = 0 \quad (12)$$

$$\text{if } C_{\text{H}} - C_{\text{OH}} < 0 \quad \text{then} \quad \Gamma_{\text{H}} = 0 \quad (13)$$

The data thus obtained were used to evaluate the amounts of hydroxyl

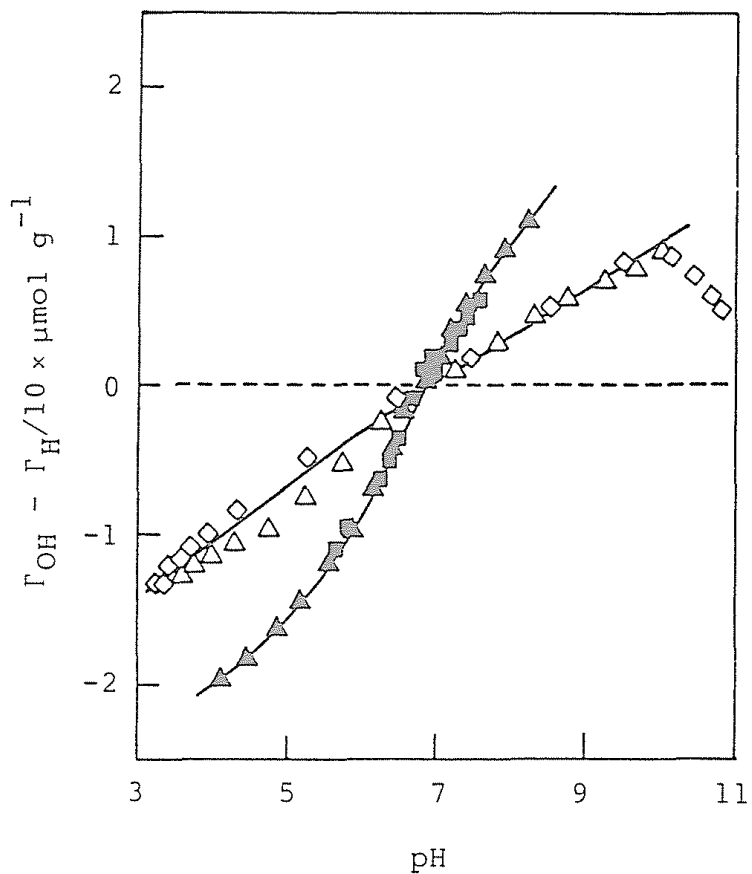
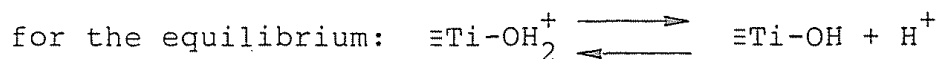


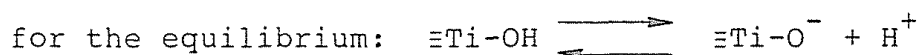
Figure 5 Excess amount of hydroxyl ( $\Gamma_{OH} - \Gamma_H$ ) on the surface of  $\text{TiO}_2(\text{A})$  (▲: 5.0 g, ■: 10.0 g) and  $\text{TiO}_2(\text{R})$  (◇: 2.5 g, △: 5.0 g).

in the protonated, neutral, and deprotonated forms, as shown in Figure 6. Though the amount of hydroxyl on the TiO<sub>2</sub>(A) surface was larger than that on the TiO<sub>2</sub>(R) surface as has been suggested above, the amphoteric nature of surface hydroxyl was essentially identical. Total amount of the surface hydroxyl (T), i.e., sum of the protonated, neutral, and deprotonated hydroxyl, was estimated by extrapolation of (1/Γ<sub>H</sub> (or 1/Γ<sub>OH</sub>) vs 1/C<sub>H</sub> (or 1/C<sub>OH</sub>)) plots and is shown in Table 1 (the total amounts obtained from Γ<sub>H</sub> and Γ<sub>OH</sub> were practically identical in each TiO<sub>2</sub> system). The total amount of surface hydroxyl on TiO<sub>2</sub>(A), 21.4 μmol g<sup>-1</sup>, was 1.4 times larger than that on TiO<sub>2</sub>(R). This may be due to the dehydration by high-temperature calcination for the crystal transformation from anatase into rutile.

From the results mentioned above, microscopic acidity constants were evaluated as follows.



$$K_{a1} = [\text{H}^+] [\equiv\text{Ti-OH}] / [\equiv\text{Ti-OH}_2^+] = C_H (T - \Gamma_H) / \Gamma_H \quad (14)$$



$$K_{a2} = [\text{H}^+] [\equiv\text{Ti-O}^-] / [\equiv\text{Ti-OH}] = C_H \Gamma_{OH} / (T - \Gamma_{OH}) \quad (15)$$

where [ ] denotes the concentration of each species. The calculated values of  $K_a$  were strongly dependent on the concentration of  $\equiv\text{Ti-OH}_2^+$  and  $\equiv\text{Ti-O}^-$ , respectively. Assuming the linear relations between  $\text{p}K_a$  and  $\Gamma$ , one can obtain;

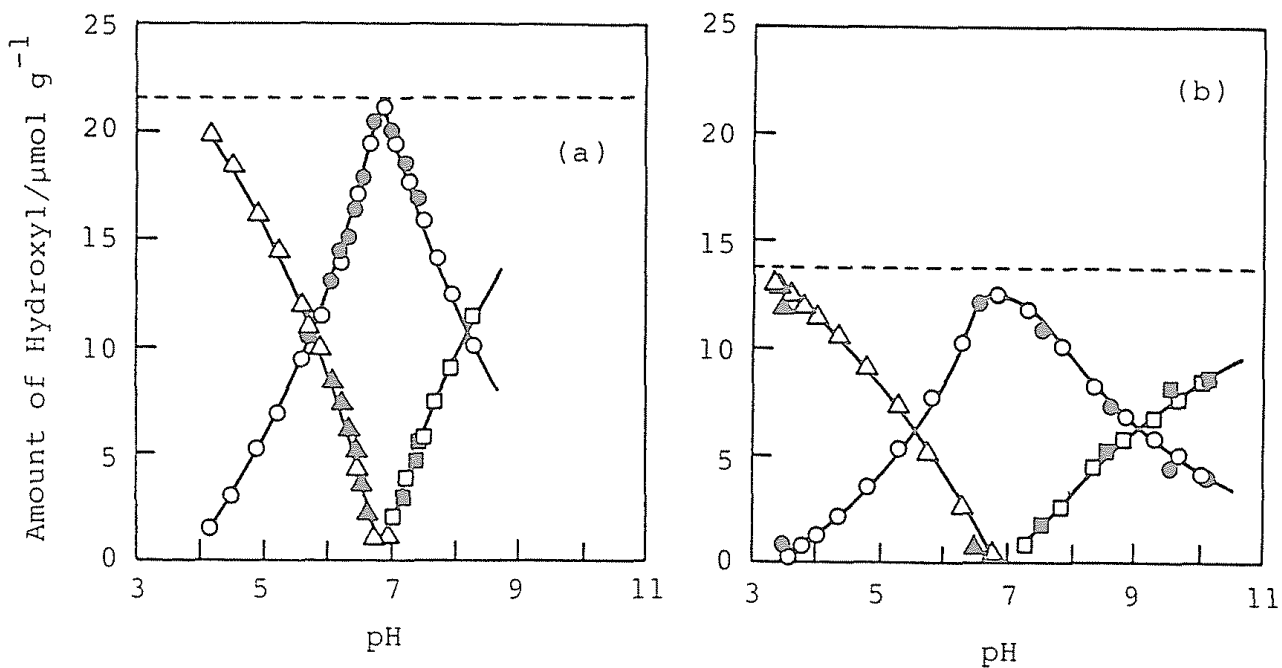


Figure 6 Distribution of protonated ( $\equiv\text{Ti-OH}_2^+$ ,  $\triangle$  and  $\blacktriangle$ ), neutral ( $\equiv\text{Ti-OH}$ ,  $\circ$  and  $\bullet$ ), and deprotonated ( $\equiv\text{Ti-O}^-$ ,  $\square$  and  $\blacksquare$ ) hydroxyl groups on (a)  $\text{TiO}_2(\text{A})$  and (b)  $\text{TiO}_2(\text{R})$  surface. Broken lines represent the total amount of hydroxyl (S, see Table 1). Open symbols are plots of data obtained using (a) 5.0 g and (b) 2.5 g of  $\text{TiO}_2$ . Closed symbols are plots of data using (a) 10.0 g and (b) 5.0 g of  $\text{TiO}_2$ .



$$pK_{a1} = a + b \Gamma_H \quad (16)$$

$$pK_{a2} = c + d \Gamma_{OH} \quad (17)$$

Observed constants for these equations obtained from Figure 7 are listed in Table 1.

Schindler and Gamsjager<sup>15</sup> pointed out this effect of surface charge of the  $TiO_2$  suspension and they proposed a quantitative interpretation on the assumption that (i) interactions between dispersed particles are negligible, (ii) the Gibbs energy of deprotonation is separable into  $\Delta G_{int}$  the Gibbs energy of dissociation, and electrical work for the removal of the proton against the electrostatic field of the charged groups from the site of dissociation into the bulk of the solution, as follows.

$$K_a = K_{a \text{ int}} \exp (F\Psi/RT) \quad (18)$$

where  $K_{a \text{ int}}$  intrinsic acidity constant, i.e., the acidity constant of the group in the absence of an electric field, and  $\Psi$  potential difference between the site of dissociation and the bulk of the solutions. Logarithm of equation (18) is formally consistent with equation (16) and (17). Therefore, intrinsic acidity constants (a and c) could be obtained (Table 1).

Furthermore, the pH value of the system at which the amounts of  $\equiv Ti-O^-$  and  $\equiv Ti-OH_2^+$  are identical ( $pH_{EABP}$  : equi-acid-base point)<sup>16</sup> can be estimated from the equations (5)-(8) because participation of

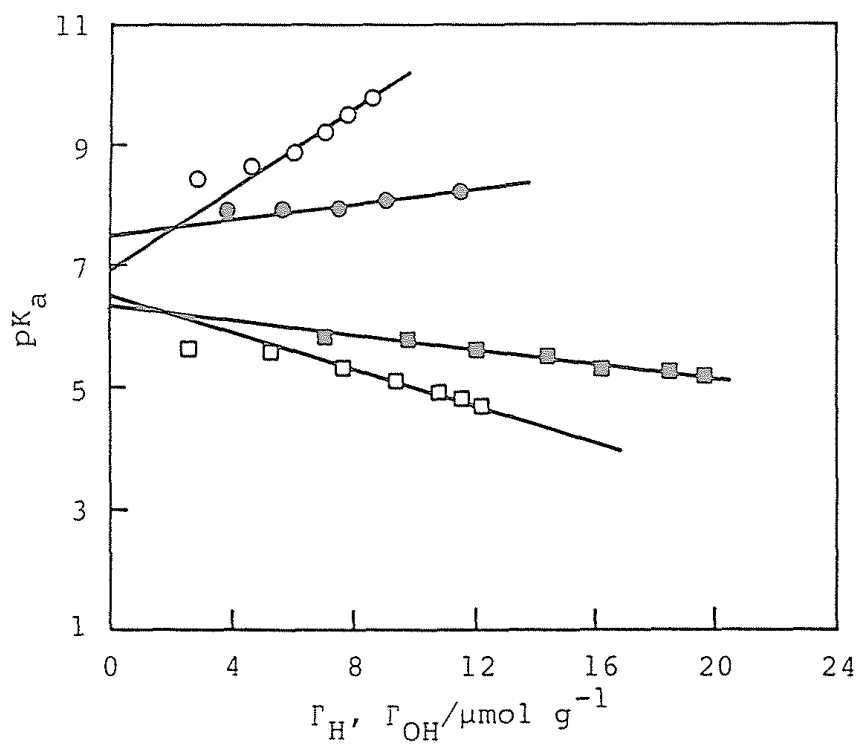


Figure 7 Dependence of  $pK_a$  on  $\Gamma_H$  and  $\Gamma_{OH}$ .

● and ○ :  $\Gamma_{OH}$  vs  $pK_{a2}$  of  $\text{TiO}_2(\text{A})$  and  $\text{TiO}_2(\text{R})$ , respectively.

■ and □ :  $\Gamma_H$  vs  $pK_{a1}$  of  $\text{TiO}_2(\text{A})$  and  $\text{TiO}_2(\text{R})$ , respectively.

electrostatic field should be negligible around  $\text{pH}_{\text{EABP}}$ , as

$$\text{pH}_{\text{EABP}} = (\text{pK}_{\text{a1 int}} + \text{pK}_{\text{a2 int}}) / 2 \quad (19)$$

Apparently good agreement between  $\text{pH}_{\text{ip}}$  and  $\text{pH}_{\text{EABP}}$  for both  $\text{TiO}_2$  powders (Table 1) shows the reasonableness of this derivation.

The reported values of a commercially available  $\text{TiO}_2$ , P-25,<sup>15</sup> are also listed in Table 1. The total amount of surface hydroxyl of P-25 ( $460 \mu\text{mol g}^{-1}$ ) and the surface area ( $56 \text{ m}^2 \text{ g}^{-1}$ ) are significantly larger than those of  $\text{TiO}_2$  used in the present investigation (ca.  $14\text{-}21 \mu\text{mol g}^{-1}$  and ca.  $11 \text{ m}^2 \text{ g}^{-1}$  ( $\text{TiO}_2(\text{A})$ ). The absolute values of the second terms of equations (15) and (16) (b and d, respectively) increased in the order, (P-25) < ( $\text{TiO}_2(\text{A})$ ) <  $\text{TiO}_2(\text{R})$ , for both  $\text{pK}_{\text{a1}}$  and  $\text{pK}_{\text{a2}}$ . Therefore, it is clarified quantitatively that the charge density (i.e., amount of positive or negative charge per unit area) predominates the term concerning the electrostatic field, independent of the crystal form of  $\text{TiO}_2$ .

Correlation between  $\text{Ag}^+$  Adsorption and pH Dependent Chemical Structure of  $\text{TiO}_2$  Surface. In this section, the  $\text{Ag}^+$  adsorption which was strongly dependent on the pH of the suspension is correlated with the pH dependent chemical structure of the  $\text{TiO}_2$  surface, in order to clarify the effect of surface charge density on the  $\text{TiO}_2$  photocatalytic reaction.

Figure 8 shows the amount of adsorbed  $\text{Ag}^+$  ( $[\text{Ag}^+]_{\text{ads}}$ ) on the anatase  $\text{TiO}_2$  ( $\text{TiO}_2(\text{A})$ ) surface as a function of the concentration of  $\text{Ag}^+$  in the solution at equilibrium ( $[\text{Ag}^+]_{\text{eq}}$ ), at given pH of the suspension derived from Figure 2. It is clear from this figure

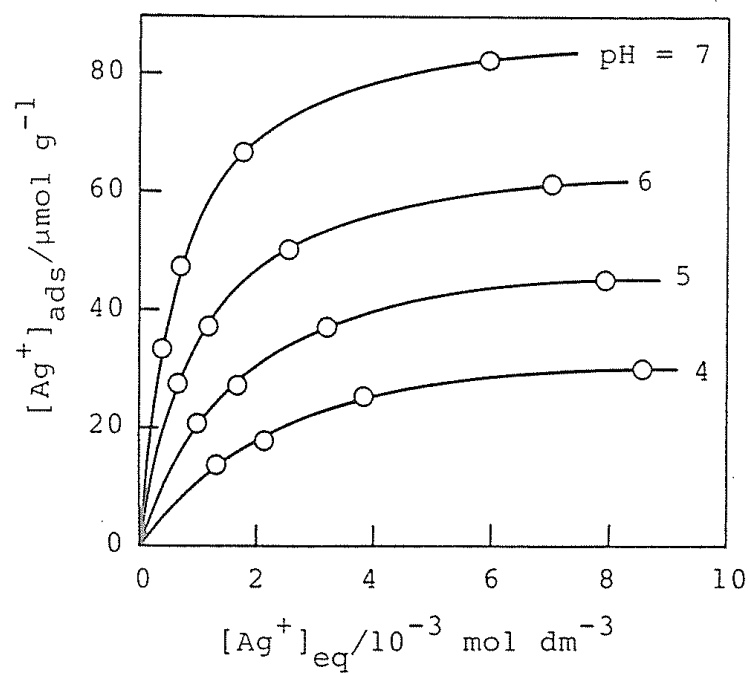
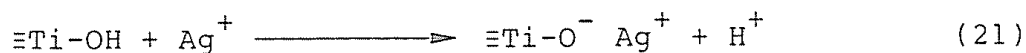


Figure 8 Amount of  $Ag^+$  adsorbed on the anatase  $TiO_2$  ( $TiO_2(A)$ ) surface ( $[Ag^+]_{ads}$ ) as a function of equilibrium concentration of  $Ag^+$  ( $[Ag^+]_{eq}$ ) in the solution.

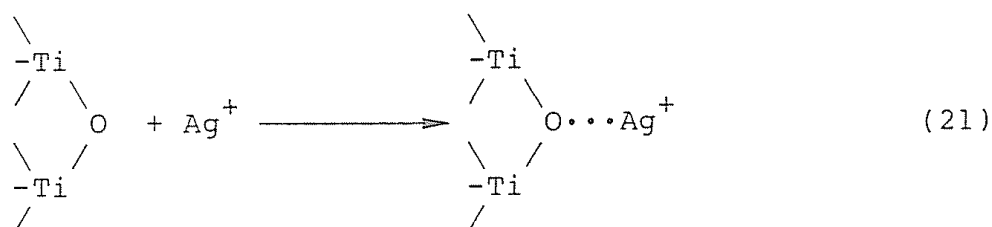
that  $[Ag^+]_{ads}$  become plateau over the  $[Ag^+]_{eq}$  range  $> 5 \text{ mmol dm}^{-3}$ ; the saturation limit increases with the increasing pH from 4 to 7 (see also Figure 2). Double reciprocal plots of data in Figure 8 are shown in Figure 9. Linear relations were obtained for each case of pH, showing reasonable fits to Langmuir relation,

$$[Ag^+]_{ads} = S K [Ag^+]_{eq} / (1 + K [Ag^+]_{eq}) \quad (20)$$

where, S and K represent limiting amount of adsorption site and adsorption constant, respectively. Both values of S and K obtained by least square approximation increased with the increase of pH (Table 2). The increase of S is presumably attributable to the increase of neutral hydroxy group the  $Ag^+$  adsorption on which is most likely as,



However,  $[Ag^+]_{ads}$  was always larger than the amount of  $\equiv Ti-OH$  (see Figure 10(a)), indicating that most part of  $Ag^+$  is adsorbed on the other sites not on  $\equiv Ti-OH$ . The most possible chemical structure of the site for such adsorption is  $-Ti-O-Ti-$  ( $Ti_2O$  structure) on the surface.



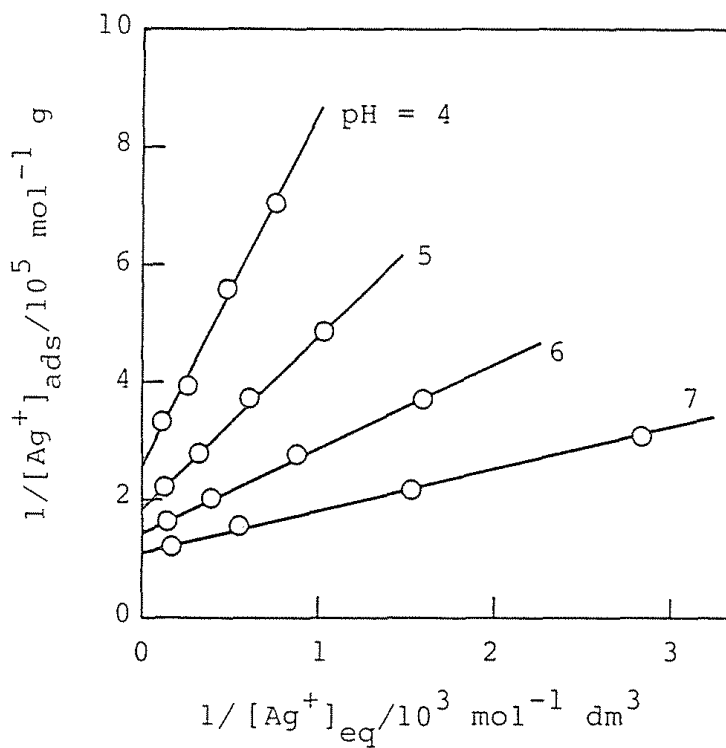


Figure 9 Reciprocal plots of  $[Ag^+]_{ads}$  and  $[Ag^+]_{eq}$  at various pH. Data were obtained from Figure 8.

Table 2 Observed constant for  $\text{Ag}^+$  adsorption on the anatase  $\text{TiO}_2$  powder ( $\text{TiO}_2(\text{A})$ ) suspended in  $\text{AgNO}_3$  solution and amount of hydroxyl group in the neutral and acidic forms.

pH	$S^a$ $\mu\text{mol g}^{-1}$	$K^b$	$\ln K$	$[\equiv\text{Ti}-\text{OH}]^c$ $\mu\text{mol g}^{-1}$	$[\equiv\text{Ti}-\text{OH}_2^+]^c$ $\mu\text{mol g}^{-1}$
7	89.5	$1.67 \times 10^3$	7.42	21.3	0
6	68.8	$1.06 \times 10^3$	6.97	13.0	8.3
5	55.0	$0.62 \times 10^3$	6.43	6.0	15.3
4	38.9	$0.44 \times 10^3$	6.08	1.1	20.2

<sup>a</sup>Limiting amount of  $\text{Ag}^+$  adsorption site on the  $\text{TiO}_2$  surface. <sup>b</sup>Equilibrium constant of  $\text{Ag}^+$  adsorption. <sup>c</sup>Obtained from Figure 6.

At pH = 7, ca. 24 % of the limiting adsorption site was attributed to  $\equiv\text{Ti-OH}$  (21.3  $\mu\text{mol}$ , see Table 2) and the rest to the  $\text{Ti}_2\text{O}$  structure (68.2  $\mu\text{mol} = 89.5 - 21.3$ ). Extrapolation of the straight line in Figure 10(a) gave a sufficient value of limiting adsorption,  $S = 38 \mu\text{mol g}^{-1}$ , at lower pH ( $< 4$ ) where the amount  $\equiv\text{Ti-OH}$  is negligible.

On the other hand, experimental results shown in Figure 2 is smaller than the expected value from this  $S$  value. The discrepancy is attributed to the decreasing value of  $K$ , adsorption equilibrium constant, which should be constant so long as the surface site remains constant. As shown in Figure 10(b), linear relation between  $\ln K$  and the amount of  $\equiv\text{Ti-OH}_2^+$  was obtained (deviation from the straight line at small amount of  $\equiv\text{Ti-OH}_2^+$  is presumably due to the error by the approximation (equation (12) in the preceding section)).

Assuming that the Gibbs energy of the  $\text{Ag}^+$  adsorption is separable into  $\Delta G_{\text{int}}$  the intrinsic Gibbs energy of adsorption, and electrical work from the bulk of the solution to the site of  $\text{Ag}^+$  adsorption on the positively charged surface against the electrostatic field, which is similar to that for the protonation and deprotonation of the surface hydroxyl, one can obtain following equation.

$$K = K_{\text{int}} \exp (F\Psi/RT) \quad (23)$$

where  $K_{\text{int}}$  intrinsic adsorption equilibrium constant (in the absence of an electric field), and  $\Psi$  potential difference between the bulk of the solution and the adsorption site. Logarithm of equation (23) is formally consistent with the results shown in Figure 10(b).



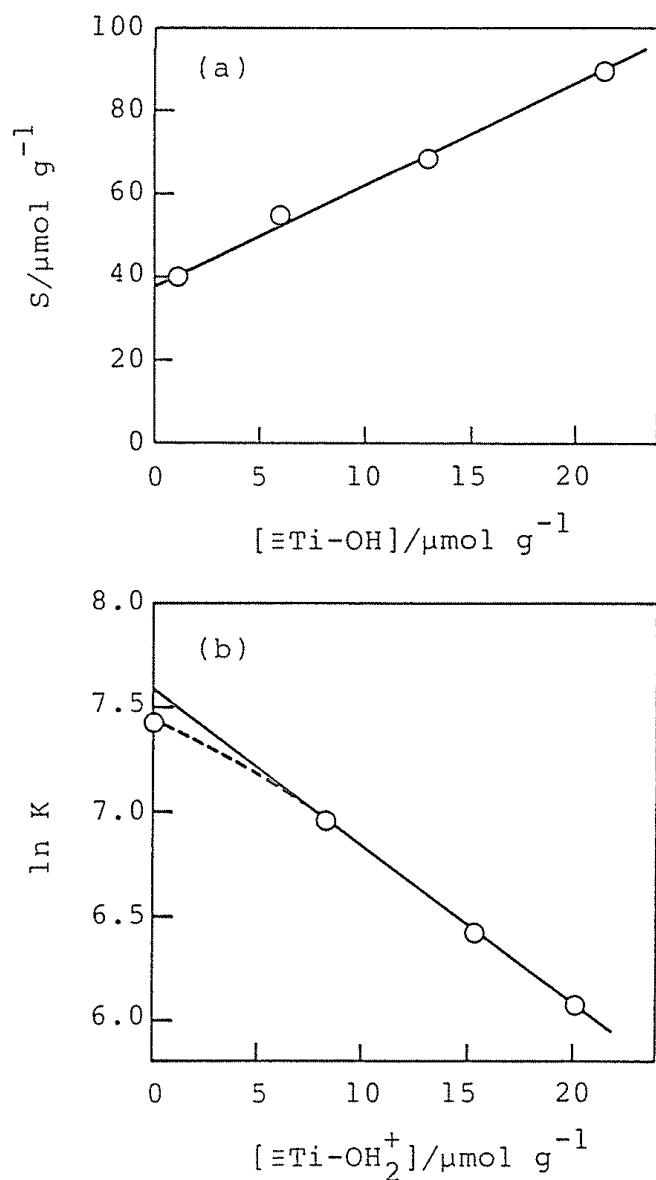


Figure 10 (a)Relation between limiting amount of  $\text{Ag}^+$  adsorption site and amount of hydroxyl group in neutral form. (b)Relation between  $\ln K$  ( $\text{Ag}^+$  adsorption equilibrium constant) and amount of hydroxyl group in acid form.

Therefore, the  $\text{Ag}^+$  adsorption on the  $\text{TiO}_2$  surface is inhibited by the protonation of surface hydroxyl under the lower pH conditions, i.e., i.e., the increase of  $\equiv\text{Ti}-\text{OH}_2^+$  leads to the decrease of both intensive (K) and extensive (S) properties of  $\text{TiO}_2$  surface to adsorb  $\text{Ag}^+$ .

In conclusion, the initial rate of the photocatalytic Ag metal deposition onto  $\text{TiO}_2$  suspended in  $\text{AgNO}_3$  solution decreased with the decrease of the initial pH. It was clarified that this pH dependence was caused by the pH dependent adsorption of  $\text{Ag}^+$  on the  $\text{TiO}_2$  surface; the amount of the adsorbed  $\text{Ag}^+$  decreased with the pH decrease owing to the protonation of the surface hydroxyl group.

## REFERENCES AND NOTES

- 1 For recent review see A. J. Bard, *J. Phys. Chem.*, 86, 172 (1982).
- 2 (a) T. Kawai and T. Sakata, *Chem. Lett.*, 81 (1981) (b) B. Kraeutler and A. J. Bard, *J. Am. Chem. Soc.*, 100, 5985 (1978).
- 3 See Chapter 6; S. Nishimoto, B. Ohtani, H. Kajiwara, and T. Kagiya, *J. Chem. Soc., Faraday Trans. 1*, 79, 2685 (1983).
- 4 G. A. Parks and P. L. de Bruyn, *J. Phys. Chem.*, 66, 967 (1962).
- 5 M. A. Butler and D. S. Ginley, *J. Electrochem. Soc.*, 125, 231 (1978).
- 6 P. D. Fleischauer, H. K. Alen Kan, and J. R. Schepherd, *J. Am. Chem. Soc.*, 94, 283 (1972).
- 7 H. Hada, Y. Yonezawa, and M. Saikawa, *Bull. Chem. Soc. Jpn*, 55, 2010 (1982).
- 8 R. F. Scarr, *J. Electrochem. Soc.*, 116, 1526 (1969).
- 9 L. D. Burke, O. J. Murphy, J. F. O'neill, and S. Venkatesan, *J. Chem. Soc., Faraday Trans. 1*, 73, 1659 (1977).
- 10 P. Salvador, *J. Electrochem. Soc.*, 129, 1895 (1981).
- 11 P. Clechet, C. Martelet, J. R. Martin, and R. Olier, *Electrochim. Acta*, 24, 457 (1979).
- 12 S. Mukai and T. Wakamatsu, *Suiyokai-shi (Kyoto University)*, 16, 601 (1968).
- 13 H. P. Boehm, *Disc. Faraday Soc.*, 52, 264 (1971).
- 14 S. Okazaki and K. Kuramochi, *Nippon Kagaku Kaishi*, 1141 (1982).
- 15 P. W. Schindler and H. Gamsjager, *Disc. Faraday Soc.*, 52, 286 (1971).

16 Equi-acid-base point (EABP) is defined as a equiadsorption point (EAP) in the case that  $H^+$  and  $OH^-$  are adsorbed on an oxide surface. On the other hand, iso-electric point (IEP, in Japanese Todenten) is estimated by the measurement of dynamic characteristics of suspension, such as electrophoresis. EABP and IEP are often called as zero point of charge (zpc). They are essentially different by definition, though it is often the case that they are practically identical. In this thesis, the term EABP was used as a strict manner; Chemical Society of Japan Ed., T. Hirai and I. Tari, Kagaku Sosetsu, 7, "Electrochemistry of Surface", Gakkai Shuppan Center, Tokyo (1975), p. 112, and references therein.

## SUMMARY

In Chapter 1, photocatalytic reaction ( $\lambda_{\text{ex}} > 300 \text{ nm}$ , under Ar at room temperature) of a series of aliphatic alcohols in aqueous suspension of  $\text{TiO}_2$  with platinum and/or ruthenium dioxide was investigated. The alcohols were dehydrogenated into carbonyl and/or dimeric derivatives. The anatase  $\text{TiO}_2$  ( $\text{TiO}_2(\text{A})$ ) with platinum black (Pt) showed the highest photocatalytic activity for these reactions while rutile  $\text{TiO}_2$  ( $\text{TiO}_2(\text{R})$ ) was ineffective. The light of wavelength  $< \text{ca. } 390 \text{ nm}$  was effective for these reactions. The linear relation between the initial rate of the photocatalytic reaction and the reported rate constant of hydrogen abstraction of the alcohols by hydroxyl radical ( $\cdot\text{OH}$ ) in homogeneous system suggested the active species  $\cdot\text{OH}$  generated via one electron oxidation of the surface hydroxyl with photogenerated positive hole.

In Chapter 2, photocatalytic reaction of 2-methyl-2-propanol in the aqueous suspension of  $\text{TiO}_2(\text{A})/\text{Pt}$  was investigated. The distribution of products, such as 2,5-dimethyl-2,5-hexanediol and acetone, was in accord with that in the oxidation induced by  $\cdot\text{OH}$  formed in the Fenton's reaction or in the  $\gamma$ -radiation in the presence of  $\text{N}_2\text{O}$ . It was clarified that 2-methyl-2-propanol is oxidized via hydrogen abstraction by  $\cdot\text{OH}$  produced by one electron oxidation of the surface hydroxyl by photogenerated positive hole, and that the intermediate 2-hydroxy-2-methylpropyl radical undergoes dimerization into 2,5-dimethyl-2,5-hexanediol or  $\beta$ -scission into acetone and methyl radical.

In Chapter 3, photocatalytic reaction of poly(vinyl alcohol) by the aqueous suspension of  $\text{TiO}_2(\text{A})/\text{Pt}$  was shown. Spectroscopic

and viscometric measurements revealed the formation of  $\beta$ -ketol and  $\alpha, \beta$ -unsaturated ketone on the polymer chain. The total amount of such ketones was approximately equimolar to that of  $H_2$  liberated simultaneously. A reaction mechanism involving an  $\alpha$ -hydroxy polymer radical liberated via hydrogen abstraction by  $\cdot OH$  on the  $TiO_2$  was discussed.

In Chapter 4, photocatalytic reaction of poly(ethylene oxide) by the aqueous suspension of  $TiO_2(A)/Pt$  was characterized. It was found that the polymer chain is degraded into acetaldehyde followed by its photolysis under the acidic conditions, while the chain is prolonged under the neutral and basic conditions. Two types of hydrogen abstractions by  $\cdot OH$  from the polymer chain adsorbed in "vertical" and "horizontal" modes on the  $TiO_2$  surface, depending on the deprotonation and protonation of surface hydroxyl, give the prolonged and degraded product in the basic and acidic conditions, respectively.

In Chapter 5, photocatalytic reaction of aliphatic amines by the aqueous suspension of  $TiO_2(A)/Pt$  was described in detail. Primary straight-chain amines were converted into secondary amines and ammonia with the liberation of  $H_2$  and aldehydes. GC-MS measurement of the product obtained in the  $D_2O$  solution indicated that secondary amine is produced by the hydrogenation, at the platinum site, of Schiff base intermediate derived from the aldehyde and the starting amine. Attempts were made to extend this photocatalytic reaction to novel synthetic process; cyclic secondary amine production from polymethylene- $\alpha, \omega$ -diamines with high selectivity.

In Chapter 6, photocatalytic formation of  $O_2$  and deposition of

Ag metal by both anatase and rutile  $\text{TiO}_2$  powders suspended in aqueous silver salt solutions were investigated. Mass spectroscopic analysis of  $\text{O}_2$  obtained from the  $\text{H}_2^{16}\text{O}/\text{H}_2^{18}\text{O}$  system revealed that the  $\text{O}_2$  formation is accounted for by the oxidative decomposition of water by photogenerated positive hole in  $\text{TiO}_2$ , along with the reduction of silver ion to form metallic Ag by photoexcited electron. The photocatalytic activities of both  $\text{TiO}_2(\text{A})$  and  $\text{TiO}_2(\text{R})$  powders were almost same. The reaction rate decreased with the irradiation time due to the decreasing pH, as a result of proton release into the suspension as the reaction proceeded by both  $\text{TiO}_2$  powders. It was clarified that salt of weak acid, silver sulfate could retain the activity of  $\text{TiO}_2$  because fluoride anion associates with the released proton to prevent the pH decrease.

In Chapter 7, effect of 2-propanol addition on the photocatalytic reaction in aqueous anatase and rutile  $\text{TiO}_2$  suspensions containing inorganic or organic silver salt was investigated. Competitive oxidations of both water and 2-propanol along with the Ag metal deposition on the  $\text{TiO}_2$  surface was characterized by the two types models of oxidation sites, one of which oxidizes both 2-propanol and water and the other only 2-propanol, on the basis of the stoichiometries of the reactions. It was also clarified that silver salt of carboxylic acid, silver acetate, was decomposed into  $\text{CO}_2$  with the simultaneous evolution of  $\text{O}_2$  and Ag metal deposition.

In Chapter 8, effect of 2-propanol and silver sulfate concentrations on the rate of photocatalytic reaction with anatase and rutile  $\text{TiO}_2$  powders suspended in aqueous solution was demonstrated. It was found that with the increasing concentration of 2-propanol

the amounts of products, Ag metal and acetone, increase along with the decrease of the  $O_2$  yield, and that these product yields also increase with the increasing concentration of silver sulfate. Characterization of these results revealed a Langmuir type adsorptions of both 2-propanol and silver ion onto the oxidation and reduction sites on the  $TiO_2$  surface, and competitive oxidations of 2-propanol and water by photogenerated positive hole at the oxidation sites, which were characterized in Chapter 7.

In Chapter 9, physical properties, such as content of anatase and rutile crystallites, specific surface area, or amount of residual sulfate anion, of  $TiO_2$  powders prepared from  $Ti(SO_4)_2$  by hydrolysis and calcination at various temperatures were shown. Photocatalytic activity of these  $TiO_2$  powders loaded with Pt black was investigated for the dehydrogenation of 2-propanol in the aqueous suspension. Correlation of the activity with the physical properties revealed that most important property controlling the photocatalytic activity of  $TiO_2$  is the crystal structure; anatase  $TiO_2$  shows sufficient activity which increases with the increase in crystallite size, while that of rutile is negligible even covered with platinum.

In Chapter 10, photocatalytic activity of  $TiO_2$  powders, which consist of anatase, rutile, and their mixture, prepared from titanium tetra-2-propoxide for the 2-propanol dehydrogenation with loaded Pt and for the oxidations of 2-propanol and water along with Ag metal deposition was demonstrated. It was found that anatase  $TiO_2$  shows sufficient photocatalytic activity in both reactions of  $H_2$  liberation with Pt and Ag metal deposition, and the activities



increase with the increase in the crystallite size. The rutile  $\text{TiO}_2$  also showed sufficient activity which was comparable to that of anatase  $\text{TiO}_2$  for the photocatalytic reduction of silver ion along with the formations of acetone and  $\text{O}_2$ , while negligible for the dehydrogenation of 2-propanol to yield  $\text{H}_2$  and acetone, even covered with platinum, in the absence of silver salt. The little activity of rutile  $\text{TiO}_2$  for the 2-propanol dehydrogenation is attributed to the lower energy of electron in its conduction band.

In Chapter 11, pH-dependent photocatalytic activity of anatase and rutile  $\text{TiO}_2$  for the  $\text{O}_2$  formation and Ag metal deposition in the aqueous solution of silver nitrate was characterized. It was clarified that the initial rate of the reaction, which decreases with decreasing pH, is in proportion to the amount of silver ion adsorbed on the  $\text{TiO}_2$  surface. Characterization of the surface properties of  $\text{TiO}_2$ , protonation and deprotonation equilibria of the surface hydroxyl, revealed that silver ion is adsorbed mainly at the  $\text{Ti}_2\text{O}$  ( $-\text{Ti}-\text{O}-\text{Ti}-$ , 76 %; at  $\equiv\text{Ti}-\text{OH}$ , 24% on anatase  $\text{TiO}_2$ ) structure on the  $\text{TiO}_2$  surface, and the extent of adsorption decreases with the increase of protonated surface hydroxyl in the lower pH region.

## LIST OF PUBLICATIONS

- Chapter 1 S. Nishimoto, B. Ohtani, and T. Kagiya, J. Chem. Soc., Faraday Trans. 1, to be submitted.
- Chapter 2 S. Nishimoto, B. Ohtani, H. Shirai, and T. Kagiya, J. Phys. Chem., to be submitted.
- Chapter 3 S. Nishimoto, B. Ohtani, H. Shirai, and T. Kagiya, J. Polym. Sci., Polym. Lett. Ed., in contribution; S. Nishimoto, B. Ohtani, and T. Kagiya, in N. S. Allen and J. F. Rabek Ed., "The New Trends in Polymer Photochemistry", Applied Science, London (1983), in press.
- Chapter 4 S. Nishimoto, B. Ohtani, T. Yoshikawa, and T. Kagiya, Macromolecules, to be submitted.
- Chapter 5 S. Nishimoto, B. Ohtani, T. Yoshikawa, and T. Kagiya, J. Am. Chem. Soc., 105, 7180 (1983).
- Chapter 6 S. Nishimoto, B. Ohtani, H. Kajiwara, and T. Kagiya, J. Chem. Soc., Faraday Trans. 1, 79, 2685 (1983).
- Chapter 7 S. Nishimoto, B. Ohtani, and T. Kagiya, J. Photochem., in contribution.
- Chapter 8 S. Nishimoto, B. Ohtani, and T. Kagiya, J. Phys. Chem., in contribution.
- Chapter 9 S. Nishimoto, B. Ohtani, A. Sakamoto, and T. Kagiya, Nippon Kagaku Kaishi, 246 (1984).
- Chapter 10 S. Nishimoto, B. Ohtani, H. Kajiwara, and T. Kagiya, J. Chem. Soc., Faraday Trans. 1, in press.
- Chapter 11 S. Nishimoto, B. Ohtani, Y. Okugawa, and T. Kagiya, to be submitted.